Entwicklung und Einsatz von Neutronentransportmethoden und Unsicherheitsanalysen für Reaktorkernberechnungen

GRS-A-3713

Gesellschaft für Anlagen- und Reaktorsicherheit (GRS) mbH

Technischer Bericht/ Technical Report

Reaktorsicherheitsforschung-Vorhabens Nr.:/
Reactor Safety Research-Project No.:
RS1503

Vorhabenstitel / Project Title:
Entwicklung und Einsatz von Neutronentransportmethoden und Unsicherheitsanalysen für Reaktorkernberechnungen

Development and Application of Neutron Transport Methods and Uncertainty Analyses for Reactor Core Calculations

Berichtstitel / Report Title:
Entwicklung und Einsatz von Neutronentransportmethoden und Unsicherheitsanalysen für Reaktorkernberechnungen

Autor / Authors:
W. Zwermann, A. Aures, W. Bernnat, L. Gallner, M. Klein, B. Krzykacz-Hausmann, M. Küntzel, I. Pasichnyk, A. Pautz, Y. Perin, F. Puente-Espel, K. Velkov, M. Zilly

Berichtszeitraum / Publication Date:
Juni 2013

Anmerkung:
Das diesem Bericht zugrunde liegende F&E-Vorhaben wird im Auftrag des Bundesministeriums für Wirtschaft und Technologie (BMWi) unter dem Kennzeichen RS1503 durchgeführt.

GRS - A - 3713

Kurzfassung

Der vorliegende Bericht dokumentiert den Zwischenstand (1. Quartal 2013) der im RS-Forschungsprojekt RS1503 „Entwicklung und Einsatz von Neutronentransportmethoden und Unsicherheitsanalysen für Reaktorkernberechnungen“ erreichten Forschungs- und Entwicklungsziele. Das übergeordnete Ziel des Projekts ist die Entwicklung, Validierung und Anwendung von Neutronentransportmethoden und Unsicherheitsanalysen für Reaktorkernberechnungen. Diese Rechenmethoden sollen im Wesentlichen für Fragestellungen, die sich mit dem Kernverhalten von Leichtwasserreaktoren und innovativen Reaktorkonzepten beschäftigen, eingesetzt werden. Dazu beitragende Einzelzielsetzungen sind die Weiterentwicklung, Validierung und Anwendung von deterministischen und stochastischen Rechenprogrammen, und von Methoden zu Unsicherheits- und Sensitivitätsanalysen, sowie die Erprobung künstlicher neuronaler Netze, zur Bereitstellung einer vollständigen nuklearen Rechenkette. Diese umfasst das Prozessieren von nuklearen Basisdaten, die Erzeugung von Multigruppen-Daten für Diffusions- und Transportcodes, die Erzeugung von Referenzlösungen für stationäre Zustände mit Monte-Carlo-Codes, die Durchführung von gekoppelten 3D-Ganzkernanalysen in Diffusionsnäherung und auch mit anderen deterministischen Methoden und Monte-Carlo-Transportprogrammen, sowie Unsicherheits- und Sensitivitätsanalysen mit dem Ziel der Propagation von Unsicherheiten durch die gesamte Berechnungskette von der Brennelement-Spektral- und Abbrandberechnung bis zur gekoppelten Transientenanalyse. Diese Rechenkette soll für Leichtwasserreaktoren, aber auch für innovative Reaktorkonzepte einsetzbar sein und muss daher entsprechend umfassend an Benchmarks und kritischen Experimenten validiert werden.

Abstract

This report documents the status of the research and development goals reached within the reactor safety research project RS1503 “Development and Application of Neutron Transport Methods and Uncertainty Analyses for Reactor Core Calculations” as of the 1st quarter of 2013. The superordinate goal of the project is the development, validation, and application of neutron transport methods and uncertainty analyses for reactor core calculations. These calculation methods will mainly be applied to problems related to the core behaviour of light water reactors and innovative reactor concepts. The contributions of this project towards achieving this goal are the further development, validation, and application of deterministic and stochastic calculation programmes and of methods for uncertainty and sensitivity analyses, as well as the assessment of artificial neutral networks, for providing a complete nuclear calculation chain. This comprises processing nuclear basis data, creating multi-group data for diffusion and transport codes, obtaining reference solutions for stationary states with Monte Carlo codes, performing coupled 3D full core analyses in diffusion approximation and with other deterministic and also Monte Carlo transport codes, and implementing uncertainty and sensitivity analyses with the aim of propagating uncertainties through the whole calculation chain from fuel assembly, spectral and depletion calculations to coupled transient analyses. This calculation chain shall be applicable to light water reactors and also to innovative reactor concepts, and therefore has to be extensively validated with the help of benchmarks and critical experiments.

Inhaltsverzeichnis

Abbildungsverzeichnis

Tabellenverzeichnis

1 Einleitung

Die Weiterentwicklung, Validierung und Anwendung von deterministischen und stochastischen Rechenprogrammen, und von Methoden zu Unsicherheits- und Sensitivitätsanalysen, sowie die Erprobung künstlicher neuronaler Netze, zur Bereitstellung einer vollständigen nuklearen Rechenkette sind Hauptgegenstand des Reaktorsicherheitsforschungsvorhabens RS1503 der GRS. Der vorliegende Bericht dokumentiert den aktuellen Stand der Arbeiten zum Ende des ersten Quartals 2013.

In Deutschland werden zur Stromerzeugung aus Kernenergie Leichtwasserreaktoren betrieben. Für diesen Reaktortyp haben sich zur Simulation von stationären und zeitabhängigen Kernzuständen reaktorphysikalische Rechenmethoden etabliert, die simultan den Neutronentransport, die Thermofluiddynamik und das thermische Verhalten der Brennstäbe beschreiben. Dies wird normalerweise mit gekoppelten Rechenprogrammen, die den Neutronentransport dreidimensional in Diffusionsnäherung und die Thermofluiddynamik des Kühlmittels mit einer auf der Lösung der Erhaltungsgleichungen für Masse, Energie und Impuls basierenden Berechnung der ein- und mehrphasigen Kühlmittelzustände beschreiben, durchgeführt.

Zur Lösung der Neutronendiffusionsgleichungen werden meist nodale Verfahren verwendet, mit denen eine hohe Genauigkeit für die Berechnung der Neutronenflüsse und der Leistung in den Volumenelementen des Rechengitters möglich ist. Diese Volumenelemente sind meist vertikale Abschnitte von Brennelementen, über die die in Wirklichkeit stark ortsabhängigen Materialeigenschaften gemittelt werden. Zusätzlich zu dieser räumlichen Homogenisierung wird die Energieabhängigkeit der nuklearen Daten auf wenige, oft nur zwei Energiegruppen reduziert. Diese im Orts- und Energieraum stark vereinfachten Parameter werden gewöhnlich in ein- oder zweidimensionalen Vorausrechnungen, in denen die tatsächliche Umgebung der Brennelemente im Reaktor nur näherungsweise berücksichtigt werden kann, vorab bestimmt. Unter der Annahme, dass sich die Eigenschaften benachbarter Brennelemente nicht stark unterscheiden, ist zur Beschreibung des Neutronentransports die Diffusionsnäherung gerechtfertigt. Mit dieser Methodik können auf moderner Rechner-Hardware stationäre Reaktorzustände und Kerntransienten problemlos beschrieben werden.

Mit fortlaufender Optimierung der Beladestrategien, MOX-Einsatz und Erhöhung der Brennstoffanreicherung und des Brennelement-Abbrands, sowie insbesondere beim Betrieb mit teilweise eingefahrenen Absorberelementen werden die Reaktorkerne zu-

nehmend heterogener; dadurch sind die Voraussetzungen zur Anwendung der Diffusionsnäherung immer weniger erfüllt. Von besonderer Bedeutung ist die genaue Berechnung der Brennstab-Leistungsverteilungen, die für die sicherheitstechnische Bewertung maßgebend ist.

Die immense Rechenleistung heutiger Computer ermöglicht Reaktorberechnungen in vertretbarer Rechenzeit unter Fallenlassen der Diffusionsnäherung auf wesentlich feineren Orts- und Energiegittern. So wird typischerweise die räumliche Homogenisierung anstatt über axiale Brennelementabschnitte über Abschnitte von Brennstabzellen durchgeführt, und anstelle der für nodale Verfahren typischen zwei Energiegruppen werden Daten mit mehr Energiegruppen (typischerweise zehn oder mehr) verwendet. Nötig ist der Einsatz solcher Verfahren z. B. für die Berechnung von Forschungsreaktoren, die einerseits wesentlich kompakter, andererseits i. A. wesentlich heterogener als Leichtwasser-Leistungsreaktoren sind. Hier hat die GRS bereits in den Vorgängervorhaben RS1128, RS1160 und RS1183 die zeitabhängigen Multigruppen-Neutronentransportcodes DORT-TD /PAU 03a/ und TORT-TD /SEU 04/ entwickelt und für stabweise 3D-Analysen mit Berücksichtigung der thermohydraulischen Rückwirkungseffekte aus ATHLET-Modellkomponenten eingesetzt /SEU 08/. Diese beiden Codes verwenden die sog. Methode der Diskreten Ordinaten. Näherungen bestehen hier im Wesentlichen in der Abbildung der tatsächlichen Energieabhängigkeit der nuklearen Daten auf eine begrenzte Anzahl von Energiegruppen, sowie die Abbildung der räumlichen Materialverteilung auf reguläre Geometrie; gegenwärtig sind in DORT-TD und TORT-TD kartesische und Zylindergeometrie implementiert.

Zur Validierung deterministischer Berechnungsmethoden werden häufig, neben der Nachrechnung von Experimenten, Referenzberechnungen für stationäre Zustände mit Monte-Carlo-Programmen herangezogen. Diese benötigen praktisch keine Vereinfachung in der räumlichen Beschreibung der Kernanordnungen; ebenso entfällt die Notwendigkeit, die kontinuierliche Energieabhängigkeit der nuklearen Daten auf Gruppen zu reduzieren. Während die Berechnung von Anordnungen mit einer begrenzten Anzahl von Materialien bei vorgegebenen thermodynamischen Bedingungen, wie kritische Experimente oder Reaktoren im leistungslosen Betrieb, mit der Monte-Carlo-Methode bereits Standard ist, wird in letzter Zeit verstärkt dazu übergegangen, stationäre Leistungszustände durch Kopplung von Monte-Carlo-Programmen, häufig dem Code MCNP /X-5 03/, mit Thermofluiddynamik-Codes zu bestimmen /PUE 09, SAN 09/. Dazu muss die betrachtete Anordnung in eine äußerst große Anzahl von Zonen mit unter-

schiedlichen thermodynamischen Parametern aufgeteilt werden; dies wird mit MCNP erst durch Modifikationen in der Verwaltung der Daten handhabbar. Die Durchführbarkeit solcher Analysen wurde in einer Kooperation zwischen dem Institut für Kernenergetik und Energiesysteme (IKE) der Universität Stuttgart und GRS demonstriert /BER 10/. Gegenwärtig werden Monte-Carlo-Kritikalitätsberechnungen praktisch ausschließlich für stationäre Zustände angewandt, wobei Untersuchungen über die Durchführbarkeit von Transientenberechnungen bereits angestellt werden /SJE 10/.

Bei dem kontinuierlichen Bestreben, Ungenauigkeiten in den Rechenmethoden, die durch Näherungsmethoden eingeführt werden, zu reduzieren, kommt gleichzeitig der Bestimmung von Unsicherheiten, die auf der unvollständigen Kenntnis von Eingangsparametern beruhen, höchste Bedeutung zu. Hinsichtlich Unsicherheiten in den thermodynamischen Parametern werden in der GRS seit langem Analysen in gekoppelten Neutronendiffusions-/Thermofluiddynamikrechnungen mit der Sampling-basierten GRS-Methode, die im Code SUSA /KRZ 94/ implementiert ist, durchgeführt.

Unsicherheits- und Sensitivitätsanalysen bezüglich Unsicherheiten in den nuklearen Basisdaten wird international zunehmend Beachtung geschenkt. Die Bedeutung von Unterschieden in den nuklearen Daten für die Ergebnisse von Leistungsverteilungen in Reaktorberechnungen wurde von der GRS anhand eines internationalen Rechenbenchmarks /KOZ 06/ demonstriert /LAN 09/. Um den Einfluss von Unsicherheiten in den nuklearen Daten auf die Ergebnisse von Kernberechnungen systematisch zu quantifizieren, beteiligt sich die GRS intensiv an internationalen Benchmarks zur Unsicherheits- und Sensitivitätsanalyse /NEA 07, UAC 08/. Eine besondere Herausforderung besteht darin, die Propagation solcher Unsicherheiten durch die mehrstufige nukleare Rechenkette aus Spektral- und Abbrandrechnungen, Erzeugung von Weniggruppen-Wirkungsquerschnitten und stationären oder transienten gekoppelten Kernberechnungen korrekt nachzuvollziehen, wie es im UAM-LWR-Benchmark angestrebt wird. Da die Sampling-basierte Vorgehensweise den einzigen bereits gangbaren Weg darstellt, dieses Ziel zu erreichen, nimmt die GRS hier durch ihr eigens zu diesem Zweck entwickeltes Programm XSUSA /ZWE 09/ eine herausragende Stellung ein. Dazu ist allerdings für die Kerntransientenanalysen in dreidimensionaler Geometrie, auch auf Multiprozessorsystemen, weiterhin der Einsatz von schnelllaufenden Programmen erforderlich; hierzu hat sich in der GRS der Diffusionscode QUABOX/CUBBOX bewährt /LAN 77a, LAN 77b, QC 78/.

Zusätzlich zur Weiterentwicklung und Anwendung etablierter Rechenverfahren zur Beschreibung des Neutronentransports, die in deterministischen und Monte-Carlo-Rechenprogrammen implementiert sind, sowie der Bestimmung von Ergebnisunsicherheiten, die auf Fertigungstoleranzen, unvollständige Kenntnis thermodynamischer Parameter und Unsicherheiten in den nuklearen Basisdaten zurückzuführen sind, ist die GRS auch bestrebt, die Anwendbarkeit innovativer Methoden zu untersuchen. Hier besteht bereits Erfahrung mit dem Einsatz von künstlichen neuronalen Netzen, die nun auch spezifisch für Untersuchungen zum Kernverhalten angewendet werden soll. Schließlich wird besonderer Wert auf die Zusammenarbeit mit nationalen und internationalen Kooperationspartnern gelegt, die teilweise im Vorgängerprojekt bereits begonnen oder geplant wurden, sowie auf den Einsatz der entwickelten Methoden auf Reaktorkonzepte, die über die Hauptanwendung für Leichtwasserreaktoren hinausgehen.

2 Zielsetzung

Die in der Einleitung dargelegten grundlegenden Fragestellungen zur Beschreibung des Kernverhaltens unter Einsatz von deterministischen und stochastischen Neutronentransportmethoden für LWR und innovative Reaktorkonzepte, sowie die Methoden für begleitende Unsicherheitsanalysen bzw. über etablierte Rechenverfahren hinausgehende Methoden werden in diesem Abschnitt durch die Formulierung von Einzelzielsetzungen für das Forschungsvorhaben RS1503 konkretisiert.

Dieses umfasst die Prozessierung von nuklearen Basisdaten, die Erzeugung von Multigruppen-Daten für Diffusions- und Transportcodes, die Erzeugung von Referenzlösungen für stationäre Zustände mit Monte-Carlo-Codes, die Durchführung von gekoppelten 3D-Ganzkernanalysen in Diffusionsnäherung bzw. mit deterministischen und Monte-Carlo-Transportprogrammen, sowie Unsicherheits- und Sensitivitätsanalysen mit dem Ziel der Propagation von Unsicherheiten durch die gesamte Berechnungskette von der Brennelement-Spektral- und Abbrandberechnung bis zur gekoppelten Transientenanalyse. Diese Rechenkette soll für Leichtwasserreaktoren, aber auch für innovative Reaktorkonzepte einsetzbar sein und muss daher entsprechend umfassend an Benchmarks und kritischen Experimenten validiert werden. Daraus ergeben sich folgende Einzelzielsetzungen.

- Methodische Weiterentwicklung, Validierung und Anwendung von deterministischen Berechnungsmethoden: Optimierung des GRS-Codes QUABOX/CUBBOX (Diffusion) bzgl. der Rechengenauigkeit, der Ausführungsgeschwindigkeit, des Einsatzbereiches und der Benutzerfreundlichkeit sowie Vergleich von Ergebnissen für gekoppelte stationäre Analysen mit entsprechenden Monte-Carlo-Ergebnissen. Die ursprünglich vorgesehene Anpassung des GRS-Codes TORT-TD für Hexagonalgeometrie wird vorerst zurückgestellt. Stattdessen ist die Teilnahme am EU-Projekt „Nuclear Reactor Safety Simulation Platform (NURESAFE)“ geplant, dessen Ziele die Entwicklung und Ausführung von Simulationsketten zur Analyse von ATWS-Transienten in Siedewasserreaktoren einschließlich der Quantifizierung von Ergebnisunsicherheiten sind. Die Teilnahme der GRS ist im Arbeitspaket „BWR ATWS with Uncertainty Quantification“ vorgesehen. Um dennoch in Zukunft solche Reaktorkernanalysen auch für Systeme jenseits von LWR-Kernanordnungen durchführen zu können (hauptsächlich mit hexagonaler Geometrie), ist es geplant, die Codes

DYN3D /GRU 00/ und nTRACER /SNU 09/ in das nukleare Berechnungssystem der GRS aufzunehmen.

- Methodische Weiterentwicklung, Validierung und Anwendung von Monte-Carlo-Berechnungsmethoden: Weiterentwicklung der Kopplung von Monte-Carlo-Neutronentransport- und thermofluiddynamischen Codes, Entwicklung von Methoden für zeitabhängige Berechnungen mit der Monte-Carlo-Methode, Erzeugung und Validierung von nuklearen Referenzdaten, Teilnahme an entsprechenden internationalen Benchmarks.

- Methodische Weiterentwicklung, Validierung und Anwendung von Methoden zur Unsicherheits- und Sensitivitätsanalyse: Vervollständigung des Programms XSUSA zur Unsicherheitsanalyse mit nuklearen Daten, Erweiterung auf kinetische Parameter, Unsicherheitsanalysen für Kerntransientenberechnungen, Propagation der Unsicherheiten durch die vollständige nukleare Berechnungskette (Spektral-/Abbrandberechnungen, Wirkungsquerschnittserzeugung, gekoppelte stationäre und zeitabhängige Kernberechnungen), Kombination von Unsicherheiten in nuklearen Daten und technologischen Parametern, Teilnahme an entsprechenden internationalen Benchmarks. Dieses Arbeitspaket soll ebenfalls bzgl. der Beteiligung am Arbeitspaket „BWR ATWS with Uncertainty Quantification“ des EU-Projekts NURESAFE erweitert werden.

- Einsatz künstlicher neuronaler Netze zur Berechnung lokaler Parameter im Reaktorkern: Entwicklung von Lösungen mit neuronalen Netzen für lokale Parameter im Reaktorkern bei unterschiedlichen Betriebszuständen aus vorgegebenen Ausgangsparametern.

Die folgenden Kapitel beschreiben die bisher durchgeführten Arbeiten zu diesen Arbeitspaketen.

3 AP1: Weiterentwicklung, Validierung und Anwendung von deterministischen Berechnungsmethoden

Der folgende Abschnitt beschreibt die bislang durchgeführten Arbeiten am nuklearen Programmsystem der GRS bezüglich deterministischer Rechenmethoden. Dies sind die Integration des direkten Ganzkern-Transport-Codes nTRACER, die Erstellung einer generischen Datenbank für Wirkungsquerschnitte und Ausgabedaten, Optimierungsarbeiten am GRS-Neutronendiffusionsprogramm QUABOX/CUBBOX, die Fortsetzung von Arbeiten zur SPH-Methode und die Durchführung eines Rechenbenchmarks mit IRSN.

3.1 Integration von nTRACER in das GRS-Programmsystem

Zur Durchführung von deterministischen stationären und transienten Reaktorberechnungen ohne die Notwendigkeit der räumlichen Homogenisierung von Teilbereichen des Reaktors (üblicherweise Brennelementen oder Stabzellen) wurde das Rechenprogramm nTRACER /SNU 09/ in das nukleare Programmsystem der GRS aufgenommen. Dabei handelt es sich um eine Entwicklung des Department of Nuclear Engineering der Universität Seoul, die auf den Konzepten des federführend vom Korean Atomic Energy Research Institute (KAERI) geschaffenen Codes DeCART beruht. Wie dieser verwendet nTRACER für die Berechnung der Neutronenfluss- und Leistungsverteilung in radialer Richtung die Planare Methode der Charakteristiken (Planar MOC), während zur Beschleunigung der Konvergenz und zur Kopplung an die axiale Dimension die Coarse-Mesh-Finite-Difference-(CMFD)-Methode benutzt wird. Bei der MOC können Multigruppen-Wirkungsquerschnittsbibliotheken ohne Homogenisierung über Stabzellen verwendet werden, weshalb nTRACER auch ein direkter Ganzkern-Transport-Code genannt wird. Der nTRACER-Code befindet sich noch in Entwicklung, daher sei zur Referenz bzgl. Theorie und Methodik auf die Dokumentation von DeCART verwiesen /ANL 05/.

Als erster Anwendungsfall wurde das C5G7-Benchmark /NEA 03/ in drei Dimensionen und bei stationären, unkontrollierten Bedingungen mit nTRACER nachgerechnet; die Ergebnisse wurden mit einer MCNP-Referenzlösung (Monte Carlo) und Ergebnissen des GRS-Codes TORT-TD (deterministisch, diskrete Ordinaten) nachgerechnet. Im C5G7-Benchmark wird eine 2x2-Brennelemente-Anordnung mit für Leichtwasserreaktoren typischen UO_2 und MOX-Brennelementen betrachtet. UO2 und MOX Brennele-

mente sind schachbrettartig angeordnet und sowohl radial wie auch axial von Reflektor (Moderator) umgeben. Das Brennelement-Layout ist in Abbildung 3-1 dargestellt. Untersucht wurden der effektive Multiplikationsfaktor für die Anordnung sowie die axial gemittelte Stableistungsverteilung.

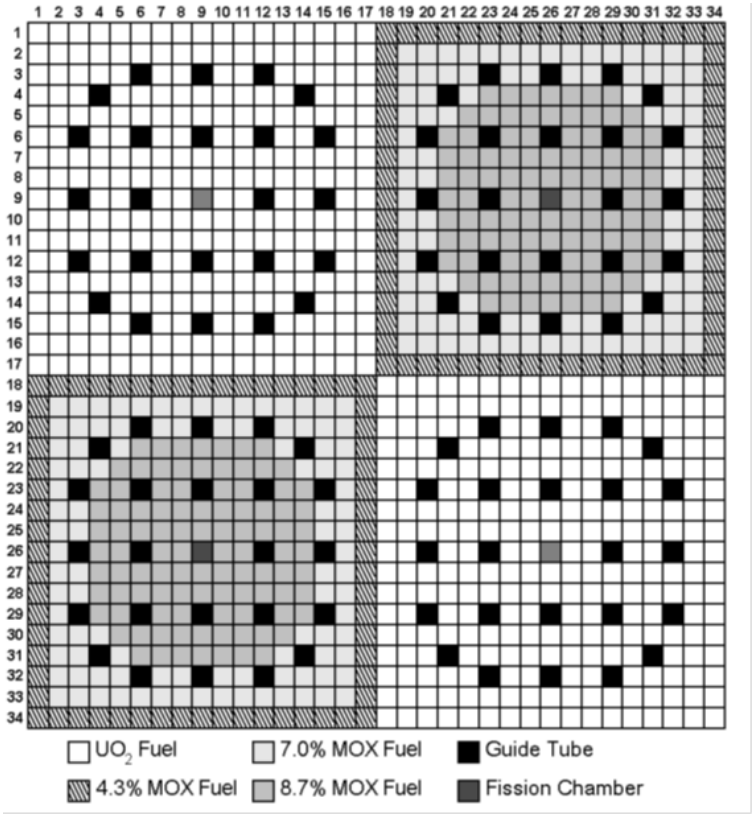

Abbildung 3-1 Brennelement-Layout des C5G7-Benchmarks

Tabelle 3-1 Ergebnisse für das C5G7-Benchmark aus MCNP, nTRACER und TORT-TD

	MCNP	nTRACER	TORT-TD
k-eff	1.14308	1.14344	1.14092
Abweichung zu MCNP:			
k-eff	-	0.00036	-0.00216
Stableistung (max.)	-	1.085%	1.489%
Stableistung (1 σ)	-	0.340%	0.448%

Die mit den drei Programmen berechneten Multiplikationsfaktoren sind in Tabelle 3-1 dargestellt, ebenso wie die Abweichungen der deterministischen Lösungen zur Monte-

Carlo-Referenzlösung. Mit nTRACER ergibt sich eine ausgezeichnete Übereinstimmung mit der MCNP-Referenzlösung.

Trotz der hohen Rechengenauigkeit ist die Laufzeit von nTRACER gering. Mit den gewählten Eingabeparametern benötigt die Rechnung auf einem Linux-Cluster mit 3-GHz-CPUs zwischen 6½ min (1 Prozessor) und 102 s (8 Prozessoren auf 1 Rechenknoten). Die deutliche Rechenzeiteinsparung wird durch die hohe Parallelisierbarkeit der planaren MOC erreicht. Zum Vergleich benötigt die entsprechende TORT-TD-Rechnung mehrere Tage Rechenzeit.

2.201	2.204	2.214	2.226	2.229	2.230	2.187	2.149	2.119	2.056	2.000	1.948	1.855	1.754	1.632	1.483	1.282	1.317	1.065	0.940	0.867	0.814	0.770	0.715	0.665	0.622	0.571	0.526	0.485	0.439	0.399	0.378	0.410	0.599
2.204	2.215	2.240	2.277	2.304	2.370	2.257	2.216	2.247	2.121	2.063	2.070	1.919	1.795	1.653	1.491	1.280	1.298	1.347	1.175	1.098	1.052	1.046	0.923	0.854	0.841	0.736	0.675	0.658	0.568	0.506	0.471	0.517	0.591
2.214	2.240	2.314	2.441	2.468	0.000	2.381	2.331	0.000	2.233	2.175	0.000	2.057	1.927	1.711	1.511	1.285	1.293	1.326	1.183	1.177	1.120	0.000	0.952	0.871	0.000	0.756	0.690	0.000	0.607	0.543	0.476	0.509	0.587
2.226	2.277	2.441	0.000	2.496	2.451	2.296	2.246	2.287	2.150	2.098	2.140	2.076	0.000	1.810	1.539	1.293	1.295	1.338	1.265	0.000	1.113	1.129	0.961	0.884	0.877	0.762	0.701	0.704	0.589	0.000	0.513	0.514	0.587
2.229	2.304	2.468	2.496	2.404	2.425	2.281	2.233	2.274	2.138	2.085	2.119	2.002	1.970	1.829	1.560	1.296	1.297	1.364	1.290	1.183	1.149	1.086	0.933	0.859	0.855	0.741	0.681	0.679	0.613	0.538	0.518	0.524	0.587
2.230	2.370	0.000	2.451	2.425	0.000	2.344	2.299	0.000	2.202	2.144	0.000	2.024	1.935	0.000	1.609	1.300	1.298	1.427	0.000	1.281	1.146	0.000	0.986	0.904	0.000	0.787	0.715	0.000	0.621	0.577	0.000	0.550	0.587
2.187	2.257	2.380	2.296	2.281	2.344	2.218	2.178	2.221	2.087	2.031	2.052	1.904	1.815	1.765	1.531	1.276	1.277	1.339	1.225	1.151	1.043	1.039	0.903	0.836	0.835	0.723	0.662	0.655	0.563	0.523	0.489	0.516	0.580
2.149	2.216	2.331	2.246	2.233	2.298	2.178	2.140	2.183	2.051	1.996	2.015	1.867	1.778	1.732	1.507	1.257	1.258	1.318	1.201	1.127	1.023	1.020	0.890	0.825	0.823	0.714	0.654	0.645	0.555	0.514	0.480	0.510	0.575
2.119	2.247	0.000	2.287	2.274	0.000	2.221	2.183	0.000	2.094	2.036	0.000	1.906	1.813	0.000	1.536	1.245	1.244	1.365	0.000	1.190	1.076	0.000	0.945	0.870	0.000	0.759	0.690	0.000	0.590	0.541	0.000	0.532	0.571
2.056	2.121	2.233	2.150	2.138	2.202	2.087	2.051	2.094	1.968	1.916	1.936	1.794	1.710	1.668	1.452	1.212	1.214	1.275	1.165	1.093	0.993	0.993	0.866	0.804	0.804	0.697	0.639	0.631	0.542	0.503	0.471	0.499	0.563
2.000	2.063	2.175	2.098	2.085	2.144	2.031	1.996	2.036	1.916	1.866	1.887	1.754	1.674	1.631	1.419	1.185	1.188	1.249	1.144	1.078	0.980	0.977	0.852	0.791	0.791	0.686	0.630	0.623	0.537	0.500	0.467	0.494	0.556
1.948	2.070	0.000	2.140	2.119	0.000	2.052	2.015	0.000	1.936	1.887	0.000	1.787	1.713	0.000	1.434	1.163	1.166	1.287	0.000	1.163	1.045	0.000	0.906	0.834	0.000	0.730	0.665	0.000	0.580	0.540	0.000	0.516	0.551
1.855	1.919	2.057	2.076	2.002	2.024	1.904	1.868	1.906	1.794	1.754	1.787	1.692	1.670	1.560	1.337	1.116	1.123	1.191	1.136	1.042	1.019	0.971	0.836	0.774	0.774	0.673	0.620	0.621	0.561	0.493	0.477	0.483	0.540
1.754	1.795	1.927	0.000	1.970	1.935	1.815	1.778	1.813	1.710	1.674	1.713	1.670	0.000	1.474	1.261	1.067	1.080	1.130	1.081	0.000	0.963	0.982	0.842	0.779	0.776	0.678	0.626	0.631	0.530	0.000	0.465	0.466	0.531
1.632	1.653	1.711	1.810	1.829	0.000	1.765	1.732	0.000	1.668	1.631	0.000	1.560	1.474	1.318	1.174	1.013	1.038	1.087	0.989	0.998	0.959	0.000	0.826	0.762	0.000	0.669	0.614	0.000	0.545	0.489	0.430	0.459	0.527
1.483	1.491	1.511	1.539	1.560	1.609	1.531	1.507	1.536	1.452	1.419	1.434	1.337	1.261	1.174	1.079	0.953	1.007	1.094	0.988	0.945	0.918	0.923	0.823	0.769	0.761	0.672	0.620	0.606	0.528	0.472	0.440	0.478	0.535
1.282	1.280	1.285	1.293	1.297	1.300	1.276	1.257	1.245	1.212	1.185	1.163	1.116	1.068	1.013	0.953	0.878	1.015	0.910	0.856	0.820	0.788	0.757	0.712	0.669	0.631	0.585	0.542	0.504	0.459	0.420	0.397	0.420	0.575
1.317	1.298	1.293	1.295	1.297	1.298	1.277	1.258	1.244	1.214	1.188	1.166	1.123	1.080	1.038	1.007	1.015	0.795	0.789	0.771	0.750	0.725	0.699	0.659	0.621	0.587	0.544	0.505	0.470	0.428	0.394	0.373	0.389	0.500
1.065	1.347	1.326	1.338	1.364	1.427	1.339	1.318	1.364	1.275	1.249	1.288	1.191	1.130	1.087	1.094	0.910	0.789	0.825	0.830	0.825	0.810	0.806	0.739	0.696	0.678	0.612	0.568	0.545	0.485	0.441	0.413	0.423	0.525
0.940	1.175	1.183	1.265	1.290	0.000	1.226	1.201	0.000	1.165	1.144	0.000	1.136	1.081	0.989	0.988	0.856	0.771	0.830	0.863	0.897	0.884	0.000	0.798	0.751	0.000	0.662	0.614	0.000	0.534	0.487	0.439	0.437	0.531
0.867	1.098	1.177	0.000	1.183	1.281	1.151	1.127	1.190	1.093	1.078	1.163	1.042	0.000	0.998	0.945	0.820	0.750	0.825	0.897	0.000	0.889	0.848	0.767	0.721	0.706	0.636	0.593	0.578	0.538	0.000	0.463	0.442	0.528
0.814	1.052	1.120	1.113	1.149	1.146	1.043	1.023	1.076	0.993	0.980	1.045	1.019	0.963	0.959	0.918	0.788	0.725	0.810	0.884	0.889	0.838	0.822	0.748	0.705	0.690	0.623	0.580	0.564	0.512	0.491	0.461	0.440	0.517
0.770	1.046	0.000	1.129	1.086	0.000	1.039	1.020	0.000	0.993	0.977	0.000	0.971	0.983	0.000	0.923	0.757	0.699	0.806	0.000	0.848	0.822	0.000	0.750	0.708	0.000	0.627	0.583	0.000	0.507	0.471	0.000	0.442	0.503
0.715	0.923	0.952	0.961	0.933	0.986	0.903	0.890	0.945	0.866	0.852	0.906	0.836	0.842	0.826	0.823	0.712	0.659	0.739	0.798	0.767	0.748	0.750	0.688	0.651	0.640	0.577	0.537	0.520	0.464	0.430	0.423	0.410	0.481
0.665	0.854	0.871	0.884	0.859	0.904	0.836	0.825	0.870	0.804	0.791	0.834	0.774	0.779	0.762	0.769	0.669	0.621	0.696	0.751	0.721	0.705	0.708	0.651	0.618	0.607	0.549	0.511	0.494	0.440	0.407	0.401	0.390	0.458
0.622	0.841	0.000	0.877	0.855	0.000	0.835	0.823	0.000	0.804	0.791	0.000	0.774	0.776	0.000	0.761	0.631	0.587	0.678	0.000	0.706	0.690	0.000	0.640	0.607	0.000	0.540	0.502	0.000	0.434	0.400	0.000	0.382	0.436
0.571	0.736	0.757	0.762	0.741	0.787	0.723	0.714	0.759	0.697	0.686	0.730	0.673	0.678	0.669	0.672	0.585	0.544	0.612	0.662	0.636	0.623	0.627	0.577	0.549	0.540	0.488	0.455	0.441	0.392	0.363	0.359	0.348	0.409
0.526	0.675	0.690	0.701	0.681	0.715	0.662	0.654	0.690	0.639	0.630	0.666	0.620	0.626	0.614	0.620	0.542	0.505	0.568	0.615	0.593	0.580	0.583	0.537	0.511	0.502	0.455	0.424	0.411	0.367	0.340	0.335	0.325	0.382
0.485	0.658	0.000	0.704	0.679	0.000	0.655	0.645	0.000	0.631	0.623	0.000	0.621	0.631	0.000	0.606	0.504	0.470	0.545	0.000	0.578	0.564	0.000	0.520	0.494	0.000	0.441	0.411	0.000	0.358	0.332	0.000	0.313	0.356
0.439	0.568	0.607	0.589	0.613	0.621	0.563	0.555	0.590	0.542	0.537	0.580	0.561	0.530	0.545	0.528	0.459	0.428	0.485	0.534	0.538	0.512	0.507	0.464	0.440	0.434	0.392	0.367	0.358	0.325	0.311	0.294	0.280	0.326
0.399	0.506	0.543	0.000	0.538	0.577	0.523	0.514	0.541	0.503	0.500	0.540	0.493	0.000	0.489	0.472	0.420	0.394	0.441	0.487	0.000	0.491	0.471	0.430	0.407	0.400	0.363	0.340	0.332	0.311	0.000	0.268	0.254	0.298
0.378	0.471	0.476	0.513	0.518	0.000	0.489	0.480	0.000	0.471	0.467	0.000	0.477	0.465	0.430	0.440	0.397	0.373	0.413	0.439	0.463	0.461	0.000	0.423	0.401	0.000	0.359	0.335	0.000	0.294	0.268	0.240	0.234	0.275
0.410	0.517	0.509	0.514	0.524	0.550	0.516	0.510	0.532	0.499	0.494	0.516	0.483	0.466	0.459	0.478	0.420	0.389	0.423	0.437	0.442	0.440	0.442	0.410	0.390	0.382	0.348	0.325	0.313	0.280	0.254	0.234	0.230	0.264
0.599	0.591	0.587	0.587	0.587	0.587	0.580	0.575	0.571	0.563	0.556	0.551	0.541	0.531	0.527	0.535	0.575	0.500	0.526	0.531	0.528	0.518	0.503	0.481	0.459	0.436	0.409	0.382	0.356	0.326	0.298	0.275	0.264	0.284

Abbildung 3-2 Axial gemittelte Stableistungsverteilung aus nTRACER für das C5G7-Benchmark

Die mit nTRACER berechnete axial gemittelte relative Stableistungsverteilung ist in Abbildung 3-2 dargestellt. Zur Verdeutlichung der Qualität der Lösung finden sich die relativen prozentuellen Abweichungen zum MCNP-Referenzergebnis in Abbildung 3-3, sowie für den Maximalwert und einen aus der Standardabweichung gebildeten repräsentativen Wert in Tabelle 3-1. Auch hier ergibt sich wieder eine ausgezeichnete Übereinstimmung der nTRACER-Lösung mit der MCNP-Referenzlösung.

0.136	0.065	0.126	0.201	0.233	0.347	0.362	0.294	0.298	0.235	0.290	0.179	0.282	0.113	0.047	-0.312	-0.466	-0.251	-0.469	-0.453	-0.628	-0.712	-0.853	-0.543	-0.739	-0.655	-0.777	-0.966	-0.673	-0.840	-0.666	-0.891	-0.893	-0.268
0.065	0.136	0.143	0.364	0.477	0.374	0.569	0.510	0.331	0.450	0.424	0.367	0.353	0.151	-0.121	-0.240	-0.468	-0.250	-0.327	-0.321	-0.291	-0.468	-0.450	-0.192	-0.190	-0.420	-0.264	-0.474	-0.702	-0.647	-0.921	-1.000	-0.527	-0.285
0.122	0.139	0.388	0.391	0.467	0.000	0.518	0.383	0.000	0.308	0.375	0.000	0.392	0.295	0.283	-0.189	-0.289	-0.186	-0.203	-0.052	-0.035	-0.153	0.000	-0.494	-0.432	0.000	-0.719	-0.569	0.000	-0.835	-0.602	-0.544	-0.407	-0.181
0.196	0.364	0.395	0.000	0.580	0.505	0.521	0.504	0.425	0.549	0.574	0.494	0.465	0.000	0.168	0.014	-0.454	-0.126	-0.054	-0.123	0.000	0.022	-0.128	-0.150	-0.345	-0.335	-0.465	-0.165	-0.471	-0.631	0.000	-0.587	-0.204	0.057
0.229	0.473	0.472	0.584	0.656	0.534	0.675	0.687	0.457	0.652	0.590	0.583	0.721	0.463	0.273	0.075	-0.235	-0.186	-0.129	-0.106	-0.135	0.309	-0.024	-0.198	-0.136	-0.338	-0.330	-0.372	-0.345	-0.208	-0.295	-0.402	0.081	0.114
0.347	0.374	0.000	0.501	0.534	0.000	0.390	0.578	0.000	0.456	0.267	0.000	0.507	0.263	0.000	0.131	-0.224	-0.108	0.133	0.000	-0.182	0.026	0.000	-0.196	-0.364	0.000	-0.512	-0.658	0.000	-0.195	-0.307	0.000	-0.248	-0.062
0.362	0.569	0.510	0.521	0.680	0.386	0.567	0.596	0.389	0.548	0.464	0.357	0.612	0.458	0.299	0.194	-0.018	-0.034	0.016	-0.090	-0.033	-0.090	-0.058	-0.294	-0.120	-0.471	-0.358	-0.292	-0.371	-0.223	-0.515	-0.424	0.135	-0.061
0.294	0.514	0.383	0.504	0.687	0.574	0.591	0.512	0.334	0.444	0.508	0.326	0.632	0.512	0.160	0.248	-0.073	-0.169	0.197	-0.274	-0.044	-0.228	0.020	-0.095	-0.395	-0.368	-0.442	-0.495	-0.389	-0.010	-0.277	-0.326	-0.069	-0.208
0.293	0.331	0.000	0.425	0.457	0.000	0.393	0.334	0.000	0.064	0.301	0.000	0.238	0.140	0.000	-0.028	-0.125	0.022	-0.037	0.000	-0.371	-0.169	0.000	-0.522	-0.578	0.000	-0.907	-0.644	0.000	-0.309	-0.484	0.000	-0.180	-0.260
0.230	0.450	0.317	0.549	0.657	0.456	0.548	0.444	0.069	0.311	0.359	0.385	0.500	0.293	0.159	0.208	-0.207	-0.097	0.170	-0.310	-0.015	0.079	-0.204	-0.208	-0.448	-0.569	-0.644	-0.576	-0.645	-0.102	-0.468	-0.445	-0.138	-0.157
0.290	0.424	0.375	0.570	0.595	0.267	0.464	0.508	0.306	0.359	0.409	0.336	0.390	0.408	0.285	0.165	-0.171	-0.076	0.158	-0.154	0.007	0.052	-0.300	-0.268	-0.195	-0.366	-0.550	-0.537	-0.536	-0.455	-0.370	-0.447	0.162	0.102
0.179	0.362	0.000	0.494	0.583	0.000	0.352	0.326	0.000	0.390	0.331	0.000	0.453	0.200	0.000	0.092	-0.086	-0.139	-0.167	0.000	-0.069	0.125	0.000	-0.404	-0.349	0.000	-0.614	-0.574	0.000	-0.137	-0.470	0.000	-0.305	-0.057
0.282	0.353	0.392	0.470	0.726	0.507	0.612	0.638	0.233	0.506	0.390	0.453	0.526	0.278	0.184	-0.004	-0.257	-0.050	-0.158	-0.199	-0.157	0.263	-0.097	0.174	-0.144	-0.325	-0.292	-0.215	-0.686	-0.356	-0.348	-0.513	-0.603	-0.158
0.113	0.151	0.295	0.000	0.463	0.263	0.458	0.512	0.140	0.293	0.408	0.205	0.272	0.000	0.143	-0.129	-0.356	-0.221	-0.278	-0.339	0.000	-0.103	-0.302	-0.098	-0.300	-0.412	-0.174	-0.357	-0.359	-0.623	0.000	-0.674	-0.287	-0.064
0.047	-0.121	0.283	0.173	0.267	0.000	0.304	0.154	0.000	0.165	0.285	0.000	0.184	0.136	0.100	-0.394	-0.547	-0.296	-0.462	-0.409	-0.187	-0.384	0.000	-0.336	-0.436	0.000	-0.460	-0.279	0.000	-0.491	-0.735	-0.207	-0.416	-0.146
-0.319	-0.240	-0.189	0.014	0.081	0.131	0.194	0.248	-0.028	0.208	0.165	0.099	-0.004	-0.129	-0.394	-0.499	-0.651	-0.473	-0.317	-0.401	-0.413	-0.327	-0.571	-0.167	-0.058	-0.356	-0.259	0.047	-0.304	-0.275	-0.646	-0.665	-0.692	-0.318
-0.458	-0.460	-0.274	-0.446	-0.228	-0.216	-0.010	-0.066	-0.117	-0.199	-0.162	-0.069	-0.248	-0.346	-0.537	-0.640	-0.539	-0.354	-0.546	-0.538	-0.469	-0.477	-0.479	-0.460	-0.502	-0.415	-0.333	-0.368	-0.481	-0.554	-0.706	-0.554	-0.672	-0.326
-0.251	-0.257	-0.193	-0.133	-0.186	-0.108	-0.042	-0.177	0.014	-0.097	-0.084	-0.139	-0.059	-0.221	-0.296	-0.473	-0.364	-0.748	-0.665	-0.613	-0.571	-0.643	-0.569	-0.468	-0.525	-0.566	-0.491	-0.465	-0.600	-1.085	-1.075	-0.897	-0.639	-0.268
-0.469	-0.327	-0.203	-0.061	-0.122	0.140	0.009	0.190	-0.045	0.170	0.166	-0.160	-0.167	-0.287	-0.471	-0.317	-0.546	-0.665	-0.780	-0.512	-0.456	-0.258	-0.416	-0.401	-0.333	-0.255	-0.136	0.012	-0.549	-0.412	-0.466	-0.646	-0.459	-0.315
-0.442	-0.329	-0.052	-0.123	-0.106	0.000	-0.082	-0.274	0.000	-0.319	-0.154	0.000	-0.190	-0.348	-0.409	-0.391	-0.538	-0.626	-0.512	-0.437	-0.394	-0.242	0.000	-0.164	-0.311	0.000	-0.059	-0.081	0.000	-0.167	-0.074	0.033	-0.392	-0.096
-0.639	-0.291	-0.035	0.000	-0.135	-0.174	-0.033	-0.044	-0.371	-0.006	0.007	-0.069	-0.157	0.000	-0.197	-0.413	-0.481	-0.571	-0.456	-0.394	0.000	0.096	0.010	0.095	-0.092	-0.133	0.015	0.083	-0.406	-0.004	0.000	-0.117	-0.082	-0.189
-0.712	-0.468	-0.153	0.022	0.309	0.026	-0.090	-0.228	-0.179	0.079	0.052	0.134	0.253	-0.103	-0.384	-0.327	-0.489	-0.643	-0.258	-0.230	0.096	0.410	0.052	0.075	-0.067	-0.079	-0.075	0.257	-0.141	0.043	0.285	0.407	-0.111	-0.076
-0.853	-0.450	0.000	-0.128	-0.024	0.000	-0.048	0.029	0.000	-0.204	-0.300	0.000	-0.097	-0.282	0.000	-0.561	-0.466	-0.555	-0.404	0.000	0.010	0.052	0.000	0.016	-0.104	0.000	-0.113	0.026	0.000	0.171	-0.076	0.000	0.026	-0.167
-0.543	-0.192	-0.505	-0.139	-0.188	-0.206	-0.294	-0.084	-0.532	-0.208	-0.268	-0.404	0.162	-0.098	-0.336	-0.167	-0.460	-0.468	-0.401	-0.164	0.095	0.075	0.016	0.018	0.015	-0.405	-0.331	0.014	0.082	0.319	0.064	-0.286	0.010	0.326
-0.739	-0.178	-0.432	-0.345	-0.136	-0.364	-0.120	-0.395	-0.578	-0.448	-0.195	-0.337	-0.144	-0.300	-0.423	-0.058	-0.516	-0.525	-0.333	-0.311	-0.092	-0.067	-0.118	0.015	-0.012	-0.338	-0.260	-0.201	0.070	0.129	0.065	-0.254	-0.001	0.230
-0.655	-0.420	0.000	-0.335	-0.338	0.000	-0.459	-0.368	0.000	-0.569	-0.366	0.000	-0.325	-0.412	0.000	-0.356	-0.431	-0.566	-0.255	0.000	-0.133	-0.079	0.000	-0.405	-0.338	0.000	-0.231	-0.163	0.000	-0.003	-0.312	0.000	0.063	0.007
-0.777	-0.264	-0.705	-0.465	-0.317	-0.512	-0.344	-0.428	-0.894	-0.644	-0.550	-0.614	-0.292	-0.174	-0.460	-0.259	-0.333	-0.509	-0.136	-0.044	0.015	-0.075	-0.113	-0.331	-0.260	-0.231	-0.184	-0.035	-0.153	-0.038	-0.019	0.045	0.009	0.181
-0.966	-0.474	-0.555	-0.165	-0.372	-0.644	-0.292	-0.495	-0.644	-0.576	-0.537	-0.559	-0.215	-0.357	-0.279	0.047	-0.368	-0.465	0.029	-0.065	0.083	0.274	0.026	0.014	-0.201	-0.163	-0.035	-0.108	-0.085	0.127	-0.038	-0.250	0.134	0.430
-0.673	-0.702	0.000	-0.471	-0.345	0.000	-0.371	-0.389	0.000	-0.629	-0.552	0.000	-0.686	-0.359	0.000	-0.304	-0.481	-0.600	-0.549	0.000	-0.406	-0.141	0.000	0.082	0.070	0.000	-0.153	-0.085	0.000	0.080	-0.263	0.000	0.007	0.205
-0.840	-0.647	-0.835	-0.631	-0.192	-0.195	-0.205	-0.010	-0.309	-0.102	-0.437	-0.137	-0.356	-0.623	-0.472	-0.275	-0.554	-1.085	-0.412	-0.167	0.014	0.043	0.171	0.319	0.129	-0.003	-0.038	0.127	0.080	0.300	0.085	0.004	0.134	0.078
-0.666	-0.921	-0.602	0.000	-0.295	-0.307	-0.515	-0.277	-0.484	-0.468	-0.370	-0.452	-0.368	0.000	-0.715	-0.625	-0.729	-1.075	-0.466	-0.054	0.000	0.285	-0.076	0.064	0.065	-0.312	-0.019	-0.038	-0.263	0.085	0.000	-0.128	0.073	0.119
-0.891	-1.000	-0.544	-0.587	-0.402	0.000	-0.424	-0.326	0.000	-0.424	-0.447	0.000	-0.513	-0.695	-0.207	-0.643	-0.554	-0.897	-0.646	0.033	-0.117	0.407	0.000	-0.286	-0.254	0.000	0.045	-0.250	0.000	-0.030	-0.128	0.091	0.142	0.230
-0.893	-0.527	-0.407	-0.204	0.100	-0.266	0.135	-0.089	-0.180	-0.138	0.162	-0.324	-0.603	-0.309	-0.416	-0.692	-0.695	-0.639	-0.459	-0.392	-0.082	-0.111	0.026	0.010	-0.001	0.063	0.009	0.134	0.007	0.134	0.073	0.142	-0.463	-0.021
-0.268	-0.285	-0.164	0.057	0.131	-0.079	-0.044	-0.208	-0.243	-0.157	0.138	-0.075	-0.139	-0.064	-0.146	-0.299	-0.326	-0.248	-0.296	-0.077	-0.170	-0.056	-0.167	0.326	0.252	0.030	0.181	0.430	0.205	0.078	0.119	0.230	-0.021	0.262

Abbildung 3-3 Relative Abweichung in % der axial gemittelten Stableistungsverteilung aus nTRACER zur MCNP-Referenzlösung für das C5G7-Benchmark

Für eine weitere Evaluierung der Möglichkeiten von nTRACER ist eine Nachrechnung des sogenannten Purdue-Benchmarks /KOZ 06/ in Vorbereitung. Anders als bei dem

oben betrachteten C5G7-Benchmark wird hier nicht ein Referenz-Wirkungsquerschnittssatz zugrunde gelegt, sondern die Wirkungsquerschnittserzeugung ist Teil der zu betrachtenden Rechenkette. Hierbei ist auch das thermohydraulische Feedback, d. h. die Rückwirkung der Leistungserzeugung auf die Temperaturverteilung und Moderatordichte, zu berücksichtigen sowie die kritische Borkonzentration zu bestimmen. In nTRACER sind Programmmodule integriert, die diese Aufgaben lösen können; ihr Einsatz wird derzeit erprobt.

3.2 Implementierung einer generischen Datenbank für Wirkungsquerschnitte und Ausgabedaten

Daten, die von einem Computerprogramm in einem bestimmten Format ausgegeben werden, sollen in praktikabler Weise als Eingabedaten in einem für ein anderes Programm benötigten anderen Format zur Weiterverarbeitung der Daten oder zu deren Visualisierung bereitgestellt werden.

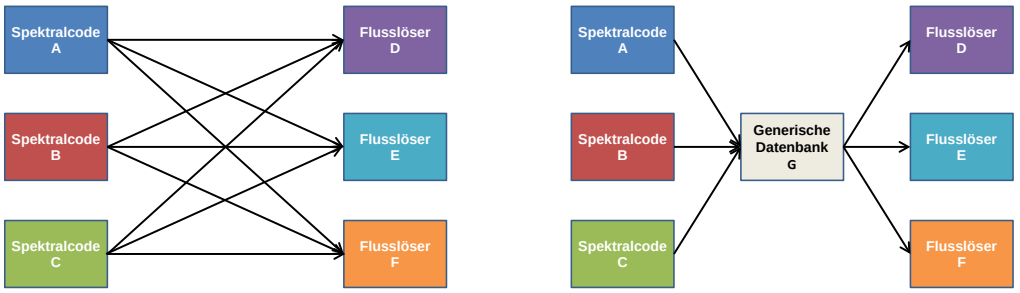

Abbildung 3-4 Datenübergabe von Spektralcodes an Transportcodes ohne und mit generischer Datenbank

Einer der in der GRS wichtigsten Anwendungsfälle ist hierbei die Bereitstellung einer generischen Wirkungsquerschnittsbibliothek. Der Vorteil einer generischen Datenbank im Zusammenspiel von Spektralcode und Transportcode wird anhand von Abbildung 3-4 leicht ersichtlich. Sollen beispielsweise mit n Spektralcodes Wirkungsquerschnitte für die Verwendung mit m Transportcodes bereitgestellt werden, so wird durch die Verwendung einer generischen Datenbank die Anzahl der notwendigen Schnittstellen von n x m auf $n + m$ reduziert. So wird auch die Verwendung eines neuen Codes in der Rechenkette erleichtert. Soll etwa ein neuer Spektralcode genutzt werden, so genügt

eine einzige Schnittstelle, um ihn in Zusammenwirkung mit einer Vielzahl von Transportcodes zu verwenden.

Für die Anwendung als Bindeglied zwischen Spektralcode und Flusslöser wurde im Berichtszeitraum eine Datenbank im HDF5-Format erprobt. Dieses hierarchische Datenformat ist in Industrie und Forschung weitverbreitet, kann plattformunabhängig eingesetzt werden und von verschiedenen Programmiersprachen wie Python, C++ oder Fortran aus gelesen bzw. geschrieben werden.

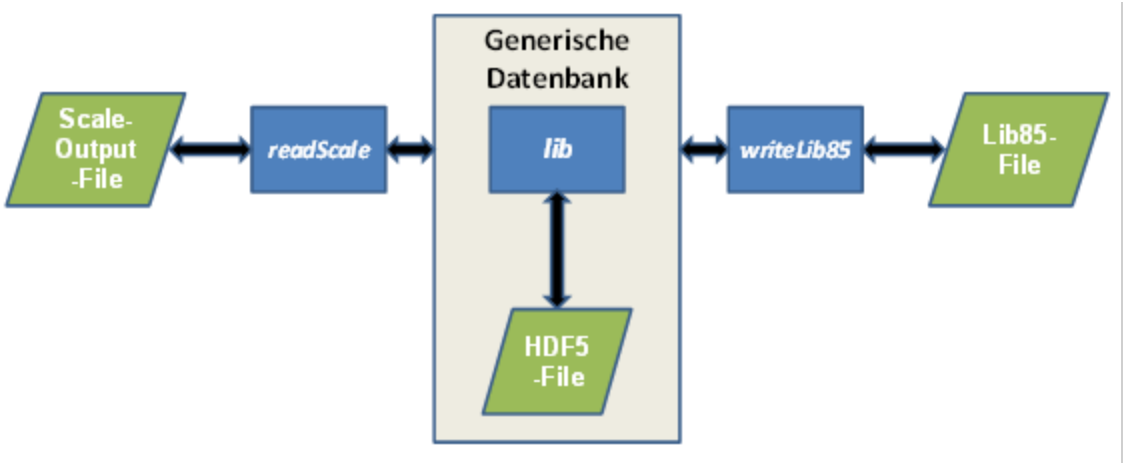

Abbildung 3-5 Derzeit implementierte Verwendung der generischen Datenbank im HDF5-Format.

Eingesetzt wurde die Datenbank bisher wie folgt. Mit dem Modul NEWT des SCALE-Programmpakets werden Wirkungsquerschnitte erzeugt (z. B. auch im Zusammenhang mit Sensitivitäts- und Unsicherheitsanalysen), welche in der SCALE-Ausgabedatei in spezifischem ASCII-Format vorliegen. Aus der SCALE-Ausgabedatei werden mit einem eigens entwickelten Python-Programm *readScale* die Wirkungsquerschnitte und weitere Daten ausgelesen. Diese Daten werden in Form eines Python-Dictionary an das Modul *lib* übergeben, welches die Lese- und Schreibroutinen für die HDF5-Datei enthält. Für die Anwendung der Wirkungsquerschnittsdaten mit dem GRS-Diffusionscode QUABOX/CUBBOX wurde ein weiteres Python-Programm *writeLib85* erstellt, welches mit einer Leseroutine von *lib* die Daten aus dem HDF5-File entnimmt und in das QUABOX/CUBBOX-Wirkungsquerschnittsdatenformat Lib85 übersetzt. Dieser Ablauf ist in Abbildung 3-5 skizziert. Dabei sind die Datenformate in grün und die Computerprogramme in blau dargestellt.

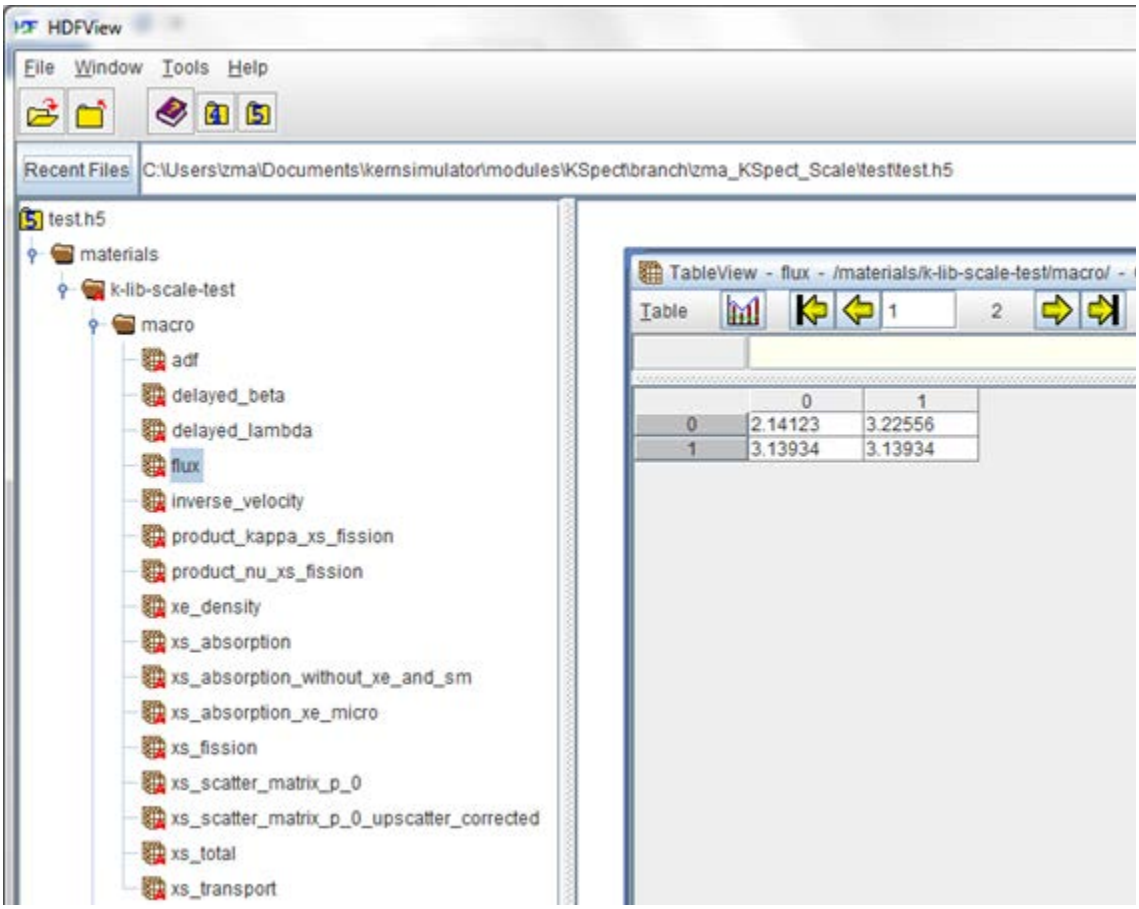

Abbildung 3-6 Darstellung eines Auszugs aus der generischen Datenbank mittels HDFView.

Eine Anzeige der in der HDF5-Datei gespeicherten Daten (von bis zu 3 Dimensionen) ist z. B. mit dem Programm HDFView möglich, siehe Abbildung 3-6. Die generische Datenbank ist wegen ihrer hierarchischen Struktur leicht erweiterbar und für die Ablage von Ausgabedaten des Flusslösers in einem weiteren Ordner sowie die Anbindung von weiteren Spektralcodes bzw. Flusslösern geeignet.

Im hierarchischen Datenformat sind die Daten gruppiert in Ordnern mit optionalen Unterordnern ähnlich der Baumstruktur eines Computer-Dateisystems. Dies ermöglicht die übersichtliche Ablage der Daten verschiedener Szenarien in einer einzigen Datei. Beispielsweise enthält in der genannten generischen Datenbank der oberste Ordner *materials* die Unterordner verschiedener benannter Brennelemente, die jeweils Unterordner für die verschiedenen erforderlichen Daten wie die makroskopischen Wirkungsquerschnitte umfassen. Die einzelnen Wirkungsquerschnitte sind dann als Vektoren bzw. Matrizen oder höherdimensionale Matrizen von Fließkommazahlen mit wählbarer Stellenzahl abgelegt. Vektoren können beispielsweise die Abhängigkeit eines Wir-

kungsquerschnitts von der Neutronenenergiegruppe widerspiegeln, in Matrixform wären dann Streuwirkungsquerschnitte dargestellt, während höherdimensionale Matrizen weitere Abhängigkeiten der Wirkungsquerschnitte etwa vom Abbrand oder thermohydraulischen Rückwirkungsparametern enthalten. Als eine weitere Dimension der Datensätze kann man sich zukünftig auch die Samples von XSUSA-Aufrufen vorstellen.

3.3 Optimierung des Neutronendiffusionsprogramms QUABOX/CUBBOX

Der Einsatz des 3D-Kernmodells für Simulationen mit QUABOX/CUBBOX (Q/C) erfordert in jedem Fall die Bereitstellung von nuklearen Daten. Die nuklearen Daten umfassen die Diffusionskonstanten und Wirkungsquerschnitte aus den Neutronendiffusionsgleichungen für zwei Energiegruppen oder zusätzliche Parameter wie mikroskopische Absorptionsquerschnitte des Xenons und Absorptionsquerschnitte des Bors. Für realistische Anwendungsprobleme werden diese Daten für die einzelnen Brennelementtypen in Abbrandrechnungen mit Brennelementauslegungsprogrammen bestimmt. Hierbei werden für jeden Brennelementtyp umfangreiche Wertetabellen berechnet, welche die Abhängigkeit der nuklearen Daten von den Zustandsgrößen enthalten. Die Zustandsgrößen und ihr Wertebereich werden zum Teil abhängig von der Problemstellung gewählt. Im Allgemeinen sind es für DWR-Bedingungen der Abbrand, die Brennstofftemperatur, die Kühlmitteltemperatur oder -dichte sowie Borkonzentration und Xenonkonzentration. Für SWR-Bedingungen sind es der Abbrand, die Brennstofftemperatur, die momentane Kühlmitteldichte und die historische Kühlmitteldichte sowie die Xenon-Konzentration. Diese nuklearen Daten werden für das steuerstabfreie Brennelement und das durch einen eingefahrenen Steuerstab kontrollierte Brennelement berechnet. Zur weiteren Nutzung dieser Daten in der Kernberechnung können diese Funktionswerte durch Näherungsfunktionen und die Bestimmung geeigneter Approximationskoeffizienten approximiert werden oder direkt durch Interpolation der Funktionstabellen ausgewertet werden. Beide Darstellungsformen und Verarbeitungsweisen können im Rahmen der Wirkungsquerschnittsbibliotheken, wie sie in Q/C implementiert sind, genutzt werden.

Aus Sicht des Lösungsverfahrens im 3D-Kernmodell Q/C müssen vor Beginn der Lösung der Neutronendiffusionsgleichungen alle notwendigen nuklearen Daten berechnet werden. Dies erfolgt durch den Aufruf des Unterprogramms CROGEN, das zur allgemeinen Bereitstellung der nuklearen Daten dient. Einfache Abhängigkeiten der nuklearen Daten können direkt in der Eingabe angegeben werden, üblicherweise erfolgt je-

doch die Bereitstellung in Form der Wirkungsquerschnittsbibliothek (WQ-Bibliothek), dann erfolgt die weitere Verarbeitung im Unterprogramm CROLRA. In diesem Modul werden alle Zustandsgrößen zur Verfügung gestellt, so dass für jedes Volumenelement des Rechengitters die aktuellen Werte der nuklearen Daten berechnet werden können. Abhängig von der Anzahl der Zustandsgrößen erfolgt die Berechnung selbst durch Aufruf des Unterprogramms LINT3D oder LINT4D, in dem alle Funktionen zur Interpolation in Tabellen zusammengefasst sind.

Function - Caller Function Tree	CPU Time:Self
⊞CROLRA	98.8%
⊞LINT4D	0.6%
⊞CUKOMR	0.2%
⊞for__acquire_lun	0.1%
⊞for__release_lun	0.0%
⊞ZSTEP	0.0%
⊞YSTEP	0.0%
⊞HLFXMR	0.0%
⊞HLFYMR	0.0%
⊞XSTEP	0.0%
⊞LDAFMR	0.0%
⊞HLFZMR	0.0%
⊞QMP4MR	0.0%

Abbildung 3-7 Hotspotanalyse des nichtoptimierten Q/C-Codes

Bei der Anwendung der sehr detaillierten WQ-Bibliothek verlangsamt sich die Q/C Simulation drastisch. Um das Laufzeitverhalten von Software zu analysieren, verwendet man sogenannte Profiler. Intel® VTune™ Amplifier XE ist ein leistungsstarkes Tool zur Performance-Analyse, das man auch zur Hotspotanalyse benutzen kann. Die WQ-Bibliothek mit 13 Brennelementtypen und vier Zustandsgrößen (Abbrand, Brennstofftemperatur, Borkonzentration und Kühlmitteldichte) hat insgesamt 127050 Zeilen. Abbildung 3-7 zeigt das Ergebnis der Hotspotanalyse, wo man eindeutig sehen kann, dass die meiste CPU-Zeit in der Routine CROLRA verbraucht wird. Intel VTune Amplifier XE ist auch in der Lage die individuellen Statement-Zeilen zu analysieren. Abbildung 3-8 zeigt die aufwendigste Schleife in der CROLRA-Routine. Die Zeile 290 verbraucht 74 % der CPU-Zeit und die Schleife selbst verursacht einen zusätzlichen CPU-Aufwand in Höhe von 24.2 % der gesamten CPU-Zeit. In den Arrays IIXS und RRXS sind die Indizes und alle Werte aus der WQ-Bibliothek dynamisch gespeichert. Beide Arrays haben 2 Dimensionen: Der erste Index bezeichnet den BE-Typ und der zweite Index nummeriert alle WQ-Werte für einen bestimmten BE-Typ. Für den betrachteten Fall sind die Dimensionen der Arrays IIXS und RRXS stark verschieden. Die erste Di-

mension hat nur 13 Elemente, während die zweite Dimension ca. 10^5 Elemente besitzt. In FORTRAN sind alle Arrays spaltenweise abgelegt, d. h. die Komponenten des FORTRAN-Arrays in Abbildung 3-9 stehen somit aufeinanderfolgend im Hauptspeicher des Rechners.

```
288              DO I50 = IEND+1,IEND + IIXS(KKEY,J+6)      0.0%
289                MM= MM+1                                 0.0%
290                TB(ISUM+MM) = RRXS(KKEY, I50)            74.0%
291              ENDDO                                      24.2%
```

Abbildung 3-8 CROLRA-Codeabschnitt mit dem gefundenen Hotspot

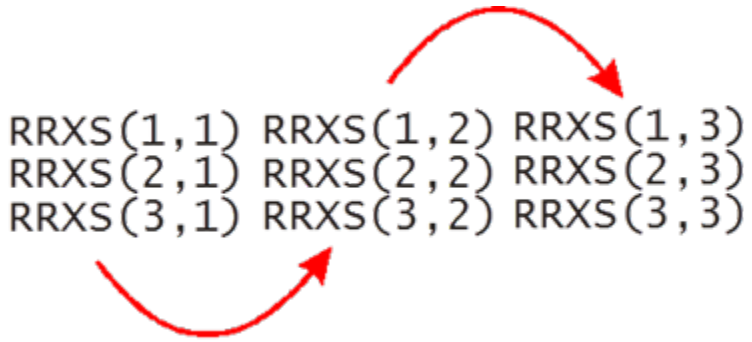

Abbildung 3-9 Belegung der Speicherplätze bei den Komponenten des Fortran-Arrays

Bei einem Speicherzugriff auf die RRXS(KKEY, I50+1) muss für den Zeiger, der auf den Inhalt des auszulesenden Datenfeldes zeigen soll, relativ zu dem Speicherplatzes des RRXS(KKEY, I50) gelten:

$$\text{Zeilendimension} * \text{Anzahl der Byte pro Datentyp} = 13 * 8\ \text{Byte} = 104\ \text{Byte}$$

Werden unmittelbar aufeinanderfolgende Speicherstellen eines Datenfeldes ausgelesen, so vermeidet man die Cache-Fehlzugriffe; dies erspart CPU-Zeit während der Pagezugriffe.

Demzufolge ist der erste Schritt zur Optimierung des Codes das Umtauschen der Dimensionen in den Arrays IIXS und RRXS, nämlich

$$IIXS(KKEY, I50) \rightarrow IIXS(I50, KKEY)$$
$$RRXS(KKEY, I50) \rightarrow RRXS(I50, KKEY)$$

Der optimierte CROLRA-Code benötigt jetzt 8 % weniger CPU-Zeit, wie in Abbildung 3-10 gezeigt. Zusätzlich verringert sich die gesamte CPU-Zeit um den Faktor 7, d. h. nach der ersten Optimierung beträgt die CPU-Zeit 204 Sekunden anstatt 1400 Sekunden mit der unveränderten CROLRA-Routine.

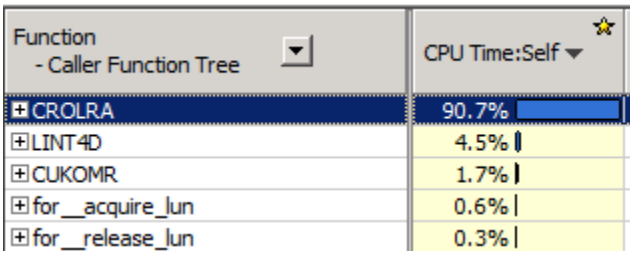

Abbildung 3-10 Hotspotanalyse nach der ersten Optimierung

Weiterhin führt die CROLRA-Routine in derselben Zeile 290 (Abbildung 3-8) eine Copy-Operation aus. Dabei muss das Runtime-System die einzelnen Datenelemente in den verwalteten Speicherraum kopieren. Diese zusätzlichen Datenverschiebungen wirken sich bei großen Arrays negativ auf die Leistung aus. Um sogenanntes „aliasing“ zu vermeiden, kann man in diesem Fall Zeiger (oder Referenzen) verwenden.

Das neue Modul QC_HEADER enthält eine Deklarierung des Arrays PRXS von Zeigern des Typs `ptr_to_arr`. Zusätzlich wird die Routine LINT4D modifiziert und nimmt als Input-Variablen die Zeiger `tp1` und `tp2` an:

```
  MODULE QC_HEADER
C     define pointers to each XS array of fuel elements
      TYPE ptr_to_arr
        REAL(8), DIMENSION(:), POINTER :: arr
      END TYPE

      TYPE(ptr_to_arr), DIMENSION(:), ALLOCATABLE :: PRXS

      INTEGER, DIMENSION(:,:), ALLOCATABLE :: IIXS

C      maximum number of records for particular xs table parameter
       INTEGER maxNRec

C      # number of table values for each fuel type
       INTEGER xs_table_val
       PARAMETER (xs_table_val = 13)

      interface lint4dmod
        subroutine lint4dmod(it, tp1, tp2, x, f)
            IMPLICIT REAL*8 (A-H,O-Z)
            dimension x(4),xt(4),it(4),nt(4),iopt(4),xt1(4)
            real(8), dimension(:), pointer :: tp1, tp2
            end subroutine
```

```
      end interface

   END MODULE
```

Das Array PRXS wird in der Routine COCTR1 dynamisch allokiert und mit den Werten aus der WQ-Bibliothek belegt:

```
   SUBROUTINE COCTR1

      USE QC_HEADER

C     temporary array for PRXS
      Real(8),Dimension(:),Allocatable :: TRXS
      <skip>

      if(allocated(PRXS)) then
        deallocate(PRXS)
      endif
      allocate(PRXS(NCOMPC))

CV      DO IJK = 1,11  or by full = 13
      DO IJK = 1, NCOMPC
        <skip>
C       read 13 XS table values  -full library
        DO J=1,xs_table_val
C         <skip>
C        allocate memory for PRXS
          If(J .EQ. 1) Then
                allocate(PRXS(IJK)%arr(IEND + nRec*xs_table_val))
             do ind = 1, size(TRXS)
                PRXS(IJK)%arr(ind) = TRXS(ind)
             enddo
             deallocate(TRXS)
          Endif

C         XS table values
          READ(303,'(5E13.6)')(PRXS(IJK)%arr(M),M=(IEND+1),
     &                          (IEND + nRec))
          IEND = IEND + IIXS(IJK,J+6)
        ENDDO
       <skip>
      ENDDO
End module
```

Schließlich verwendet die modifizierte CROLRA-Routine die Zeiger auf Abschnitte des Arrays PRXS:

```
C    pointer to the XS table of fuel type KKEY
     pa => PRXS(KKEY)%arr(:)
     <skip>
     tp1 => pa(1:ISUM)
     <skip>
     tp2 => pa(IEND+1:IEND+IIXS(KKEY,J+6))
                    <skip>
     CALL LINT4DMOD (IT, tp1, tp2, X,FF)
```

Die Einführung von intelligenten Zeiger-Objekten erlaubt eine weitere deutliche Beschleunigung der CPU-Rechenzeit um den zusätzlichen Faktor 20. Die Hotspotanalyse des optimierten QUABOX-CUBBOX Code zeigt, dass die CROLRA-Routine deutlich nach unten rutscht (Abbildung 3-11).

Function - Caller Function Tree	CPU Time:Self
LINT4DMOD	22.5%
CUKOMR	21.6%
for__release_lun	8.0%
for__acquire_lun	6.7%
HLFZMR	4.6%
YSTEP	4.1%
CROLRA	4.0%
XSTEP	3.8%
HLFYMR	3.8%
QMP4MR	2.9%
HLFXMR	2.5%
ZSTEP	2.4%
LDAFMR	2.0%
HALFMR	1.6%

Abbildung 3-11 Hotspotanalyse des optimierten Q/C-Codes

Als Ergebnis der Optimierungen ist die CPU-Gesamtzeit für die Ausführung von QUABOX/CUBBOX für den untersuchten Anwendungsfall um den Faktor 140 reduziert worden.

3.4 Weiterentwicklung und Anwendung der SPH-Methode mit QUABOX/CUBBOX

Um eine konsistente Homogenisierung von Wirkungsquerschnitten auf Stabzellbasis zu erreichen, wurde die Entwicklung und Anwendung der sog. „Superhomogenization“-Methode (SPH) im Zusammenspiel mit dem Diffusionscode QUABOX/CUBBOX und dem Transportcode NEWT weitergeführt. Nachdem die bisherigen Ergebnisse für die berechneten 2D-Anordnungen vielversprechend waren (siehe hierzu auch Anhang B8), wurde damit begonnen die Methodik für die dritte Dimension (z-Achse) zu erweitern.

Weiterhin wurden die berechneten 2D-Kerne noch detaillierter im QUABOX/CUBBOX-Modell abgebildet. Dazu wurde der ca. 1,5 mm breite Wasserspalt, welcher sich zwischen zwei Brennelementen befindet, modelliert. Hierzu wurden verschiedene Ansätze zur Nodalisierung in den NEWT- und QUABOX/CUBBOX-Modellen erprobt.

Die Anwendung der mittels der SPH-Methode erzeugten Wirkungsquerschnitte auf ein 3D-Modell wurde zuerst an der 3D-Version des C5G7-Benchmarks durchgeführt. Dazu wurde ein QUABOX/CUBBOX-Modell eines Viertelkerns (einschließlich Reflektor) detailliert mit über 50000 Rechenknoten erstellt. In Abb. 3-12 sind die unterschiedlichen Materialzonen dargestellt, links ein horizontaler, rechts ein vertikaler Schnitt durch die Anordnung. Reflektierende Randbedingungen sind als graue Balken angedeutet.

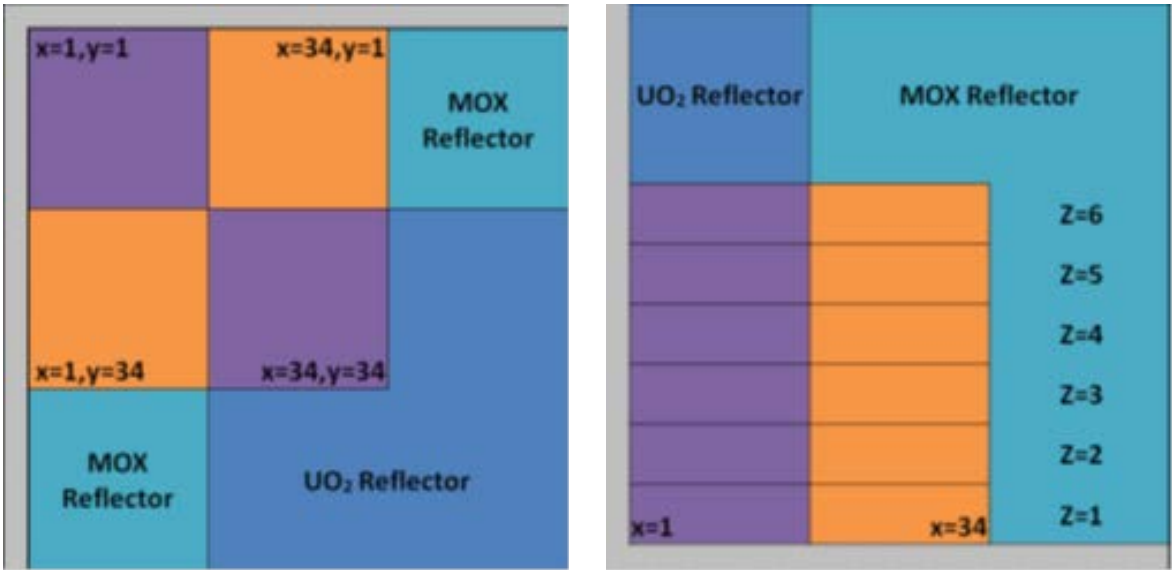

Abbildung 3-12 3D-Modell des C5G7-Benchmarks für QUABOX/CUBBOX.

Die Wirkungsquerschnitte für die einzelnen Brennelemente und den Reflektor wurden aus dem 2D-Modell übernommen. Die ersten Ergebnisse zeigen, dass QUABOX/CUBBOX in der Lage ist diese detaillierte Darstellung des Kerns zu berechnen. Die mittlere und maximale relative Stableistung Abweichungen zu der Monte-Carlo-Referenzrechnung sind in Tabelle 3-2 dargestellt.

Die Ergebnisse für die Leistungsverteilung in den Ebenen Z=1 bis Z=5 sind zwar deutlich, allerdings wird die maximale relative Abweichung immer dort beobachtet, wo die Leistung am geringsten ist. In der Ebene Z=6 ist die Leistungsverteilung noch nicht zufriedenstellend; hier sind die mittlere und maximale Abweichung deutlich größer als in den anderen Ebenen. Außerdem können große Abweichungen in Brennstäben mit hoher Leistung auftreten. Dieses Ergebnis ist insbesondere auf die einfache Modellierung des axialen Reflektors zurückzuführen.

Eine erste Verbesserung ist durch Erstellung unterschiedlicher Reflektormodelle für die axiale und die radiale Richtung zu erwarten. Eine weitere Verbesserungsmöglichkeit

besteht darin, den Reflektor in unterschiedliche Ebenen aufzuteilen und für jede Ebene eigene Wirkungsquerschnitte zu erzeugen.

Tabelle 3-2 Mittlere und maximale relative Stableistung Abweichungen zwischen QUABOX/CUBBOX und die Monte-Carlo-Referenzrechnung

Ebene	Mittlere Abweichung (%)	Maximale Abweichung (%)
Z=1	2.14	10.05
Z=2	2.15	10.17
Z=3	2.24	10.08
Z=4	2.47	11.03
Z=5	3.17	13.03
Z=6	11.96	23.29

Für das detaillierte 2D-Modell (inkl. Wasserspalt) gibt es zwei Modellierungsstrategien für NEWT und QUABOX/CUBBOX. Im ersten Modell sind die äußeren Brennstabzellen größer (1.335 cm breit statt 1.26 cm). Im zweiten Modell wird das Volumen des Wasserspalts auf alle Brennstabzellen gleichmäßig verteilt. In diesem Fall ist jeder Zellabstand 1.2688 cm.

Tabelle 3-3 Vergleich von mit KENO und QUABOX/CUBBOX mit SPH berechneten Leistungsverteilungen in zwei Brennelementtypen

KENO – Q/C	Relative Abweichung (%)	UO2 Brennelement	MOX Brennelement
Modell 1	Mittlere Abweichung	2.22	2.94
	Maximale Abweichung	10.26	12.16
Modell 2	Mittlere Abweichung	0.67	1.22
	Maximale Abweichung	1.96	3.43

Es stellt sich heraus (siehe Tabelle 3-3), dass das Modell mit Rechenknoten mit gleichen Abständen die besten Rechenergebnisse liefert. Dies ist auf den Lösungsalgorithmus von QUABOX/CUBBOX zurückzuführen.

Allerdings sind die Abweichungen zu den Monte-Carlo-Referenzergebnissen etwa doppelt so groß wie ohne die Modellierung des Wasserspalts, wenn der ganze zweidimensionale C5G7-Kern simuliert wird. Dies könnte zum einen an den zugrunde liegenden NEWT-Modellen liegen. Zum anderen muss überprüft werden, ob die im Programm implementierte verallgemeinerte Selengut-Normierung für die geänderte Geometrie richtig anwendbar ist.

3.5 Rechenbenchmark mit IRSN

Im Rahmen einer Zusammenarbeit mit dem IRSN (Institut de Radioprotection et de Sûreté Nucléaire), wird ein Benchmark durchgeführt. Ziel dieses Benchmarks ist ein Vergleich der Ergebnisse der gekoppelten „Multi-Scale/Multi-Physics“-Rechensysteme von GRS und IRSN.

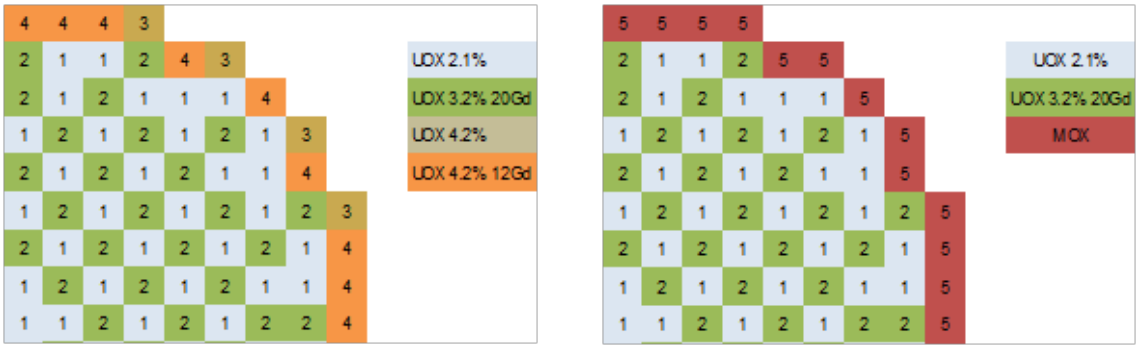

Abbildung 3-13 Generische EPR-basierte Kernbeladungen aus dem UAM-LWR-Benchmark mit UOX und UOX/MOX

Für die erste Phase des Benchmarks „Stand-Alone Neutronentransport“ liegen bereits Ergebnisse vor. Die Wirkungsquerschnitte für zwei generische EPR-basierte Kernbeladungen aus dem UAM-LWR-Benchmark wurden mit den jeweiligen Spektralcodes erzeugt. Die beiden Kernbeladungen mit UOX und UOX/MOX sind in Abbildung 3-13 dargestellt. Ein direkter Vergleich der Wirkungsquerschnitte wurde durchgeführt. Zunächst wurden die Wirkungsquerschnitte in einem Diffusionscode benutzt um die Kern-Leistungsverteilung zu berechnen. Schließlich wurden die berechneten Leistungsverteilungen verglichen.

Von der GRS wurde der Spektralcode TRITON verwendet. Auf der IRSN-Seite wurden die Codes APOLLO2 und DRAGON benutzt. Die verwendeten nuklearen Daten sind ENDF/B-VII mit TRITON und JEF-2.2 mit APOLLO2.

Die Kern-Leistungsverteilungen wurden von GRS und IRSN mit QUABOX/CUBBOX (Q/C) beziehungsweise CRONOS berechnet. Der Vergleich der Leistungsverteilungen für den UOX-Kern ist in Abbildung 3-14 dargestellt, für den UOX/MOX-Kern in Abbildung 3-15.

Der Vergleich der Leistungsverteilungen für die UOX-Kernbeladung zeigt eine gute Übereinstimmung; größere Abweichungen sind bei den Leistungsverteilungen der MOX/UOX-Kernbeladung zu beobachten.

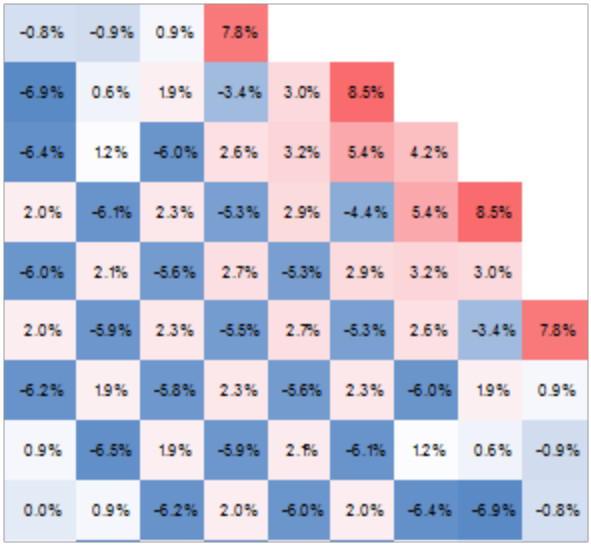

Abbildung 3-14 Vergleich der mit CRONOS und QUABOX/CUBBOX berechneten Leistungsverteilungen des EPR-UOX-Kerns

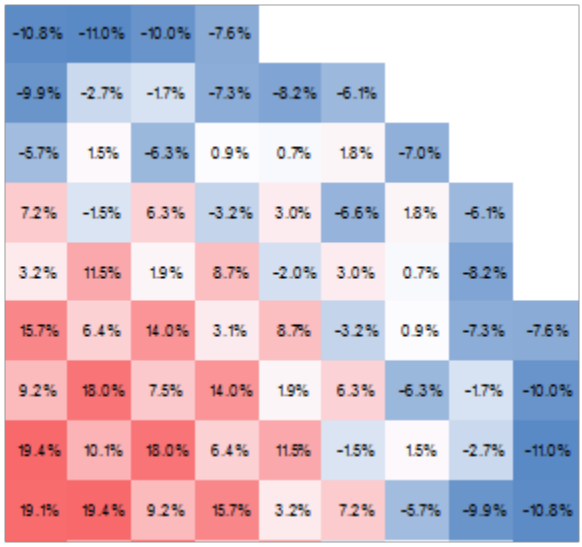

Abbildung 3-15 Vergleich der mit CRONOS und QUABOX/CUBBOX berechneten Leistungsverteilungen des EPR-UOX/MOX-Kerns

Der Vergleich der Wirkungsquerschnitte für jeden Brennelementtyp zeigt systematische Abweichungen. So sind etwa die Werte für $\kappa\Sigma_f$ (Energie x Spaltwirkungsquerschnitt) bei APOLLO2 immer größer als bei NEWT. Die Abweichung der thermischen $\kappa\Sigma_f$ ist ca. doppelt so groß in den UOX-Brennelementen mit Gadolinium (+4 %) und im MOX-Brennelement (>5 %) als in den UOX-Brennelementen ohne Gadolinium (+2 %). Generell sind die Abweichungen in den UOX-Brennelementen mit Gadolinium und im MOX-Brennelement größer als in den UOX-Brennelementen ohne Gadolinium.

Als mögliche Ursachen für die Abweichungen in den Leistungsverteilungen kommen auch die Reflektor-Wirkungsquerschnitte in Frage. Deshalb werden die von GRS und IRSN verwendeten Reflektormodelle gegenwärtig verglichen.

4 AP2: Weiterentwicklung, Validierung und Anwendung von Monte-Carlo-Berechnungsmethoden

Der folgende Abschnitt beschreibt die bislang durchgeführten Arbeiten am nuklearen Programmsystem der GRS bezüglich Monte-Carlo-Berechnungsmethoden. Dies sind Arbeiten am Monte-Carlo-Programms MCNP für hohe Ortsauflösung, insbesondere für die Durchführung von gekoppelten Berechnungen mit einem Thermohydraulik-Code, sowie die eigene Erstellung von nuklearen Datenbibliotheken mit dem Programmsystem NJOY.

4.1 Weiterentwicklung und Validierung des Monte-Carlo-Programms MCNP für hohe Ortsauflösung

Ein Verfahren, mit welchem reaktorphysikalische Aufgabenstellungen sehr genau berechnet werden können, ist das Monte-Carlo-Verfahren, das die Energieabhängigkeit der Wirkungsquerschnitte kontinuierlich repräsentiert und insbesondere die räumliche Verteilung der Reaktormaterialien sehr detailliert beschreiben kann. Die Leistungsfähigkeit der Methode wurde bereits vielfach demonstriert und stellt somit auch eine Referenzmethode zur Verifikation von Auslegungs-Programmen und zur Interpretation von Experimenten und Benchmarks mit frischem und abgebranntem Brennstoff und einen wichtigen Baustein der reaktorphysikalischen Rechenmethoden dar.

Das vom Los Alamos National Laboratory (USA) entwickelte Programm MCNP /X-5 03/ ist derzeit das flexibelste und meistangewandte Monte-Carlo-Programm für Teilchen- und Strahlentransport im Bereich der Reaktorphysik. Insbesondere können Brennstabgitter von Forschungs- und Leistungsreaktoren geometrisch mit Hilfe von sog. „Repeated Structures“ detailliert dargestellt werden. Für gleichartige Materialverteilung im Gitter lässt sich ein Reaktorkern mit relativ geringem Aufwand detailliert darstellen. Die Realität ist allerdings eine sehr heterogene Verteilung der Brennstoff- und Moderatormaterialien und deren Temperaturen. Die Darstellung einer heterogenen Materialverteilung für einen ganzen Reaktorkern (brennstabweise) ist mit MCNP trotz der „Repeated Structures“ sehr aufwendig und überschreitet u. U. interne feste Speichergrenzen wie z. B. die maximal zulässige Anzahl von geometrischen Zellen. Aus diesem Grund wurde das Programm MCNP dahingehend erweitert, dass detaillierte Teilchendichte- und Temperaturverteilungen auch für hohe Ortsauflösung effizient berücksichtigt werden können, siehe auch Anhang B2. Dadurch sollen insbesondere Anordnungen mit regu-

lären Gittern (rechteckig, hexagonal) mit Hilfe der in MCNP vorgesehenen „Repeated Structures“ geometrisch für homogene Materialverteilung beschrieben werden, die reale Material- und Temperaturspezifikation soll jedoch über interne Funktionen berücksichtigt werden. Damit kann z. B. die stabweise Beschreibung eines vollständigen Reaktorkernes mit detaillierter Materialspezifikation (durch Abbrand und Thermodynamik) realisiert werden. Dazu sind diverse Änderungen im Programmcode erforderlich, mit welchen die im MCNP-Input eingegebenen homogenen Material- und Temperaturverteilungen durch heterogene ersetzt werden. Ferner ist es erforderlich, zur effizienten Berechnung von stabweisen Reaktionsraten und Leistungsverteilungen eine generell anwendbare sogenannte „User Tally“ Routine zu realisieren.

Die bisher durchgeführten Erweiterungen wurden durch detaillierte Tests und Vergleiche mit dem Standardverfahren (mit vereinfachter Problemstellung) validiert. Insbesondere wurde die Berücksichtigung der Temperaturabhängigkeit der Doppler-Verbreiterung und der Streuung thermischer Neutronen mittels Interpolation getestet.

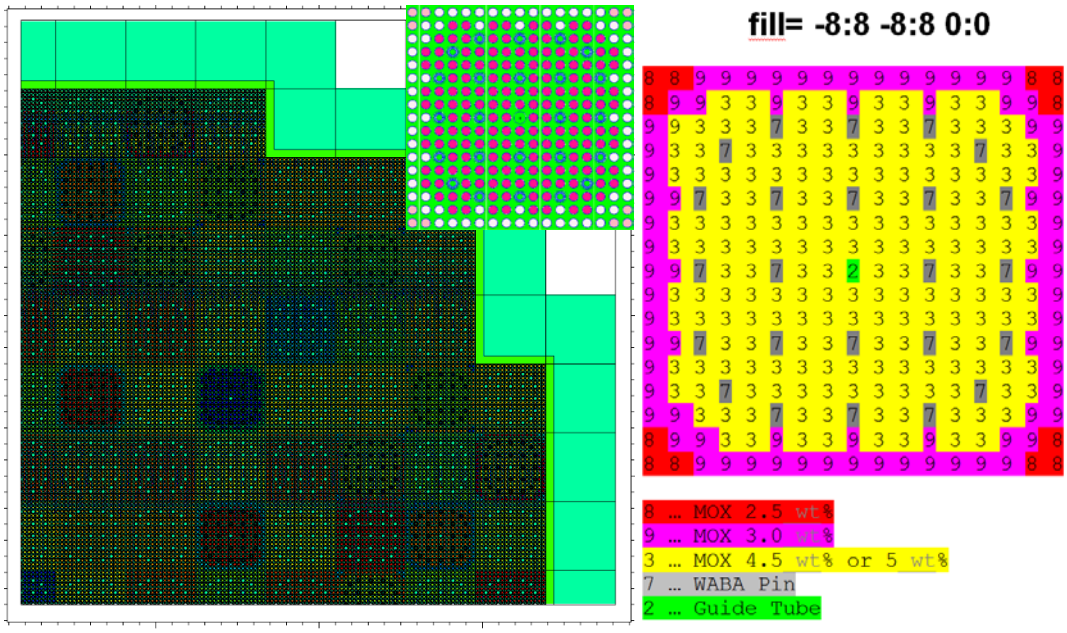

Abbildung 4-1 MCNP-Modell eines DWR-Viertel-Reaktorkern basierend auf “Repeated Structurs”. Eingabebeispiel für ein MOX-Brennelement mit unterschiedlichen Pu-fiss-Gehalten und WABA-Absorberstäben

Für die Erweiterungen wurde aktuellste Programmversion von MCNP aus dem Package: MCNP6_BETA-V / MCNP5 / MCNPX /X-5 12/ zugrunde gelegt, z. Zt. in der Version

V=2. MCNP6 ist eine Zusammenfassung der bisher getrennt entwickelten Versionen MCNP5 und MCNPX.

Eine hohe Ortsauflösung wird erreicht, wenn z. B. der Reaktorkern stabweise dargestellt wird. In Abbildung 4-1 wird dies illustriert. Der Reaktorkern ist ein DWR mit 17x17 Brennstäben je Brennelement, davon 24 Positionen für Absorberstäbe und einer zentral gelegenen Instrumentierungsposition. Das Beispiel zeigt zusätzlich ein Brennelement (BE) mit 5 verschiedenen Stabzelltypen. Obwohl das BE 264 Brennstäbe aufweist, müssen nur 5 verschiedene Zellen definiert werden, mit welchen über eine sog. „fill"-Anweisung ein BE komplett beschrieben werden kann. Das Beispiel zeigt eine 2D-Darstellung, bei realistischen 3D-Anordnungen muss jeder Brennstab ggf. noch in vertikaler Richtung aufgeteilt werden, um axiale Temperatur- und Materialverteilungen zu berücksichtigen.

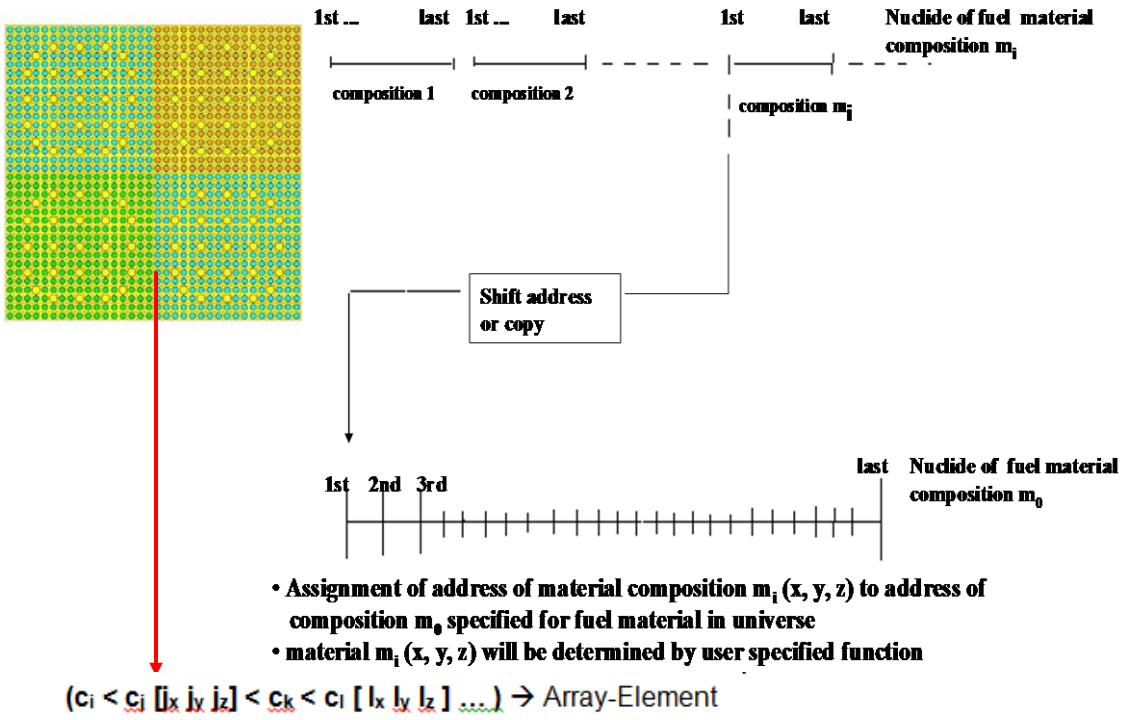

Abbildung 4-2 Interne Funktion zur Zuweisung der Materialspezifikation und Temperatur für ein Gitter-Element (Stabzelle)

Eine homogene Verteilung der Materialien und ggf. Brennstoff- und Moderatortemperaturen im Brennelement liegt nur bei frischem Brennstoff und Nulllast vor. Für alle anderen Zustände sind diese Verteilungen heterogen. Um dies über die MCNP-Standard-Input-Anweisungen zu realisieren, müssten für jeden Brennstab jedes Brennelements

für alle vertikalen Schichten Zellen mit dem entsprechenden Material und der entsprechenden Temperatur definiert werden. Für das obige Beispiel würde dies bedeuten, dass 191000 Zellen mit unterschiedlichem Material definiert werden müssten (bei 15 vertikalen Schichten). Als Alternative dazu werden mittels spezieller Programm-Modifikationen bei MCNP6 die Materialzusammensetzung und die Temperatur intern während der Simulation des Partikelwegs durch die heterogenen Geometriezonen für die Berechnung der makroskopischen Wirkungsquerschnitte und der Bestimmung der Kernreaktion am jeweiligen Ort der Kollision des Partikels mit einem Targetnuklid beschrieben, sozusagen „on the fly“. Die Identifikation des Gitterelements am Ort der Kollision liefert dabei MCNP. Bei mehrfach geschachtelten Gittern (Brennstabgitter, Brennelementgitter, …) kann die Adresse für den infrage kommenden Brennstabs aus den Level-Informationen, die MCNP in dem Datensatz pbl%i bzw. pbl%r bereitstellt (ci < cj [jx jy jz] < ck < cl [lx ly lz] …), ermittelt werden. Dabei wird die Materialzusammensetzung des Inputs für die homogene Verteilung durch die aktuelle für den identifizierten Brennstab (allgemeiner für die identifizierte Zone) ersetzt (siehe Abbildung 4-2). Dasselbe wird ggf. für die Temperatur durchgeführt.

Die entscheidenden Variablen zur Beschreibung von Materialzusammensetzung und Temperatur sind mat(icl) (beschreibt relative Nuklid-Anteile), rho(icl) (beschreibt totale Anzahl von Nukliden (je barn-cm) im Material) und tmp(icl) (beschreibt Temperatur in MeV). Die Zell-Variable icl ist bei MCNP6 identisch mit pbl%i%icl. Die Zahl und die Reihenfolge der Nuklide für das ersetzte und das Ersatzmaterial müssen allerdings identisch sein. Die zu ersetzenden Daten (Materialzusammensetzung, Dichte, Temperatur) werden in geeigneter Reihenfolge auf einer anwenderspezifischen Datei bereitgestellt und entsprechend der bei der Kollision identifizierten Adresse übertragen.

Die Wirkungsquerschnitte zur Beschreibung der verschiedenen Kernreaktionen sind abhängig von der Relativgeschwindigkeit (Energie) zwischen Partikel (Neutron) und Target-Nuklid. Da bei Temperaturen > 0 K die Target-Nuklide bewegt sind, spielt die Temperatur für die Simulation von Kernreaktionen eine wichtige Rolle. Insbesondere sind Resonanzreaktionen davon betroffen sowie die Streuung thermischer Neutronen.

Die bisherige Vorgehensweise für die Berücksichtigung der Temperatur war die Voraberstellung von gemittelten Querschnittssätzen für bestimmte Target-Temperaturen. Da solche Querschnittssätze z. T. mehrere 10000 Daten enthalten, ist die Anzahl solcher Target-Temperaturen begrenzt. Um dennoch Querschnitte für die aktuellen Temperaturen am Kollisionsort einzusetzen, bietet sich eine Interpolation an. Hierbei wird

die Temperaturabhängigkeit der Resonanz- und Streuquerschnitte über eine $T^{1/2}$-Interpolation aus jeweils 2 Datensätzen für definierte Temperaturen entsprechend der vorgegebenen Temperatur berücksichtigt. Zur effektiven Berücksichtigung der Temperaturabhängigkeit der Resonanzquerschnitte (auch für den unaufgelösten Resonanzbereich) und der Streugesetze für thermische Neutronen wurden durch Vergleich von Parametern, die mit für die Temperatur direkt berechneten und durch Temperaturinterpolation berechneten Daten umfangreiche Untersuchungen durchgeführt, siehe Abbildung 4-3. Eine weitere Möglichkeit zur Berücksichtigung der Target-Bewegung ist die über eine Verteilungsfunktion (Maxwell-Verteilung) bestimmte zufällige Target-Geschwindigkeit relativ zum Teilchen („on the fly“) /BRO 12/.

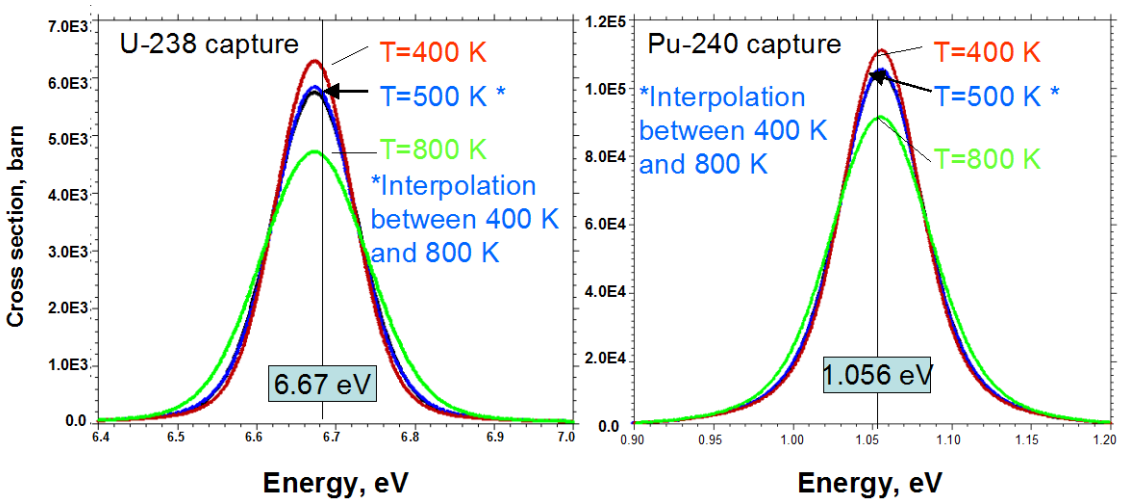

Abbildung 4-3 Vergleich von temperaturverbreiterten Resonanzquerschnitten für U-238 und Pu-240, berechnet direkt für 500K und interpoliert zwischen 400 und 800K

Umfangreiche Untersuchungen wurden durchgeführt, um die Funktionsfähigkeit der neu eingeführten internen Funktionen zu überprüfen. Als Beispiel ist in Abbildung 4-4 die Berechnung eines 2x2-BE-Clusters mit DWR-Brennelementen (die Spezifikation wurde dem Purdue-DWR-Benchmark /KOZ 06/ entnommen) ausgeführt mit MCNP5 und dem Standard-Input, sowie ausgeführt mittels der internen Funktionen. In Abbildung 4-4 ist der relative Unterschied bezüglich der axial gemittelten Leistungsverteilung dargestellt. Die stabweisen Leistungen unterscheiden sich lediglich im Rahmen des (hier sehr kleinen) statistischen Fehlers. Mittels der internen Funktionen wurde für quadratische und hexagonale Brennstab- und Brennelementgitter eine Reihe von Beispielen berechnet. Konkret wurden Beispiele für quadratische und hexagonale DWR-Gitter (Purdue- bzw. WWER-Benchmark), für ein hexagonales SFR (Natriumgekühlter

Schneller Reaktor)- Benchmark und für hexagonale Gitter experimenteller Anordnungen (TRX-1 bis TRX-4) mit z. T. unterschiedlichen Gitterweiten erstellt und berechnet.

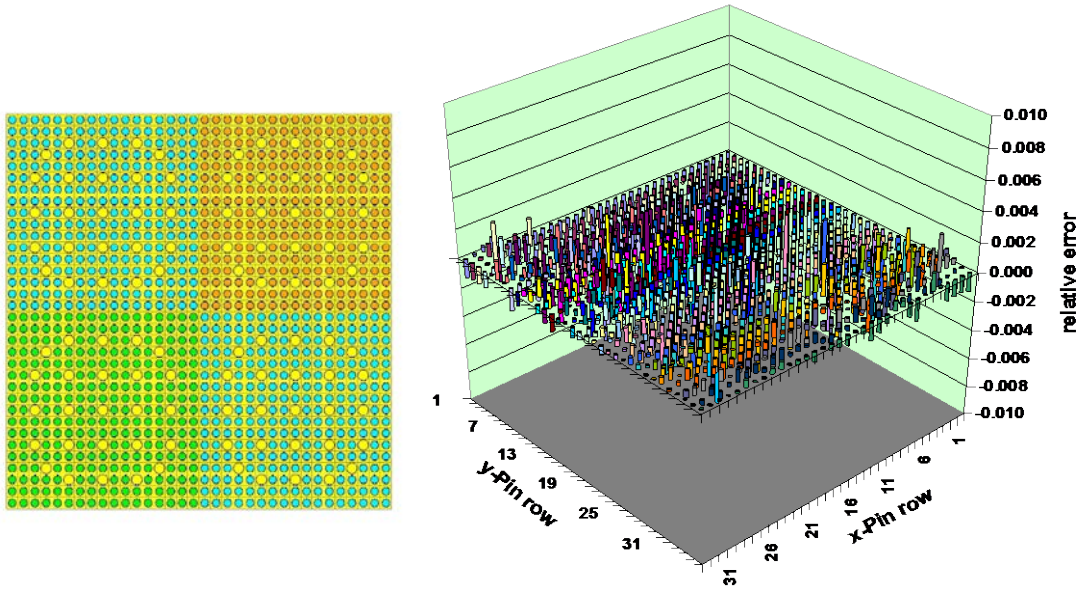

Abbildung 4-4 Relativer Unterschied bezüglich der Leistungsverteilung, berechnet mit Standard-Input und mittels interner Funktion für ein 2x2-BE-Cluster

Für quadratische und hexagonale Brennstabgitter konnte gezeigt werden, dass die Material-, Temperatur- und Zelldichtespezifikation über eine interne Funktion dargestellt werden kann. Vergleiche von Leistungsdichte-Ergebnissen für die angegebenen Anordnungen, berechnet mit dem Standard-Input und mit dem Input mittels interner Funktionen, zeigten Übereinstimmung im Rahmen des statistischen Fehlers (< 0.1 %). Für hexagonale Gitter wie z. B. bei schnellen Reaktoren oder bei den WWER-Reaktoren, ist die Zahl der Brennstäbe je Reihe unterschiedlich. D. h. nicht alle Positionen des hexagonalen Gitters sind mit Brennstäben besetzt. Dasselbe gilt, wenn Symmetrieeigenschaften berücksichtigt werden. Um eine große Zahl von nicht besetzten Positionen in der Ergebnis-Datei (und der Eingabe-Datei) zu vermeiden, kann eine Zuordnungsliste erstellt werden, welche nur die besetzen Positionen berücksichtigt. Damit kann der Speicherbedarf erheblich reduziert werden.

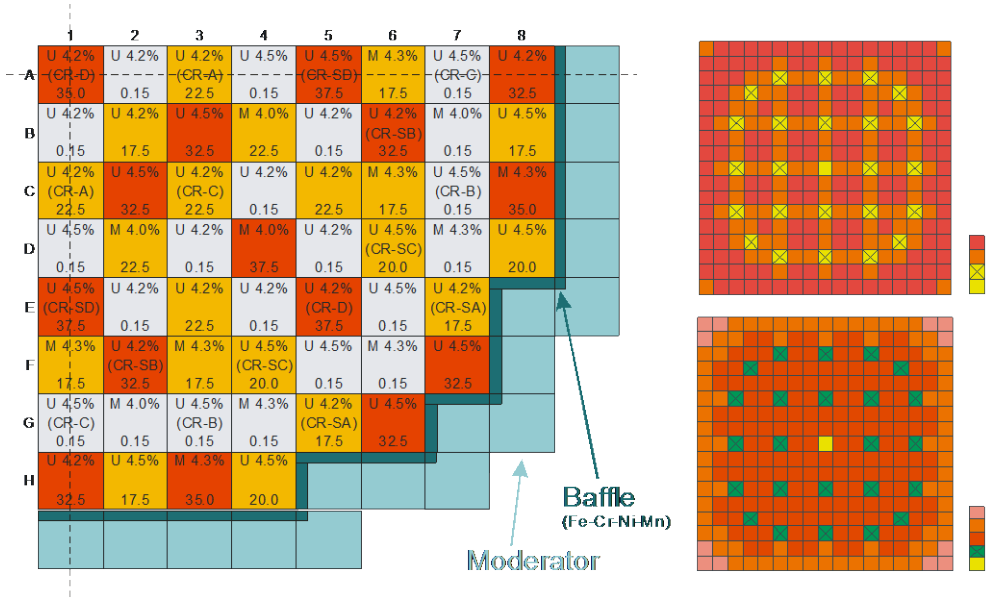

Abbildung 4-5 Kernkonfiguration und BE-Spezifikation des UOX/MOX DWR–(Purdue) Benchmarks

Eine weitere Anwendung besteht in der Kopplung von MCNP mit dem Thermohydraulik-Code ATHLET /LER 98/ am Beispiel des für den beim Purdue-Benchmark /KOZ 06/ spezifizierten DWR. Die berechnete Kernkonfiguration ist aus Abbildung 4-5 ersichtlich. In dieser Abbildung sind auch die Spezifikationen für UOX- und MOX-Brennelemente dargestellt.

Die Berechnung dieser Anordnung wurde aus Symmetriegründen für einen Viertelkern durchgeführt. Es wurde die stationäre Leistungs- und Temperaturverteilung bei Volllast berechnet. Bis zum Erreichen der Konvergenz wurden abwechselnd MCNP und ATHLET ausgeführt, wobei mit einer geschätzten Anfangstemperaturverteilung begonnen wurde. Die Leistungsverteilung wurde von MCNP mittels eines speziellen „Tallies“ berechnet und über ein Interface an ATHLET übergeben. Die von ATHLET berechneten Brennstoff- und Moderatortemperaturverteilungen sowie die Moderatordichteverteilung wurden über ein zweites Interface an MCNP übergeben. Diese Daten wurden nicht über den Standard-MCNP-Input, sondern an die für MCNP entwickelten internen Funktionen übergeben.

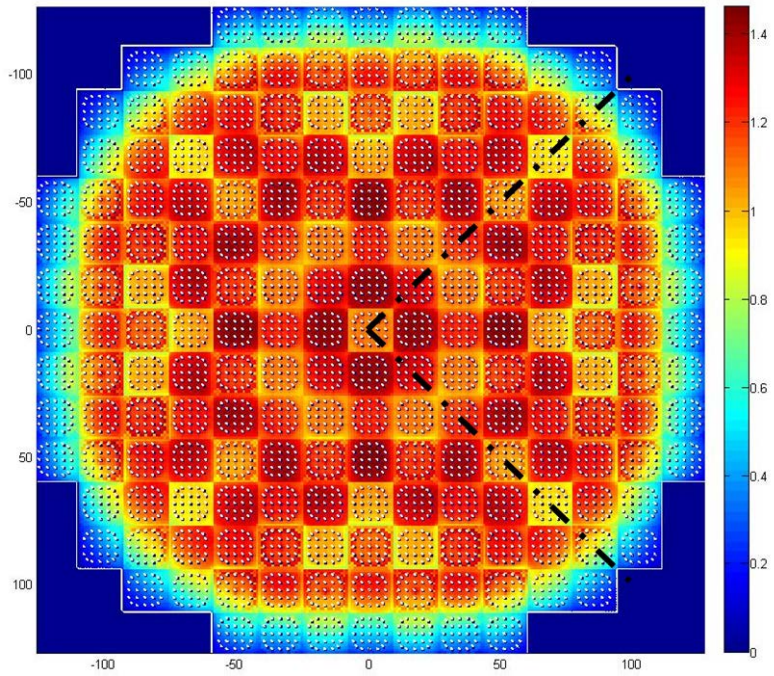

Abbildung 4-6 Axial gemittelte Brennelementleistungen für das UOX/MOX DWR–(Purdue) Benchmark, berechnet mit MCNP

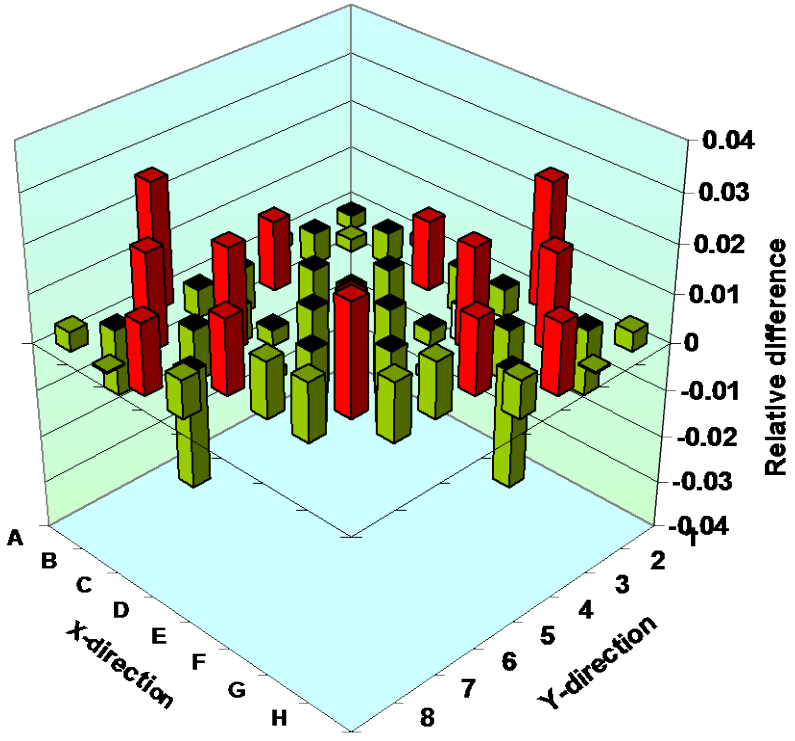

Abbildung 4-7 Relative Unterschiede der Brennelementleistungen für das UOX/MOX DWR–(Purdue) Benchmark: QUABOX/CUBBOX/ATHLET und MCNP/ATHLET

Ausgewählte Ergebnisse aus diesen Berechnungen sind in Abbildung 4-6 und Abbildung 4-7 dargestellt. Abbildung 4-6 zeigt die axial gemittelte relative Leistungsverteilung (stabweise). Abbildung 4-7 zeigt einen Vergleich der mit MCNP/ATHLET berechneten Brennelementleistungen mit entsprechenden Leistungen, die mit QUABOX/ CUBBOX/ATHLET /LAN 04/ berechnet wurden. Obwohl die beiden Methoden und die dabei eingesetzten Wirkungsquerschnitte unterschiedlich waren, sind die Unterschiede in den BE-Leistungen relativ gering. Dasselbe gilt auch für die stabweisen Leistungsverteilungen für ausgewählte Brennelemente im Vergleich der Ergebnisse aus gekoppelten Neutronentransport-/Thermohydraulik-Berechnungen mit MCNP/ ATHLET und PARCS/TRACE /DOW 02/, siehe Abbildung 4-8.

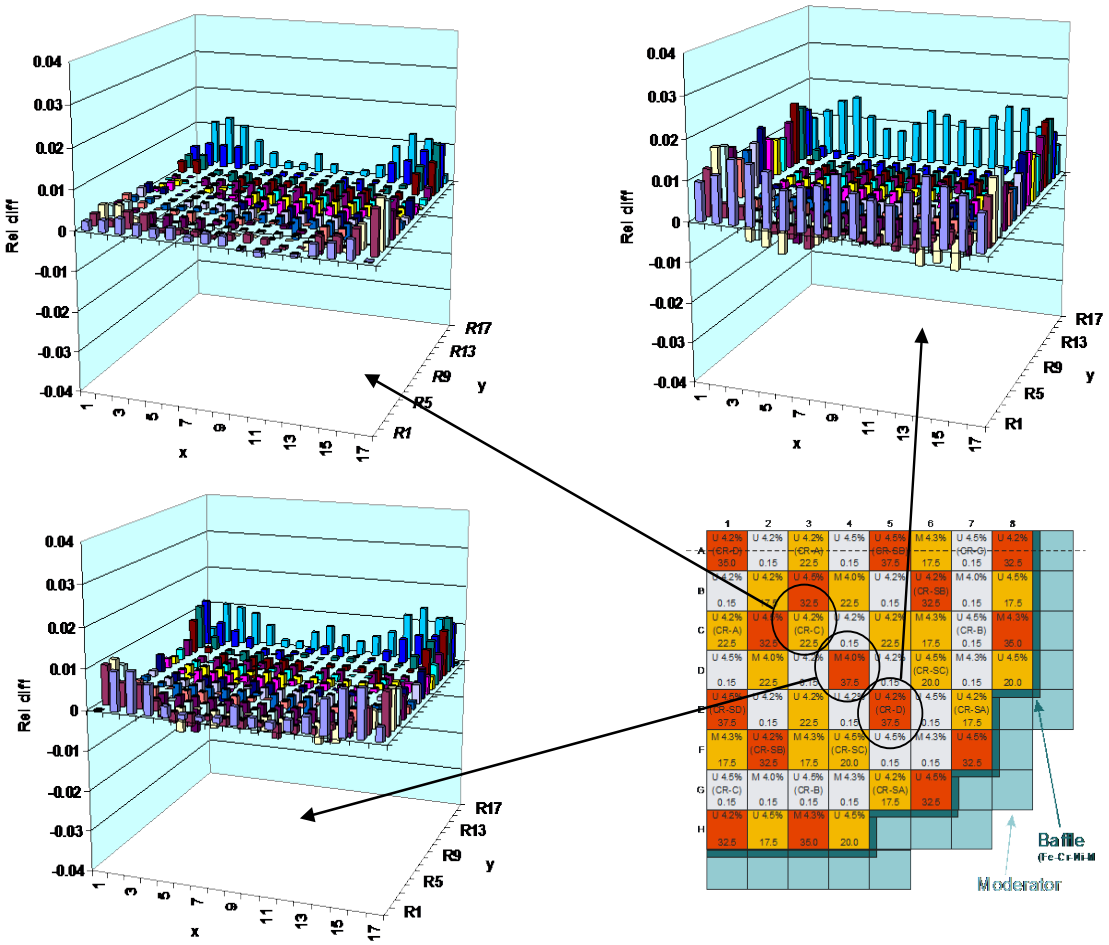

Abbildung 4-8 Vergleich der axial gemittelten Brennstableistungen für das UOX/MOX DWR–(Purdue) Benchmark, berechnet mit MCNP/ ATHLET und PARCS/TRACE für ausgewählte Brennelemente

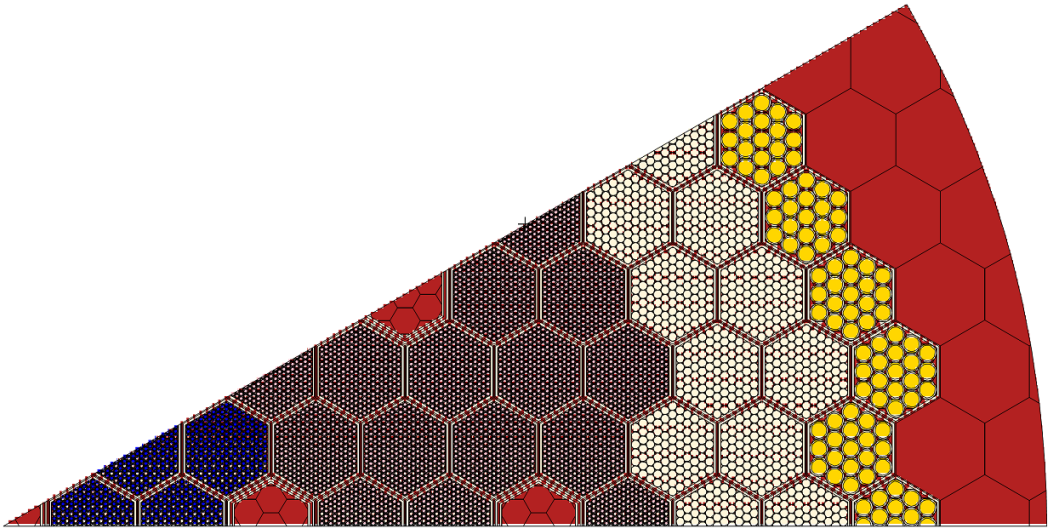

Abbildung 4-9 MCNP-Modell des SFR-Benchmark-Kerns (radiales 30°-Segment)

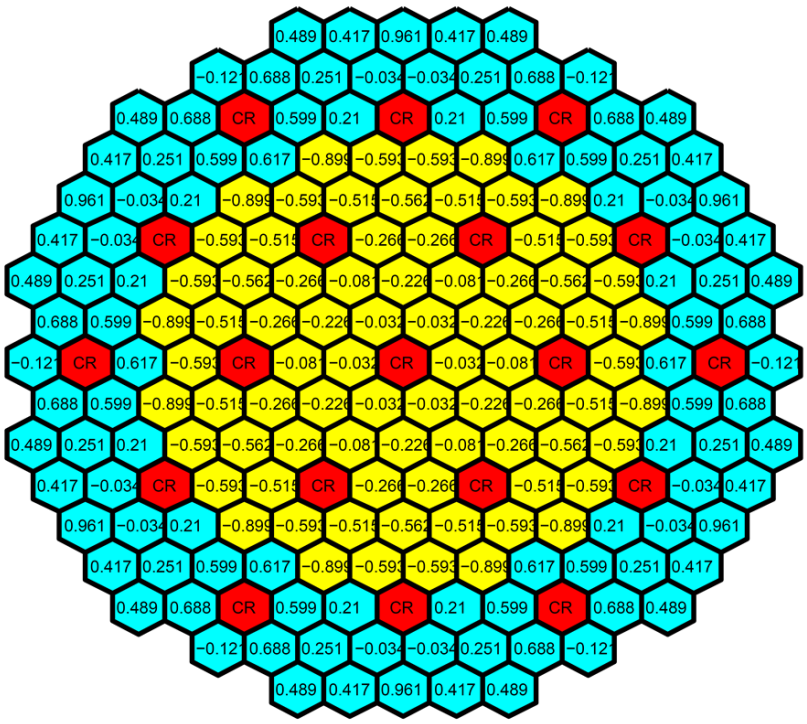

Abbildung 4-10 Vergleich der axial gemittelten Brennelementleistungen (relativer Unterschied in %) zwischen MCNP und deterministischer Methode bei dem SFR-Benchmark

Als Beispiel für hexagonale Gitter wurde ein Benchmark für natriumgekühlte schnelle Reaktoren berechnet /BLA 12/. Ausgewählt wurde ein „Medium Size“ Kern mit 1000 MW thermischer Leistung. Einen 30°-Ausschnitt des Kernmodells zeigt Abbildung 4-9.

Für das Benchmark-Modell wurden mit der Standard-Eingabe und mittels der internen Funktionen die Nuklidzusammensetzungen der Brennstäbe an MCNP übergeben. Die Ergebnisse (k-eff, Fluss- und Leistungsverteilungen) aus diesen Vergleichen unterschieden sich ebenfalls nur im Rahmen des sehr kleinen statistischen Fehlers. Ein Vergleich der Leistungsverteilungen, berechnet mit MCNP (mit internen Funktionen und speziellem Tally) und einer deterministischen Methode /KIM 12/ zeigt Abbildung 4-10. Die maximalen relativen Abweichungen liegen dabei bei ca. 1 %.

4.2 Erstellung von nuklearen Daten

Mit dem nuklearen Datenverarbeitungssystem NJOY wurden Wirkungsquerschnitte kontinuierlicher Energie bei unterschiedlichen Temperaturen erzeugt; die Temperaturgitterweite beträgt ein Grad Kelvin. Zur Automatisierung der Wirkungsquerschnittserzeugung wurde ein Skript erstellt, das die NJOY-Eingabedaten erzeugt, die NJOY-Rechenläufe ausführt und die entsprechenden Ausgabedaten, die für die MCNP5-Berechnungen benötigt werden, extrahiert. Zusätzlich wurde eine entsprechende Reihe von Wirkungsquerschnittsbibliotheken bei gleichen Temperaturen erzeugt, jedoch wurde dazu eine Interpolationsmethode verwendet. Die Interpolation wurde mit der Quadratwurzel der Temperatur durchgeführt. Schließlich wurden mehrere MCNP5-Berechnungen bei verschiedenen Temperaturen mit den unterschiedlich erzeugten Wirkungsquerschnittsbibliotheken (direkt mit NJOY erzeugt bzw. interpoliert) durchgeführt. Dazu wurde ein Brennstab-Zell-Modell des SWR Peach Bottom 2 (PB-2) verwendet.

Tabelle 4-1 MCNP-Ergebnisse für eine Stabzelle des SWR Peach Bottom 2, mit direkt erzeugten und temperaturinterpolierten Daten

Temperatur (°C)	k-inf (direkt)	k-inf (interpoliert)	Differenz
301	1.36974+/-0.00033	1.37019+/-0.00033	0.00045
302	1.36939+/-0.00032	1.37001+/-0.00033	0.00062
303	1.36940+/-0.00033	1.36975+/-0.00033	0.00035

In Tabelle 4-1 werden die Ergebnisse für die PB-2-Stabzelle bei unterschiedlichen Temperaturen verglichen. Die Wirkungsquerschnittsvariation mit der Temperatur wurde dabei für U-238 durchgeführt. Dabei ergeben sich Unterschiede zwischen den Ergebnissen mit den beiden Berechnungsmethoden (Wirkungsquerschnitte direkt bei der je-

weiligen Temperatur mit NJOY erzeugt bzw. interpoliert), die kleiner sind als zwei Standardabweichungen aus der statistischen Unsicherheit der Monte-Carlo-Rechnungen. Es gibt also keine Hinweise, dass die Temperaturinterpolation nicht ausreichend genaue Ergebnisse liefern würde, siehe auch Abbildung 4-3.

Tabelle 4-2 MCNP-Ergebnisse für die VENUS-7-Anordnungen mit ENDF/B-VII- und JEFF-3.1.1-Daten: Multiplikationsfaktoren und effektiver Anteil verzögerter Neutronen

Configuration Nr.	MCNP5 ENDF/B-VII		MCNP5 JEFF-3.1.1	
	k-eff	β-eff (pcm)	k-eff	β-eff (pcm)
7a	0.99469	658	0.99449	676
7b	0.99623		0.99595	
7b subst. 3/1	0.99535		0.99514	
7b subst. 4/0	0.99743		0.99727	
7c	0.99578		0.99557	
7d	0.99593		0.99577	
7d subst. 2/2.7	0.99527		0.99515	
7/1a	0.99576	671	0.99558	684
7/1b	0.99699		0.99694	
7/1c	0.99637		0.99630	
7/3	0.99630	701	0.99621	721

Zur Validierung der erstellten JEFF-3.1.1-Bibliothek /SAN 09a/ im ACE-Format für MCNP wurden alle Anordnungen aus der Serie von VENUS7-Experimenten /ZWE 08/ nochmals mit erhöhter statistischer Genauigkeit sowohl auf herkömmliche Art wie auch im prompten Modus (d. h. ohne Berücksichtigung der verzögerten Neutronen) nachgerechnet und die Ergebnisse mit denen aus ENDF/B-VII-Daten /HER 11/ verglichen. Die Ergebnisse sind in Tabelle 4-2 zusammengestellt.

Zur Ermittlung des effektiven verzögerten Neutronenanteils wurde die „prompt k ratio“-Methode /BRE 97/ verwendet, die in Abschnitt 5 näher beschrieben wird. Die Berechnungen wurden alle mit 10^9 Neutronenschicksalen durchgeführt; die resultierende statistische Unsicherheit ist 0.00002 im Multiplikationsfaktor und 3 pcm im effektiven verzögerten Neutronenanteil. Für alle Anordnungen aus der Serie von VENUS7-Experimenten ergibt sich ausgezeichnete Übereinstimmung im Multiplikationsfaktor zwischen den Ergebnissen mit JEFF-3.1.1- und ENDF/B-VII-Daten. Etwas größere Abweichungen zeigen sich bei der Ermittlung des Anteils von verzögerten Neutronen, der zwar auf die Kritikalität keinen Einfluss hat, aber für das dynamische Verhalten eines Systems mit Spaltmaterial eine wesentliche Rolle spielt. Dies legt die Durchführung von systematischen Unsicherheitsanalysen für β-eff bezüglich der nuklearen Daten nahe. Derartige Unsicherheits- und Sensitivitätsanalysen werden in Abschnitt 5 beschrieben.

5 AP3: Weiterentwicklung, Validierung und Anwendung von Methoden zur Unsicherheits- und Sensitivitätsanalyse

Der folgende Abschnitt beschreibt die bislang durchgeführten Arbeiten am nuklearen Programmsystem der GRS bezüglich Methoden zur Unsicherheits- und Sensitivitätsanalyse. Dies sind Arbeiten zum UAM-LWR-Benchmark Phase 1, die Durchführung von Unsicherheitsanalysen für eine gekoppelte Kerntransientenberechnung, die Erstellung von Kovarianzdaten für die Multiplizität verzögerter Neutronen und deren Anwendung für Unsicherheits- und Sensitivitätsanalysen in Bezug auf den effektiven verzögerten Neutronenanteil in kritischen Anordnungen, sowie die Entwicklung einer Methode zur höchsteffizienten Durchführung von Unsicherheits- und Sensitivitätsanalyse bei der Verwendung von Monte Carlo-Codes zur Simulation des Neutronentransports („schnelle GRS-Methode“).

5.1 Ergebnisse zum UAM-LWR-Benchmark Phase 1

Die GRS beteiligt sich mit dem Programmsystem XSUSA zur Sensitivitäts- und Unsicherheitsanalyse bezüglich nuklearer Daten am „BENCHMARK FOR UNCERTAINTY ANALYSIS IN MODELING (UAM) FOR DESIGN, OPERATION AND SAFETY ANALYSIS OF LWRs“ /NEA 07/. Die jetzt nahezu abgeschlossene Phase 1 beschreibt die einzelnen Schritte der „Stand-Alone“-Neutronentransportberechnungen, von der Spektralberechnung für Stabzellen bis zur stationären Kernsimulation ohne thermohydraulische Rückwirkungen. Die GRS hat zu allen Teilen des Benchmarks Rechenergebnisse eingereicht.

Für das UAM-LWR-Benchmark Phase I liegt damit ein nahezu vollständiger Satz von Ergebnissen aus Unsicherheitsanalysen mit XSUSA und den entsprechenden Neutronentransportprogrammen für die einzelnen Teile (NEWT für Exercise 1 - Zellberechnungen und Exercise 2 - Gitterberechnungen, KENO und QUABOX/CUBBOX für Exercise 3 - Kernberechnungen) vor: Zell- und Gitterberechnungen für die Reaktoren Three Mile Island 1, Peach Bottom 2, Kozloduy 6, zwei EPR-Kerne mit Uran- und MOX-Beladung, sowie die kritische Anordnung KRITZ 2, Kernberechnungen für Three Mile Island 1 und die EPR-Kerne.

Die Ergebnisse werden vom Benchmark-Team ausgewertet und mit den Lösungen anderer Benchmark-Teilnehmer verglichen. Diese Auswertung ist noch nicht abgeschlos-

sen. Damit lassen sich auch noch keine endgültigen Schlüsse aus den Vergleichen der unterschiedlichen Ergebnisse ziehen. Jedoch lässt sich bereits feststellen, dass für die Unsicherheiten von Multiplikationsfaktoren, die auch mit Störungstheorie erster Ordnung, wie sie im Programm TSUNAMI aus dem SCALE-System /SCA 09/ implementiert ist, in allen Fällen sehr gute Übereinstimmung erzielt wird; dies wird auch immer wieder durch Vergleiche mit eigenen TSUNAMI-Berechnungen sichergestellt, siehe z. B. /ZWE 10a, ZWE 10b, ZWE 11/.

Die vollständigen Ergebnisse zum Benchmark liegen in einer Technischen Notiz vor, siehe Anhang A. Besonders interessant sind die Ergebnisse von Ganzkernberechnungen für zwei repräsentative Reaktorkerne der Generation III (ein Uran-Kern und ein Uran/MOX-Kern auf EPR-Basis), siehe auch Anhang B7. Zur Berechnung der Brennelement-Wirkungsquerschnitte wurde das SCALE-Programm NEWT verwendet, für die Ganzkern-Leistungsverteilungen QUABOX/CUBBOX. Die beiden Kernanordnungen sind in Abbildung 5-1 dargestellt, die Ergebnisse für die Multiplikationsfaktoren und deren Unsicherheiten in Tabelle 5-1, für die Leistungsverteilungen in Abbildung 5-2, und für die entsprechenden Unsicherheiten in den Brennelement-Leistungen in Abbildung 5-3.

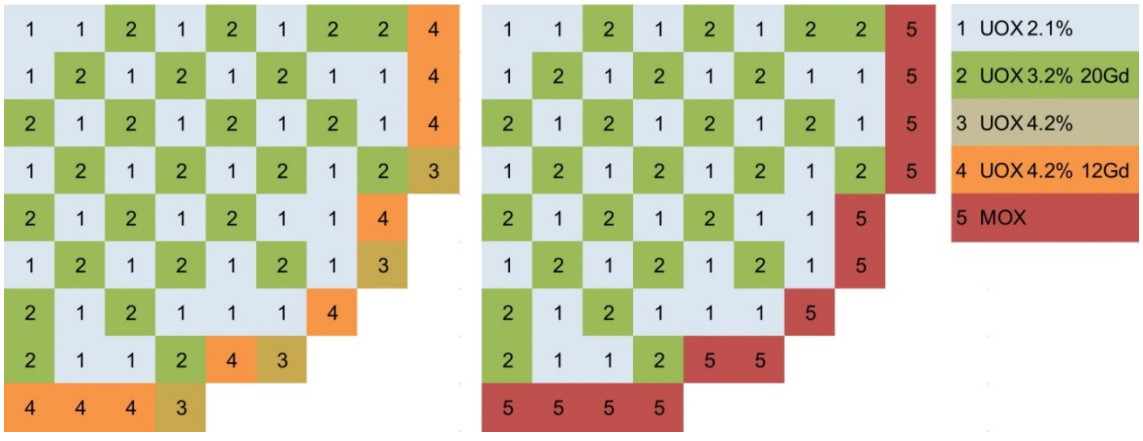

Abbildung 5-1 Kernbeladungen der UO_2- und UO_2/MOX-Kerne der Generation III auf EPR-Basis

Tabelle 5-1 Mittelwerte und Unsicherheiten (1 σ) der Leistungsverteilungen der UO_2- und UO_2/MOX-Kerne der Generation III, berechnet mit XSUSA-QUABOX/CUBBOX

k_{eff}	Mittelwert	Unsicherheit
UOX	1.00292	0.00513
MOX/UOX	1.00063	0.00488

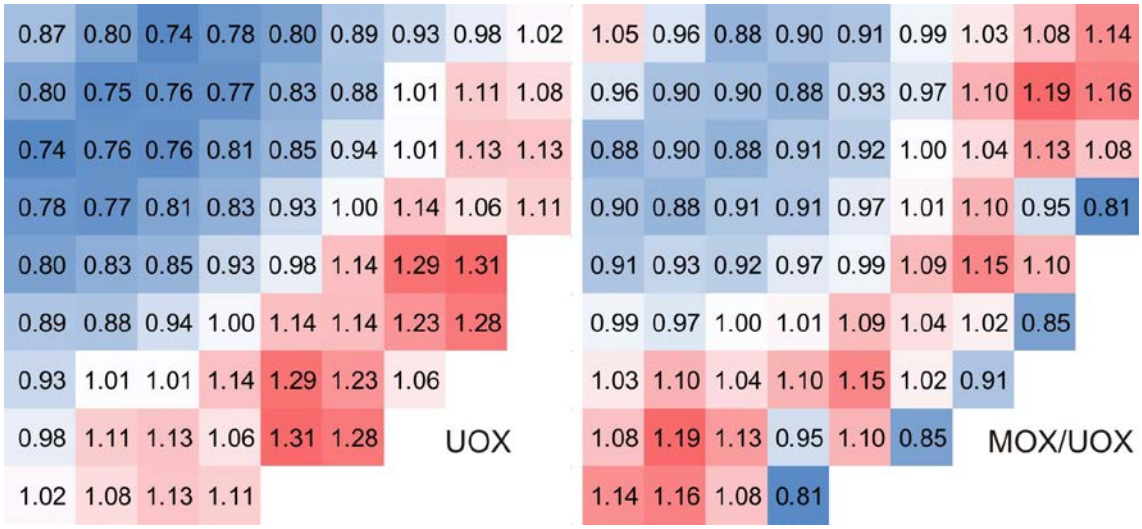

Abbildung 5-2 Mittelwerte der Leistungsverteilungen der UO_2- und UO_2/MOX-Kerne der Generation III, berechnet mit XSUSA-QUABOX/CUBBOX

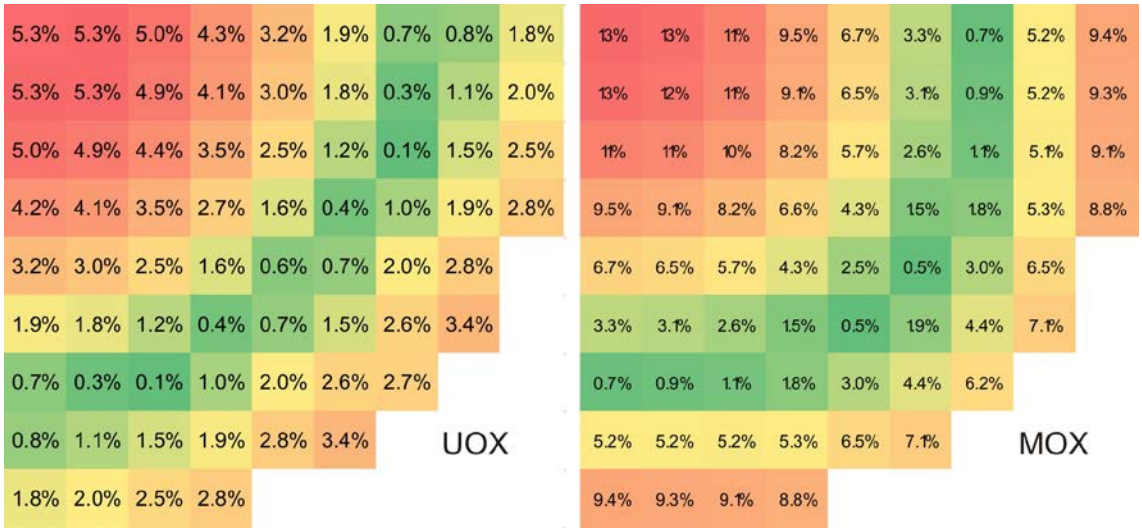

Abbildung 5-3 Unsicherheiten der Leistungsverteilungen der UO_2- und UO_2/MOX-Kerne der Generation III, berechnet mit XSUSA-QUABOX/CUBBOX

Während die Unsicherheiten der Multiplikationsfaktoren in der Größenordnung von 0.5 % liegen, wie es bei LWR-Stabgitter-Systemen mit vorwiegend Uran-Brennstoff bei Verwendung der SCALE-Kovarianzdaten zu erwarten ist, weisen die Leistungsverteilungen erheblich größere Unsicherheiten auf. Bei dem Uran/MOX-Kern erreicht die Unsicherheit der radialen Leistungsverteilung am Kernrand nahezu 10 %, im Kernzentrum noch deutlich höhere Werte. Dies ist mit noch nicht veröffentlichten CEA-Ergebnissen, die auf dem UAM-7-Workshop vorgestellt wurden, qualitativ konsistent. Ähnliche Beobachtungen für andere LWR-Kerne sind auch in Anhang B1 und B11 beschrieben.

5.2 Unsicherheitsanalysen für eine Kerntransientenberechnung

Nach der derzeitigen Praxis sind zur Auslegung und Sicherheitsanalyse von Kernkraftwerken konservativen Annahmen und Modelle erforderlich, um die Erfüllung der Akzeptanzkriterien zu bestätigen. In den letzten Jahren ist ein neuer Trend zu beobachten, nämlich der Übergang von konservativen Analysen zu Best-Estimate-Berechnungen in Kombination mit der Durchführung von Unsicherheits- und Sensitivitätsanalysen („Best Estimate Plus Uncertainty“ - BEPU). Best-Estimate-Analysen für eine große Klasse von Transienten und Sicherheitsanalysen erfordern die Anwendung von gekoppelten Neutronentransport-/Thermohydraulik-Codes. Ein Fernziel des OECD-Benchmarks „Uncertainty Analysis in Modeling“ (UAM) ist es, die Konfidenzin-

tervalle von Ergebnissen von Simulationen und Analysen des Reaktorverhaltens zu untersuchen. Eines der diskutierten Referenz-Szenarien für den UAM-Benchmark ist ein Reaktivitätsstörfall (RIA) in einem Druckwasserreaktor.

Für einen ersten Einsatz der XSUSA-Methode zur Abschätzung der Unsicherheiten in einer Kerntransientenberechnung (siehe auch Anhang B6) wurde das „Pressurized Water Reactor MOX/UO_2 Core Transient Benchmark“ /KOZ 06/ herangezogen, das in der GRS als eines der Standard-Benchmarks zum Neutronentransport verwendet wird. Das Benchmark besteht aus mehreren Teilen stationärer und transienter Kernberechnungen; für die Ergebnisse stationärer Berechnungen wurden bereits Unsicherheitsanalysen mit XSUSA durchgeführt /ZWE 10a/.

Ein Überblick über die gesamte Berechnungskette ist in Abbildung 5-4 gegeben. Wie üblich werden dazu in Spektralberechnungen für die einzelnen Stabzellen eines Brennelements und anschließenden Brennelementberechnungen mit einem zweidimensionalen Transportcode (hier NEWT) Wirkungsquerschnitte in zwei Energiegruppen sowie kinetische Parameter aller Brennelemente der Kernanordnung erzeugt. Dies geschieht auf einem grobmaschigen Gitter für die relevanten Parameter (Brennstofftemperatur, Kühlmitteldichte, Borkonzentration). Die Wirkungsquerschnitte und kinetischen Parameter bei den während der Kernsimulation benötigten Parameterwerten werden dann durch Interpolation zwischen den Stützstellen ermittelt. Die Transientenberechnungen werden mit den Wirkungsquerschnitten, die sich durch Variation der nuklearen Daten ergeben, immer wieder ausgeführt.

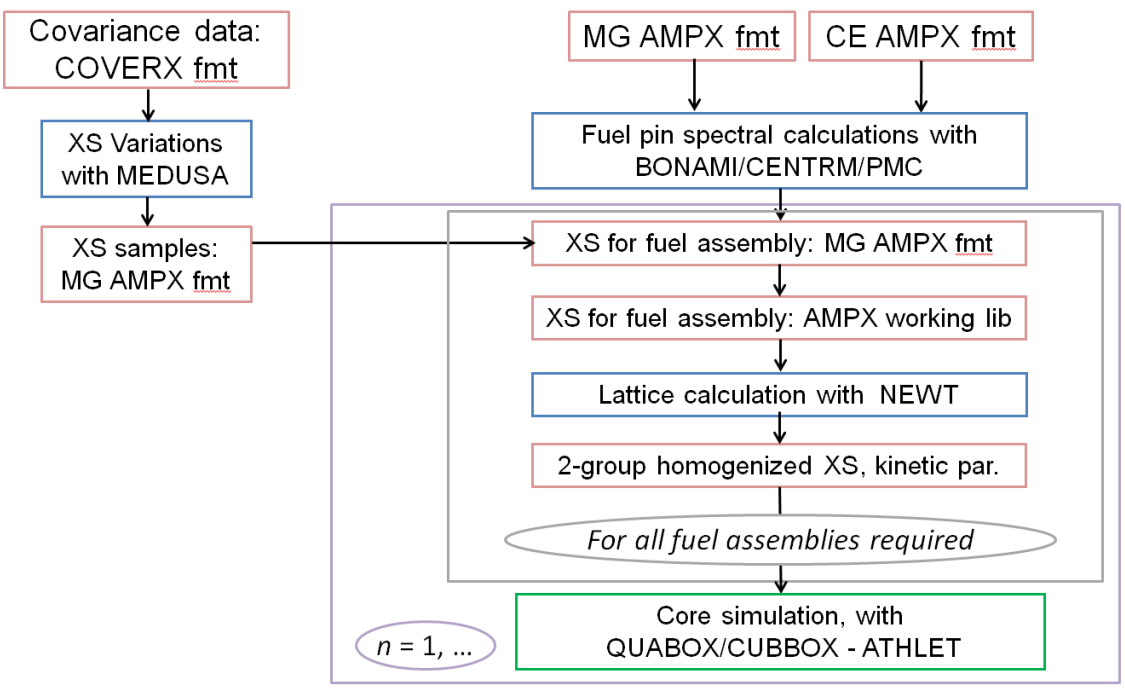

Abbildung 5-4 Berechnungskette für Unsicherheitsanalysen mit XSUSA für Kerntransientenberechnungen

Abbildung 5-5 zeigt zunächst einen Vergleich für die Unsicherheiten in der radialen Leistungsverteilung in der stationären Kernanordnung, ermittelt in einer Referenz-Monte-Carlo-Berechnung mit KENO, und einer nodalen Diffusionsrechnung mit QUABOX/CUBBOX /KLE 11/, für die vorab wie oben beschrieben nodale Zwei-Gruppen-Daten erzeugt wurden. Die Übereinstimmung ist ausgezeichnet; Dies verdeutlicht, dass die Unsicherheiten mit der Sampling-basierten XSUSA-Methode korrekt auch durch eine mehrstufige Berechnungskette propagiert werden.

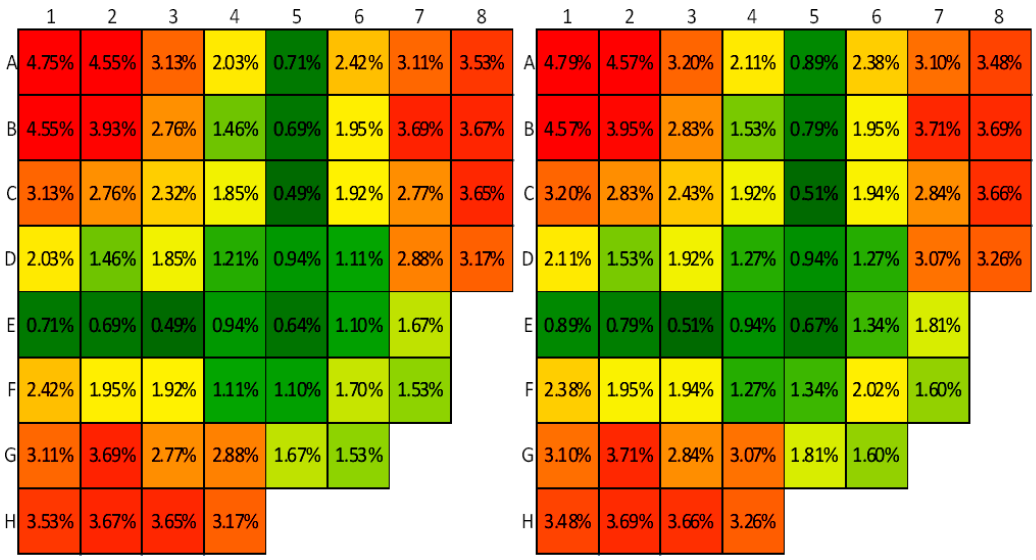

Abbildung 5-5 Unsicherheiten für die radiale Leistungsverteilung in einem DWR-Kern, ermittelt mit XSUSA/KENO (links) und XSUSA/QUABOX/CUBBOX (rechts)

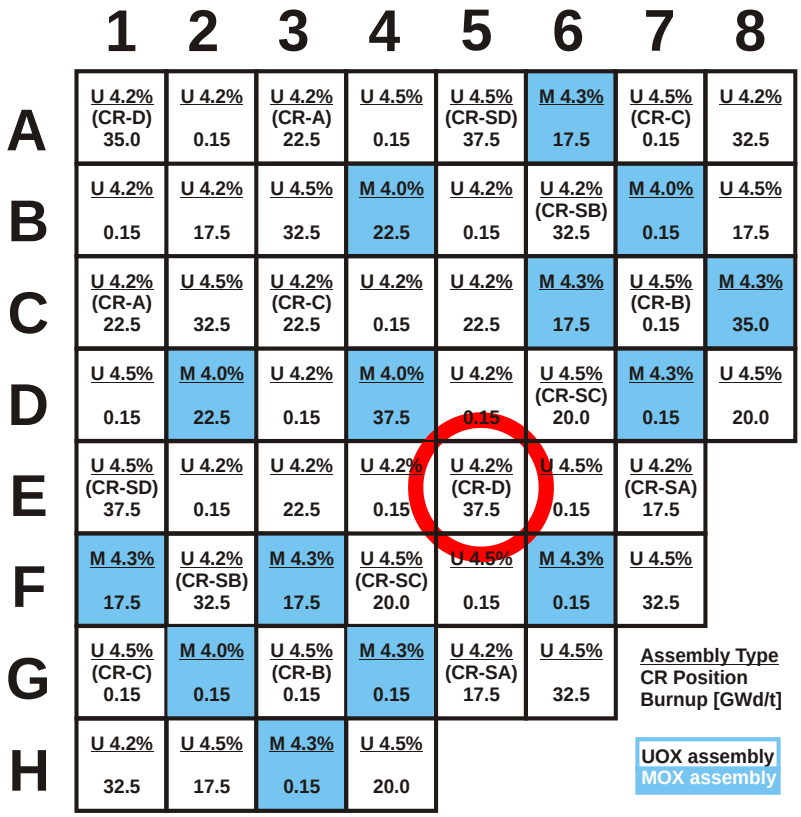

Abbildung 5-6 Kernanordnung für eine Steuerstabauswurf-Transiente

Abbildung 5-6 zeigt die Kernanordnung für die spezifizierte Transiente: alle Regelstäbe (CR-A, CR-B, CR-C, CR-D) sind vollständig eingefahren, alle Abschaltstäbe (CR-SA,

CR-SB, CR-SC, CR-SD) sind ausgefahren, die Position des Brennelements, in dem der Steuerstabauswurf stattfindet, ist durch einen Kreis markiert. Es ist darauf hinzuweisen, dass die nicht dargestellten drei Viertelkerne dieselbe Brennelement- und Steuerstabanordnung besitzen, der Steuerstabauswurf aber auf das dargestellte Kernviertel beschränkt ist, so dass bei der Transientenberechnung keine Symmetrien ausgenutzt werden können.

In Abbildung 5-7 sind zunächst die Ergebnisse für die Leistung als Funktion der Zeit der ursprünglichen Benchmark-Lösungen dargestellt. Dabei ist zu beachten, dass die Schar der „ähnlichen“ Lösungen zwar mit unterschiedlichen Rechenprogrammen erhalten wurde, die verwendeten Wirkungsquerschnitte jedoch identisch waren. Lediglich der davon stark abweichenden Lösung liegt ein anderer Satz von nuklearen Daten zu Grunde.

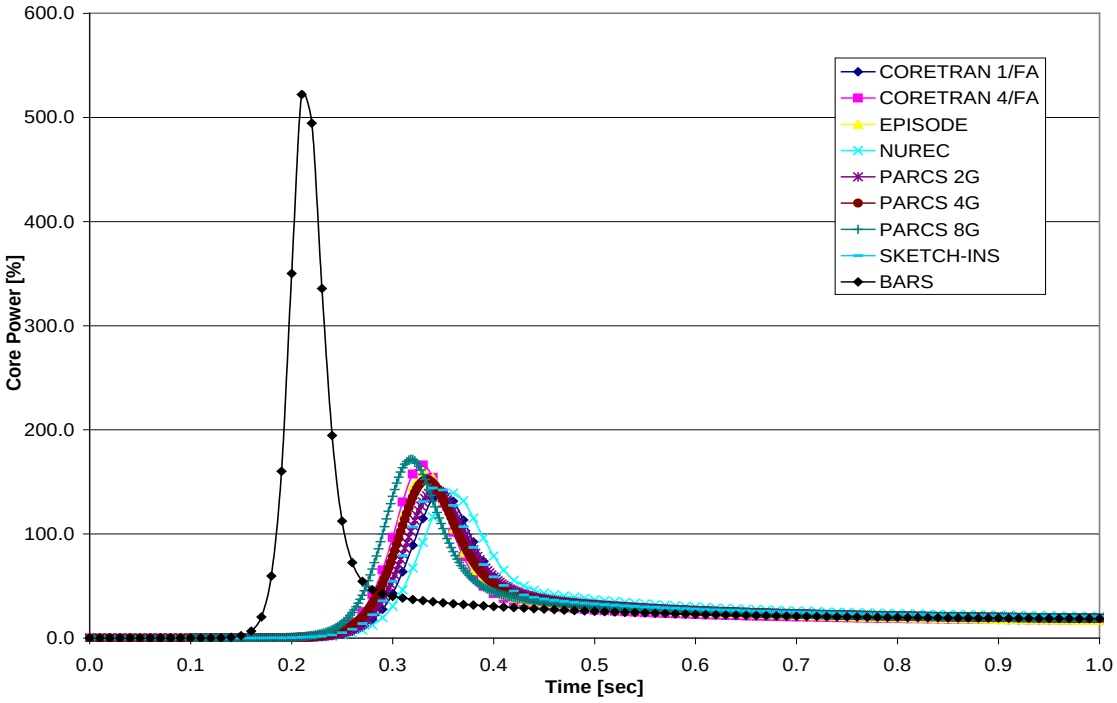

Abbildung 5-7 Gesamtleistung bei einer Steuerstabauswurf-Transiente aus unterschiedlichen Rechenprogrammen

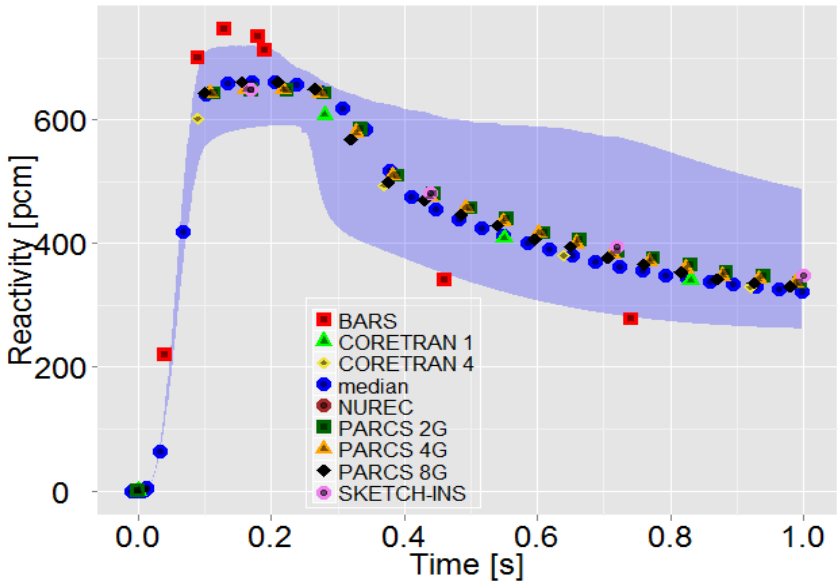

Abbildung 5-8 Reaktivität und deren Unsicherheit für eine Steuerstabauswurf-Transiente

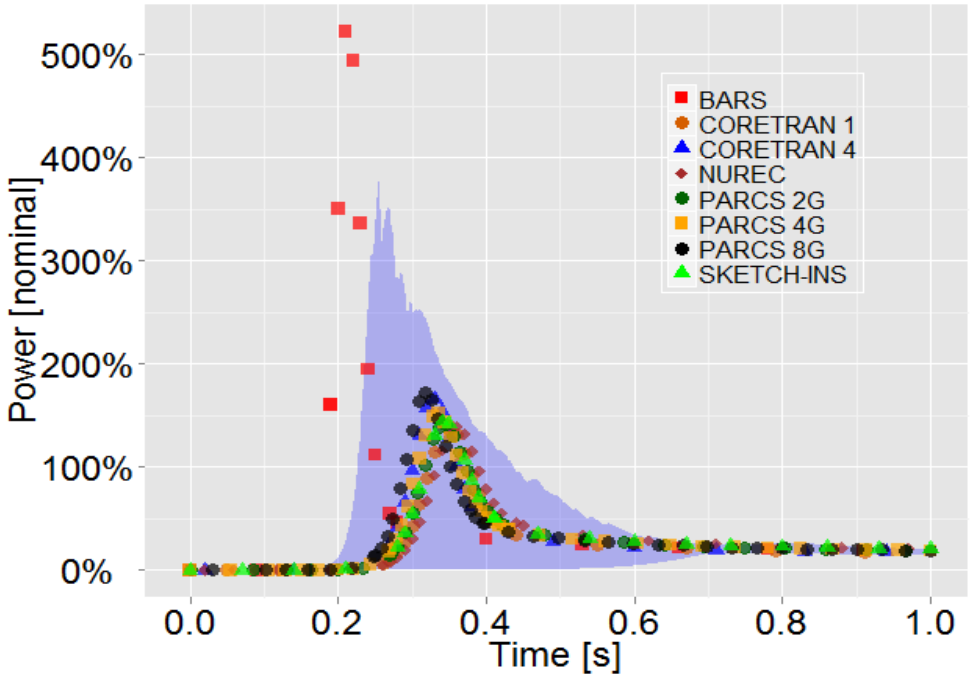

Abbildung 5-9 Gesamtleistung und deren Unsicherheit für eine Steuerstabauswurf-Transiente

Abbildung 5-8 und Abbildung 5-9 zeigen die wesentlichen Ergebnisse der Unsicherheitsanalysen bzgl. nuklearer Daten mit XSUSA, im Vergleich mit den Ergebnissen der ursprünglichen Benchmark-Beiträge. Die blaue Fläche in Abbildung 5-8 skizziert das Unsicherheitsband der durch die Transiente zugefügten Reaktivität. Am Maximum bei

ca. 0.15 sec ergibt sich ein relativ moderater Bereich von etwa 650 +/- 70 pcm. Der jeweilige Wert ist jedoch entscheidend dafür, ob das System prompt oder nur verzögert überkritisch wird. Dementsprechend deutlich ist die Unsicherheit in der Gesamtleistung im Verlauf der Transiente, Abbildung 5-9: der Leistungsanstieg variiert zwischen einem praktisch vernachlässigbaren Wert und ca. 350 % der Nominal-Reaktorleistung.

Die oben beschriebenen Analysen wurden mit insgesamt 100 Variationen der nuklearen Daten durchgeführt. Dies ist zwar ausreichend, um die Unsicherheit zuverlässig zu ermitteln, für eine Sensitivitätsanalyse, d. h. zur Ermittlung der Hauptbeiträge zu dieser Unsicherheit, sind deutlich mehr Variationen nötig.

5.3 Kovarianzdaten für die Multiplizität verzögerter Neutronen

Der effektive verzögerte Neutronenanteil β-eff ist ein wesentlicher Parameter der Reaktorsicherheit; er beeinflusst sowohl die Ergebnisse von Berechnungen von Steuerstabreaktivitäten als auch Transientenanalysen, und spielt damit eine wichtige Rolle bei der Analyse von Reaktivitätsstörfällen. Die Genauigkeit von β-eff sollte daher genau ermittelt und bewertet werden. Das Interesse an der Berechnung kinetischer Parameter und der Fortpflanzung der entsprechenden Unsicherheiten wurde innerhalb des Projekts „Uncertainty Analysis in Modelling“ (UAM) der OECD/NEA betont.

Für die Berechnung des effektiven verzögerten Neutronenanteils spielt die Multiplizität der verzögerten Neutronen $\nu_{delayed}$ eine wesentliche Rolle. Deshalb ist zu erwarten, dass für die Unsicherheit von β-eff auch die Unsicherheit in der Multiplizität der verzögerten Neutronen einen wesentlichen Beitrag liefert. Das Problem hierbei ist, dass die normalerweise mit XSUSA verwendeten Kovarianzdaten aus dem Programmsystem SCALE 6 keine Daten für $\nu_{delayed}$ enthalten. Eine Überprüfung der wichtigsten evaluierten nuklearen Datenbibliotheken JEFF-3.1, ENDF/B-VII und JENDL-4.0 hat ergeben, dass nur JENDL-4.0 einen umfangreichen Satz von Unsicherheitsdaten für $\nu_{delayed}$ für die wichtigsten Aktiniden beinhaltet.

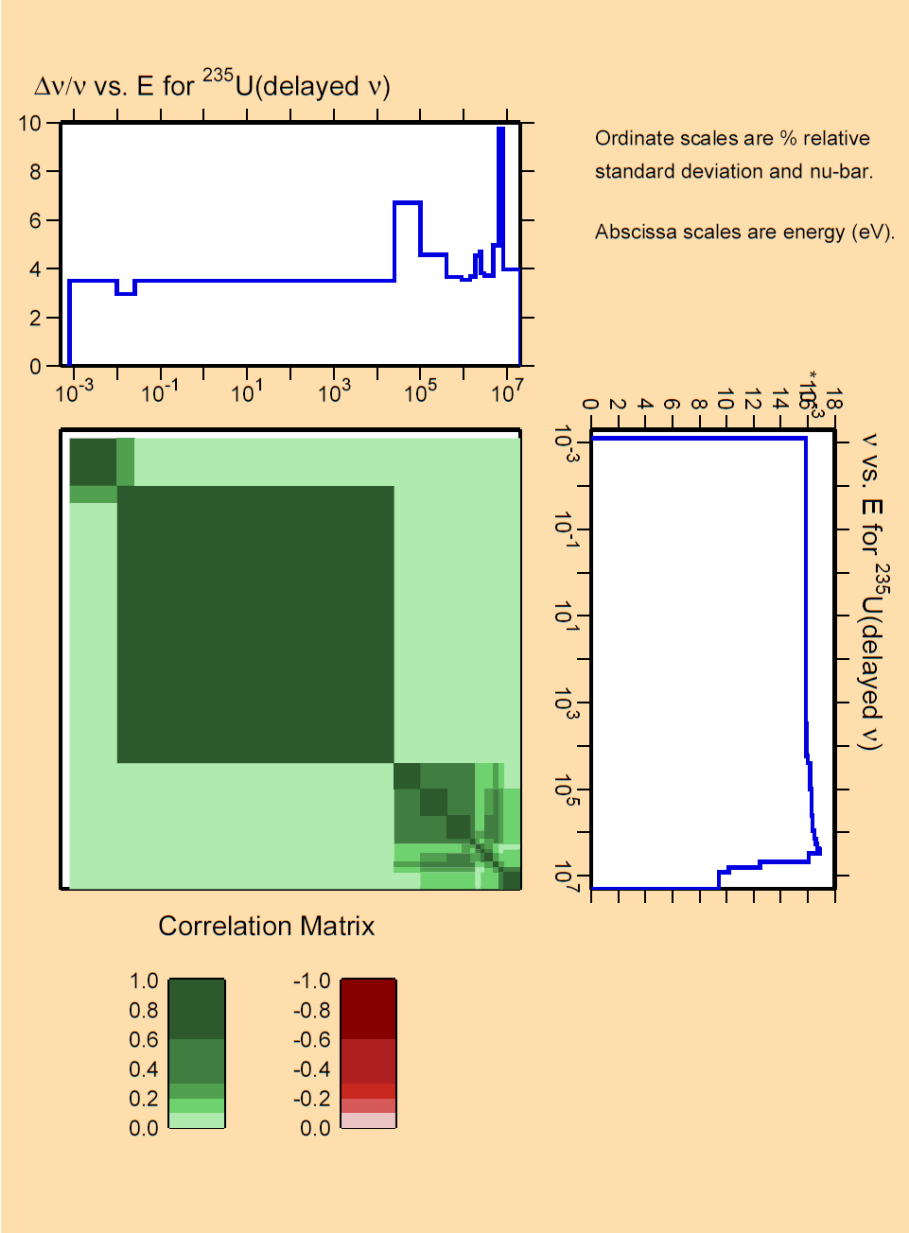

Abbildung 5-10 Unsicherheit und Korrelationsmatrix der Multiplizität der verzögerten Neutronen von U-235 aus den JENDL-4.0-Daten

Zur Erzeugung von Kovarianzmatrizen für die Multiplizität der verzögerten Neutronen in der 44-Gruppen-Struktur, in der auch die SCALE-Kovarianzmatrizen vorliegen, wurde das Programmsystem NJOY99 verwendet. Die derart erstellten Daten liegen schließlich im BOXER-Format vor, das mit den Programmen aus dem SCALE-System, und auch mit XSUSA, nicht direkt nutzbar ist. Deshalb war es nötig ein Hilfsmodul zu erstellen, mit dem die Kovarianzmatrizen im mit SCALE und XSUSA kompatiblen COVERX-Format erzeugt werden. Zur Überprüfung der Berechnungskette wurden die Daten

ebenfalls mit dem Code PUFF-IV /WIA 06/, der Stand-Alone-Version eines entsprechenden Moduls des AMPX-Systems /GRE 01/, prozessiert.

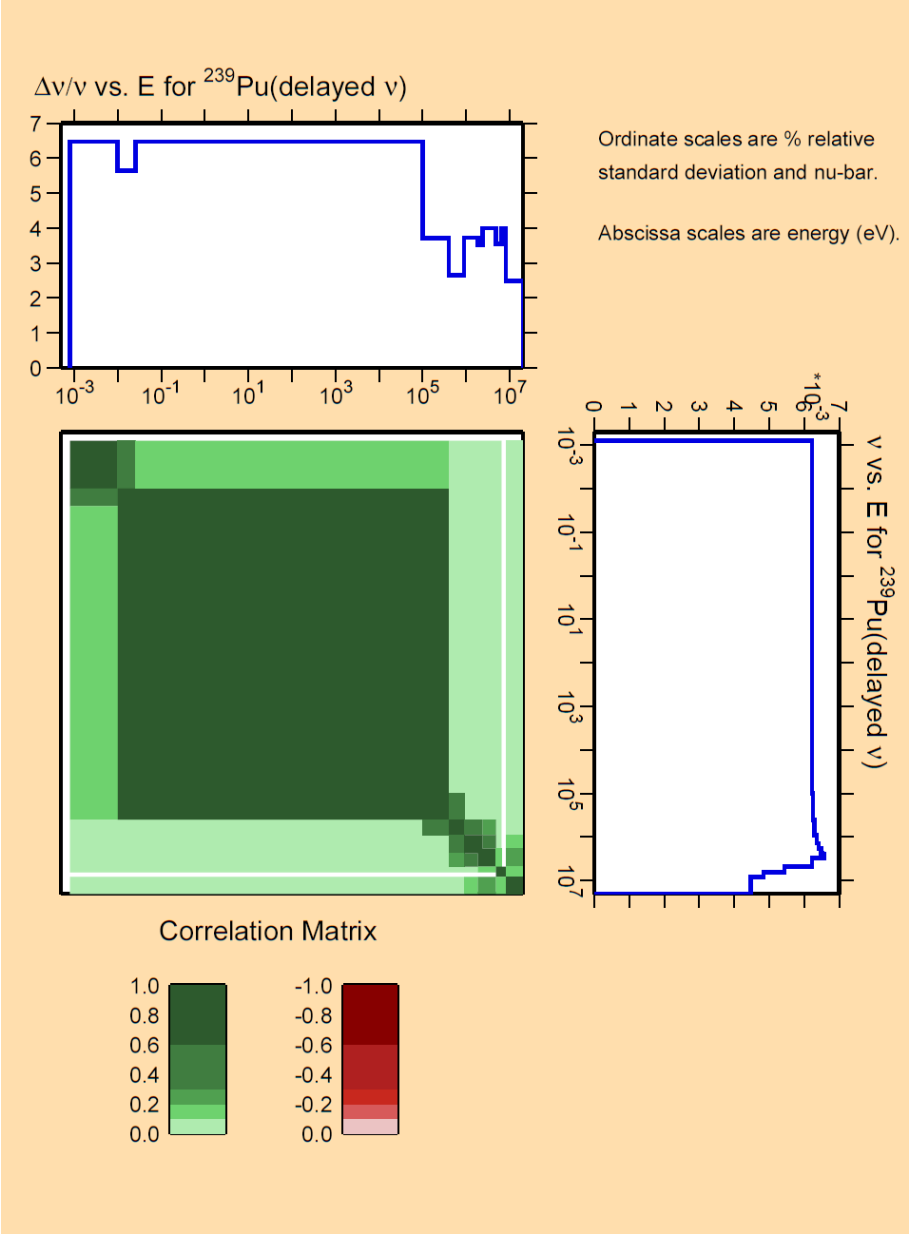

Abbildung 5-11 Unsicherheit und Korrelationsmatrix der Multiplizität der verzögerten Neutronen von Pu-239 aus den JENDL-4.0-Daten

Abbildung 5-10 und Abbildung 5-11 zeigen die prozessierten Daten für U-235 und Pu-239 in der üblichen Darstellung mit Nominalwerten (rechts), relativen Standardabweichungen (oben) und Korrelationsmatrix zwischen den Daten bei den verschiedenen Energiegruppen. Für die relativen Standardabweichungen sind Werte von 4 % – 10 %

zu beobachten; diese legen nahe, dass der Einfluss auf die Unsicherheiten im effektiven verzögerten Neutronenanteil nicht zu vernachlässigen ist.

Für die entsprechenden Unsicherheitsanalysen müssen zunächst für die betrachteten Anordnungen die Nominalwerte des effektiven verzögerten Neutronenanteils β-eff bestimmt werden. Dazu eignet sich am besten die „prompt k ratio"-Methode /BRE 97/. Dabei müssen für dieselbe Anordnung zwei Kritikalitätsrechnungen durchgeführt werden, die eine auf gewöhnliche Art unter Berücksichtigung aller Spaltneutronen, die andere nur mit prompten Spaltneutronen, d. h. unter Vernachlässigung der verzögerten Neutronen. Der effektive verzögerte Neutronenanteil ergibt sich dann in sehr guter Näherung als $\beta\text{-eff} = 1 - k_p/k$; dabei ist k der herkömmliche, k_p der prompte Multiplikationsfaktor. Leider bieten normalerweise Spektral- und Multigruppen-Transportcodes keine Möglichkeit, programmintern nur prompte Neutronen zu berücksichtigen. Deshalb war es erforderlich, SCALE-Module zur Handhabung von Daten im AMPX-Format derart zu erweitern, dass es möglich ist, die totalen Neutronenmultiplizitäten durch die der verzögerten Neutronen zu ersetzen.

Zur Anwendung wurden drei kritische Anordnungen herangezogen: JEZEBEL (eine Kugel aus Pu-239), TOPSY (eine Kugel aus U-235 mit einem Reflektor aus Natururan) und POPSY (eine Kugel aus Pu-239 mit einem Reflektor aus Natururan). Die Beschreibungen der Anordnungen sind im „International Handbook of Evaluated Criticality Safety Benchmark Experiments" /NEA 11/ zu finden. Die jeweiligen Unsicherheiten sind in Tabelle 5-2, Tabelle 5-3 und Tabelle 5-4 angegeben. Dabei bedeuten (n,n') inelastische Streuung, (n,f) Spaltung, (n,γ) Einfang, sowie ν_{del} und ν_{pmt} die Multiplizitäten verzögerter und prompter Neutronen. Zum Vergleich wurden störungstheoretische Ergebnisse herangezogen. Da TSUNAMI in der gegenwärtigen Version verzögerte Neutronen nicht explizit berücksichtigen kann, wurde dazu, in einer Zusammenarbeit mit dem Institut Jožef Stefan in Ljubljana, das Programm SUSD3D /KOD 11/ verwendet, siehe auch Anhang B12. Dabei wurden mit XSUSA „One-at-a-time"-Variationen durchgeführt; es wurden also nicht nur alle Reaktionen gleichzeitig variiert, sondern auch individuell.

Wie erwartet liefert die Unsicherheit in der Multiplizität der verzögerten Neutronen in allen Fällen einen wesentlichen Beitrag zur Ergebnisunsicherheit. Überraschenderweise liefert für POPSY die Unsicherheit in der inelastischen Streuung am Reflektormaterial U-238 den Hauptbeitrag. Allgemein sind die Ergebnisse von SUSD3D und XSUSA in

guter Übereinstimmung. Ein deutlicherer Unterschied zeigt sich bei der inelastischen Streuung an U-238 für die POPSY-Anordnung. Hier ist die Unsicherheit im Wirkungsquerschnitt erheblich (bis zu 30 %), was zur Folge hat, dass störungstheoretische Ansätze ihren Gültigkeitsbereich verlassen.

Tabelle 5-2 Unsicherheiten (1 σ) im effektiven verzögerten Neutronenanteil bei der kritischen Anordnung JEZEBEL

	(n,n')	(n,f)	ν_{del}	ν_{pmt}
SUSD3D	0.25	0.26	2.13	1.76
XSUSA	0.26		2.37	1.80

Tabelle 5-3 Unsicherheiten (1 σ) im effektiven verzögerten Neutronenanteil bei der kritischen Anordnung TOPSY

		(n,n')	(n,f)	(n,γ)	ν_{del}	ν_{pmt}
SUSD3D	U-235	0.09	0.08	1.01	2.41	0.14
	U-238	0.88	0.02	0.02	0.51	0.16
XSUSA	U-235			1.02	2.40	
	U-238	1.17			0.58	

Tabelle 5-4 Unsicherheiten (1 σ) im effektiven verzögerten Neutronenanteil bei der kritischen Anordnung POPSY

		(n,n')	(n,f)	(n,γ)	ν_{del}	ν_{pmt}
SUSD3D	U-238	3.24	0.18	0.065	1.21	0.11
	Pu-239	0.65	0.28	0.151	1.36	1.40
XSUSA	U-238	4.18			1.39	
	Pu-239	0.72			1.38	1.40

5.4 Die „schnelle GRS-Methode“

Sampling-basierte Methoden zur Sensitivitäts- und Unsicherheitsanalyse werden sowohl mit deterministischen als auch mit Monte-Carlo-Transportprogrammen angewendet. Wenn ein Monte-Carlo-Programm zur direkten Simulation des Neutronentransport verwendet wird, wird dabei eine zusätzliche Unsicherheitsquelle eingeführt, die sich aus der endlichen Anzahl von Neutronenschicksalen ergibt, die im Verlauf der Monte-Carlo-Simulation ausgewertet werden („aleatorische Unsicherheit“). Diese kommt noch zu der Unsicherheit hinzu, die durch eine unvollständige Kenntnis von Eingabeparametern, hier der nuklearen Daten, zustande kommt („epistemische Unsicherheit“). Deshalb wählt man, falls ein Monte-Carlo-Code zur Lösung des Transportproblems eingesetzt wird, normalerweise für jede Rechnung mit variierten nuklearen Daten die Anzahl der Neutronenschicksale so groß, dass die aleatorische Sampling-Unsicherheit vernachlässigbar klein wird, und die beobachtete Sampling-Unsicherheit der Ergebnisse praktisch ausschließlich auf die epistemische Unsicherheit durch die Variation der nuklearen Daten zurückgeführt werden kann. Das bedeutet, dass für jeden Rechenlauf mit variierten nuklearen Daten dieselbe hohe Anzahl von Neutronenschicksalen verwendet wird wie für die Referenzrechnung. Die Rechenzeiten werden offenbar bei dieser Vorgehensweise enorm hoch, wenn man es mit vielen variierten Datensätzen zu tun hat.

Im Folgenden wird eine Methode vorgestellt, mit der es möglich ist, die Rechenzeit deutlich zu verringern. Dabei wird gezeigt, dass es in vielen Anwendungsfällen nicht nötig ist, die gesamte Serie von Rechenläufen mit hoher statistischer Genauigkeit durchzuführen. In der Tat ist es möglich, zuverlässige Ergebnisse für die epistemische Unsicherheit mit einer wesentlich reduzierten Anzahl von Neutronenschicksalen in jedem Rechenlauf zu erhalten; dabei kann unter günstigen Umständen die Gesamtzahl von Neutronenschicksalen für die komplette Serie aller Rechenläufe von derselben Größenordnung sein wie für einen einzigen Rechenlauf mit hoher Genauigkeit, d. h. mit geringer aleatorischer Unsicherheit.

Dabei wird folgendermaßen vorgegangen:

Es werden zwei Serien von Rechenläufen durchgeführt.

1. Serie: gewöhnliches zweidimensionales aleatorisches/epistemisches verschachteltes Sampling:

- Äußere (epistemische) Schleife: Sample von der Größe N_e bzgl. der nuklearen Daten.
- Innere (aleatorische) Schleife: Monte-Carlo-Transportsimulation mit reduzierter Sample-Größe N_a.

2. Serie: zusätzliches zweidimensionales aleatorisches/epistemisches verschachteltes Sampling:

- Äußere (epistemische) Schleife: Sample von der Größe N_e bzgl. der nuklearen Daten, identisch zum Sample der ersten Serie.
- Innere (aleatorische) Schleife: neue Monte-Carlo-Transportsimulation mit reduzierter Sample-Größe N_a mit Variationen, die statistisch unabhängig von denen der ersten Serie sind.

Schließlich wird die Sample-Kovarianz dieses zweidimensionalen Samples gebildet. Diese stellt näherungsweise die Varianz der Verteilung dar, die dem epistemischen Anteil der Sampling-Unsicherheit entspricht, nachdem der Einfluss des aleatorischen Anteils eliminiert wurde.

Die Genauigkeit der Ergebnisse mit dieser Methode hängt invers vom relativen Beitrag der aleatorischen Sampling-Unsicherheit ab. Die Genauigkeit kann also nötigenfalls erhöht werden, indem die aleatorische Sample-Größe, also die Anzahl der Neutronenschicksale je Rechenlauf erhöht wird. Andererseits wird bei gleichbleibender aleatorischer Sample-Größe die Genauigkeit auch durch eine Erhöhung der epistemischen Sample-Größe, also durch mehr Rechenläufe, zunehmen.

Die Anwendung der Methode wird anhand des EG-UACSA-Benchmarks Phase II /NEU 10/ demonstriert. Dabei handelt es sich um eine zweidimensionale Darstellung eines unendlichen Gitters von Brennelementen, die ein Brennelementlager simuliert. Die Brennelemente bestehen aus 17x17 Stabzellen, auf 25 Positionen sind Instrumentierungs- oder Steuerstabführungsrohre. Der Brennstoff ist frisches UO_2 mit einer U-235-Anreicherung von 4 %. Unterkritikalität wird durch Borstahl erreicht, der die Brennstabgitter umschließt.

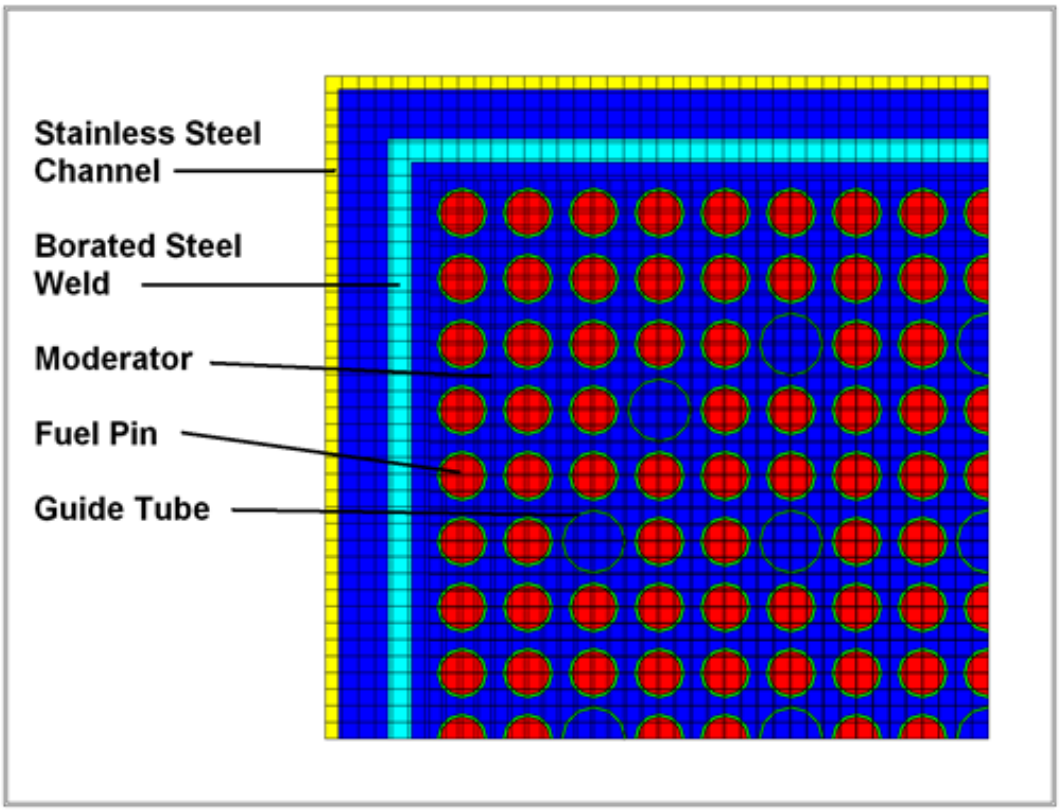

Abbildung 5-12 NEWT-Modell für die Anordnung des EG-UACSA-Benchmarks Phase II

Tabelle 5-5 Multiplikationsfaktoren des EG-UACSA-Benchmarks Phase II und deren relative Unsicherheiten (1 σ) aus XSUSA mit einer Sample-Größe von 1000

	k	Δk/k (%)	CPU-Zeit pro Lauf
NEWT (Ref.)	0.99212		
KENO (Ref.)	0.99293		
XSUSA/NEWT	0.99226	0.424	25 min
XSUSA/KENO (1000 lange Läufe)	0.99308	0.418	25 min
XSUSA/KENO (1000 kurze Läufe)	0.99306	0.544	5 sec
XSUSA/KENO (2 x 1000 kurze Läufe)	0.99305	0.411	5 sec (x2)

Die deterministischen Berechnungen wurden mit dem 2-d Transportcode NEWT durchgeführt, die Monte-Carlo-Berechnungen mit KENO. Abbildung 5-12 stellt das NEWT-Modell dar, die Modellierung mit KENO ist entsprechend. Aus Symmetriegrün-

den reicht es aus, ein Viertel der Anordnung zu beschreiben. Die Unsicherheits- und Sensitivitätsanalysen mit XSUSA wurden mit einer Sample-Größe von 1000 durchgeführt.

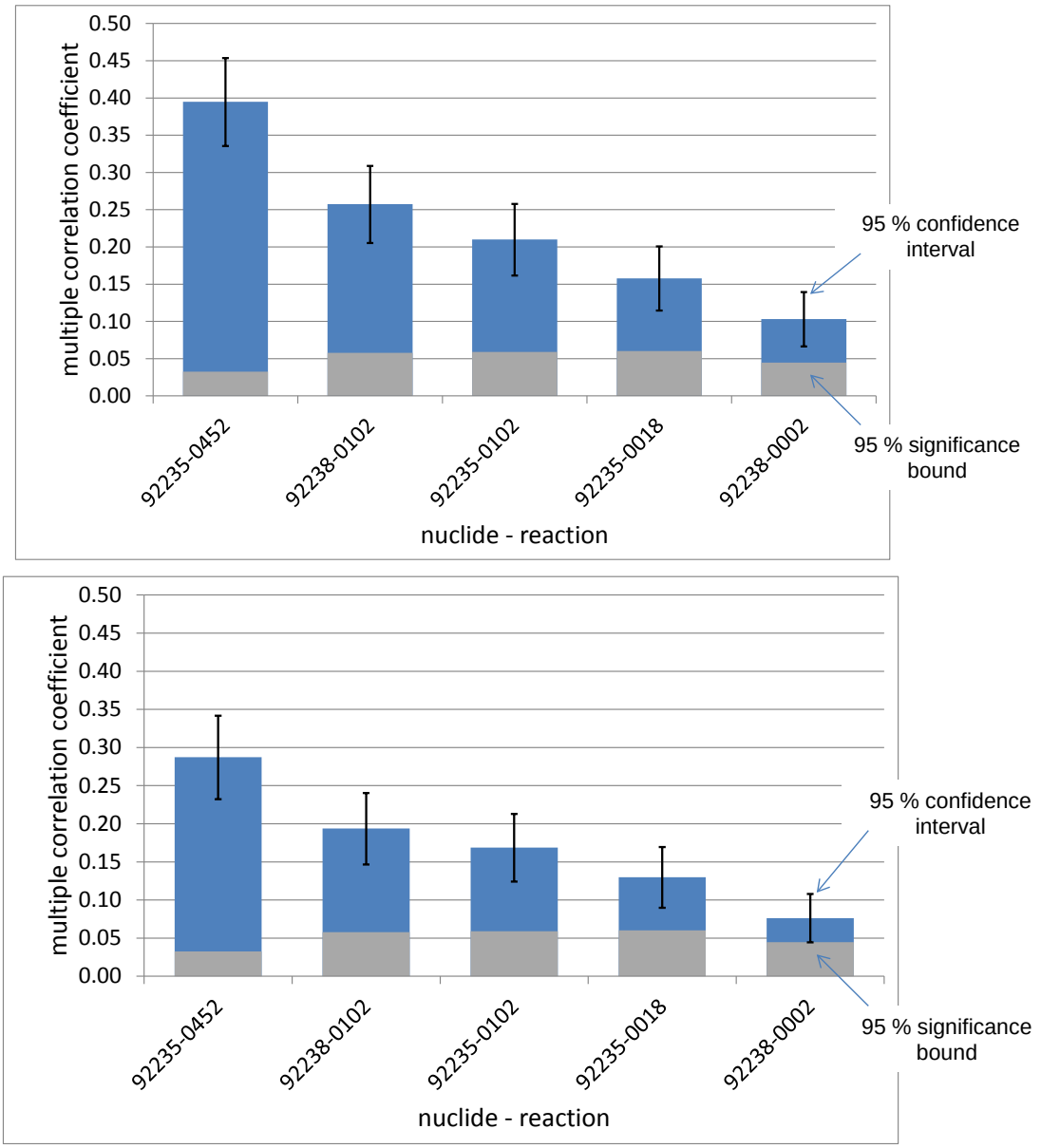

Abbildung 5-13 Sensitivitätsergebnisse für das EG-UACSA-Benchmark Phase II. Quadrierte multiple Korrelationskoeffizienten (R2) aus 1000 langen KENO-Rechenläufen (oben) und nach der „schnellen GRS-Methode“ (unten)

Die wesentlichen Ergebnisse für die Unsicherheit des Multiplikationsfaktors sind in Tabelle 5-5 zusammengefasst. Sowohl die deterministische Berechnung mit NEWT als auch die Monte-Carlo-Berechnung mit KENO benötigen pro Rechenlauf ca. 25 Minu-

ten; die KENO-Rechnung wurde mit 50 x 10^6 Neutronenschicksalen durchgeführt. Bei 1000 Rechenläufen entspricht dies einer Gesamtrechenzeit von ca. 17 Tagen. Bei der Monte-Carlo-Rechnung kann diese Rechenzeit gemäß der oben beschriebenen Methode drastisch reduziert werden. Verwendet man nur noch 50 x 10^3 Neutronenschicksale, reduziert sich die Rechenzeit pro Rechenlauf auf ca. 5 Sekunden. (Die Rechenzeit skaliert nicht mit der Anzahl der Neutronenschicksale, da für sehr geringe Anzahlen die Rechenzeit durch Lese- und Schreiboperationen etc. deutlich mitbeeinflusst wird.) Die resultierende Unsicherheit liegt deutlich über der tatsächlichen epistemischen Unsicherheit, da nun die aleatorische Unsicherheit einen deutlichen Beitrag zur Gesamtunsicherheit leistet. Führt man nun eine weitere Serie von kurzen Rechenläufen durch, erhält man durch Kovarianzbildung eine ausgezeichnete Abschätzung für die epistemische Unsicherheit. Die gesamte Rechenzeit hat sich dadurch auf ca. 3 Stunden reduziert, also gegenüber der ursprünglichen Rechenzeit von 17 Tagen um mehr als einen Faktor 100.

Mit der „schnellen GRS-Methode“ ist es nicht nur möglich, bei Unsicherheitsanalysen mit Monte-Carlo-Transportrechnungen die Unsicherheit mit einem geringen Aufwand an CPU-Zeit sehr gut abzuschätzen, siehe auch Anhang B5 und B9. und B13. Ähnliches gilt für die Sensitivitätsanalyse, d. h. die Bestimmung der Hauptbeiträge zur Ergebnisunsicherheit. In einer Zusammenarbeit mit dem NRG, Petten wurde eine ähnliche Methode unter der Bezeichnung „fast TMC“ in das Programmsystem TMC („Total Monte Carlo“) /KON 08/ integriert, siehe auch Anhang B13.

In Abbildung 5-13 sind als Sensitivitätsindikatoren die „quadrierten multiplen Korrelationskoeffizienten (R^2)“ für das EG-UACSA-Benchmark Phase II dargestellt. Dabei sind nur Beiträge berücksichtigt, die tatsächlich statistisch signifikant sind, d. h. die oberhalb der 95 %-Signifikanzgrenze liegen. Ein Vergleich der Ergebnisse aus einer herkömmlichen Rechenserie mit 1000 langen KENO-Rechenläufen und gemäß der „schnellen GRS-Methode“, d. h. mit zwei Serien mit je 1000 kurzen Rechenläufen liefert dieselbe Reihenfolge der Beiträge. Leidglich die quantitativen Werte der Sensitivitätsindikatoren sind bei der „schnellen GRS-Methode“ niedriger, was auf den Anteil der aleatorischen Unsicherheit zurückzuführen ist.

Zusätzlich zu den bereits genannten Kooperationen mit IJS, Ljubljana und NRG, Petten werden auch gemeinsame Arbeitet mit ORNL, Oak Ridge, und der University of Michigan durchgeführt, siehe Anhang B3, B4 und B10.

6 AP4: Einsatz künstlicher neuronaler Netze zur Berechnung lokaler Parameter im Reaktorkern

Der folgende Abschnitt beschreibt die bislang durchgeführten Arbeiten am nuklearen Programmsystem der GRS bezüglich der Erprobung der Anwendbarkeit neuronaler Netze für Fragestellungen bei der Rektorkernsimulation.

Künstliche neuronale Netzwerke (KNN) /BIS 96/ wurden im Hinblick auf ihre Einsatzmöglichkeit im Bereich der Verarbeitung von nuklearen Daten untersucht. Speziell soll in diesem Arbeitspunkt die explizite, tabellarische Speicherung von hochdimensionalen Wirkungsquerschnittsdaten und deren lineare Interpolation an Zwischenstellen, wie z. B. im Neutronenkinetik-Programm QUABOX/CUBBOX /QC 78/ praktiziert, durch kontinuierliche, analytische Modelle ersetzt werden. Davon verspricht man sich bei Wirkungsquerschnittsbibliotheken mit wenigen Stützstellen, also Kombinationen von Werten der diskretisierten freien Variablen wie z. B. Brennstofftemperatur oder Borkonzentration, an denen Werte vorliegen, ein verbessertes Interpolationsergebnis und insbesondere bei hoch abgetasteten Daten eine Speicherplatzersparnis durch die kodierte Darstellung.

6.1 Eigenschaften und Funktionsprinzip

Ein Vorteil von neuronalen Netzwerken bei Regressionsanalysen, also der Anpassung von analytischen Modellen an eine Menge von Stützstelle-Wert-Paaren, besteht darin, dass dabei keine speziell auf das Problem zugeschnittenen, sondern generische Funktionen zum Einsatz kommen. Auf der anderen Seite führt eine solche quasi theoriefreie Herangehensweise nicht zu einem besseren Verständnis der Daten, was aber im vorliegenden Fall auch nicht das Ziel ist. Man fasst diese Klasse von Ansätzen unter dem Begriff der nicht-parametrischen Statistik zusammen. Die mathematische Grundlage für den Erfolg der Methode bildet ein Approximationstheorem von Kolmogorov /KOL91/. Das Arbeitsgebiet der künstlichen neuronale Netzwerke hat seinen Ursprung in der theoretischen Hirnforschung, weswegen viele Begriffe biologisch inspiriert sind.

Die hier verwendeten, nicht-rückgekoppelten „feed-forward“-Netzwerke bestehen aus einer Eingabeschicht, mindestens einer sogenannten versteckten Schicht und einer Gruppe von Ausgabeneuronen (siehe Abbildung 6-1). Das i-te Neuron einer Schicht bildet dabei jeweils die gewichtete Summe der Signale x_j der N_i Neuronen aus der vo-

rangegangenen Schicht, mit denen es synaptisch verbunden ist, wendet darauf eine nichtlineare Aktivierungsfunktion σ an und reicht sein eigenes Signal $y_i(x)$ unidirektional an die nächste Ebene weiter:

$$y_i\,(\boldsymbol{x}) = \sigma\left(\sum_{j}^{N_i} w_{ij}x_j + \theta_j\right)$$

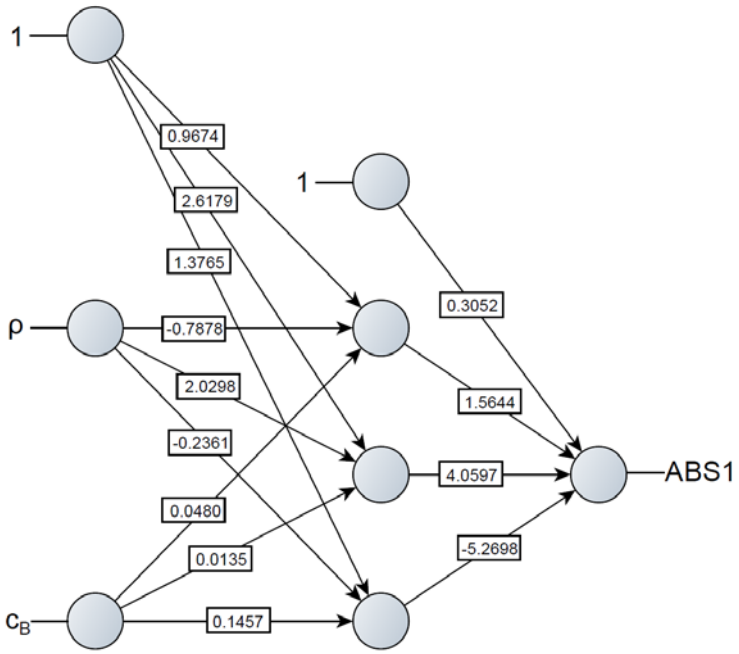

Abbildung 6-1 Architektur und synaptische Gewichte eines trainierten neuronalen Netzwerks

Dabei symbolisieren die Koeffizienten w_{ij} die synaptischen Gewichte und θ_j einen Schwellenwert, der auch als weiteres Gewicht für einen konstanten Eingabewert angesehen werden kann. Der Regressionsvorgang besteht bei neuronalen Netzen in einem Lernprozess, während dessen die Eingangsgewichte jedes Neurons durch Vergleich der Ausgabe des Netzwerks mit den bekannten Zielwerten über eine Fehlerfunktion adaptiert werden („supervised learning“). Sind alle Datenpunkte vorab bekannt, liegt ein klassisches nichtlineares Optimierungsproblem vor. Ein Vorteil von neuronalen Netzen gegenüber Ansätzen mit anderen generischen Funktionen wie Polynomen besteht darin, dass die freien Parameter nichtlinear in die Ausgleichsfunktion eingehen und dadurch ihre Anzahl, die zur Beschreibung benötigt wird, nicht exponentiell mit der Dimension wächst.

6.2 Fragen bei der praktischen Umsetzung

Wir setzen eine spezielle Klasse von „feed-forward“-Netzwerken, das „multi-layer perceptron“ (MLP), ein, bei dem die Aktivierungsfunktionen der Neuronen eine sigmoidale Form haben, und das häufig für Regressionsaufgaben verwendet wird. Leider macht das Kolmogorov-Theorem keine Aussage über die Anzahl der versteckten Schichten und der darin enthaltenen Neuronen, die man zur Approximation einer gegebenen Funktion benötigt. Angemessene Werte für diese auch als Hyper-Parameter des Netzwerks bezeichneten und für die meisten Algorithmen vor dem Lernprozess festzulegenden Größen hängen von der Komplexität der Funktion ab, eine Eigenschaft die nicht gut quantifizierbar ist und in keinen direkten Zusammenhang mit den gesuchten Parametern gebracht werden kann. Heuristische Argumente und Modellsysteme liefern zwar Anhaltspunkte für die Größenordnungen, man ist aber in der praktischen Anwendung gezwungen, den Raum der Hyperparameter in gewissen Grenzen nach geeigneten Werten abzusuchen. Für Regressionsprobleme werden in der Regel höchstens zwei versteckte Schichten verwendet. Bei Fragestellungen aus dem Bereich der Mustererkennung erhofft man sich aufgrund von Forschungen zur Struktur der Großhirnrinde bessere Ergebnisse von einer tieferen Staffelung („deep learning“). Solche Netzwerke sind allerdings nur schwierig zur Konvergenz zu bringen. Erst in den letzten Jahren hat man in dieser Richtung Fortschritte durch verbesserte Initialisierungsalgorithmen erzielt.

Die Anzahl der synaptischen Gewichte eines Netzwerks bestimmt sein Potential, sich flexibel an vorgegebene Daten anzupassen und diese widerzugeben. Gleichzeitig bewirkt eine zu hohe Zahl von freien Parametern eine Überanpassung und damit den Verlust der Verallgemeinerungsfähigkeit, also der Qualität der Vorhersage (hier: Interpolation) von Werten bei der Präsentation von nicht gelernten Eingabedaten. Diesen Umstand bezeichnet man auch als „bias-variance“-Dilemma. Zur Sicherstellung der Vorhersagekraft von neuronalen Netzwerken kommen unterschiedliche Techniken zum Einsatz:

- In Anwendung des heuristischen „lex parsimonae“ („Occam's razor“): Auswahl des Modells mit der geringsten Anzahl von freien Parametern, das die Daten in einem vorgegebenen Fehlerrahmen erklärt.
- Regularisierung, d. h. Hinzufügen von Termen zur Fehlerfunktion aufgrund von Vorwissen über Eigenschaften wie z. B. die Glattheit der zu approximierenden Funktion.

- Kreuzvalidierung („cross validation“).

Bei der Kreuzvalidierung werden die Trainingsdaten (unter Umständen mehrfach) in eine Lern- und eine Validierungsuntermenge aufgeteilt. Während des Trainingsvorgangs passt ein Algorithmus die synaptischen Gewichte auf der Basis der Daten aus der Lernmenge an, der eigentliche Lernerfolg wird aber anhand der Abweichung der Ausgabe des neuronalen Netzwerks von den Validierungsdaten bewertet.

Unabhängig vom „bias-variance“-Dilemma setzen die Anzahl und damit zusammenhängend die Qualität der verfügbaren Trainingsdaten, also ihre Repräsentativität, der Approximation mit neuronalen Netzen Grenzen. In diesem Zusammenhang ist es wichtig zu erwähnen, dass es nur Sinn ergibt, Werte im Inneren des durch die Daten vorgegebenen Definitionsbereichs vorhersagen zu lassen. Im erweiterten Sinne zur Datenqualität gehört insbesondere bei verrauschten Werten auch das Größenverhältnis zwischen der Anzahl der freien Parameter und der Menge an Trainingsbeispielen. Problematisch ist die Tatsache, dass mit wachsender Dimensionalität die Menge der benötigten Abtaststellen exponentiell anwächst, was als „curse of dimensionality“ in die Literatur eingegangen ist. Wenn das Problem es zulässt, versucht man deshalb vor der Regressionsanalyse eine Dimensionsreduktion durchzuführen.

Die Formulierung des Lernprozesses als nichtlineares Optimierungsproblem weist auf weitere Schwierigkeiten beim Training von neuronalen Netzwerken hin. Insbesondere ist das Resultat eines lokalen Minimierungsalgorithmus aufgrund der typischerweise vielen lokalen Minima der Fehlerfunktion von den Anfangswerten der freien Parameter abhängig. Dem versucht man einerseits durch Vermeidung von a-priori ungünstigen Initialisierungsbereichen und andererseits durch den wiederholten Neustart des Lernalgorithmus mit neu initialisierten Anfangswerten zu begegnen.

6.3 Anwendung auf Wirkungsquerschnittsdaten

Bei der Umsetzung diente als Softwareumgebung die Programmiersprache Python in Kombination mit der Programmbibliothek Neurolab /ZUE 13/. Damit erzeugten wir ein voll vernetztes MLP mit tanh(x)-förmigen Aktivierungsfunktionen und wendeten es in einer Regressionsanalyse zunächst auf eine niedrigdimensionale, aus einer Wirkungsquerschnittsbibliothek für einen Druckwasserreaktor stammende Größe an, die nur von der Moderatordichte und der Borkonzentration abhängt. Zum Ausschluss von Domi-

nanzeffekten unter den Eingabegrößen und zur Verbesserung der Konvergenz wurden sowohl Ein- als auch Ausgabe der Trainingsdaten auf das Intervall [-1,1] reskaliert. Wir verwendeten ein stochastisches Initialisierungsverfahren von Bengio und Glorot /GLO10/ um Anfangswerte für das verwendete nichtlineare Optimierungsverfahren von Broyden, Fletcher, Goldfarb und Shanno (BGFS-Algorithmus) zu generieren, was in ersten Tests die Konvergenzeigenschaften gegenüber der einfachen stochastischen Initialisierung zu verbessern schien.

Um die Generalisierungsfähigkeit des Netzwerks zu gewährleisten, wurde die einfachste Form von „cross validation“ („holdout“) verwendet. Die dazu programmierten Funktionen erlauben die regelmäßige oder stochastische Stichprobenziehung der Validierungsdaten, wobei die Randpunkte ausgenommen bleiben, um das Definitionsgebiet zu erhalten. Aus dem manuell abgesuchten Raum der Hyperparameter wählten wir das Modell mit den wenigsten synaptischen Gewichten. Das Resultat der Vorhersage der Validierungsdaten des so konfigurierten neuronalen Netzwerks mit einer versteckten Ebene und insgesamt 13 synaptischen Gewichten (siehe Abbildung 6-2) verglichen wir mit linearer und kubischer Interpolation.

Wie aus Abbildung. 6-2 deutlich wird, gibt das neuronale Netzwerk im vorliegenden Beispiel die gelernten Daten zufriedenstellend wieder und seine Vorhersagen für die Validierungsdaten sind von ähnlicher Qualität. Im Vergleich mit den Resultaten der anderen beiden Interpolationsformen in Abbildung 6-3 liefert das KNN insbesondere in stark nichtlinearen Regionen deutlich bessere und ansonsten vergleichbare Ergebnisse. Statt durch die tabellierten 36 Datenpunkte kann der untersuchte Wirkungsquerschnitt also auch durch die 13 Gewichte des neuronalen Netzwerks beschrieben werden.

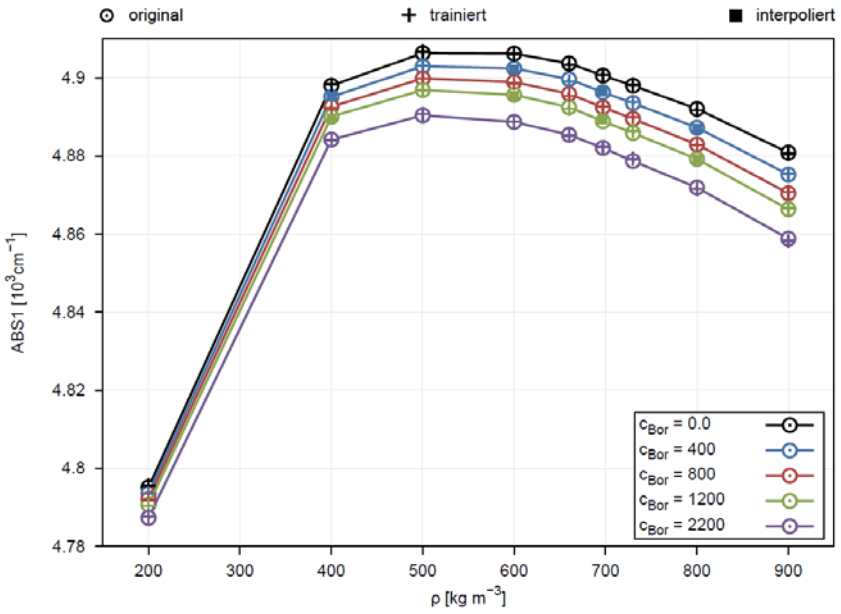

Abbildung 6-2 Vergleich der Wirkungsquerschnittsdaten mit den Vorhersagen des neuronalen Netzwerks für gelernte und unbekannte Stützstellen

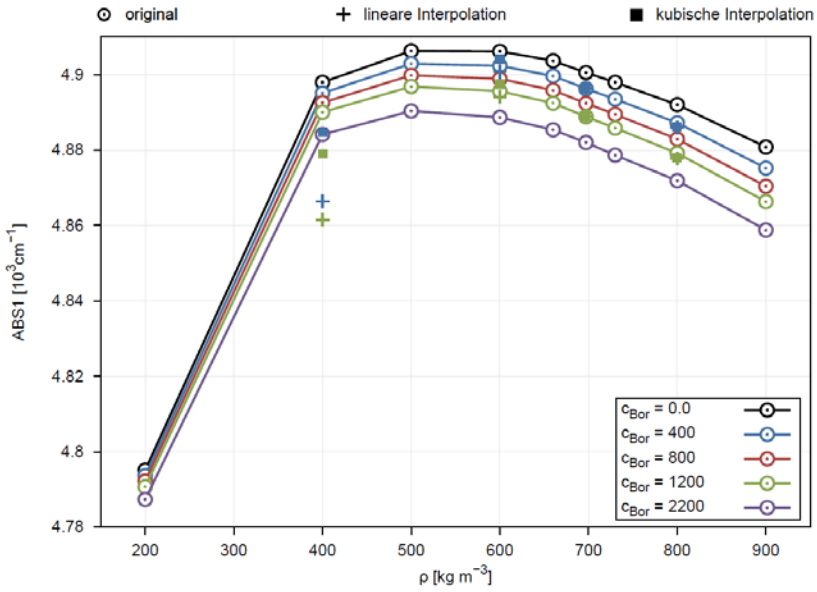

Abbildung 6-3 Vergleich der Wirkungsquerschnittsdaten mit den Ergebnissen von linearer und kubischer Interpolation an den Stützstellen der Validierungsdaten

Wie sich die verbesserte Approximation auf das Resultat einer Neutronenkinetik-Rechnung auswirkt ist noch zu untersuchen. Als weitere Schritte sind die Anwendung

der Regressionsanalyse auf Wirkungsquerschnitte, die von mehr als zwei Variablen abhängen, und die Automatisierung des Konfigurationsprozesses geplant. Um die Ergebnisse der Regressionsanalysen einfach beurteilen zu können wurde mit der Entwicklung eines dem Problem angepassten Visualisierungsprogramms für tabellierte hochdimensionale Daten und ihre KNN-Modelle begonnen (siehe Abbildung 6-4).

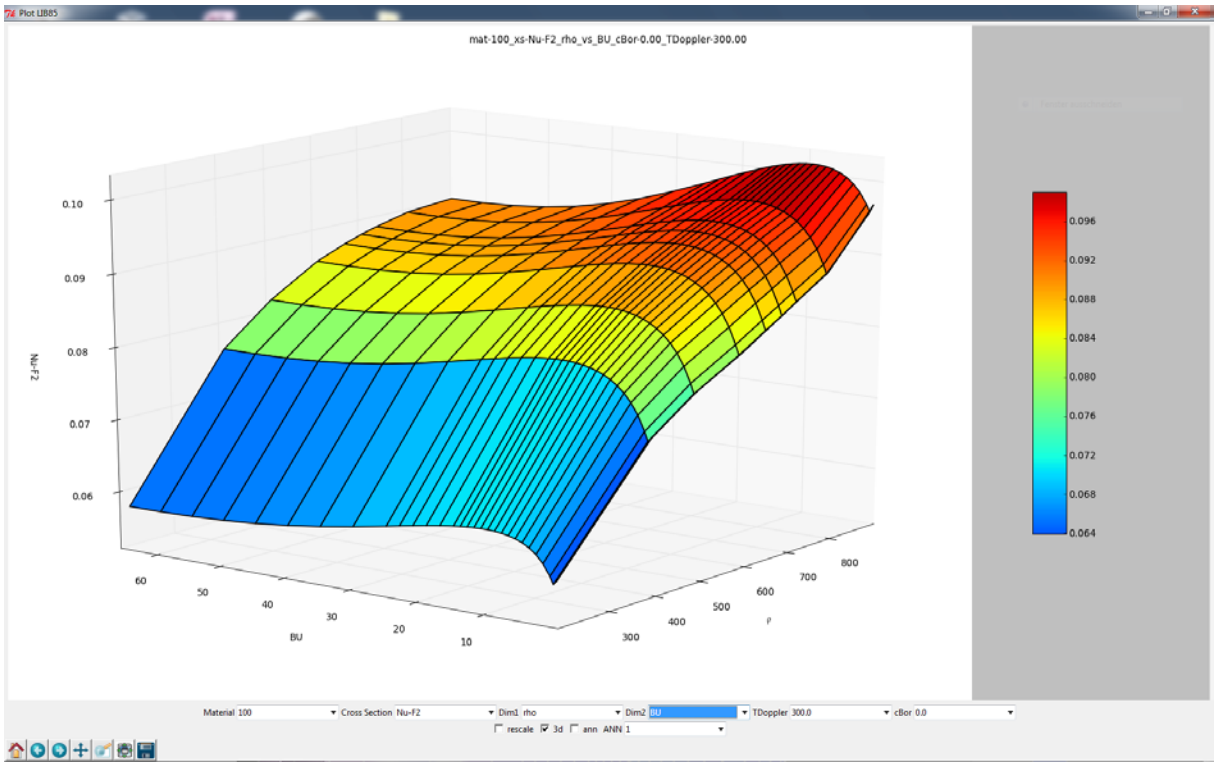

Abbildung 6-4 Visualisierungsprogramm zur Darstellung von hochdimensionalen (d>3) Wirkungsquerschnittsdaten

7 Zusammenfassung

Der vorliegende Bericht gibt den Stand der Arbeiten am BMWi-Forschungsvorhaben RS1503 „Entwicklung und Einsatz von Neutronentransportmethoden und Unsicherheitsanalysen für Reaktorkernberechnungen“ zum Ende des 1. Quartals 2013 wieder. Die durchgeführten Arbeiten dienen dem Ziel der Weiterentwicklung, Validierung und Anwendung von deterministischen und stochastischen Rechenprogrammen, und von Methoden zu Unsicherheits- und Sensitivitätsanalysen, sowie der Erprobung künstlicher neuronaler Netze, zur Bereitstellung einer vollständigen nuklearen Rechenkette.

Bezüglich deterministischer Rechenmethoden wurde damit begonnen, das Programm nTRACER, das den Neutronentransport mittels der Methode der Charakteristiken beschreibt, in das nukleare Programmsystem der GRS zu integrieren. Die bisher durchgeführten Berechnungen zeigen sehr gute Übereinstimmung mit Monte-Carlo-Referenzlösungen. Hinsichtlich einer effizienten und codeübergreifend vereinheitlichten Wirkungsquerschnittsdatenbank wurde ein plattformunabhängiges Programm FILEREADER entwickelt, welches mittels der TRITON-Sequenz erzeugte Wirkungsquerschnittsdaten aus dem SCALE-eigenen ASCII-Format in das weitverbreitete hierarchische HDF5-Datenformat überführt. Die so erzeugte Datenbank ist leicht erweiterbar und auch für die Aufnahme zusätzlicher Daten wie Ergebnissen der Flussberechnung geeignet. Der für die Berechnung von Kerntransienten, insbesondere auch im Rahmen von Unsicherheitsanalysen, nach wie vor benötigte Diffusionscode QUABOX/CUBBOX wurde einer substantiellen Modernisierungen unterzogen. Die zunehmende Komplexität des Codes erforderte die Umstrukturierung und die Aufteilung des Codes in klar definierte Module sowie deren Schnittstellen. Durch eine Verbesserung der in QUABOX/CUBBOX verwendeten Prozeduren wurde für Testfälle die benötigte CPU-Zeit um mehr als zwei Größenordnungen reduziert. Zur konsistenten Homogenisierung von Wirkungsquerschnitten auf Stabzellbasis wurde die Entwicklung und Anwendung der sog. „Superhomogenization“-Methode (SPH) für den Diffusionscode QUABOX/CUBBOX und den Transportcode NEWT weitergeführt und auf drei Raumdimensionen erweitert. Die Ergebnisse sind noch nicht völlig zufriedenstellend, was vermutlich an einer noch nicht optimalen Reflektormodellierung liegt. Im Rahmen eines Rechenbenchmarks mit IRSN wurden Ganzkernberechnungen für zwei generische EPR-Kerne durchgeführt. Auch hier kommen für Unterschiede in den Leistungsverteilungen zwischen den Ergebnissen der verschiedenen Simulationscodes hauptsächlich Unterschiede in den Reflektormodellen in Frage.

Bezüglich der Monte-Carlo-Rechenmethoden wurde das Programm MCNP5 dahingehend erweitert, dass detaillierte Teilchendichte- und Temperaturverteilungen für hohe Ortsauflösung effizient berücksichtigt werden können. Dadurch werden insbesondere Anordnungen mit regulären Gittern (rechteckig, hexagonal) mit Hilfe der in MCNP vorgesehenen "Repeated Structures" geometrisch beschrieben, die Material- und Temperaturspezifikation jedoch über interne Funktionen berücksichtigt. Über die eingeführten internen Funktionen können detaillierte Nukliddichte- und Temperaturverteilungen für Brennstoff, Moderator und Strukturmaterialien definiert werden. Die bisher durchgeführten Modifikationen an MCNP wurden durch Testrechnungen an Systemen mit Rechtecks- und hexagonaler Geometrie überprüft; diese zeigten korrekte Ergebnisse. Ferner kann die Temperaturinterpolation über die internen Funktionen vorgenommen werden, ohne dass der Standard-Input geändert werden muss. Vergleichsrechnungen mit Daten bei spezifizierten Temperaturen und entsprechenden Daten, die durch Interpolation auf einem groben Netz von Stützstellen erzeugt wurden, legen nahe, dass die Daten aus der Interpolation ausreichend genaue Ergebnisse liefern. MCNP-Berechnungen mit JEFF-3.1.1- und ENDF/B-VII-Daten für alle Anordnungen aus der Serie von VENUS7-Experimenten liefern ausgezeichnete Übereinstimmung im Multiplikationsfaktor. Etwas größere Abweichungen zeigen sich bei der Ermittlung des Anteils von verzögerten Neutronen, der zwar auf die Kritikalität keinen Einfluss hat, aber für das dynamische Verhalten eines Systems mit Spaltmaterial eine wesentliche Rolle spielt.

Bezüglich der Methoden zur Unsicherheits- und Sensitivitätsanalyse wurden die Arbeiten zum UAM-LWR-Benchmark Phase I (Neutronenphysik) vervollständigt. Die Ergebnisse wurden beim UAM-6-Workshop 2012, vorgestellt und dem Benchmark-Team übergeben. Damit liegt ein nahezu vollständiger Satz von Ergebnissen aus Unsicherheitsanalysen mit XSUSA und den entsprechenden Neutronentransportprogrammen für die einzelnen Teile vor: Zell-und Gitterberechnungen für die Reaktoren Three Mile Island 1, Peach Bottom 2, Kozloduy 6, zwei EPR-Kerne mit Uran-und MOX-Beladung, sowie die kritische Anordnung KRITZ 2, Kernberechnungen für Three Mile Island 1 und generische EPR-Kerne. Die stationären Unsicherheitsanalysen von Ganzkernanordnungen das "PWR MOX/UO_2 Core Transient Benchmark" wurden auf den Fall "Steuerstabauswurf-Transiente" erweitert. Es wurden 100 Rechnungen durchgeführt und statistisch ausgewertet. Die Ergebnisse der Unsicherheitsanalysen zeigen erheblichen Einfluss der nuklearen Kovarianzdaten auf Ergebnisgrößen wie den Zeitverlauf der Reaktorleistung. Auf der Basis von JENDL-4 wurden in Ergänzung zu den SCALE-

Kovarianzmatrizen Unsicherheitsdaten für die pro Spaltung erzeugte Anzahl von verzögerten Neutronen erstellt. Mit den so ergänzten Unsicherheitsdaten wurden Berechnungen durchgeführt, um den Einfluss der Unsicherheit der nuklearen Daten auf den effektiven verzögerten Neutronenanteil zu ermitteln. Dabei spielt die Unsicherheit in der pro Spaltung erzeugten Anzahl von verzögerten Neutronen eine wesentliche Rolle. Vergleiche mit störungstheoretischen Analysen zeigen sehr gute Übereistimmung. Für die Verwendung mit Monte-Carlo-Codes zur direkten Simulation des Neutronentransports wurde eine Methode entwickelt, bei der Unsicherheitsanalysen mit XSUSA bei gleichzeitiger Berücksichtigung aleatorischer und epistemischer Unsicherheiten durchgeführt werden können („schnelle GRS-Methode“). Die Anwendung dieser Methode mit Kritikalitätsberechnungen liefert Ergebnisse, die mit den Ergebnissen nach der herkömmlichen Methode konsistent sind, bei erheblichen Rechenzeiteinsparungen.

Künstliche neuronale Netze wurden zur Interpolation von diskreten nuklearen Wirkungsquerschnittsdaten eingesetzt. An einem zweidimensionalen Testproblem zeigten sich die Vorteile dieser Methode gegenüber der Interpolation mit Polynomen erster und dritter Ordnung in stark nichtlinearen Bereichen der zu approximierenden Funktion. Im nächsten Schritt ist zu klären, ob die eingesetzten Techniken zur Initialisierung und zur Sicherstellung der Verallgemeinerungsfähigkeit der neuronalen Modelle auch bei höherdimensionalen Beispielen eine gute Rekonstruktion der vorliegenden Daten ermöglichen.

8 Literaturverzeichnis

/ANL 05/ Argonne National Laboratory, Korea Atomic Energy Research Institute, Purdue University, Seoul National University, *The Numerical Nuclear Reactor for High Fidelity Integrated Simulation of Neutronic, Thermal-Hydraulic and Thermo-Mechanical Phenomena*, (2005)

/BER 10/ W. Bernnat, M. Mattes, A. Pautz, W. Zwermann, *Monte Carlo Applications with Consideration of Detailed Material Composition and Temperature Distributions in LWR and HTR*, SNA+MC 2010, Tokyo, Oct. 18-21, 2010

/BIS 96/ C.M. Bishop, *Neural Networks for Pattern Recognition*, Oxford University Press, (1996)

/BLA 12/ D. Blanchet, L. Buiron, N. Stauff, T.- K. Kim, T. Taiwo, *AEN – WPRS Sodium Fast Reactor Core Definitions*, http://www.oecd-nea.org/science/wprs/sfr-taskforce/WPRS-AEN-SFR-Cores-V1.2.pdf

/BRE 97/ M. M. Bretscher, *Evaluation of Reactor Kinetics Parameters Without the Need for Perturbation Codes*, Proc. Int. Meeting on Reduced Enrichment for Research & Test Reactors, Jackson Hole, Wyoming. USA, Okt. 1997.

/BRO 12/ F.B. Brown, W.-R. Martin, G. Yesilyurt, S. Wilderman, *Progress with On-The-Fly neutron Doppler Broadening in MCNP*, Trans. Am. Nuc. Soc. 106 (2012)

/C5G7 03/ *Benchmark on Deterministic Transport Calculations Without Spatial Homogenisation - A 2-D/3-D MOX Fuel Assembly Benchmark*, OECD, Paris, (2003)

/DOW 02/ T. Downar, et al., *PARCS: Purdue Advanced Reactor Core Simulator*, PHYSOR 2002, Oct. 7 – 10, Seoul, Korea (2002)

/GLO 10/ X. Glorot, Y. Bengio, *Understanding the Difficulty of Training Deep Feedforward Neural Networks*, JMLR W&CP: Proceedings of the Thirteenth International Conference on Artificial Intelligence and Statistics; 249-256 (2010)

/GRE 01/ N.M. Greene, M.E. Dunn, *The AMPX-2000 Operating System for Producing Continuous Energy and Multi-Group Cross Sections from Basic Data Libraries Using the ENDF/B-6 Formats*, International Conference on Nuclear Data for Science and Technology (ND2001), Tsukuba, Japan (2001)

/GRU 00/ U. Grundmann, U. Rohde, S. Mittag, *DYN3D – Three Dimensional Core Model for Steady-State and Transient Analysis of Thermal Reactors*, ANS Int. Topical Meeting on Advances in Reactor Physics, PHYSOR 2000, Pittsburgh, USA, May 7-11, 2000

/HER 11/ M. Herman, *Development of ENDF/B-VII.1 and Its Covariance Components*, Journal of the Korean Physical Society, 59, pp.1034–1039 (2011)

/KIM 12/ T.-K. Kim, B. Feng, N. Stauff, and T. Taiwo, *Numerical Results for 1000 MWth Sodi-um-cooled Fast Reactor Benchmark*, Progress Meeting of SFR Benchmark Task Force, OECD/NEA-WPRS, Chicago, USA (2012)

/KLE 11/ M. Klein, L. Gallner, B. Krzykacz-Hausmann, A. Pautz, W. Zwermann, Influence of Nuclear Data Uncertainties on Reactor Core Calculations. Kerntechnik 76(2011)03, S. 174-178.

/KOD 11/ I. Kodeli, *The SUSD3D Code for Cross-Section Sensitivity and Uncertainty Analysis – Recent Development*, Trans. Am. Nucl. Soc., 104, S.791-793 (2011).

/KOL 91/ V.A. Kolmogorov, *On the Representation of Continuous Functions of Several Variables as Superpositions of Continuous Functions of one Variable and Addition*, In: V.M. Tikhomirov: Selected Works of A. N. Kolmogorov; Mathematics and Its Applications; 383-387; Springer (1991)

/KON 08/ J. Koning, D. Rochman, *Towards Sustainable Nuclear Energy: Putting Nuclear Physics to Work*, Annals of Nucl. Energy, 35, pp.2024-2030 (2008).

/KOZ 06/ T. Kozlowski, T. J. Downar, *Pressurised Water Reactor MOX/UO_2 Core Transient Benchmark, Final Report,* December 2006, NEA/NSC/DOC(2006)

/KRZ 94/ B. Krzykacz, E. Hofer, M. Kloos, *A Software System for Probabilistic Uncertainty and Sensitivity Analysis of Results from Computer Models*, International Conference on Probabilistic Safety Assessment and Management (PSAM-II), San Diego (1994)

/LAN 04/ S. Langenbuch, K.-D. Schmidt, K. Velkov, *Analysis of OECD/NRC Turbine Trip Benchmark by the Coupled-Code System ATHLET-QUABOX/CUBBOX*, Nucl. Sci. Eng. 148, pp. 270-280 (2004)

/LAN 09/ S. Langenbuch, A. Pautz and W. Zwermann, W. Bernnat, M. Mattes, *Influence of Nuclear Data Evaluations on Full Scale Reactor Core Calculations,* M&C 2009, Saratoga Springs, New York, May 3-7, (2009)

/LER 98/ G. Lerchl, H. Austregesilo, *ATHLET Mod 1.2 Cycle A, User's Manual, Rev. 1*, GRS-P-1/Vol. 1 (1998)

/NEA 07/ *OECD Benchmark for Uncertainty Analysis in Best-Estimate Modeling (UAM) for Design, Operation and Safety Analysis of LWRs*, NEA/NSC/DOC(2007)4

/NEA 11/ *International Handbook of Evaluated Criticality Safety Benchmark Experiments*, OECD/NEA, NEA/NSC/DOC(95)03, Paris (2011).

/NEU 10/ J. C. Neuber, *Proposal for an UACSA benchmark study on the reactivity impacts of manufacturing tolerances of parameters characterizing a fuel assembly configuration*, http://www.oecd-nea.org/science/wpncs/UACSA/

/PAU 03a/ A. Pautz, A. Birkhofer, *DORT-TD: A Transient Neutron Transport Code with Fully Implicit Time Integration*, Nucl. Sci. Eng. Vol. 145, pp. 299-319, (2003)

/PUE 09/ F. Puente Espel, M. Avramova, K. Ivanov, *High Accuracy Modeling for Advanced Nuclear Reactor Core Designs Using Monte Carlo Based Coupled Calculations,* M&C 2009, Saratoga Springs, New York, May 3-7, (2009)

/QC 78/ *QUABOX/CUBBOX, Version 02: Ein Grobgitterverfahren zur Lösung von Neutronendiffusionsgleichungen, Programmbeschreibung*, GRS-A-160 (1978)

/SAN 09/ V. Sanchez, A. Al-Hamry, *Development OF A Coupling Scheme between MCNP and COBRA-TF for the Prediction of the Pin Power of a PWR Fuel Assembly*, M&C 2009, Saratoga Springs, New York, May 3-7, (2009)

/SAN 09a/ A. Santamarina et al., *The JEFF-3.1.1 Nuclear Data Library*, JEFF Report 22, ISBN 978-92-64-99074-6, (2009)

/SCA 09/ *SCALE: A Modular Code System for Performing Standardized Computer Analyses for Licensing, Version 6,* ORNL/TM-2005/39, (2009)

/SEU 04/ A. Seubert, S. Langenbuch, W. Zwermann, *Entwicklung des zeitabhängigen 3D-S_N-Neutronen-Transportcodes TORT-TD*, GRS-A-3237, Nov. 2004

/SEU 08/ A. Seubert, K. Velkov, S. Langenbuch, *The Time-Dependent 3D Discrete Ordinates Code TORT-TD with Thermal-Hydraulic Feedback by ATHLET Models*, PHYSOR 2008, September 14-19, Interlaken, Switzerland, (2008)

/SJE 10/ B. L. Sjenitzer, J. E. Hoogenboom, *A Monte Carlo Method for Calculation on the Dynamic Behaviour of Nuclear Reactors*, SNA+MC 2010, Tokyo, Oct. 18-21, (2010)

/SNU 09/ Seoul National University, Department of Nuclear Engineering, nTRACER Homepage: http://neutron.snu.ac.kr/research02-1.html

/UAC 08/ Expert Group on Uncertainty Analyses for Criticality Safety Assessment, *http://www.oecd-nea.org/science/wpncs/UACSA*

/WIA 06/ D. Wiarda, M.E. Dunn, PUFF-IV: *A Code for Processing ENDF Uncertainty Data into Multigroup Covariance Matrices*, ORNL/TM-2006/147/R1, Okt. 2006.

/X-5 03/ X-5 Monte Carlo Team, *MCNP – A General Monte Carlo N-Particle Transport Code, Version 5*, LA-UR-03-1987 (2003)

/X-5 12/ *Initial MCNP6 Release Overview MCNP6 Beta 2*, Los Alamos National Laboratory, Report LA-UR-11-07082.

/ZUE 13/ E. Zuev, Neurolab Homepage: https://code.google.com/p/neurolab/

/ZWE 08/ W. Zwermann, S. Langenbuch, B.-C. Na, E. Sartori, U.-K. Wehmann, *Summary of the Results of the VENUS-7 Benchmark*, PHYSOR 2008, September 14-19, Interlaken, Switzerland, (2008)

/ZWE 09/ W. Zwermann, B. Krzykacz-Hausmann, L. Gallner, A. Pautz, *Influence of Nuclear Covariance Data on Reactor Core Calculations*, WONDER 2009, Sep. 29 – Oct. 2, Cadarache (2009)

/ZWE 10a/ W. Zwermann, B. Krzykacz-Hausmann, L. Gallner, A. Pautz, *Uncertainty Analyses with Nuclear Covariance Data in Reactor Core Calculations*, Jahrestagung Kerntechnik 2010, May 04-06, Berlin, (2010)

/ZWE 10b/ W. Zwermann, B. Krzykacz-Hausmann, L. Gallner, A. Pautz, M. Mattes, *Uncertainty Analyses with Nuclear Covariance Data in Reactor Core Calculations*. Int. Conf. Nuclear Data for Science and Technology ND 2010, Jeju, Korea (2010)

/ZWE 11/ W. Zwermann, L. Gallner, M. Klein, B. Krzykacz-Hausmann, A. Pautz, D. Wiarda, M. L. Williams, M. A. Jessee, B. T. Rearden, *Nuclear Data Uncertainty Analysis for a Fuel Assembly Criticality Benchmark.* Intl. Conf. on Nuclear Criticality (ICNC) 2011, Edinburgh (2011).

9 Anhänge

Anhang A: Technische Notiz

L. Gallner, M. Klein, W. Zwermann: Sensitivitäts- und Unsicherheitsanalysen mit XSUSA zum „BENCHMARK FOR UNCERTAINTY ANALYSIS IN MODELING (UAM) FOR DESIGN, OPERATION AND SAFETY ANALYSIS OF LWRs (Phase 1)“

Anhang B: Veröffentlichungen

B1: L. Gallner, M. Klein, B. Krzykacz-Hausmann, A. Pautz, K. Velkov, W. Zwermann, "Sampling Based Nuclear Data Uncertainty Analysis in Mixed LWR Calculations", IAEA Technical Meeting on Fuel Design and Licensing of Mixed Cores for Water Cooled Reactors, Wien, 12.-14.12.2011.

B2: W. Bernnat, M. Buck, M. Mattes, W. Zwermann, I. Pasichnyk, K. Velkov, "Coupled Monte Carlo Neutronics and Thermal Hydraulics for Power Reactors", PHYSOR, Knoxville, TN, USA, 15.-20.04.2012.

B3: A. Yankov, M. Klein, M. A. Jessee, W. Zwermann, K. Velkov, A. Pautz, B. Collins, T. Downar, "Comparison of XSUSA and TWO-STEP Approaches for Full-Core Uncertainty Quantification", PHYSOR, Knoxville, TN, USA, 15.-20.04.2012.

B4: M. Williams, D. Wiarda, H. Smith, M. A. Jessee, B. T. Rearden, W. Zwermann, M. Klein, A. Pautz, B. Krzykacz-Hausmann, L. Gallner, "Development of a Statistical Sampling Method for Uncertainty Analysis with Scale", PHYSOR, Knoxville, TN, USA, 15.-20.04.2012.

B5: W. Zwermann, B. Krzykacz-Hausmann, L. Gallner, M. Klein, A. Pautz, K.Velkov, "Aleatoric and Epistemic Uncertainties in Sampling Based Nuclear Data Uncertainty and Sensitivity Analyses", PHYSOR, Knoxville, TN, USA, 15.-20.04.2012.

B6: I. Pasichnyk, M. Klein, K. Velkov, W. Zwermann, A. Pautz, "Nuclear Data Uncertainties by the PWR MOX/UO2 Core Rod Ejection Benchmark", PHYSOR, Knoxville, TN, USA, 15.-20.04.2012.

B7: M. Klein, L. Gallner, B. Krzykacz-Hausmann, A. Pautz, K. Velkov, W. Zwermann, "Interaction of Loading Pattern and Nuclear Data Uncertainties in Reactor Core Calculations", PHYSOR, Knoxville, TN, USA, 15.-20.04.2012.

B8: E. Lemarchand, M. Klein, I. Pasichnyk, K. Velkov, W. Zwermann, "Pin-by-Pin Calculations with QUABOX/CUBBOX using the Super Homogenization Method", Jahrestagung Kerntechnik, Stuttgart, 22.-24.05.2012..

B9: L. Gallner, M. Klein, B. Krzykacz-Hausmann, A. Pautz, K. Velkov, W. Zwermann, "Application of XSUSA with Aleatoric and Epistemic Uncertainties", Jahrestagung Kerntechnik, Stuttgart, 22.-24.05.2012.

B10: A. Yankov, B. Collins, M. Klein, M.A. Jessee, W. Zwermann, K. Velkov, A. Pautz, T. Downar, "A Two-Step Approach to Uncertainty Quantification of Core Simulators", Science and Technology of Nuclear Installations, Volume 2012, (2012), Article ID 767096.

B11: W. Zwermann, L. Gallner, M. Klein, B. Krzykacz-Hausmann, I. Pasichnyk, A. Pautz, K. Velkov, "Status of XSUSA for Sampling Based Nuclear Data Uncertainty and Sensitivity Analysis", EPJ Web of Conferences 42, 03003 (2013).

B12: I. Kodeli, W. Zwermann, "Evaluation of Uncertainties in β_{eff} by Means of Deterministic and Monte Carlo Methods", International Conference on Nuclear Data for Science and Technology, New York, 4.-8. März 2013.

B13: D. Rochman, S.C. van der Marck, A.J. Koning, H. Sjöstrand, W. Zwermann, "Uncertainty Propagation with Fast Monte Carlo Techniques", International Conference on Nuclear Data for Science and Technology, 4.-8. März 2013.

Anhang A

Technische Notiz: Sensitivitäts- und Unsicherheitsanalysen mit XSUSA zum „BENCHMARK FOR UNCERTAINTY ANALYSIS IN MODELING (UAM) FOR DESIGN, OPERATION AND SAFETY ANALYSIS OF LWRs (Phase 1)“

L. Gallner, M. Klein, W. Zwermann

Gesellschaft für Anlagen- und Reaktorsicherheit (GRS) mbH
Forschungszentrum, Boltzmannstraße 14
85748 Garching

März 2013

Diese Notiz enthält die Beiträge der GRS zum „BENCHMARK FOR UNCERTAINTY ANALYSIS IN MODELING (UAM) FOR DESIGN, OPERATION AND SAFETY ANALYSIS OF LWRs (Phase 1)“, die in der Originalfassung in Form von Excel-Dateien abgegeben wurden, in Textform. Zur besseren Zuordnung der Ergebnisse zu den spezifizierten Problemen /NEA 07/ werden die englischen Originalbezeichnungen beibehalten. Die Ergebnisse wurden im Februar/März 2012 eingereicht, auf dem UAM-6-Workshop, Mai 2012, Karlsruhe, vorgestellt, und seitdem an die Formatvorlagen angepasst.

1 Exercise I-1: Cell Physics

1.1 BWR PB-2 (Peach Bottom 2)

Name of Participant(s)		E-mail Address	
Markus Klein		markus.klein@grs.de	
Winfried Zwermann		winfried.zwermann@grs.de	
Organization	Gesellschaft für Anlagen- und Reaktorsicherheit (GRS)mbH		
Country	Germany		
Reactor Name	*PB-2*		
Operating Condition	*Hot Zero Power*		
Reactor type	*BWR*		
Nuclear Data Library Used	*ENDF/B-VII*		
Covariance Data Library Used	*SCALE 6.0 (44groups)*		
Computer Code Used	*XSUSA / NEWT*		
Criticality Calculation Method	*two-dimensional (2-D) discrete-ordinates transport*		
Uncertainty Calculation Method	*sampling method*		
k_{inf} (forward)	**k_{inf} (adjoint)**	**uncertainties** absolute Δk	**uncertainties** relative Δk/k [%]
1.34366		*0.00701*	*0.52%*
Top 5 contributors the uncertainty in k_{inf}		**uncertainties** absolute Δk	**uncertainties** relative Δk/k [%]
one-group microscopic cross-section	**mean value**	**uncertainty** absolute standard deviation	**uncertainty** (% relative standard deviation)
absorption			
U235	*6.06367E+01*	*6.85171E-01*	*1.13%*
U238	*9.29471E-01*	*8.79288E-03*	*0.95%*
fission			
U235	*4.98429E+01*	*5.70359E-01*	*1.14%*
U238	*9.38947E-02*	*4.08522E-03*	*4.35%*

Name of Participant(s)		E-mail Address	
Markus Klein		markus.klein@grs.de	
Winfried Zwermann		winfried.zwermann@grs.de	
Organization	Gesellschaft für Anlagen- und Reaktorsicherheit (GRS)mbH		
Country	Germany		
Reactor Name	*PB-2*		
Operating Condition	*Hot Full Power*		
Reactor type	*BWR*		
Nuclear Data Library Used	*ENDF/B-VII*		
Covariance Data Library Used	*SCALE 6.0 (44groups)*		
Computer Code Used	*XSUSA / NEWT*		
Criticality Calculation Method	*two-dimensional (2-D) discrete-ordinates transport*		
Uncertainty Calculation Method	*sampling method*		
k_{inf} (forward)	**k_{inf} (adjoint)**	**uncertainties** absolute Δk	**uncertainties** relative Δk/k [%]
1.22760		*0.00762*	*0.62%*
Top 5 contributors the uncertainty in k_{inf}		**uncertainties** absolute Δk	**uncertainties** relative Δk/k [%]
one-group microscopic cross-section	**mean value**	**uncertainty** absolute standard deviation	**uncertainty** (% relative standard deviation)
absorption			
U235	*4.07302E+01*	*5.58987E-01*	*1.37%*
U238	*8.63286E-01*	*8.22706E-03*	*0.95%*
fission			
U235	*3.28357E+01*	*4.53670E-01*	*1.38%*
U238	*8.83916E-02*	*4.65950E-03*	*5.27%*

1.2 PWR TMI-1 (Three Mile Island 1)

Name of Participant(s)		E-mail Address	
Markus Klein		markus.klein@grs.de	
Winfried Zwermann		winfried.zwermann@grs.de	
Organization	Gesellschaft für Anlagen- und Reaktorsicherheit (GRS)mbH		
Country	Germany		
Reactor Name	*TMI-1*		
Operating Condition	*Hot Zero Power*		
Reactor type	*PWR*		
Nuclear Data Library Used	*ENDF/B-VII*		
Covariance Data Library Used	*SCALE 6.0 (44groups)*		
Computer Code Used	*XSUSA / NEWT*		
Criticality Calculation Method	*two-dimensional (2-D) discrete-ordinates transport*		
Uncertainty Calculation Method	*sampling method*		
k_{inf} (forward)	**k_{inf} (adjoint)**	**uncertainties** absolute Δk	**uncertainties** relative Δk/k [%]
1.42471		*0.00691*	*0.49%*
Top 5 contributors the uncertainty in k_{inf}		**uncertainties** absolute Δk	**uncertainties** relative Δk/k [%]
one-group microscopic cross-section	**mean value**	**uncertainty** absolute standard deviation	**uncertainty** (% relative standard deviation)
absorption			
U235	*4.35600E+01*	*5.15294E-01*	*1.18%*
U238	*9.27480E-01*	*8.66190E-03*	*0.93%*
fission			
U235	*3.52838E+01*	*4.21658E-01*	*1.20%*
U238	*1.01025E-01*	*4.24205E-03*	*4.20%*

Name of Participant(s)		E-mail Address	
Markus Klein		markus.klein@grs.de	
Winfried Zwermann		winfried.zwermann@grs.de	
Organization	Gesellschaft für Anlagen- und Reaktorsicherheit (GRS)mbH		
Country	Germany		
Reactor Name	*TMI-1*		
Operating Condition	*Hot Full Power*		
Reactor type	*PWR*		
Nuclear Data Library Used	*ENDF/B-VII*		
Covariance Data Library Used	*SCALE 6.0 (44groups)*		
Computer Code Used	*XSUSA / NEWT*		
Criticality Calculation Method	*two-dimensional (2-D) discrete-ordinates transport*		
Uncertainty Calculation Method	*sampling method*		
k_{inf} (forward)	**k_{inf} (adjoint)**	**uncertainties** absolute Δk	**uncertainties** relative Δk/k [%]
1.40628		*0.00692*	*0.49%*
Top 5 contributors the uncertainty in k_{inf}		**uncertainties** absolute Δk	**uncertainties** relative Δk/k [%]
one-group microscopic cross-section	**mean value**	**uncertainty** absolute standard deviation	**uncertainty** (% relative standard deviation)
absorption			
U235	*4.24358E+01*	*5.08250E-01*	*1.20%*
U238	*9.48317E-01*	*8.92300E-03*	*0.94%*
fission			
U235	*3.43171E+01*	*4.14991E-01*	*1.21%*
U238	*1.01027E-01*	*4.27881E-03*	*4.24%*

1.3 VVER KOZ-6 (Kozloduy 6)

Name of Participant(s)		E-mail Address	
Markus Klein		markus.klein@grs.de	
Winfried Zwermann		winfried.zwermann@grs.de	
Organization	Gesellschaft für Anlagen- und Reaktorsicherheit (GRS)mbH		
Country	Germany		
Reactor Name	*KOZ-6*		
Operating Condition	*Hot Zero Power*		
Reactor type	*VVER 1000*		
Nuclear Data Library Used	*ENDF/B-VII*		
Covariance Data Library Used	*SCALE 6.0 (44groups)*		
Computer Code Used	*XSUSA / NEWT*		
Criticality Calculation Method	*two-dimensional (2-D) discrete-ordinates transport*		
Uncertainty Calculation Method	*sampling method*		
k_{inf} (forward)	**k_{inf} (adjoint)**	**uncertainties** absolute Δk	**uncertainties** relative Δk/k [%]
1.33937		*0.00686*	*0.51%*
Top 5 contributors the uncertainty in k_{inf}		**uncertainties** absolute Δk	**uncertainties** relative Δk/k [%]
one-group microscopic cross-section	**mean value**	**uncertainty** absolute standard deviation	**uncertainty** (% relative standard deviation)
absorption			
U235	*5.87926E+01*	*6.44932E-01*	*1.10%*
U238	*1.00690E+00*	*9.64511E-03*	*0.96%*
fission			
U235	*4.81994E+01*	*5.36014E-01*	*1.11%*
U238	*9.43542E-02*	*3.84410E-03*	*4.07%*

Name of Participant(s)		E-mail Address	
Markus Klein		markus.klein@grs.de	
Winfried Zwermann		winfried.zwermann@grs.de	
Organization	Gesellschaft für Anlagen- und Reaktorsicherheit (GRS)mbH		
Country	Germany		
Reactor Name	*KOZ-6*		
Operating Condition	*Hot Full Power*		
Reactor type	*VVER 1000*		
Nuclear Data Library Used	*ENDF/B-VII*		
Covariance Data Library Used	*SCALE 6.0 (44groups)*		
Computer Code Used	*XSUSA / NEWT*		
Criticality Calculation Method	*two-dimensional (2-D) discrete-ordinates transport*		
Uncertainty Calculation Method	*sampling method*		
k_{inf} (forward)	**k_{inf} (adjoint)**	**uncertainties** absolute Δk	**uncertainties** relative Δk/k [%]
1.32179		*0.00685*	*0.52%*
Top 5 contributors the uncertainty in k_{inf}		**uncertainties** absolute Δk	**uncertainties** relative Δk/k [%]
one-group microscopic cross-section	**mean value**	**uncertainty** absolute standard deviation	**uncertainty** (% relative standard deviation)
absorption			
U235	*5.74500E+01*	*6.37231E-01*	*1.11%*
U238	*1.02935E+00*	*9.88036E-03*	*0.96%*
fission			
U235	*4.70496E+01*	*5.28813E-01*	*1.12%*
U238	*9.44567E-02*	*3.87383E-03*	*4.10%*

1.4 PWR GEN-III (Generation-III European Pressurized Water Reactor)

Name of Participant(s)		E-mail Address	
Markus Klein		markus.klein@grs.de	
Winfried Zwermann		winfried.zwermann@grs.de	
Organization	Gesellschaft für Anlagen- und Reaktorsicherheit (GRS)mbH		
Country	Germany		
Reactor Name	*GEN-III*		
Operating Condition	*Hot Full Power*		
Reactor type	*PWR*		
Nuclear Data Library Used	*ENDF/B-VII*		
Covariance Data Library Used	*SCALE 6.0 (44groups)*		
Computer Code Used	*XSUSA / NEWT*		
Criticality Calculation Method	*two-dimensional (2-D) discrete-ordinates transport*		
Uncertainty Calculation Method	*sampling method*		
k_{inf} (forward)	**k_{inf} (adjoint)**	**uncertainties** absolute Δk	**uncertainties** relative Δk/k [%]
1.10332		*0.01015*	*0.92%*
Top 5 contributors the uncertainty in k_{inf}		**uncertainties** absolute Δk	**uncertainties** relative Δk/k [%]
one-group microscopic cross-section	**mean value**	**uncertainty** absolute standard deviation	**uncertainty** (% relative standard deviation)
absorption			
U235	*1.52596E+01*	*2.19256E-01*	*1.44%*
U238	*9.05526E-01*	*8.63827E-03*	*0.95%*
fission			
U235	*1.10591E+01*	*1.41729E-01*	*1.28%*
U238	*1.17829E-01*	*4.68205E-03*	*3.97%*

1.5 KRITZ-2 (Uranium and MOX Fuel Critical Assemblies)

Name of Participant(s)		E-mail Address	
Markus Klein		markus.klein@grs.de	
Winfried Zwermann		winfried.zwermann@grs.de	
Organization	Gesellschaft für Anlagen- und Reaktorsicherheit (GRS)mbH		
Country	Germany		
Reactor Name	*KRITZ-2*		
Operating Condition	*Cold/Hot Zero Power*		
Reactor type	*LWR critical assembly*		
Nuclear Data Library Used	*ENDF/B-VII*		
Covariance Data Library Used	*SCALE 6.0 (44groups)*		
Computer Code Used	*XSUSA / XSDRN*		
Criticality Calculation Method	*one-dimensional (1-D) discrete-ordinates transport*		
Uncertainty Calculation Method	*sampling method*		
k_{inf} (forward)	**k_{inf} (adjoint)**	**uncertainties** absolute Δk	**uncertainties** relative Δk/k [%]
1.23374		*0.00701*	*0.568%*
1.18802		*0.00726*	*0.611%*
1.26609		*0.00664*	*0.524%*
1.23891		*0.00682*	*0.551%*
1.28041		*0.01465*	*1.144%*
1.29757		*0.01471*	*1.134%*
in the order:	KRITZ-2:1 cold		
	KRITZ-2:1 hot		
	KRITZ-2:13 cold		
	KRITZ-2:13 hot		
	KRITZ-2:19 cold		
	KRITZ-2:19 hot		

2 Exercise I-2: Lattice Physics

2.1 BWR PB-2 (Peach Bottom 2)

Name of Participant(s)	E-mail Address
Markus Klein	markus.klein@grs.de
Winfried Zwermann	winfried.zwermann@grs.de

Organization	Gesellschaft für Anlagen- und Reaktorsicherheit (GRS)mbH
Country	Germany

Reactor Name	*PB-2*
Operating Condition	*Hot Zero Power*
Reactor type	*BWR*
Nuclear Data Library Used	*ENDF/B-VII*
Covariance Data Library Used	*SCALE 6.0 (44groups)*
Computer Code Used	*XSUSA / NEWT*
Criticality Calculation Method	*two-dimensional (2-D) discrete-ordinates transport*
Uncertainty Calculation Method	*sampling method*

		(mean) value	uncertainty	rel. uncertainty
k_eff		1.10158E+00	5.55000E-03	0.50382%

homogenized XS	energy group	(mean) value	uncertainty	rel. uncertainty
total	1	5.35135E-01	4.57977E-03	0.85582%
	2	1.39690E+00	1.76490E-03	0.12634%
transport	1	2.11168E-01	4.96109E-03	2.34936%
	2	8.22898E-01	1.49446E-03	0.18161%
diffusion	1	1.57940E+00	3.72865E-02	2.36080%
	2	4.05074E-01	7.35491E-04	0.18157%
absorption	1	6.70218E-03	5.37512E-05	0.80200%
	2	4.83300E-02	9.31002E-05	0.19263%
nu_fission	1	4.46852E-03	5.62935E-05	1.25978%
	2	5.92485E-02	2.69244E-04	0.45443%
kappa_fission	1	5.38948E-14	5.14825E-16	0.95524%
	2	7.55710E-13	2.47675E-15	0.32774%
flux	1	6.76873E-01	2.71701E-03	0.40141%
	2	3.23127E-01	2.71702E-03	0.84085%
inv_velocity	1	2.14326E-08	2.58786E-10	1.20744%
	2	2.30676E-06	1.15573E-09	0.05010%
fission	1	1.76615E-03	1.85202E-05	1.04862%
	2	2.43106E-02	7.96839E-05	0.32777%
scatter	1 -> 1	5.05397E-01	4.27238E-03	0.84535%
	1 -> 2	2.30753E-02	2.83338E-04	1.22788%
	2 -> 1	0.00000E+00	0.00000E+00	#DIV/0!
	2 -> 2	1.34857E+00	1.76715E-03	0.13104%
delayed_lambda	1	1.24938E-02	2.57177E-06	0.02058%
	2	3.07524E-02	5.00623E-06	0.01628%
	3	1.13579E-01	9.16021E-05	0.08065%
	4	3.06451E-01	1.85963E-04	0.06068%
	5	1.18882E+00	8.32412E-04	0.07002%
	6	3.18043E+00	3.13782E-03	0.09866%
delayed_beta	1	2.22884E-04	3.29667E-08	0.01479%
	2	1.51579E-03	2.60498E-06	0.17186%
	3	1.40429E-03	4.47206E-06	0.31846%
	4	2.92689E-03	1.23033E-05	0.42035%
	5	9.99558E-04	9.64376E-06	0.96480%
	6	3.41676E-04	3.16734E-06	0.92700%
adf	1	9.55426E-01	1.10216E-03	0.11536%
	2	1.24024E+00	7.24704E-04	0.05843%

pin power distribution

mean values

WWC	1	2	3	4	5	6	7
1	1.1025	1.1769	1.051	1.1182	1.1131	1.1639	1.1321
2	1.1769	1.0385	1.19	1.1398	1.1373	1.1805	1.0305
3	1.0511	1.19	0.2616	0.8774	0.874	0.2627	1.1826
4	1.1182	1.1399	0.8775	0.8367	0.8041	0.8851	1.1561
5	1.1131	1.1375	0.8741	0.804	0.2515	0.9487	1.2232
6	1.1639	1.1806	0.2627	0.885	0.9487	1.1254	0.9825
7	1.1321	1.0306	1.1825	1.1559	1.2231	0.9824	1.1132

WWC = wide-wide corner

rel. uncertainties

WWC	1	2	3	4	5	6	7
1	0.10%	0.08%	0.07%	0.04%	0.04%	0.04%	0.06%
2	0.08%	0.09%	0.04%	0.04%	0.04%	0.03%	0.03%
3	0.07%	0.04%	0.76%	0.06%	0.06%	0.76%	0.06%
4	0.04%	0.04%	0.06%	0.06%	0.06%	0.06%	0.09%
5	0.04%	0.04%	0.06%	0.07%	0.76%	0.06%	0.11%
6	0.04%	0.03%	0.76%	0.06%	0.06%	0.09%	0.07%
7	0.06%	0.03%	0.06%	0.09%	0.11%	0.07%	0.12%

Name of Participant(s)	E-mail Address
Winfried Zwermann	winfried.zwermann@grs.de
Markus Klein	markus.klein@grs.de

Organization	Gesellschaft für Anlagen- und Reaktorsicherheit (GRS)mbH
Country	Germany

Reactor Name	*PB-2*
Operating Condition	*Hot Full Power*
Reactor type	*BWR*
Nuclear Data Library Used	*ENDF/B-VII*
Covariance Data Library Used	*SCALE 6.0 (44groups)*
Computer Code Used	*XSUSA / NEWT*
Criticality Calculation Method	*two-dimensional (2-D) discrete-ordinates transport*
Uncertainty Calculation Method	*sampling method*

		(mean) value	uncertainty	rel. uncertainty
k_eff		1.05943E+00	5.96000E-03	0.56257%

homogenized XS	energy group	(mean) value	uncertainty	rel. uncertainty
total	1	3.90751E-01	3.52936E-03	0.90322%
	2	8.66029E-01	1.20772E-03	0.13945%
transport	1	1.75920E-01	4.39942E-03	2.50081%
	2	5.24842E-01	1.10100E-03	0.20978%
diffusion	1	1.89599E+00	4.76889E-02	2.51525%
	2	6.35114E-01	1.33194E-03	0.20972%
absorption	1	6.45488E-03	5.60808E-05	0.86881%
	2	4.29345E-02	8.15686E-05	0.18998%
nu_fission	1	4.12246E-03	5.52349E-05	1.33985%
	2	5.39552E-02	2.45408E-04	0.45484%
kappa_fission	1	4.99551E-14	5.24792E-16	1.05053%
	2	6.88195E-13	2.25413E-15	0.32754%
flux	1	7.59646E-01	2.58619E-03	0.34045%
	2	2.40354E+00	2.58620E-03	0.10760%
inv_velocity	1	2.10953E-08	2.86109E-10	1.35627%
	2	2.06001E-06	1.37050E-09	0.06653%
fission	1	1.63492E-03	1.86664E-05	1.14173%
	2	2.21387E-02	7.25194E-05	0.32757%
scatter	1 -> 1	3.70743E-01	3.31167E-03	0.89325%
	1 -> 2	1.35860E-02	1.88730E-04	1.38915%
	2 -> 1	0.00000E+00	0.00000E+00	#DIV/0!
	2 -> 2	8.23094E-01	1.21322E-03	0.14740%
delayed_lambda	1	1.25274E-02	3.83183E-06	0.03059%
	2	3.08492E-02	7.32270E-06	0.02374%
	3	1.14434E-01	1.37887E-04	0.12049%
	4	3.08283E-01	2.79639E-04	0.09071%
	5	1.20799E+00	1.20458E-03	0.09972%
	6	3.24661E+00	4.56685E-03	0.14067%
delayed_beta	1	2.23790E-04	5.42117E-08	0.02422%
	2	1.52896E-03	3.96793E-06	0.25952%
	3	1.43041E-03	6.79732E-06	0.47520%
	4	3.01211E-03	1.86443E-05	0.61898%
	5	1.07052E-03	1.45963E-05	1.36348%
	6	3.58273E-04	4.82165E-06	1.34580%
adf	1	9.78673E-01	7.62657E-04	0.07793%
	2	1.16557E+00	4.89651E-04	0.04201%

pin power distribution

mean values

WWC	1	2	3	4	5	6	7
1	1.0521	1.1464	1.0326	1.0948	1.0811	1.1158	1.0601
2	1.1464	1.0477	1.2326	1.1719	1.1603	1.1913	0.9959
3	1.0326	1.2327	0.3537	0.9309	0.9224	0.3504	1.17
4	1.0948	1.1719	0.9309	0.8808	0.8471	0.9115	1.1316
5	1.0812	1.1604	0.9225	0.8471	0.3357	0.9588	1.1777
6	1.1158	1.1913	0.3504	0.9115	0.9587	1.0983	0.9222
7	1.0601	0.996	1.17	1.1315	1.1776	0.9222	1.0161

WWC = wide-wide corner

rel. uncertainties

WWC	1	2	3	4	5	6	7
1	0.09%	0.07%	0.05%	0.05%	0.05%	0.06%	0.08%
2	0.07%	0.05%	0.06%	0.05%	0.05%	0.06%	0.03%
3	0.05%	0.06%	0.82%	0.08%	0.07%	0.80%	0.07%
4	0.05%	0.05%	0.08%	0.09%	0.11%	0.05%	0.07%
5	0.05%	0.05%	0.07%	0.11%	0.86%	0.04%	0.09%
6	0.06%	0.06%	0.80%	0.05%	0.04%	0.06%	0.03%
7	0.08%	0.03%	0.07%	0.07%	0.09%	0.03%	0.09%

2.2 PWR TMI-1 (Three Mile Island 1)

Name of Participant(s)	E-mail Address
Markus Klein	markus.klein@grs.de
Winfried Zwermann	winfried.zwermann@grs.de

Organization	Gesellschaft für Anlagen- und Reaktorsicherheit (GRS)mbH
Country	Germany
Reactor Name	*TMI-1*
Operating Condition	*Hot Zero Power*
Reactor type	*PWR*
Nuclear Data Library Used	*ENDF/B-VII*
Covariance Data Library Used	*SCALE 6.0 (44groups)*
Computer Code Used	*XSUSA / NEWT*
Criticality Calculation Method	*two-dimensional (2-D) discrete-ordinates transport*
Uncertainty Calculation Method	*sampling method*

		(mean) value	uncertainty	rel. uncertainty
k_eff		1.41469E+00	6.49000E-03	0.45876%

homogenized XS	energy group	(mean) value	uncertainty	rel. uncertainty
total	1	5.61835E-01	4.77988E-03	0.85076%
	2	1.44441E+00	1.81426E-03	0.12561%
transport	1	2.24937E-01	5.43004E-03	2.41403%
	2	9.44607E-01	1.55680E-03	0.16481%
diffusion	1	1.48276E+00	3.57887E-02	2.41365%
	2	3.52881E-01	5.81626E-04	0.16482%
absorption	1	1.04281E-02	9.08820E-05	0.87151%
	2	1.10253E-01	2.33091E-04	0.21141%
nu_fission	1	9.00225E-03	4.82318E-05	0.53577%
	2	1.91419E-01	8.62313E-04	0.45048%
kappa_fission	1	1.11337E-13	3.95787E-16	0.35549%
	2	2.44197E-12	7.63492E-15	0.31265%
flux	1	8.61714E-01	1.49071E-03	0.17299%
	2	1.38286E-01	1.49071E-03	1.07799%
inv_velocity	1	5.62338E-08	6.77422E-10	1.20465%
	2	2.42460E-06	8.29350E-10	0.03421%
fission	1	3.56745E-03	1.37880E-05	0.38649%
	2	7.85560E-02	2.45705E-04	0.31278%
scatter	1 -> 1	5.33490E-01	4.49957E-03	0.84342%
	1 -> 2	1.79567E-02	2.20246E-04	1.22654%
	2 -> 1	1.64042E-03	4.36074E-06	0.26583%
	2 -> 2	1.33251E+00	1.82131E-03	0.13668%
delayed_lambda	1	1.25089E-02	2.41437E-06	0.01930%
	2	3.08276E-02	4.72865E-06	0.01534%
	3	1.13623E-01	8.57608E-05	0.07548%
	4	3.06679E-01	1.74222E-04	0.05681%
	5	1.20581E+00	7.89532E-04	0.06548%
	6	3.23556E+00	2.96877E-03	0.09175%
delayed_beta	1	2.24610E-04	3.14384E-08	0.01400%
	2	1.50089E-03	2.43466E-06	0.16221%
	3	1.38380E-03	4.18150E-06	0.30218%
	4	2.88985E-03	1.15073E-05	0.39820%
	5	9.76556E-04	9.02126E-06	0.92378%
	6	3.24414E-04	2.96048E-06	0.91256%
adf	1	9.86165E-01	4.16587E-04	0.04224%
	2	1.02919E+00	2.62485E-04	0.02550%

pin power distribution

mean values

	1	2	3	4	5	6	7	8
1	IT	1.0873	1.0336	1.0064	0.9993	1.0027	0.9864	0.995
2	1.0873	1.0613	1.0837	1.0326	1.0273	1.0602	1.0069	0.9995
3	1.0336	1.0837	CR	1.098	1.0983	CR	1.0549	1.0055
4	1.0064	1.0326	1.098	1.0774	1.1126	1.0902	1.005	0.9886
5	0.9993	1.0273	1.0983	1.1126	CR	1.0521	0.9608	0.9609
6	1.0027	1.0602	CR	1.0902	1.0521	0.9554	0.881	0.9165
7	0.9864	1.0069	1.0549	1.005	0.9608	0.881	0.3276	0.8689
8	0.995	0.9995	1.0055	0.9886	0.9609	0.9165	0.8689	0.8683

CR = control rod position
IT = instrumentation tube

rel. uncertainties

.	1	2	3	4	5	6	7	8
1	IT	0.03%	0.02%	0.02%	0.02%	0.02%	0.02%	0.01%
2	0.03%	0.03%	0.03%	0.02%	0.02%	0.02%	0.01%	0.01%
3	0.02%	0.03%	CR	0.03%	0.03%	CR	0.02%	0.01%
4	0.02%	0.02%	0.03%	0.03%	0.04%	0.03%	0.01%	0.01%
5	0.02%	0.02%	0.03%	0.04%	CR	0.01%	0.02%	0.02%
6	0.02%	0.02%	CR	0.03%	0.01%	0.02%	0.06%	0.04%
7	0.02%	0.01%	0.02%	0.01%	0.02%	0.06%	0.58%	0.07%
8	0.01%	0.01%	0.01%	0.01%	0.02%	0.04%	0.07%	0.05%

Name of Participant(s)	E-mail Address
Winfried Zwermann	winfried.zwermann@grs.de
Markus Klein	markus.klein@grs.de

Organization	Gesellschaft für Anlagen- und Reaktorsicherheit (GRS)mbH
Country	Germany
Reactor Name	*TMI-1*
Operating Condition	*Hot Zero Power (rodded case)*
Reactor type	*PWR*
Nuclear Data Library Used	*ENDF/B-VII*
Covariance Data Library Used	*SCALE 6.0 (44groups)*
Computer Code Used	*XSUSA / NEWT*
Criticality Calculation Method	*two-dimensional (2-D) discrete-ordinates transport*
Uncertainty Calculation Method	*sampling method*

		(mean) value	uncertainty	rel. uncertainty
k_eff		1.08582E+00	5.18000E-03	0.47706%

homogenized XS	energy group	(mean) value	uncertainty	rel. uncertainty
total	1	5.54705E-01	4.58745E-03	0.82701%
	2	1.41567E+00	1.77650E-03	0.12549%
transport	1	2.29937E-01	5.31881E-03	2.31316%
	2	9.36691E-01	1.53315E-03	0.16368%
diffusion	1	1.45045E+00	3.35464E-02	2.31283%
	2	3.55864E-01	5.82509E-04	0.16369%
absorption	1	1.27967E-02	1.12457E-04	0.87880%
	2	1.36520E-01	2.47166E-04	0.18105%
nu_fission	1	8.73684E-03	4.76777E-05	0.54571%
	2	1.95149E-01	8.81434E-04	0.45167%
kappa_fission	1	1.08030E-13	3.90220E-16	0.36121%
	2	2.48956E-12	7.82701E-15	0.31439%
flux	1	9.01758E-01	1.09608E-03	0.12155%
	2	9.82420E-02	1.09607E-03	1.11568%
inv_velocity	1	5.09781E-08	6.08106E-10	1.19288%
	2	2.34280E-06	8.23556E-10	0.03515%
fission	1	3.46398E-03	1.36429E-05	0.39385%
	2	8.00870E-02	2.51888E-04	0.31452%
scatter	1 -> 1	5.26638E-01	4.31570E-03	0.81948%
	1 -> 2	1.50910E-02	1.83804E-04	1.21797%
	2 -> 1	1.99764E-03	4.94232E-06	0.24741%
	2 -> 2	1.27715E+00	1.78651E-03	0.13988%
delayed_lambda	1	1.25364E-02	2.82191E-06	0.02251%
	2	3.09100E-02	5.37701E-06	0.01740%
	3	1.14289E-01	1.01891E-04	0.08915%
	4	3.08121E-01	2.06502E-04	0.06702%
	5	1.22233E+00	8.84208E-04	0.07234%
	6	3.29224E+00	3.35221E-03	0.10182%
delayed_beta	1	2.25481E-04	4.25872E-08	0.01889%
	2	1.50963E-03	2.94536E-06	0.19510%
	3	1.40202E-03	5.04090E-06	0.35955%
	4	2.95223E-03	1.38104E-05	0.46780%
	5	1.02927E-03	1.08068E-05	1.04995%
	6	3.35577E-04	3.57813E-06	1.06626%
adf	1	1.02310E+00	3.42155E-04	0.03344%
	2	1.35036E+00	3.65734E-04	0.02708%

pin power distribution

mean values

	1	2	3	4	5	6	7	8
1	IT	1.1312	1.0218	1.0056	1.0046	1.0123	1.0726	1.1426
2	1.1312	1.045	0.9399	0.9623	0.9616	0.9396	1.0419	1.1343
3	1.0218	0.9399	CR	0.8653	0.8603	CR	0.9775	1.1197
4	1.0056	0.9623	0.8653	0.8743	0.8358	0.88	1.0229	1.1292
5	1.0046	0.9616	0.8603	0.8358	CR	0.9188	1.0503	1.1392
6	1.0123	0.9396	CR	0.88	0.9188	0.9949	1.0331	1.1339
7	1.0726	1.0419	0.9775	1.0229	1.0503	1.0331	0.4272	1.1172
8	1.1426	1.1343	1.1197	1.1292	1.1392	1.1339	1.1172	1.1347

CR = control rod position
IT = instrumentation tube

rel. uncertainties

.	1	2	3	4	5	6	7	8
1	IT	0.03%	0.02%	0.02%	0.02%	0.01%	0.03%	0.05%
2	0.03%	0.02%	0.04%	0.03%	0.03%	0.03%	0.02%	0.04%
3	0.02%	0.04%	CR	0.07%	0.07%	CR	0.01%	0.04%
4	0.02%	0.03%	0.07%	0.06%	0.07%	0.05%	0.02%	0.05%
5	0.02%	0.03%	0.07%	0.07%	CR	0.03%	0.03%	0.05%
6	0.01%	0.03%	CR	0.05%	0.03%	0.02%	0.03%	0.06%
7	0.03%	0.02%	0.01%	0.02%	0.03%	0.03%	0.47%	0.06%
8	0.05%	0.04%	0.04%	0.05%	0.05%	0.06%	0.06%	0.09%

Name of Participant(s)	E-mail Address
Winfried Zwermann	winfried.zwermann@grs.de
Markus Klein	markus.klein@grs.de

Organization	Gesellschaft für Anlagen- und Reaktorsicherheit (GRS)mbH
Country	Germany

reflector model

Reactor Name	*TMI-1*
Operating Condition	*Hot ZeroPower*
Reactor type	*PWR*
Nuclear Data Library Used	*ENDF/B-VII*
Covariance Data Library Used	*SCALE 6.0 (44groups)*
Computer Code Used	*XSUSA / NEWT*
Criticality Calculation Method	*two-dimensional (2-D) discrete-ordinates transport*
Uncertainty Calculation Method	*sampling method*

		(mean) value	uncertainty	rel. uncertainty
k_eff		1.22333E+00	5.93000E-03	0.48474%

homogenized XS	energy group	(mean) value	uncertainty	rel. uncertainty
total	1	6.37179E-01	4.68630E-03	0.73548%
	2	1.95844E+00	2.55503E-03	0.13046%
transport	1	2.24580E-01	3.04280E-03	1.35488%
	2	1.23904E+00	1.79033E-03	0.14449%
diffusion	1	1.48452E+00	2.01211E-02	1.35539%
	2	2.69026E-01	3.88605E-04	0.14445%
absorption	1	1.29433E-03	1.59608E-05	1.23313%
	2	1.68178E-02	7.29689E-05	0.43388%
nu_fission	1	0.00000E+00	0.00000E+00	#DIV/0!
	2	0.00000E+00	0.00000E+00	#DIV/0!
kappa_fission	1	0.00000E+00	0.00000E+00	#DIV/0!
	2	0.00000E+00	0.00000E+00	#DIV/0!
flux	1	7.60047E-01	6.94549E-04	0.09138%
	2	2.39953E-01	6.94535E-04	0.28945%
inv_velocity	1	7.80492E-08	8.69723E-10	1.11433%
	2	2.87653E-06	4.16462E-10	0.01448%
fission	1	0.00000E+00	0.00000E+00	#DIV/0!
	2	0.00000E+00	0.00000E+00	#DIV/0!
scatter	1 -> 1	6.11956E-01	4.47484E-03	0.73124%
	1 -> 2	2.35592E-02	1.98112E-04	0.84091%
	2 -> 1	1.16819E-03	1.17793E-05	1.00834%
	2 -> 2	1.94045E+00	2.58829E-03	0.13339%
delayed_lambda	1	0.00000E+00	0.00000E+00	#DIV/0!
	2	0.00000E+00	0.00000E+00	#DIV/0!
	3	0.00000E+00	0.00000E+00	#DIV/0!
	4	0.00000E+00	0.00000E+00	#DIV/0!
	5	0.00000E+00	0.00000E+00	#DIV/0!
	6	0.00000E+00	0.00000E+00	#DIV/0!
delayed_beta	1	0.00000E+00	0.00000E+00	#DIV/0!
	2	0.00000E+00	0.00000E+00	#DIV/0!
	3	0.00000E+00	0.00000E+00	#DIV/0!
	4	0.00000E+00	0.00000E+00	#DIV/0!
	5	0.00000E+00	0.00000E+00	#DIV/0!
	6	0.00000E+00	0.00000E+00	#DIV/0!
adf	1	9.97997E-01	3.98770E-03	0.39957%
	2	2.59527E-01	1.99179E-03	0.76747%

2.3 VVER KOZ-6 (Kozloduy 6)

Name of Participant(s)	E-mail Address
Markus Klein	markus.klein@grs.de
Winfried Zwermann	winfried.zwermann@grs.de

Organization	Gesellschaft für Anlagen- und Reaktorsicherheit (GRS)mbH
Country	Germany
Reactor Name	*KOZ-6*
Operating Condition	*Hot Zero Power*
Reactor type	*VVER 1000*
Nuclear Data Library Used	*ENDF/B-VII*
Covariance Data Library Used	*SCALE 6.0 (44groups)*
Computer Code Used	*XSUSA / NEWT*
Criticality Calculation Method	*two-dimensional (2-D) discrete-ordinates transport*
Uncertainty Calculation Method	*sampling method*

		(mean) value	uncertainty	rel. uncertainty
k_eff		1.33210E+00	4.91000E-03	0.36859%

homogenized XS	energy group	(mean) value	uncertainty	rel. uncertainty
total	1	5.59636E-01	1.92450E-03	0.34388%
	2	1.37306E+00	8.50000E-04	0.06191%
transport	1	2.29324E-01	2.19600E-03	0.95760%
	2	9.12513E-01	6.58000E-04	0.07211%
diffusion	1	1.45368E+00	1.39204E-02	0.95760%
	2	3.65292E-01	2.63407E-04	0.07211%
absorption	1	9.38167E-03	1.19850E-05	0.12775%
	2	8.31107E-02	8.34500E-05	0.10041%
nu_fission	1	6.57057E-03	2.13300E-05	0.32463%
	2	1.37842E-01	3.41500E-04	0.24775%
kappa_fission	1	8.07856E-14	3.31150E-16	0.40991%
	2	1.76100E-01	3.00500E-15	0.00000%
flux	1	8.22128E-01	1.35250E-03	0.16451%
	2	1.77872E-01	1.35300E-03	0.76066%
inv_velocity	1	5.88361E-08	4.38350E-10	0.74504%
	2	2.50698E-06	5.35000E-10	0.02134%
fission	1	2.60637E-03	9.84500E-06	0.37773%
	2	5.66503E-02	9.63000E-05	0.16999%
scatter	1 -> 1	5.32033E-01	1.77500E-03	0.33363%
	1 -> 2	1.82603E-02	1.51000E-04	0.82693%
	2 -> 1	1.29445E-03	3.55000E-07	0.02742%
	2 -> 2	1.28865E+00	9.35000E-04	0.07256%
delayed_lambda	1	1.24684E-02	1.25000E-06	0.01003%
	2	3.06952E-02	2.60000E-06	0.00847%
	3	1.12758E-01	4.20000E-05	0.03725%
	4	3.04760E-01	8.50000E-05	0.02789%
	5	1.17855E+00	4.45000E-04	0.03776%
	6	3.14321E+00	1.65000E-03	0.05249%
delayed_beta	1	2.22869E-04	7.00000E-09	0.00314%
	2	1.49524E-03	1.11500E-06	0.07457%
	3	1.36812E-03	1.93000E-06	0.14107%
	4	2.82403E-03	5.40500E-06	0.19139%
	5	9.17891E-04	4.26000E-06	0.46411%
	6	3.16533E-04	1.35700E-06	0.42871%

2.4 PWR GEN-III (Generation-III European Pressurized Water Reactor)

Name of Participant(s)	E-mail Address
Markus Klein	markus.klein@grs.de
Winfried Zwermann	winfried.zwermann@grs.de

Organization	Gesellschaft für Anlagen- und Reaktorsicherheit (GRS)mbH
Country	Germany

Type 1: UOX 2.1% without UO2-Gd2O3 rods

Reactor Name	*GEN-III*
Operating Condition	*Hot Full Power*
Reactor type	*PWR*
Nuclear Data Library Used	*ENDF/B-VII*
Covariance Data Library Used	*SCALE 6.0 (44groups)*
Computer Code Used	*XSUSA / NEWT*
Criticality Calculation Method	*two-dimensional (2-D) discrete-ordinates transport*
Uncertainty Calculation Method	*sampling method*

		(mean) value	uncertainty	rel. uncertainty
k_eff		1.04640E+00	5.88000E-03	0.56193%

homogenized XS	energy group	(mean) value	uncertainty	rel. uncertainty
total	1	5.32158E-01	4.60554E-03	0.86545%
	2	1.28850E+00	1.91469E-03	0.14860%
transport	1	2.16416E-01	5.51716E-03	2.54933%
	2	8.56722E-01	1.72376E-03	0.20120%
diffusion	1	1.54125E+00	3.95375E-02	2.56529%
	2	3.89082E-01	7.82509E-04	0.20112%
absorption	1	8.95641E-03	7.53848E-05	0.84169%
	2	7.30922E-02	1.82065E-04	0.24909%
nu_fission	1	5.25516E-03	5.93581E-05	1.12952%
	2	9.39320E-02	4.24421E-04	0.45184%
kappa_fission	1	6.39061E-14	5.51864E-16	0.86355%
	2	1.19784E-12	4.02589E-15	0.33610%
flux	1	8.10734E-01	2.01427E-03	0.24845%
	2	1.89266E-01	2.01428E-03	1.06426%
inv_velocity	1	5.87081E-08	7.46346E-10	1.27128%
	2	2.47471E-06	8.12032E-10	0.03281%
fission	1	2.08427E-03	1.97168E-05	0.94598%
	2	3.85334E-02	1.29534E-04	0.33616%
scatter	1 -> 1	5.05844E-01	4.34566E-03	0.85909%
	1 -> 2	1.73943E-02	2.23070E-04	1.28243%
	2 -> 1	1.41555E-03	5.34241E-06	0.37741%
	2 -> 2	1.21399E+00	1.90535E-03	0.15695%
delayed_lambda	1	1.24827E-02	2.55365E-06	0.02046%
	2	3.07199E-02	5.03330E-06	0.01638%
	3	1.13305E-01	9.04076E-05	0.07979%
	4	3.05860E-01	1.83711E-04	0.06006%
	5	1.18233E+00	8.42624E-04	0.07127%
	6	3.15813E+00	3.16481E-03	0.10021%
delayed_beta	1	2.22559E-04	2.98968E-08	0.01343%
	2	1.51189E-03	2.54793E-06	0.16853%
	3	1.39637E-03	4.38119E-06	0.31376%
	4	2.90042E-03	1.20799E-05	0.41649%
	5	9.77359E-04	9.47653E-06	0.96961%
	6	3.36731E-04	3.09896E-06	0.92031%
adf	1	9.99859E-01	1.11682E-04	0.01117%
	2	1.01737E+00	9.27890E-05	0.00912%

pin power distribution

mean values

	1	2	3	4	5	6	7	8	9	
1	0.9669	0.9729	1.0061	CR	1.0229	1.0237	CR	1.0128	0.9936	
2	0.9729	0.9742	0.9903	1.0201	1.0027	1.0034	1.0214	0.9946	0.9899	CR = control rod position
3	1.0061	0.9903	0.9971	1.024	1.0057	1.0063	1.0228	0.9948	0.9895	
4	CR	1.0201	1.024	CR	1.0333	1.0352	CR	1.0127	0.9918	
5	1.0229	1.0027	1.0057	1.0333	1.0232	1.0383	1.0283	0.9908	0.984	
6	1.0237	1.0034	1.0063	1.0352	1.0383	CR	1.0155	0.9785	0.9769	
7	CR	1.0214	1.0228	CR	1.0283	1.0155	0.9829	0.9664	0.9708	
8	1.0128	0.9946	0.9948	1.0127	0.9908	0.9785	0.9664	0.9611	0.97	
9	0.9936	0.9899	0.9895	0.9918	0.984	0.9769	0.9708	0.97	0.9261	

rel. uncertainties

.	1	2	3	4	5	6	7	8	9	
1	0.03%	0.02%	0.01%	CR	0.01%	0.01%	CR	0.01%	0.01%	
2	0.02%	0.02%	0.01%	0.01%	0.00%	0.00%	0.01%	0.00%	0.01%	
3	0.01%	0.01%	0.01%	0.01%	0.00%	0.00%	0.01%	0.00%	0.01%	
4	CR	0.01%	0.01%	CR	0.01%	0.02%	CR	0.01%	0.01%	
5	0.01%	0.00%	0.00%	0.01%	0.01%	0.02%	0.02%	0.00%	0.01%	
6	0.01%	0.00%	0.00%	0.02%	0.02%	CR	0.01%	0.01%	0.01%	
7	CR	0.01%	0.01%	CR	0.02%	0.01%	0.01%	0.02%	0.01%	
8	0.01%	0.00%	0.00%	0.01%	0.00%	0.01%	0.02%	0.02%	0.01%	
9	0.01%	0.01%	0.01%	0.01%	0.01%	0.01%	0.01%	0.01%	0.01%	

Name of Participant(s)	E-mail Address
Winfried Zwermann	winfried.zwermann@grs.de
Markus Klein	markus.klein@grs.de

Organization	Gesellschaft für Anlagen- und Reaktorsicherheit (GRS)mbH
Country	Germany

Type 1: UOX 4.2% without UO2-Gd2O3 rods

Reactor Name	*GEN-III*
Operating Condition	*Hot Full Power*
Reactor type	*PWR*
Nuclear Data Library Used	*ENDF/B-VII*
Covariance Data Library Used	*SCALE 6.0 (44groups)*
Computer Code Used	*XSUSA / NEWT*
Criticality Calculation Method	*two-dimensional (2-D) discrete-ordinates transport*
Uncertainty Calculation Method	*sampling method*

		(mean) value	uncertainty	rel. uncertainty
k_eff		1.25517E+00	6.10000E-03	0.48599%

homogenized XS	energy group	(mean) value	uncertainty	rel. uncertainty
total	1	5.30042E-01	4.62447E-03	0.87247%
	2	1.31065E+00	1.92776E-03	0.14708%
transport	1	2.15124E-01	5.44893E-03	2.53293%
	2	8.64146E-01	1.72499E-03	0.19962%
diffusion	1	1.55049E+00	3.95230E-02	2.54907%
	2	3.85739E-01	7.69686E-04	0.19954%
absorption	1	1.03506E-02	8.93688E-05	0.86342%
	2	1.06730E-01	2.25461E-04	0.21124%
nu_fission	1	8.00089E-03	4.46764E-05	0.55839%
	2	1.66874E-01	7.36702E-04	0.44147%
kappa_fission	1	9.87462E-14	3.76689E-16	0.38147%
	2	2.12800E-12	6.80711E-15	0.31988%
flux	1	8.69523E-01	1.48855E-03	0.17119%
	2	1.30477E-01	1.48855E-03	1.14085%
inv_velocity	1	5.55809E-08	7.13833E-10	1.28431%
	2	2.34815E-06	8.26177E-10	0.03518%
fission	1	3.17197E-03	1.33018E-05	0.41935%
	2	6.84560E-02	2.19002E-04	0.31992%
scatter	1 -> 1	5.03412E-01	4.36016E-03	0.86612%
	1 -> 2	1.63151E-02	2.11335E-04	1.29533%
	2 -> 1	1.99562E-03	7.00582E-06	0.35106%
	2 -> 2	1.20192E+00	1.91099E-03	0.15899%
delayed_lambda	1	1.24877E-02	2.10571E-06	0.01686%
	2	3.07604E-02	4.14503E-06	0.01348%
	3	1.13151E-01	7.46370E-05	0.06596%
	4	3.05642E-01	1.51608E-04	0.04960%
	5	1.19208E+00	6.94168E-04	0.05823%
	6	3.18887E+00	2.60543E-03	0.08170%
delayed_beta	1	2.23780E-04	2.64572E-08	0.01182%
	2	1.49670E-03	2.11065E-06	0.14102%
	3	1.37369E-03	3.62716E-06	0.26405%
	4	2.85100E-03	9.99179E-06	0.35047%
	5	9.42664E-04	7.83571E-06	0.83123%
	6	3.18827E-04	2.56690E-06	0.80511%
adf	1	9.99591E-01	1.19739E-04	0.01198%
	2	1.03392E+00	1.33238E-04	0.01289%

pin power distribution

mean values

	1	2	3	4	5	6	7	8	9	
1	0.9515	0.96	1.0092	CR	1.0305	1.0315	CR	1.0181	0.9894	
2	0.96	0.9621	0.9851	1.0272	1.0007	1.0015	1.029	0.9908	0.9849	CR = control rod position
3	1.0092	0.9851	0.9939	1.0323	1.0047	1.0054	1.0313	0.9913	0.9846	
4	CR	1.0272	1.0323	CR	1.0445	1.0474	CR	1.0189	0.9878	
5	1.0305	1.0007	1.0047	1.0445	1.0302	1.0544	1.0416	0.9873	0.9784	
6	1.0315	1.0015	1.0054	1.0474	1.0544	CR	1.0236	0.9696	0.9696	
7	CR	1.029	1.0313	CR	1.0416	1.0236	0.9771	0.9541	0.9625	
8	1.0181	0.9908	0.9913	1.0189	0.9873	0.9696	0.9541	0.9481	0.9624	
9	0.9894	0.9849	0.9846	0.9878	0.9784	0.9696	0.9625	0.9624	0.9246	

rel. uncertainties

.	1	2	3	4	5	6	7	8	9	
1	0.03%	0.02%	0.00%	CR	0.01%	0.01%	CR	0.01%	0.01%	
2	0.02%	0.02%	0.01%	0.01%	0.00%	0.00%	0.01%	0.00%	0.01%	
3	0.00%	0.01%	0.01%	0.01%	0.00%	0.00%	0.01%	0.00%	0.01%	
4	CR	0.01%	0.01%	CR	0.01%	0.02%	CR	0.01%	0.01%	
5	0.01%	0.00%	0.00%	0.01%	0.01%	0.02%	0.02%	0.00%	0.01%	
6	0.01%	0.00%	0.00%	0.02%	0.02%	CR	0.01%	0.01%	0.01%	
7	CR	0.01%	0.01%	CR	0.02%	0.01%	0.01%	0.02%	0.01%	
8	0.01%	0.00%	0.00%	0.01%	0.00%	0.01%	0.02%	0.02%	0.01%	
9	0.01%	0.01%	0.01%	0.01%	0.01%	0.01%	0.01%	0.01%	0.01%	

Name of Participant(s)	E-mail Address
Winfried Zwermann	winfried.zwermann@grs.de
Markus Klein	markus.klein@grs.de

Organization	Gesellschaft für Anlagen- und Reaktorsicherheit (GRS)mbH
Country	Germany

Type 2: UOX 4.2% with 12 UO2-Gd2O3 rods

Reactor Name	*GEN-III*
Operating Condition	*Hot Full Power*
Reactor type	*PWR*
Nuclear Data Library Used	*ENDF/B-VII*
Covariance Data Library Used	*SCALE 6.0 (44groups)*
Computer Code Used	*XSUSA / NEWT*
Criticality Calculation Method	*two-dimensional (2-D) discrete-ordinates transport*
Uncertainty Calculation Method	*sampling method*

		(mean) value	uncertainty	rel. uncertainty
k_eff		1.12438E+00	5.55000E-03	0.49361%

homogenized XS	energy group	(mean) value	uncertainty	rel. uncertainty
total	1	5.30064E-01	4.61955E-03	0.87151%
	2	1.32206E+00	1.92236E-03	0.14541%
transport	1	2.15118E-01	5.43676E-03	2.52734%
	2	8.70826E-01	1.71868E-03	0.19736%
diffusion	1	1.55054E+00	3.94353E-02	2.54333%
	2	3.82780E-01	7.55152E-04	0.19728%
absorption	1	1.05268E-02	9.07808E-05	0.86238%
	2	1.16974E-01	2.23627E-04	0.19118%
nu_fission	1	7.84330E-03	4.49089E-05	0.57258%
	2	1.60605E-01	7.09762E-04	0.44193%
kappa_fission	1	9.67487E-14	3.76331E-16	0.38898%
	2	2.04806E-12	6.56033E-15	0.32032%
flux	1	8.80537E-01	1.37626E-03	0.15630%
	2	1.19463E-01	1.37625E-03	1.15203%
inv_velocity	1	5.51586E-08	7.07887E-10	1.28337%
	2	2.32321E-06	7.85973E-10	0.03383%
fission	1	3.10938E-03	1.33336E-05	0.42882%
	2	6.58842E-02	2.11061E-04	0.32035%
scatter	1 -> 1	5.03410E-01	4.35566E-03	0.86523%
	1 -> 2	1.61644E-02	2.09294E-04	1.29478%
	2 -> 1	2.16854E-03	7.30121E-06	0.33669%
	2 -> 2	1.20292E+00	1.90952E-03	0.15874%
delayed_lambda	1	1.25319E-02	3.35606E-06	0.02678%
	2	3.08770E-02	6.36877E-06	0.02063%
	3	1.14393E-01	1.21323E-04	0.10606%
	4	3.08257E-01	2.45860E-04	0.07976%
	5	1.21445E+00	1.04353E-03	0.08593%
	6	3.26728E+00	3.96413E-03	0.12133%
delayed_beta	1	2.24521E-04	4.98870E-08	0.02222%
	2	1.52115E-03	3.50942E-06	0.23071%
	3	1.41911E-03	6.00657E-06	0.42326%
	4	2.98895E-03	1.64534E-05	0.55047%
	5	1.05485E-03	1.28749E-05	1.22054%
	6	3.49134E-04	4.26385E-06	1.22126%
adf	1	1.00969E+00	1.11571E-04	0.01105%
	2	1.09768E+00	2.54704E-04	0.02320%

pin power distribution

mean values

	1	2	3	4	5	6	7	8	9	
1	1.0172	1.0209	1.0583	CR	1.0457	1.0734	CR	1.1066	1.0848	
2	1.0209	1.0172	1.0244	1.0344	0.9638	1.0202	1.0943	1.0751	1.0784	CR = control rod position
3	1.0583	1.0244	1.0039	0.9828	0.2	0.9795	1.0858	1.0712	1.0751	
4	CR	1.0344	0.9828	CR	0.9968	1.0618	CR	1.0962	1.0733	
5	1.0457	0.9638	0.2	0.9968	1.0381	1.0875	1.0856	1.0501	1.0538	
6	1.0734	1.0202	0.9795	1.0618	1.0875	CR	1.0049	0.9984	1.0304	
7	CR	1.0943	1.0858	CR	1.0856	1.0049	0.201	0.9355	1.0103	
8	1.1066	1.0751	1.0712	1.0962	1.0501	0.9984	0.9355	0.9745	1.021	
9	1.0848	1.0784	1.0751	1.0733	1.0538	1.0304	1.0103	1.021	0.9906	

rel. uncertainties

.	1	2	3	4	5	6	7	8	9
1	0.02%	0.02%	0.01%	CR	0.02%	0.02%	CR	0.04%	0.04%
2	0.02%	0.01%	0.01%	0.02%	0.03%	0.01%	0.03%	0.03%	0.04%
3	0.01%	0.01%	0.01%	0.03%	1.25%	0.02%	0.03%	0.03%	0.04%
4	CR	0.02%	0.03%	CR	0.03%	0.02%	CR	0.04%	0.03%
5	0.02%	0.03%	1.25%	0.03%	0.02%	0.04%	0.03%	0.02%	0.03%
6	0.02%	0.01%	0.02%	0.02%	0.04%	CR	0.02%	0.01%	0.02%
7	CR	0.03%	0.03%	CR	0.03%	0.02%	1.24%	0.02%	0.01%
8	0.04%	0.03%	0.03%	0.04%	0.02%	0.01%	0.02%	0.01%	0.02%
9	0.04%	0.04%	0.04%	0.03%	0.03%	0.02%	0.01%	0.02%	0.03%

Name of Participant(s)	E-mail Address
Winfried Zwermann	winfried.zwermann@grs.de
Markus Klein	markus.klein@grs.de

Organization	Gesellschaft für Anlagen- und Reaktorsicherheit (GRS)mbH
Country	Germany

Type 3: UOX 3.2% with 20 UO2-Gd2O3 rods

Reactor Name	*GEN-III*
Operating Condition	*Hot Full Power*
Reactor type	*PWR*
Nuclear Data Library Used	*ENDF/B-VII*
Covariance Data Library Used	*SCALE 6.0 (44groups)*
Computer Code Used	*XSUSA / NEWT*
Criticality Calculation Method	*two-dimensional (2-D) discrete-ordinates transport*
Uncertainty Calculation Method	*sampling method*

		(mean) value	uncertainty	rel. uncertainty
k_eff		9.58060E-01	5.11000E-03	0.53337%

homogenized XS	energy group	(mean) value	uncertainty	rel. uncertainty
total	1	5.30864E-01	4.60662E-03	0.86776%
	2	1.31864E+00	1.91348E-03	0.14511%
transport	1	2.15572E-01	5.45561E-03	2.53076%
	2	8.70491E-01	1.71645E-03	0.19718%
diffusion	1	1.54727E+00	3.94036E-02	2.54665%
	2	3.82927E-01	7.54748E-04	0.19710%
absorption	1	1.00391E-02	8.54607E-05	0.85128%
	2	1.09645E-01	2.05126E-04	0.18708%
nu_fission	1	6.54083E-03	5.01342E-05	0.76648%
	2	1.25577E-01	5.60318E-04	0.44619%
kappa_fission	1	8.02282E-14	4.28222E-16	0.53375%
	2	1.60137E-12	5.23504E-15	0.32691%
flux	1	8.71137E-01	1.46471E-03	0.16814%
	2	1.28863E-01	1.46470E-03	1.13663%
inv_velocity	1	5.62128E-08	7.18009E-10	1.27731%
	2	2.35351E-06	7.53556E-10	0.03202%
fission	1	2.59344E-03	1.53904E-05	0.59344%
	2	5.15148E-02	1.68426E-04	0.32695%
scatter	1 -> 1	5.04338E-01	4.34420E-03	0.86137%
	1 -> 2	1.65227E-02	2.12967E-04	1.28894%
	2 -> 1	2.04945E-03	6.82103E-06	0.33282%
	2 -> 2	1.20694E+00	1.90545E-03	0.15787%
delayed_lambda	1	1.25385E-02	3.77428E-06	0.03010%
	2	3.08816E-02	7.16653E-06	0.02321%
	3	1.14714E-01	1.36478E-04	0.11897%
	4	3.08885E-01	2.76588E-04	0.08954%
	5	1.21442E+00	1.17326E-03	0.09661%
	6	3.26877E+00	4.45816E-03	0.13639%
delayed_beta	1	2.24102E-04	5.55185E-08	0.02477%
	2	1.53313E-03	3.94600E-06	0.25738%
	3	1.43878E-03	6.75414E-06	0.46944%
	4	3.03968E-03	1.85047E-05	0.60877%
	5	1.09355E-03	1.44798E-05	1.32411%
	6	3.63554E-04	4.79420E-06	1.31870%
adf	1	1.02538E+00	4.75010E-04	0.04633%
	2	1.16236E+00	5.11278E-04	0.04399%

pin power distribution

mean values

	1	2	3	4	5	6	7	8	9	
1	1.0182	1.016	1.0336	CR	1.0001	0.927	CR	1.1327	1.1423	
2	1.016	0.992	0.9566	1.0184	0.95	0.2164	1.0378	1.1066	1.1395	CR = control rod position
3	1.0336	0.9566	0.2141	0.9798	0.9885	0.9875	1.0981	1.1227	1.1441	
4	CR	1.0184	0.9798	CR	0.9983	1.0713	CR	1.1558	1.149	
5	1.0001	0.95	0.9885	0.9983	0.2184	1.0428	1.117	1.1165	1.1336	
6	0.927	0.2164	0.9875	1.0713	1.0428	CR	1.0426	1.069	1.1137	
7	CR	1.0378	1.0981	CR	1.117	1.0426	0.2226	1.0079	1.0971	
8	1.1327	1.1066	1.1227	1.1558	1.1165	1.069	1.0079	1.0606	1.1142	
9	1.1423	1.1395	1.1441	1.149	1.1336	1.1137	1.0971	1.1142	1.0817	

rel. uncertainties

.	1	2	3	4	5	6	7	8	9	
1	0.03%	0.03%	0.03%	CR	0.04%	0.06%	CR	0.04%	0.05%	
2	0.03%	0.04%	0.05%	0.04%	0.05%	1.29%	0.02%	0.04%	0.05%	
3	0.03%	0.05%	1.31%	0.05%	0.03%	0.03%	0.04%	0.04%	0.06%	
4	CR	0.04%	0.05%	CR	0.04%	0.03%	CR	0.06%	0.06%	
5	0.04%	0.05%	0.03%	0.04%	1.28%	0.03%	0.04%	0.05%	0.06%	
6	0.06%	1.29%	0.03%	0.03%	0.03%	CR	0.02%	0.04%	0.06%	
7	CR	0.02%	0.04%	CR	0.04%	0.02%	1.26%	0.02%	0.05%	
8	0.04%	0.04%	0.04%	0.06%	0.05%	0.04%	0.02%	0.05%	0.07%	
9	0.05%	0.05%	0.06%	0.06%	0.06%	0.06%	0.05%	0.07%	0.08%	

Name of Participant(s)	E-mail Address
Winfried Zwermann	winfried.zwermann@grs.de
Markus Klein	markus.klein@grs.de

Organization	Gesellschaft für Anlagen- und Reaktorsicherheit (GRS)mbH
Country	Germany

Type 4: MOX

Reactor Name	*GEN-III*
Operating Condition	*Hot Full Power*
Reactor type	*PWR*
Nuclear Data Library Used	*ENDF/B-VII*
Covariance Data Library Used	*SCALE 6.0 (44groups)*
Computer Code Used	*XSUSA / NEWT*
Criticality Calculation Method	*two-dimensional (2-D) discrete-ordinates transport*
Uncertainty Calculation Method	*sampling method*

		(mean) value	uncertainty	rel. uncertainty
k_eff		1.11480E+00	1.00900E-02	0.90510%

homogenized XS	energy group	(mean) value	uncertainty	rel. uncertainty
total	1	5.29912E-01	4.72444E-03	0.89155%
	2	1.53249E+00	2.07046E-03	0.13510%
transport	1	2.13198E-01	5.28566E-03	2.47923%
	2	1.04679E+00	1.81016E-03	0.17292%
diffusion	1	1.56446E+00	3.89356E-02	2.48876%
	2	3.18435E-01	5.50377E-04	0.17284%
absorption	1	1.55184E-02	1.45604E-04	0.93827%
	2	2.86495E-01	7.03251E-04	0.24547%
nu_fission	1	1.19520E-02	9.13157E-05	0.76402%
	2	4.48469E-01	4.78623E-03	1.06724%
kappa_fission	1	1.32398E-13	6.60656E-16	0.49899%
	2	5.01126E-12	3.23323E-14	0.64519%
flux	1	9.60633E-01	5.11981E-04	0.05330%
	2	3.93666E-02	5.11975E-04	1.30053%
inv_velocity	1	4.37496E-08	5.59423E-10	1.27869%
	2	2.18102E-06	1.21909E-09	0.05590%
fission	1	4.12447E-03	2.41514E-05	0.58556%
	2	1.56224E-01	1.00817E-03	0.64534%
scatter	1 -> 1	5.02524E-01	4.45496E-03	0.88652%
	1 -> 2	1.19171E-02	1.55582E-04	1.30554%
	2 -> 1	4.31046E-03	1.42591E-05	0.33080%
	2 -> 2	1.24169E+00	1.92806E-03	0.15528%
delayed_lambda	1	1.20926E-02	5.96132E-06	0.04930%
	2	2.86789E-02	1.68791E-05	0.05886%
	3	1.19532E-01	9.22302E-05	0.07716%
	4	3.09285E-01	2.21939E-04	0.07176%
	5	1.10914E+00	1.36897E-03	0.12343%
	6	2.76691E+00	5.72097E-03	0.20676%
delayed_beta	1	8.62301E-05	5.26105E-07	0.61012%
	2	8.06747E-04	5.91074E-06	0.73266%
	3	6.80255E-04	8.15187E-06	1.19836%
	4	1.31671E-03	2.08565E-05	1.58399%
	5	5.63802E-04	1.29528E-05	2.29740%
	6	1.85602E-04	4.30572E-06	2.31987%
adf	1	9.93511E-01	3.17525E-04	0.03196%
	2	1.34336E+00	7.51131E-04	0.05591%

pin power distribution

mean values

	1	2	3	4	5	6	7	8	9	
1	0.9273	0.9401	1.0482	CR	1.0764	1.0886	CR	0.9029	0.8868	
2	0.9401	0.9457	0.9931	1.0709	1.0153	1.0245	1.1033	1.0717	0.8762	CR = control rod position
3	1.0482	0.9931	1.0057	1.0774	1.0204	1.0295	1.1076	1.0733	0.8764	
4	CR	1.0709	1.0774	CR	1.0971	1.1113	CR	0.9063	0.8869	
5	1.0764	1.0153	1.0204	1.0971	1.0776	1.1433	1.1439	1.071	0.8733	
6	1.0886	1.0245	1.0295	1.1113	1.1433	CR	1.1041	1.028	0.8694	
7	CR	1.1033	1.1076	CR	1.1439	1.1041	1.0355	1.0451	0.9025	
8	0.9029	1.0717	1.0733	0.9063	1.071	1.028	1.0451	0.8867	0.6932	
9	0.8868	0.8762	0.8764	0.8869	0.8733	0.8694	0.9025	0.6932	0.7106	

rel. uncertainties

.	1	2	3	4	5	6	7	8	9	
1	0.06%	0.06%	0.02%	CR	0.03%	0.03%	CR	0.04%	0.05%	
2	0.06%	0.05%	0.03%	0.03%	0.02%	0.02%	0.04%	0.03%	0.05%	
3	0.02%	0.03%	0.03%	0.03%	0.02%	0.02%	0.04%	0.03%	0.05%	
4	CR	0.03%	0.03%	CR	0.04%	0.04%	CR	0.04%	0.05%	
5	0.03%	0.02%	0.02%	0.04%	0.03%	0.05%	0.05%	0.03%	0.05%	
6	0.03%	0.02%	0.02%	0.04%	0.05%	CR	0.04%	0.03%	0.06%	
7	CR	0.04%	0.04%	CR	0.05%	0.04%	0.02%	0.04%	0.06%	
8	0.04%	0.03%	0.03%	0.04%	0.03%	0.03%	0.04%	0.07%	0.22%	
9	0.05%	0.05%	0.05%	0.05%	0.05%	0.06%	0.06%	0.22%	0.18%	

2.5 KRITZ-2 (Uranium and MOX Fuel Critical Assemblies)

Name of Participant(s)		E-mail Address	
Markus Klein		markus.klein@grs.de	
Winfried Zwermann		winfried.zwermann@grs.de	
Organization	Gesellschaft für Anlagen- und Reaktorsicherheit (GRS)mbH		
Country	Germany		
Reactor Name	*KRITZ-2:13 cold*		
Operating Condition	*Cold*		
Reactor type	*LWR critical assembly*		
Nuclear Data Library Used	*ENDF/B-VII*		
Covariance Data Library Used	*SCALE 6.0 (44groups)*		
Computer Code Used	*XSUSA / KENO-Va*		
Criticality Calculation Method	*three-dimensional (3-D) multi-group Monte Carlo*		
Uncertainty Calculation Method	*sampling method*		

k_{inf} (forward)	k_{inf} (adjoint)	uncertainties absolute Δk	uncertainties relative Δk/k [%]
0.99645		*0.00527*	*0.529%*

pin fission rate (forward)		uncertainties absolute Δf	uncertainties relative Δf/f [%]	pin coordinates
0.2820		*0.0044*	*1.569%*	03 03
0.7528		*0.0050*	*0.669%*	03 23
0.2820		*0.0044*	*1.571%*	03 42
0.6999		*0.0032*	*0.462%*	04 23
1.0393		*0.0013*	*0.120%*	08 23
1.2253		*0.0020*	*0.162%*	10 23
1.4620		*0.0033*	*0.229%*	13 23
1.6409		*0.0045*	*0.276%*	16 23
1.7556		*0.0053*	*0.300%*	19 23
1.0393		*0.0012*	*0.116%*	22 08
1.3103		*0.0024*	*0.183%*	22 11
1.5284		*0.0037*	*0.242%*	22 14
1.6865		*0.0048*	*0.286%*	22 17
1.7790		*0.0053*	*0.299%*	22 20
1.8023		*0.0056*	*0.310%*	22 23
1.7557		*0.0053*	*0.299%*	22 26
1.6408		*0.0045*	*0.277%*	22 29
1.4619		*0.0034*	*0.231%*	22 32
1.2251		*0.0019*	*0.155%*	22 35
1.0391		*0.0012*	*0.118%*	22 37
0.6998		*0.0032*	*0.461%*	22 41
0.7527		*0.0050*	*0.666%*	22 42
1.8023		*0.0056*	*0.310%*	23 22
1.7790		*0.0054*	*0.302%*	25 23
1.6865		*0.0048*	*0.284%*	28 23
1.5283		*0.0037*	*0.244%*	31 23
1.3100		*0.0024*	*0.181%*	34 23
1.0392		*0.0013*	*0.122%*	37 23
0.2820		*0.0044*	*1.571%*	42 03
0.2819		*0.0044*	*1.576%*	42 42

Notes:

Pin coordinates are defined as in the Final Report NEA/NSC/DOC(2005)24.

Fission rates are normalized to the total number of fuel pins (1600).
This does not correspond to the experimental values.

3 Exercise I-1: Core Physics

3.1 PWR TMI-1 (Three Mile Island 1)

Name of Participant(s)	E-mail Address
Markus Klein	markus.klein@grs.de
Winfried Zwermann	winfried.zwermann@grs.de

Organization	Gesellschaft für Anlagen- und Reaktorsicherheit (GRS)mbH
Country	Germany

TMI-1 core, steady state

Reactor Name	*TMI-1*
Operating Condition	*Hot Zero Power*
Reactor type	*PWR*
Nuclear Data Library Used	*ENDF/B-VII*
Covariance Data Library Used	*SCALE 6.0 (44groups)*
Computer Code Used	*XSUSA / KENO Va*
	XSUSA / QUABOX-CUBBOX
Criticality Calculation Method	*KENO Va: Monte Carlo*
	QUABOX-CUBBOX: Nodal Diffusion Code
Uncertainty Calculation Method	*sampling method*

		(mean) value	uncertainty	rel. uncertainty
XSUSA/KENO Va	k_eff	1.30280	0.00606	0.465%
XSUSA/QUABOX-CUBBOX	k_eff	1.30025	0.00598	0.460%

radial power distribution

XSUSA/KENO Va

mean values

					0.51	0.66	0.75	0.66	0.51					
			0.38	0.74	1.02	1.15	1.24	1.15	1.02	0.74	0.38			
		0.72	1.20	1.25	0.96	1.29	1.01	1.29	0.96	1.25	1.20	0.72		
	0.38	1.20	1.46	1.10	1.27	0.97	1.22	0.97	1.27	1.10	1.46	1.20	0.38	
	0.74	1.25	1.10	1.32	0.97	1.17	0.92	1.17	0.97	1.32	1.10	1.25	0.74	
0.51	1.02	0.96	1.27	0.97	1.18	0.89	1.13	0.89	1.18	0.97	1.27	0.96	1.02	0.51
0.66	1.15	1.29	0.97	1.17	0.89	1.11	0.86	1.11	0.89	1.17	0.97	1.29	1.15	0.66
0.75	1.24	1.01	1.22	0.92	1.13	0.86	1.04	0.86	1.13	0.92	1.22	1.01	1.24	0.75
0.66	1.15	1.29	0.97	1.17	0.89	1.11	0.86	1.11	0.89	1.17	0.97	1.29	1.15	0.66
0.51	1.02	0.96	1.27	0.97	1.18	0.89	1.13	0.89	1.18	0.97	1.27	0.96	1.02	0.51
	0.74	1.25	1.10	1.32	0.97	1.17	0.92	1.17	0.97	1.32	1.10	1.25	0.74	
	0.38	1.20	1.46	1.10	1.27	0.97	1.22	0.97	1.27	1.10	1.46	1.20	0.38	
		0.72	1.20	1.25	0.96	1.29	1.01	1.29	0.96	1.25	1.20	0.72		
			0.38	0.74	1.02	1.15	1.24	1.15	1.02	0.74	0.38			
					0.51	0.66	0.75	0.66	0.51					

relative uncertainties

					1.18%	1.31%	1.42%	1.31%	1.18%					
			1.14%	1.20%	1.21%	1.18%	1.21%	1.18%	1.21%	1.20%	1.14%			
		1.96%	1.96%	1.27%	0.41%	0.35%	0.12%	0.35%	0.41%	1.27%	1.96%	1.96%		
	1.14%	1.96%	1.58%	0.47%	0.28%	0.88%	0.87%	0.88%	0.28%	0.47%	1.58%	1.96%	1.14%	
	1.20%	1.27%	0.47%	0.29%	1.23%	1.62%	1.91%	1.62%	1.23%	0.29%	0.47%	1.27%	1.20%	
1.18%	1.21%	0.41%	0.28%	1.23%	1.83%	2.47%	2.48%	2.47%	1.83%	1.23%	0.28%	0.41%	1.21%	1.18%
1.31%	1.18%	0.35%	0.88%	1.62%	2.47%	2.78%	3.09%	2.78%	2.47%	1.62%	0.88%	0.35%	1.18%	1.31%
1.42%	1.21%	0.12%	0.87%	1.91%	2.48%	3.09%	3.15%	3.09%	2.48%	1.91%	0.87%	0.12%	1.21%	1.42%
1.31%	1.18%	0.35%	0.88%	1.62%	2.47%	2.78%	3.09%	2.78%	2.47%	1.62%	0.88%	0.35%	1.18%	1.31%
1.18%	1.21%	0.41%	0.28%	1.23%	1.83%	2.47%	2.48%	2.47%	1.83%	1.23%	0.28%	0.41%	1.21%	1.18%
	1.20%	1.27%	0.47%	0.29%	1.23%	1.62%	1.91%	1.62%	1.23%	0.29%	0.47%	1.27%	1.20%	
	1.14%	1.96%	1.58%	0.47%	0.28%	0.88%	0.87%	0.88%	0.28%	0.47%	1.58%	1.96%	1.14%	
		1.96%	1.96%	1.27%	0.41%	0.35%	0.12%	0.35%	0.41%	1.27%	1.96%	1.96%		
			1.14%	1.20%	1.21%	1.18%	1.21%	1.18%	1.21%	1.20%	1.14%			
					1.18%	1.31%	1.42%	1.31%	1.18%					

XSUSA/QUABOX-CUBBOX

mean values

					0.51	0.64	0.74	0.64	0.51					
			0.37	0.73	1.02	1.14	1.23	1.14	1.02	0.73	0.37			
		0.71	1.20	1.25	0.95	1.29	0.99	1.29	0.95	1.25	1.20	0.71		
	0.37	1.20	1.47	1.09	1.27	0.96	1.23	0.96	1.27	1.09	1.47	1.20	0.37	
	0.73	1.25	1.09	1.33	0.97	1.19	0.92	1.19	0.97	1.33	1.09	1.25	0.73	
0.51	1.02	0.95	1.27	0.97	1.20	0.90	1.15	0.90	1.20	0.97	1.27	0.95	1.02	0.51
0.64	1.14	1.29	0.96	1.19	0.90	1.14	0.87	1.14	0.90	1.19	0.96	1.29	1.14	0.64
0.74	1.23	0.99	1.23	0.92	1.15	0.87	1.07	0.87	1.15	0.92	1.23	0.99	1.23	0.74
0.64	1.14	1.29	0.96	1.19	0.90	1.14	0.87	1.14	0.90	1.19	0.96	1.29	1.14	0.64
0.51	1.02	0.95	1.27	0.97	1.20	0.90	1.15	0.90	1.20	0.97	1.27	0.95	1.02	0.51
	0.73	1.25	1.09	1.33	0.97	1.19	0.92	1.19	0.97	1.33	1.09	1.25	0.73	
	0.37	1.20	1.47	1.09	1.27	0.96	1.23	0.96	1.27	1.09	1.47	1.20	0.37	
		0.71	1.20	1.25	0.95	1.29	0.99	1.29	0.95	1.25	1.20	0.71		
			0.37	0.73	1.02	1.14	1.23	1.14	1.02	0.73	0.37			
					0.51	0.64	0.73	0.64	0.51					

relative uncertainties

					1.08%	1.24%	1.35%	1.23%	1.08%					
			1.10%	1.27%	1.35%	1.29%	1.29%	1.29%	1.35%	1.27%	1.10%			
		2.06%	2.27%	1.47%	0.41%	0.37%	0.06%	0.37%	0.41%	1.47%	2.27%	2.06%		
	1.10%	2.27%	1.85%	0.53%	0.26%	0.98%	0.93%	0.98%	0.26%	0.53%	1.85%	2.27%	1.10%	
	1.27%	1.47%	0.53%	0.23%	1.33%	1.73%	2.08%	1.73%	1.33%	0.23%	0.53%	1.47%	1.27%	
1.08%	1.35%	0.41%	0.26%	1.33%	1.93%	2.65%	2.63%	2.65%	1.93%	1.33%	0.26%	0.41%	1.35%	1.08%
1.24%	1.29%	0.37%	0.98%	1.73%	2.65%	2.94%	3.29%	2.94%	2.65%	1.73%	0.98%	0.37%	1.29%	1.23%
1.35%	1.30%	0.06%	0.93%	2.08%	2.63%	3.29%	3.31%	3.29%	2.63%	2.08%	0.93%	0.06%	1.29%	1.35%
1.23%	1.29%	0.37%	0.98%	1.73%	2.65%	2.94%	3.29%	2.93%	2.65%	1.72%	0.98%	0.37%	1.29%	1.24%
1.08%	1.35%	0.41%	0.26%	1.33%	1.93%	2.65%	2.63%	2.65%	1.93%	1.33%	0.26%	0.41%	1.35%	1.08%
	1.27%	1.47%	0.53%	0.23%	1.33%	1.73%	2.08%	1.73%	1.33%	0.23%	0.53%	1.47%	1.27%	
	1.10%	2.27%	1.85%	0.53%	0.26%	0.98%	0.93%	0.98%	0.26%	0.53%	1.85%	2.27%	1.10%	
		2.06%	2.27%	1.47%	0.41%	0.37%	0.06%	0.37%	0.41%	1.47%	2.27%	2.06%		
			1.10%	1.27%	1.35%	1.29%	1.29%	1.29%	1.35%	1.27%	1.10%			
					1.08%	1.24%	1.35%	1.24%	1.08%					

3.2 PWR GEN-III (Generation-III European Pressurized Water Reactor, UO_2 Core)

Name of Participant(s)	E-mail Address
Markus Klein	markus.klein@grs.de
Winfried Zwermann	winfried.zwermann@grs.de

Organization	Gesellschaft für Anlagen- und Reaktorsicherheit (GRS)mbH
Country	Germany

GEN-III UOX core, steady state

Reactor Name	*GEN-III*
Operating Condition	*Hot Full Power*
Reactor type	*PWR*
Nuclear Data Library Used	*ENDF/B-VII*
Covariance Data Library Used	*SCALE 6.0 (44groups)*
Computer Code Used	*XSUSA / KENO Va*
	XSUSA / QUABOX-CUBBOX
Criticality Calculation Method	*KENO Va: Monte Carlo*
	QUABOX-CUBBOX: Nodal Diffusion Code
Uncertainty Calculation Method	*sampling method*

		(mean) value	uncertainty	rel. uncertainty
XSUSA/KENO Va	k_eff	1.00806	0.00519	0.515%
XSUSA/QUABOX-CUBBOX	k_eff	1.00292	0.00513	0.512%

radial power distribution

mean values – XSUSA/KENO Va

					1.1143	1.1114	1.0639	1.0064	1.0639	1.1114	1.1143					
			1.2895	1.3113	1.0674	1.1095	1.0870	0.9803	1.0870	1.1095	1.0674	1.3113	1.2895			
		1.0805	1.1990	1.2705	1.1213	1.0298	0.9962	0.9379	0.9962	1.0298	1.1213	1.2705	1.1990	1.0805		
	1.2895	1.1990	1.1643	1.1236	1.0211	0.9343	0.8972	0.8740	0.8972	0.9343	1.0211	1.1236	1.1643	1.1990	1.2895	
	1.3113	1.2705	1.1236	1.0021	0.9167	0.8654	0.8253	0.8198	0.8253	0.8654	0.9167	1.0021	1.1236	1.2705	1.3113	
1.1143	1.0674	1.1213	1.0211	0.9167	0.8554	0.8049	0.7866	0.7739	0.7866	0.8049	0.8554	0.9167	1.0211	1.1213	1.0674	1.1143
1.1114	1.1095	1.0298	0.9343	0.8654	0.8049	0.7789	0.7615	0.7657	0.7615	0.7789	0.8049	0.8654	0.9343	1.0298	1.1095	1.1114
1.0639	1.0870	0.9962	0.8972	0.8253	0.7866	0.7615	0.7779	0.8009	0.7779	0.7615	0.7866	0.8253	0.8972	0.9962	1.0870	1.0639
1.0064	0.9803	0.9379	0.8740	0.8198	0.7739	0.7657	0.8009	0.8687	0.8009	0.7657	0.7739	0.8198	0.8740	0.9379	0.9803	1.0064
1.0639	1.0870	0.9962	0.8972	0.8253	0.7866	0.7615	0.7779	0.8009	0.7779	0.7615	0.7866	0.8253	0.8972	0.9962	1.0870	1.0639
1.1114	1.1095	1.0298	0.9343	0.8654	0.8049	0.7789	0.7615	0.7657	0.7615	0.7789	0.8049	0.8654	0.9343	1.0298	1.1095	1.1114
1.1143	1.0674	1.1213	1.0211	0.9167	0.8554	0.8049	0.7866	0.7739	0.7866	0.8049	0.8554	0.9167	1.0211	1.1213	1.0674	1.1143
	1.3113	1.2705	1.1236	1.0021	0.9167	0.8654	0.8253	0.8198	0.8253	0.8654	0.9167	1.0021	1.1236	1.2705	1.3113	
	1.2895	1.1990	1.1643	1.1236	1.0211	0.9343	0.8972	0.8740	0.8972	0.9343	1.0211	1.1236	1.1643	1.1990	1.2895	
		1.0805	1.1990	1.2705	1.1213	1.0298	0.9962	0.9379	0.9962	1.0298	1.1213	1.2705	1.1990	1.0805		
			1.2895	1.3113	1.0674	1.1095	1.0870	0.9803	1.0870	1.1095	1.0674	1.3113	1.2895			
					1.1143	1.1114	1.0639	1.0064	1.0639	1.1114	1.1143					

relative uncertainties – XSUSA/KENO Va

					2.56%	2.29%	1.89%	1.71%	1.89%	2.29%	2.56%					
			3.02%	2.56%	1.85%	1.50%	1.13%	0.89%	1.13%	1.50%	1.85%	2.56%	3.02%			
		2.56%	2.43%	1.88%	0.98%	0.24%	0.24%	0.53%	0.24%	0.24%	0.98%	1.88%	2.43%	2.56%		
	3.02%	2.43%	1.51%	0.75%	0.29%	1.05%	1.56%	1.73%	1.56%	1.05%	0.29%	0.75%	1.51%	2.43%	3.02%	
	2.56%	1.88%	0.75%	0.50%	1.45%	2.24%	2.74%	2.93%	2.74%	2.24%	1.45%	0.50%	0.75%	1.88%	2.56%	
2.56%	1.85%	0.98%	0.29%	1.45%	2.46%	3.24%	3.75%	3.91%	3.75%	3.24%	2.46%	1.45%	0.29%	0.98%	1.85%	2.56%
2.29%	1.50%	0.24%	1.05%	2.24%	3.24%	4.02%	4.47%	4.63%	4.47%	4.02%	3.24%	2.24%	1.05%	0.24%	1.50%	2.29%
1.89%	1.13%	0.24%	1.56%	2.74%	3.75%	4.47%	4.87%	4.95%	4.87%	4.47%	3.75%	2.74%	1.56%	0.24%	1.13%	1.89%
1.71%	0.89%	0.53%	1.73%	2.93%	3.91%	4.63%	4.95%	4.96%	4.95%	4.63%	3.91%	2.93%	1.73%	0.53%	0.89%	1.71%
1.89%	1.13%	0.24%	1.56%	2.74%	3.75%	4.47%	4.87%	4.95%	4.87%	4.47%	3.75%	2.74%	1.56%	0.24%	1.13%	1.89%
2.29%	1.50%	0.24%	1.05%	2.24%	3.24%	4.02%	4.47%	4.63%	4.47%	4.02%	3.24%	2.24%	1.05%	0.24%	1.50%	2.29%
2.56%	1.85%	0.98%	0.29%	1.45%	2.46%	3.24%	3.75%	3.91%	3.75%	3.24%	2.46%	1.45%	0.29%	0.98%	1.85%	2.56%
	2.56%	1.88%	0.75%	0.50%	1.45%	2.24%	2.74%	2.93%	2.74%	2.24%	1.45%	0.50%	0.75%	1.88%	2.56%	
	3.02%	2.43%	1.51%	0.75%	0.29%	1.05%	1.56%	1.73%	1.56%	1.05%	0.29%	0.75%	1.51%	2.43%	3.02%	
		2.56%	2.43%	1.88%	0.98%	0.24%	0.24%	0.53%	0.24%	0.24%	0.98%	1.88%	2.43%	2.56%		
			3.02%	2.56%	1.85%	1.50%	1.13%	0.89%	1.13%	1.50%	1.85%	2.56%	3.02%			
					2.56%	2.29%	1.89%	1.71%	1.89%	2.29%	2.56%					

mean values – XSUSA/QUABOX-CUBBOX

					1.1070	1.1280	1.0770	1.0230	1.0770	1.1280	1.1070					
			1.2830	1.3130	1.0640	1.1310	1.1110	0.9780	1.1110	1.1310	1.0640	1.3120	1.2820			
		1.0560	1.2260	1.2930	1.1350	1.0110	1.0110	0.9270	1.0110	1.0100	1.1350	1.2930	1.2260	1.0550		
	1.2830	1.2260	1.1440	1.1380	1.0010	0.9430	0.8780	0.8850	0.8780	0.9430	1.0010	1.1380	1.1430	1.2260	1.2820	
	1.3130	1.2930	1.1390	0.9820	0.9250	0.8450	0.8300	0.7990	0.8300	0.8450	0.9250	0.9810	1.1380	1.2930	1.3120	
1.1070	1.0640	1.1350	1.0010	0.9250	0.8350	0.8090	0.7650	0.7760	0.7650	0.8090	0.8340	0.9250	1.0010	1.1350	1.0640	1.1070
1.1280	1.1320	1.0110	0.9440	0.8450	0.8090	0.7570	0.7630	0.7430	0.7630	0.7570	0.8090	0.8450	0.9430	1.0100	1.1310	1.1280
1.0780	1.1110	1.0110	0.8790	0.8310	0.7650	0.7630	0.7540	0.8000	0.7540	0.7630	0.7650	0.8300	0.8780	1.0110	1.1110	1.0770
1.0230	0.9780	0.9270	0.8850	0.8000	0.7760	0.7430	0.8000	0.8670	0.8000	0.7430	0.7760	0.7990	0.8850	0.9270	0.9780	1.0230
1.0780	1.1110	1.0110	0.8790	0.8310	0.7650	0.7630	0.7540	0.8000	0.7540	0.7630	0.7650	0.8300	0.8780	1.0110	1.1110	1.0770
1.1280	1.1320	1.0110	0.9440	0.8450	0.8090	0.7570	0.7630	0.7430	0.7630	0.7570	0.8090	0.8450	0.9430	1.0100	1.1310	1.1280
1.1070	1.0640	1.1360	1.0010	0.9250	0.8350	0.8090	0.7650	0.7760	0.7650	0.8090	0.8340	0.9250	1.0010	1.1350	1.0640	1.1070
	1.3130	1.2930	1.1390	0.9820	0.9250	0.8450	0.8310	0.7990	0.8300	0.8450	0.9250	0.9820	1.1380	1.2930	1.3120	
	1.2830	1.2270	1.1440	1.1390	1.0010	0.9440	0.8790	0.8850	0.8790	0.9440	1.0010	1.1380	1.1430	1.2260	1.2830	
		1.0560	1.2270	1.2930	1.1350	1.0110	1.0110	0.9270	1.0110	1.0110	1.1350	1.2930	1.2260	1.0560		
			1.2830	1.3130	1.0640	1.1320	1.1110	0.9780	1.1110	1.1310	1.0640	1.3120	1.2830			
					1.1070	1.1280	1.0780	1.0230	1.0770	1.1280	1.1070					

relative uncertainties – XSUSA/QUABOX-CUBBOX

					2.82%	2.50%	2.02%	1.79%	2.02%	2.50%	2.82%					
			3.36%	2.81%	1.94%	1.53%	1.13%	0.80%	1.13%	1.53%	1.94%	2.81%	3.36%			
		2.72%	2.62%	2.00%	0.98%	0.14%	0.28%	0.66%	0.28%	0.14%	0.98%	2.00%	2.62%	2.72%		
	3.36%	2.62%	1.51%	0.75%	0.37%	1.19%	1.77%	1.92%	1.77%	1.19%	0.37%	0.75%	1.50%	2.61%	3.36%	
	2.82%	2.00%	0.75%	0.61%	1.61%	2.48%	3.00%	3.23%	3.00%	2.48%	1.61%	0.61%	0.75%	2.00%	2.81%	
2.83%	1.94%	0.98%	0.37%	1.61%	2.73%	3.53%	4.11%	4.26%	4.11%	3.53%	2.73%	1.61%	0.37%	0.98%	1.93%	2.82%
2.50%	1.53%	0.14%	1.19%	2.48%	3.53%	4.39%	4.85%	5.04%	4.85%	4.39%	3.53%	2.48%	1.19%	0.14%	1.53%	2.50%
2.02%	1.12%	0.28%	1.76%	2.99%	4.11%	4.85%	5.28%	5.30%	5.28%	4.85%	4.11%	3.00%	1.76%	0.28%	1.13%	2.02%
1.79%	0.80%	0.66%	1.92%	3.23%	4.24%	5.04%	5.30%	5.26%	5.30%	5.04%	4.26%	3.23%	1.92%	0.66%	0.80%	1.79%
2.02%	1.13%	0.29%	1.76%	2.99%	4.11%	4.85%	5.28%	5.30%	5.28%	4.85%	4.11%	3.00%	1.77%	0.28%	1.13%	2.02%
2.50%	1.53%	0.14%	1.19%	2.48%	3.53%	4.39%	4.85%	5.04%	4.85%	4.39%	3.53%	2.48%	1.19%	0.14%	1.53%	2.50%
2.83%	1.94%	0.98%	0.37%	1.61%	2.73%	3.53%	4.11%	4.24%	4.11%	3.53%	2.73%	1.61%	0.37%	0.98%	1.94%	2.82%
	2.82%	2.00%	0.75%	0.61%	1.61%	2.48%	2.99%	3.23%	3.00%	2.48%	1.61%	0.61%	0.75%	2.00%	2.81%	
	3.36%	2.62%	1.51%	0.75%	0.37%	1.19%	1.76%	1.92%	1.77%	1.19%	0.37%	0.75%	1.51%	2.62%	3.36%	
		2.72%	2.61%	2.00%	0.98%	0.14%	0.28%	0.66%	0.28%	0.14%	0.98%	2.00%	2.62%	2.72%		
			3.36%	2.81%	1.94%	1.53%	1.12%	0.80%	1.12%	1.52%	1.94%	2.81%	3.36%			
					2.83%	2.50%	2.02%	1.79%	2.02%	2.50%	2.82%					

3.3 PWR GEN-III (Generation-III European Pressurized Water Reactor, MOX Core)

Name of Participant(s)	E-mail Address
Markus Klein	markus.klein@grs.de
Winfried Zwermann	winfried.zwermann@grs.de

Organization	Gesellschaft für Anlagen- und Reaktorsicherheit (GRS)mbH
Country	Germany
GEN-III MOX core, steady state	
Reactor Name	*GEN-III*
Operating Condition	*Hot Full Power*
Reactor type	*PWR*
Nuclear Data Library Used	*ENDF/B-VII*
Covariance Data Library Used	*SCALE 6.0 (44groups)*
Computer Code Used	*XSUSA / KENO Va*
	XSUSA / QUABOX-CUBBOX
Criticality Calculation Method	*KENO Va: Monte Carlo*
	QUABOX-CUBBOX: Nodal Diffusion Code
Uncertainty Calculation Method	*sampling method*

		(mean) value	uncertainty	rel. uncertainty
XSUSA/KENO Va	k_eff	1.00499	0.00490	0.487%
XSUSA/NEWT/QUABOX-CUBBOX	k_eff	1.00063	0.00488	0.488%

radial power distribution

mean values

Model																	
						0.8097	1.0556	1.1445	1.1210	1.1445	1.0556	0.8097					
XSUSA/KENO Va				0.8622	1.1042	0.9116	1.0727	1.1369	1.0506	1.1369	1.0727	0.9116	1.1042	0.8622			
			0.9426	0.9662	1.1096	1.0738	1.0578	1.0767	1.0328	1.0767	1.0578	1.0738	1.1096	0.9662	0.9426		
		0.8622	0.9662	1.0549	1.0726	1.0301	0.9945	0.9916	0.9801	0.9916	0.9945	1.0301	1.0726	1.0549	0.9662	0.8622	
		1.1042	1.1096	1.0726	1.0112	0.9711	0.9555	0.9393	0.9423	0.9393	0.9555	0.9711	1.0112	1.0726	1.1096	1.1042	
	0.8097	0.9116	1.0738	1.0301	0.9711	0.9459	0.9218	0.9225	0.9150	0.9225	0.9218	0.9459	0.9711	1.0301	1.0738	0.9116	0.8097
	1.0556	1.0727	1.0578	0.9945	0.9555	0.9218	0.9197	0.9175	0.9293	0.9175	0.9197	0.9218	0.9555	0.9945	1.0578	1.0727	1.0556
	1.1445	1.1369	1.0767	0.9916	0.9393	0.9225	0.9175	0.9535	0.9869	0.9535	0.9175	0.9225	0.9393	0.9916	1.0767	1.1369	1.1445
	1.1210	1.0506	1.0328	0.9801	0.9423	0.9150	0.9293	0.9869	1.0750	0.9869	0.9293	0.9150	0.9423	0.9801	1.0328	1.0506	1.1210
	1.1445	1.1369	1.0767	0.9916	0.9393	0.9225	0.9175	0.9535	0.9869	0.9535	0.9175	0.9225	0.9393	0.9916	1.0767	1.1369	1.1445
	1.0556	1.0727	1.0578	0.9945	0.9555	0.9218	0.9197	0.9175	0.9293	0.9175	0.9197	0.9218	0.9555	0.9945	1.0578	1.0727	1.0556
	0.8097	0.9116	1.0738	1.0301	0.9711	0.9459	0.9218	0.9225	0.9150	0.9225	0.9218	0.9459	0.9711	1.0301	1.0738	0.9116	0.8097
		1.1042	1.1096	1.0726	1.0112	0.9711	0.9555	0.9393	0.9423	0.9393	0.9555	0.9711	1.0112	1.0726	1.1096	1.1042	
		0.8622	0.9662	1.0549	1.0726	1.0301	0.9945	0.9916	0.9801	0.9916	0.9945	1.0301	1.0726	1.0549	0.9662	0.8622	
			0.9426	0.9662	1.1096	1.0738	1.0578	1.0767	1.0328	1.0767	1.0578	1.0738	1.1096	0.9662	0.9426		
				0.8622	1.1042	0.9116	1.0727	1.1369	1.0506	1.1369	1.0727	0.9116	1.1042	0.8622			
						0.8097	1.0556	1.1445	1.1210	1.1445	1.0556	0.8097					
						0.8080	1.0750	1.1620	1.1430	1.1620	1.0750	0.8080					
XSUSA/NEWT/QUABOX-CUBBOX				0.8480	1.0950	0.9500	1.1260	1.1920	1.0790	1.1920	1.1260	0.9500	1.0950	0.8480			
			0.9070	1.0170	1.1530	1.0960	1.0440	1.0970	1.0250	1.0970	1.0440	1.0960	1.1530	1.0170	0.9070		
		0.8480	1.0180	1.0410	1.0870	1.0080	1.0000	0.9650	0.9850	0.9650	1.0000	1.0080	1.0870	1.0400	1.0170	0.8480	
		1.0950	1.1540	1.0870	0.9850	0.9710	0.9230	0.9330	0.9070	0.9330	0.9230	0.9710	0.9850	1.0870	1.1530	1.0950	
	0.8090	0.9510	1.0960	1.0080	0.9710	0.9100	0.9110	0.8810	0.9000	0.8810	0.9110	0.9100	0.9710	1.0080	1.0960	0.9500	0.8080
	1.0750	1.1260	1.0440	1.0000	0.9230	0.9110	0.8760	0.8980	0.8800	0.8980	0.8760	0.9110	0.9230	1.0000	1.0440	1.1260	1.0750
	1.1620	1.1920	1.0970	0.9650	0.9330	0.8810	0.8980	0.9020	0.9620	0.9020	0.8980	0.8810	0.9330	0.9650	1.0970	1.1920	1.1620
	1.1430	1.0790	1.0250	0.9860	0.9070	0.9010	0.8800	0.9620	1.0480	0.9620	0.8800	0.9000	0.9070	0.9850	1.0250	1.0790	1.1430
	1.1620	1.1920	1.0970	0.9660	0.9330	0.8810	0.8980	0.9020	0.9620	0.9020	0.8980	0.8810	0.9330	0.9650	1.0970	1.1920	1.1620
	1.0750	1.1260	1.0440	1.0000	0.9230	0.9110	0.8760	0.8980	0.8800	0.8980	0.8760	0.9110	0.9230	1.0000	1.0440	1.1260	1.0750
	0.8090	0.9510	1.0960	1.0080	0.9710	0.9110	0.9110	0.8810	0.9010	0.8810	0.9110	0.9100	0.9710	1.0080	1.0960	0.9500	0.8080
		1.0950	1.1540	1.0870	0.9850	0.9710	0.9230	0.9330	0.9070	0.9330	0.9230	0.9710	0.9850	1.0870	1.1530	1.0950	
		0.8480	1.0180	1.0410	1.0870	1.0080	1.0000	0.9650	0.9860	0.9650	1.0000	1.0080	1.0870	1.0410	1.0170	0.8480	
			0.9080	1.0180	1.1540	1.0960	1.0440	1.0970	1.0250	1.0970	1.0440	1.0960	1.1530	1.0170	0.9070		
				0.8480	1.0950	0.9510	1.1260	1.1920	1.0790	1.1920	1.1260	0.9500	1.0950	0.8480			
						0.8090	1.0750	1.1620	1.1430	1.1620	1.0750	0.8080					

relative uncertainties

Model																	
						9.76%	9.97%	10.13%	10.29%	10.13%	9.97%	9.76%					
XSUSA/KENO Va				8.13%	7.34%	5.95%	5.78%	5.74%	5.78%	5.74%	5.78%	5.95%	7.34%	8.13%			
			7.27%	5.22%	3.67%	2.28%	1.46%	1.19%	0.93%	1.19%	1.46%	2.28%	3.67%	5.22%	7.27%		
		8.13%	5.22%	2.63%	0.76%	1.35%	2.56%	3.17%	3.42%	3.17%	2.56%	1.35%	0.76%	2.63%	5.22%	8.13%	
		7.34%	3.67%	0.76%	2.31%	4.39%	5.86%	6.76%	7.03%	6.76%	5.86%	4.39%	2.31%	0.76%	3.67%	7.34%	
	9.76%	5.95%	2.28%	1.35%	4.39%	6.78%	8.55%	9.57%	9.94%	9.57%	8.55%	6.78%	4.39%	1.35%	2.28%	5.95%	9.76%
	9.97%	5.78%	1.46%	2.56%	5.86%	8.55%	10.45%	11.64%	12.00%	11.64%	10.45%	8.55%	5.86%	2.56%	1.46%	5.78%	9.97%
	10.13%	5.74%	1.19%	3.17%	6.76%	9.57%	11.64%	12.83%	13.26%	12.83%	11.64%	9.57%	6.76%	3.17%	1.19%	5.74%	10.13%
	10.29%	5.78%	0.93%	3.42%	7.03%	9.94%	12.00%	13.26%	13.61%	13.26%	12.00%	9.94%	7.03%	3.42%	0.93%	5.78%	10.29%
	10.13%	5.74%	1.19%	3.17%	6.76%	9.57%	11.64%	12.83%	13.26%	12.83%	11.64%	9.57%	6.76%	3.17%	1.19%	5.74%	10.13%
	9.97%	5.78%	1.46%	2.56%	5.86%	8.55%	10.45%	11.64%	12.00%	11.64%	10.45%	8.55%	5.86%	2.56%	1.46%	5.78%	9.97%
	9.76%	5.95%	2.28%	1.35%	4.39%	6.78%	8.55%	9.57%	9.94%	9.57%	8.55%	6.78%	4.39%	1.35%	2.28%	5.95%	9.76%
		7.34%	3.67%	0.76%	2.31%	4.39%	5.86%	6.76%	7.03%	6.76%	5.86%	4.39%	2.31%	0.76%	3.67%	7.34%	
		8.13%	5.22%	2.63%	0.76%	1.35%	2.56%	3.17%	3.42%	3.17%	2.56%	1.35%	0.76%	2.63%	5.22%	8.13%	
			7.27%	5.22%	3.67%	2.28%	1.46%	1.19%	0.93%	1.19%	1.46%	2.28%	3.67%	5.22%	7.27%		
				8.13%	7.34%	5.95%	5.78%	5.74%	5.78%	5.74%	5.78%	5.95%	7.34%	8.13%			
						9.76%	9.97%	10.13%	10.29%	10.13%	9.97%	9.76%					
						8.80%	9.07%	9.27%	9.40%	9.27%	9.08%	8.80%					
XSUSA/NEWT/QUABOX-CUBBOX				7.12%	6.46%	5.26%	5.15%	5.17%	5.24%	5.16%	5.15%	5.26%	6.47%	7.11%			
			6.24%	4.41%	3.05%	1.79%	1.08%	0.91%	0.70%	0.91%	1.08%	1.78%	3.05%	4.40%	6.24%		
		7.12%	4.41%	1.95%	0.52%	1.52%	2.58%	3.12%	3.31%	3.12%	2.58%	1.53%	0.52%	1.94%	4.40%	7.11%	
		6.47%	3.05%	0.52%	2.46%	4.34%	5.67%	6.48%	6.73%	6.48%	5.67%	4.35%	2.46%	0.52%	3.05%	6.47%	
	8.80%	5.26%	1.79%	1.52%	4.34%	6.57%	8.19%	9.15%	9.47%	9.15%	8.18%	6.57%	4.35%	1.53%	1.78%	5.26%	8.80%
	9.09%	5.16%	1.09%	2.58%	5.67%	8.18%	10.00%	11.11%	11.46%	11.11%	10.00%	8.18%	5.67%	2.58%	1.08%	5.15%	9.08%
	9.27%	5.17%	0.91%	3.12%	6.47%	9.15%	11.11%	12.26%	12.67%	12.26%	11.11%	9.15%	6.48%	3.12%	0.91%	5.17%	9.26%
	9.41%	5.24%	0.71%	3.31%	6.72%	9.48%	11.46%	12.66%	13.00%	12.67%	11.46%	9.48%	6.73%	3.31%	0.70%	5.23%	9.39%
	9.27%	5.18%	0.91%	3.12%	6.47%	9.13%	11.11%	12.25%	12.66%	12.26%	11.11%	9.15%	6.48%	3.12%	0.91%	5.17%	9.26%
	9.09%	5.16%	1.09%	2.57%	5.67%	8.19%	10.00%	11.11%	11.46%	11.11%	10.00%	8.18%	5.67%	2.58%	1.08%	5.15%	9.08%
	8.81%	5.27%	1.78%	1.52%	4.34%	6.56%	8.19%	9.13%	9.47%	9.15%	8.18%	6.57%	4.35%	1.53%	1.79%	5.26%	8.80%
		6.47%	3.05%	0.53%	2.46%	4.34%	5.67%	6.47%	6.72%	6.48%	5.67%	4.35%	2.46%	0.52%	3.05%	6.47%	
		7.11%	4.41%	1.95%	0.52%	1.52%	2.57%	3.12%	3.31%	3.12%	2.58%	1.52%	0.53%	1.94%	4.40%	7.10%	
			6.24%	4.41%	3.05%	1.78%	1.09%	0.91%	0.71%	0.91%	1.08%	1.79%	3.05%	4.40%	6.24%		
				7.11%	6.47%	5.26%	5.16%	5.17%	5.24%	5.17%	5.16%	5.26%	6.47%	7.12%			
						8.80%	9.08%	9.27%	9.40%	9.27%	9.08%	8.80%					

4 PWR Burnup Pin-Cell Benchmark

Name of Participant(s)	E-mail Address
Lucia Gallner	lucia.gallner@grs.de
Markus Klein	markus.klein@grs.de
Winfried Zwermann	winfried.zwermann@grs.de
Organization	Gesellschaft für Anlagen- und Reaktorsicherheit (GRS)mbH
Country	Germany

Reactor Name	*TMI-1*
Operating Condition	*Hot Full Power*
Reactor type	*PWR*
Nuclear Data Library Used	*ENDF/B-VII*
Covariance Data Library Used	*SCALE 6.0 (44groups)*
Computer Code Used	*XSUSA / TRITON (BONAMI-CENTRM-NEWT-ORIGENS)*
Criticality Calculation Method	*two-dimensional (2-D) discrete-ordinates transport*
Uncertainty Calculation Method	*sampling method*

In the following tables, the quantities given are:

1. Multiplication factor k-eff
2. Main contributions to k-eff (squared multiple correlation coefficient)
3. Neutron flux
4. Reaction rates
5. Cross sections
6. Nuclide Inventories

	0 GWd/MTU		10 GWd/MTU		20 GWd/MTU	
	mean	rel. std. dev.	mean	rel. std. dev.	mean	rel. std. dev.
k-eff	1.4029	0.48%	1.2474	0.49%	1.1623	0.55%
	92238-0102	0.352	92238-0102	0.288	94239-0452	0.294
	92235-0452	0.289	92238-0002	0.199	92238-0102	0.193
	92235-0102	0.258	92235-0102	0.176	92238-0002	0.185
	92238-0002	0.173	92235-0452	0.168	94239-0102	0.141
	92235-0002	0.128	94239-0452	0.147	94239-0018	0.139
flux	2.002E+01	0.92%	1.973E+01	0.92%	1.968E+01	0.92%
u235-cap	1.279E-01	1.39%	9.080E-02	1.42%	6.883E-02	1.40%
u235-fis	5.406E-01	0.44%	3.703E-01	0.62%	2.781E-01	0.73%
u238-cap	2.581E-01	0.82%	2.519E-01	0.75%	2.506E-01	0.70%
u238-fis	3.002E-02	4.78%	3.010E-02	4.59%	3.008E-02	4.48%
pu239-cap			4.903E-02	1.25%	6.981E-02	1.16%
pu239-fis			8.615E-02	0.90%	1.238E-01	0.80%
pu240-cap			2.111E-02	1.26%	4.070E-02	1.06%
pu240-fis			7.578E-05	3.29%	1.955E-04	3.25%
pu241-cap			1.423E-03	1.67%	5.182E-03	1.46%
pu241-fis			3.915E-03	1.60%	1.436E-02	1.35%
abs-1	1.159E-02	0.90%	1.202E-02	0.91%	1.236E-02	0.92%
abs-2	1.164E-01	0.23%	1.306E-01	0.35%	1.323E-01	0.50%
fis-1	3.873E-03	0.38%	3.447E-03	0.40%	3.076E-03	0.51%
fis-2	8.663E-02	0.32%	8.504E-02	0.36%	8.110E-02	0.51%
nufis-1	9.761E-03	0.50%	8.818E-03	0.54%	7.973E-03	0.65%
nufis-2	2.111E-01	0.44%	2.156E-01	0.51%	2.105E-01	0.69%
diff-1	1.414E+00	2.37%	1.418E+00	2.35%	1.422E+00	2.33%
diff-2	3.745E-01	0.18%	3.655E-01	0.17%	3.618E-01	0.17%
42095	0.000E+00		8.372E-06	0.08%	2.238E-05	0.13%
43099	0.000E+00		1.481E-05	0.07%	2.875E-05	0.14%
44101	0.000E+00		1.291E-05	0.05%	2.572E-05	0.05%
44106	0.000E+00		1.789E-06	0.61%	3.955E-06	0.54%
45103	0.000E+00		6.462E-06	0.40%	1.412E-05	0.69%
47109	0.000E+00		4.376E-07	0.87%	1.332E-06	0.91%
55133	0.000E+00		1.541E-05	0.18%	3.013E-05	0.36%
55134	0.000E+00		4.787E-07	5.01%	1.795E-06	4.83%
55135	0.000E+00		6.240E-06	2.53%	1.238E-05	2.54%
55137	0.000E+00		1.511E-05	0.02%	2.992E-05	0.02%
57139	0.000E+00		1.538E-05	0.04%	3.024E-05	0.05%
58140	0.000E+00		1.398E-05	0.04%	2.863E-05	0.05%
58142	0.000E+00		1.392E-05	0.07%	2.734E-05	0.07%
58144	0.000E+00		9.138E-06	0.07%	1.302E-05	0.09%
60142	0.000E+00		3.801E-08	0.40%	1.835E-07	0.44%
60143	0.000E+00		1.229E-05	0.28%	2.339E-05	0.58%
60145	0.000E+00		9.113E-06	0.29%	1.729E-05	0.61%
60146	0.000E+00		7.531E-06	0.35%	1.533E-05	0.68%
60148	0.000E+00		4.200E-06	0.29%	8.348E-06	0.31%
60150	0.000E+00		1.762E-06	0.21%	3.630E-06	0.20%
62147	0.000E+00		4.254E-07	0.49%	1.420E-06	0.88%
62148	0.000E+00		4.499E-07	3.38%	1.743E-06	2.87%
62149	0.000E+00		1.170E-07	1.69%	1.227E-07	1.82%

62150	0.000E+00	2.758E-06	0.32%	5.931E-06	0.56%
62151	0.000E+00	3.909E-07	1.72%	4.724E-07	2.28%
62152	0.000E+00	1.274E-06	0.76%	2.506E-06	1.29%
62154	0.000E+00	2.511E-07	0.34%	5.759E-07	0.31%
63151	0.000E+00	5.924E-10	1.93%	7.837E-10	2.73%
63153	0.000E+00	6.876E-07	1.20%	1.884E-06	1.67%
63154	0.000E+00	6.975E-08	5.21%	3.025E-07	5.93%
63155	0.000E+00	4.358E-08	4.69%	1.028E-07	6.05%
64154	0.000E+00	1.467E-09	4.97%	1.251E-08	5.50%
64155	0.000E+00	5.151E-10	4.87%	1.212E-09	5.93%
64156	0.000E+00	1.561E-07	1.23%	5.511E-07	2.08%
64158	0.000E+00	6.062E-08	0.70%	1.782E-07	1.03%
64160	0.000E+00	3.584E-09	0.76%	1.101E-08	0.67%
92233	0.000E+00	5.899E-11	15.51%	1.002E-10	15.17%
92234	1.166E-05	1.034E-05	0.81%	9.097E-06	1.69%
92235	1.126E-03	8.716E-04	0.11%	6.660E-04	0.28%
92236	0.000E+00	4.870E-05	1.59%	8.633E-05	1.57%
92238	2.181E-02	2.167E-02	0.01%	2.153E-02	0.01%
93237	0.000E+00	1.695E-06	5.95%	4.878E-06	4.33%
94238	0.000E+00	1.233E-07	7.36%	7.333E-07	5.29%
94239	0.000E+00	8.072E-05	1.15%	1.232E-04	1.28%
94240	0.000E+00	9.364E-06	1.61%	2.452E-05	1.72%
94241	0.000E+00	3.545E-06	1.63%	1.348E-05	1.44%
94242	0.000E+00	1.983E-07	2.03%	1.672E-06	2.04%
95241	0.000E+00	3.648E-08	1.74%	2.764E-07	1.69%
95243	0.000E+00	9.627E-09	9.64%	1.778E-07	9.03%
96244	0.000E+00	5.641E-10	10.10%	2.323E-08	9.58%
96246	0.000E+00	1.172E-13	16.34%	2.199E-11	15.95%

	30 GWd/MTU		40 GWd/MTU		50 GWd/MTU	
	mean	rel. std. dev.	mean	rel. std. dev.	mean	rel. std. dev.
k-eff	1.0913	0.60%	1.0270	0.65%	0.9688	0.70%
	94239-0452	0.388	94239-0452	0.449	94239-0452	0.487
	92238-0002	0.172	94239-0102	0.176	94239-0102	0.174
	94239-0102	0.166	94239-0018	0.171	94239-0018	0.168
	94239-0018	0.161	92238-0002	0.165	92238-0002	0.164
	92238-0004	0.121	92238-0004	0.135	92238-0004	0.146
flux	1.971E+01	0.91%	1.977E+01	0.91%	1.984E+01	0.91%
u235-cap	5.223E-02	1.33%	3.889E-02	1.22%	2.817E-02	1.13%
u235-fis	2.108E-01	0.80%	1.575E-01	0.85%	1.147E-01	0.90%
u238-cap	2.508E-01	0.65%	2.514E-01	0.60%	2.520E-01	0.55%
u238-fis	3.000E-02	4.42%	2.989E-02	4.38%	2.975E-02	4.37%
pu239-cap	8.039E-02	1.11%	8.639E-02	1.07%	8.968E-02	1.04%
pu239-fis	1.436E-01	0.76%	1.552E-01	0.76%	1.618E-01	0.76%
pu240-cap	5.438E-02	1.00%	6.501E-02	0.98%	7.324E-02	0.97%
pu240-fis	3.149E-04	3.30%	4.261E-04	3.37%	5.208E-04	3.46%
pu241-cap	9.502E-03	1.39%	1.335E-02	1.36%	1.655E-02	1.34%
pu241-fis	2.642E-02	1.25%	3.721E-02	1.19%	4.621E-02	1.14%
abs-1	1.255E-02	0.94%	1.268E-02	0.95%	1.278E-02	0.97%
abs-2	1.307E-01	0.67%	1.274E-01	0.86%	1.235E-01	1.07%
fis-1	2.758E-03	0.69%	2.478E-03	0.92%	2.240E-03	1.17%
fis-2	7.567E-02	0.70%	6.971E-02	0.94%	6.388E-02	1.22%
nufis-1	7.239E-03	0.82%	6.591E-03	1.03%	6.035E-03	1.26%
nufis-2	2.001E-01	0.90%	1.875E-01	1.13%	1.744E-01	1.40%
diff-1	1.425E+00	2.32%	1.428E+00	2.31%	1.431E+00	2.30%
diff-2	3.600E-01	0.18%	3.592E-01	0.18%	3.588E-01	0.18%
42095	3.563E-05	0.19%	4.783E-05	0.27%	5.902E-05	0.34%
43099	4.152E-05	0.21%	5.335E-05	0.28%	6.422E-05	0.36%
44101	3.837E-05	0.06%	5.077E-05	0.06%	6.289E-05	0.07%
44106	6.115E-06	0.48%	8.149E-06	0.41%	1.003E-05	0.35%
45103	2.110E-05	0.99%	2.722E-05	1.27%	3.240E-05	1.54%
47109	2.520E-06	0.99%	3.901E-06	1.11%	5.400E-06	1.26%
55133	4.359E-05	0.55%	5.578E-05	0.74%	6.668E-05	0.94%
55134	3.717E-06	4.64%	6.070E-06	4.45%	8.711E-06	4.26%
55135	1.826E-05	2.56%	2.387E-05	2.60%	2.924E-05	2.63%
55137	4.444E-05	0.02%	5.867E-05	0.02%	7.258E-05	0.02%
57139	4.470E-05	0.05%	5.879E-05	0.05%	7.252E-05	0.04%
58140	4.363E-05	0.05%	5.843E-05	0.06%	7.306E-05	0.06%
58142	4.035E-05	0.07%	5.300E-05	0.07%	6.532E-05	0.07%
58144	1.450E-05	0.10%	1.488E-05	0.11%	1.476E-05	0.11%
60142	4.517E-07	0.51%	8.586E-07	0.60%	1.421E-06	0.71%
60143	3.243E-05	0.91%	3.948E-05	1.26%	4.463E-05	1.63%
60145	2.464E-05	0.94%	3.119E-05	1.30%	3.697E-05	1.67%
60146	2.349E-05	0.98%	3.206E-05	1.26%	4.106E-05	1.50%
60148	1.246E-05	0.32%	1.654E-05	0.34%	2.058E-05	0.36%
60150	5.585E-06	0.19%	7.613E-06	0.18%	9.703E-06	0.17%
62147	2.582E-06	1.26%	3.678E-06	1.63%	4.583E-06	2.00%
62148	3.660E-06	2.44%	6.067E-06	2.10%	8.862E-06	1.81%
62149	1.147E-07	2.00%	1.100E-07	2.15%	1.041E-07	2.34%

62150	9.285E-06	0.77%	1.265E-05	0.96%	1.595E-05	1.16%
62151	5.268E-07	2.68%	5.685E-07	3.02%	6.026E-07	3.28%
62152	3.459E-06	1.81%	4.203E-06	2.25%	4.804E-06	2.60%
62154	9.609E-07	0.28%	1.398E-06	0.25%	1.881E-06	0.22%
63151	8.303E-10	3.24%	8.305E-10	3.72%	8.090E-10	4.16%
63153	3.327E-06	2.04%	4.800E-06	2.44%	6.172E-06	2.87%
63154	6.760E-07	6.61%	1.117E-06	7.23%	1.555E-06	7.77%
63155	1.988E-07	6.33%	3.185E-07	6.11%	4.452E-07	5.77%
64154	4.238E-08	6.02%	9.589E-08	6.51%	1.722E-07	6.96%
64155	2.312E-09	5.96%	3.588E-09	5.61%	4.836E-09	5.34%
64156	1.336E-06	2.98%	2.699E-06	3.35%	4.778E-06	3.35%
64158	3.598E-07	1.68%	6.257E-07	2.54%	1.011E-06	3.53%
64160	2.173E-08	0.60%	3.546E-08	0.54%	5.201E-08	0.50%
92233	1.252E-10	14.99%	1.367E-10	14.91%	1.379E-10	14.87%
92234	7.940E-06	2.62%	6.874E-06	3.60%	5.906E-06	4.63%
92235	4.980E-04	0.51%	3.623E-04	0.85%	2.554E-04	1.31%
92236	1.151E-04	1.55%	1.361E-04	1.52%	1.502E-04	1.49%
92238	2.137E-02	0.02%	2.120E-02	0.03%	2.102E-02	0.03%
93237	8.759E-06	3.72%	1.285E-05	3.40%	1.679E-05	3.23%
94238	2.072E-06	4.36%	4.233E-06	3.82%	7.152E-06	3.46%
94239	1.447E-04	1.45%	1.546E-04	1.64%	1.577E-04	1.85%
94240	4.000E-05	1.85%	5.405E-05	1.97%	6.593E-05	2.10%
94241	2.470E-05	1.41%	3.434E-05	1.47%	4.164E-05	1.61%
94242	4.960E-06	2.33%	9.939E-06	2.73%	1.621E-05	3.15%
95241	7.147E-07	1.90%	1.219E-06	2.25%	1.659E-06	2.71%
95243	8.158E-07	8.37%	2.161E-06	7.69%	4.263E-06	7.05%
96244	1.740E-07	9.01%	6.592E-07	8.42%	1.727E-06	7.86%
96246	4.165E-10	15.50%	3.118E-09	15.00%	1.401E-08	14.45%

	60 GWd/MTU		shutdown		1 year cooling time	
	mean	rel. std. dev.	mean	rel. std. dev.	mean	rel. std. dev.
k-eff	0.9169	0.75%	0.9102	0.75%	0.9246	0.77%
	94239-0452	0.507	94239-0452	0.508	94239-0452	0.499
	92238-0002	0.169	92238-0002	0.170	92238-0002	0.169
	94239-0102	0.162	94239-0102	0.159	94239-0102	0.167
	94239-0018	0.156	94239-0018	0.153	94239-0018	0.163
	92238-0004	0.152	92238-0004	0.153	92238-0004	0.152
flux	1.992E+01	0.91%	1.993E+01	0.91%	1.997E+01	0.91%
u235-cap	1.968E-02	1.16%	1.873E-02	1.18%	1.903E-02	1.19%
u235-fis	8.068E-02	1.03%	7.686E-02	1.07%	7.862E-02	1.08%
u238-cap	2.525E-01	0.50%	2.525E-01	0.50%	2.536E-01	0.50%
u238-fis	2.957E-02	4.36%	2.955E-02	4.36%	2.956E-02	4.37%
pu239-cap	9.134E-02	1.02%	9.145E-02	1.02%	9.394E-02	1.01%
pu239-fis	1.654E-01	0.77%	1.657E-01	0.78%	1.706E-01	0.78%
pu240-cap	7.969E-02	0.95%	8.045E-02	0.95%	8.083E-02	0.95%
pu240-fis	5.987E-04	3.56%	6.081E-04	3.57%	6.094E-04	3.57%
pu241-cap	1.898E-02	1.31%	1.920E-02	1.30%	1.866E-02	1.29%
pu241-fis	5.307E-02	1.09%	5.367E-02	1.08%	5.222E-02	1.07%
abs-1	1.287E-02	0.99%	1.288E-02	0.99%	1.290E-02	0.99%
abs-2	1.195E-01	1.27%	1.190E-01	1.30%	1.165E-01	1.29%
fis-1	2.040E-03	1.42%	2.017E-03	1.45%	2.012E-03	1.45%
fis-2	5.854E-02	1.52%	5.788E-02	1.56%	5.797E-02	1.56%
nufis-1	5.572E-03	1.49%	5.517E-03	1.52%	5.502E-03	1.52%
nufis-2	1.620E-01	1.68%	1.604E-01	1.72%	1.606E-01	1.72%
diff-1	1.434E+00	2.29%	1.435E+00	2.29%	1.435E+00	2.29%
diff-2	3.588E-01	0.19%	3.589E-01	0.19%	3.590E-01	0.19%
42095	6.922E-05	0.43%	7.046E-05	0.44%	7.607E-05	0.41%
43099	7.412E-05	0.45%	7.535E-05	0.46%	7.556E-05	0.46%
44101	7.467E-05	0.08%	7.615E-05	0.08%	7.615E-05	0.08%
44106	1.174E-05	0.32%	1.195E-05	0.32%	6.046E-06	0.32%
45103	3.665E-05	1.79%	3.713E-05	1.82%	3.976E-05	1.70%
47109	6.960E-06	1.41%	7.161E-06	1.43%	7.171E-06	1.43%
55133	7.627E-05	1.14%	7.741E-05	1.17%	7.786E-05	1.16%
55134	1.152E-05	4.08%	1.188E-05	4.06%	8.493E-06	4.06%
55135	3.442E-05	2.68%	3.508E-05	2.68%	3.511E-05	2.68%
55137	8.620E-05	0.03%	8.791E-05	0.03%	8.591E-05	0.03%
57139	8.589E-05	0.04%	8.757E-05	0.04%	8.758E-05	0.04%
58140	8.756E-05	0.06%	8.934E-05	0.06%	9.026E-05	0.06%
58142	7.732E-05	0.06%	7.884E-05	0.06%	7.884E-05	0.06%
58144	1.442E-05	0.11%	1.437E-05	0.11%	5.913E-06	0.11%
60142	2.154E-06	0.84%	2.261E-06	0.85%	2.265E-06	0.85%
60143	4.800E-05	2.03%	4.830E-05	2.08%	4.911E-05	2.05%
60145	4.201E-05	2.06%	4.260E-05	2.11%	4.261E-05	2.11%
60146	5.052E-05	1.70%	5.176E-05	1.73%	5.176E-05	1.73%
60148	2.459E-05	0.38%	2.510E-05	0.39%	2.510E-05	0.39%
60150	1.185E-05	0.16%	1.213E-05	0.16%	1.213E-05	0.16%
62147	5.250E-06	2.37%	5.318E-06	2.41%	7.296E-06	2.27%
62148	1.195E-05	1.57%	1.236E-05	1.55%	1.248E-05	1.55%
62149	9.834E-08	2.55%	1.030E-07	2.57%	1.509E-07	1.76%

62150	1.912E-05	1.37%	1.949E-05	1.40%	1.949E-05	1.40%
62151	6.326E-07	3.46%	6.368E-07	3.47%	6.415E-07	3.42%
62152	5.308E-06	2.87%	5.366E-06	2.89%	5.367E-06	2.89%
62154	2.406E-06	0.19%	2.475E-06	0.18%	2.475E-06	0.18%
63151	7.815E-10	4.56%	7.767E-10	4.61%	5.733E-09	3.52%
63153	7.381E-06	3.28%	7.520E-06	3.33%	7.566E-06	3.32%
63154	1.944E-06	8.21%	1.988E-06	8.26%	1.834E-06	8.26%
63155	5.649E-07	5.47%	5.800E-07	5.43%	5.002E-07	5.43%
64154	2.665E-07	7.36%	2.795E-07	7.41%	4.335E-07	7.68%
64155	5.954E-09	5.29%	6.058E-09	5.31%	8.586E-08	5.31%
64156	7.629E-06	3.20%	8.050E-06	3.18%	8.307E-06	3.15%
64158	1.548E-06	4.53%	1.628E-06	4.65%	1.628E-06	4.65%
64160	7.124E-08	0.48%	7.388E-08	0.48%	7.388E-08	0.48%
92233	1.322E-10	14.85%	1.312E-10	14.85%	1.380E-10	14.14%
92234	5.043E-06	5.70%	4.940E-06	5.83%	5.031E-06	5.73%
92235	1.741E-04	1.92%	1.654E-04	2.01%	1.654E-04	2.01%
92236	1.582E-04	1.47%	1.589E-04	1.47%	1.589E-04	1.47%
92238	2.082E-02	0.04%	2.080E-02	0.04%	2.080E-02	0.04%
93237	2.030E-05	3.13%	2.071E-05	3.12%	2.101E-05	3.11%
94238	1.061E-05	3.21%	1.107E-05	3.18%	1.161E-05	3.04%
94239	1.574E-04	2.05%	1.573E-04	2.07%	1.593E-04	2.05%
94240	7.533E-05	2.23%	7.635E-05	2.25%	7.649E-05	2.25%
94241	4.667E-05	1.79%	4.713E-05	1.82%	4.491E-05	1.82%
94242	2.332E-05	3.55%	2.427E-05	3.59%	2.427E-05	3.59%
95241	1.970E-06	3.22%	2.001E-06	3.29%	4.217E-06	2.34%
95243	7.004E-06	6.46%	7.389E-06	6.39%	7.394E-06	6.39%
96244	3.588E-06	7.35%	3.890E-06	7.29%	3.751E-06	7.29%
96246	4.522E-08	13.86%	5.159E-08	13.78%	5.158E-08	13.78%

	3 years cooling time		5 years cooling time		10 years cooling time	
	mean	rel. std. dev.	mean	rel. std. dev.	mean	rel. std. dev.
k-eff	0.9124	0.79%	0.9011	0.81%	0.8777	0.85%
	94239-0452	0.488	94239-0452	0.478	94239-0452	0.456
	94239-0102	0.173	94239-0102	0.177	94239-0102	0.187
	92238-0002	0.172	92238-0002	0.174	94239-0018	0.181
	94239-0018	0.168	94239-0018	0.173	92238-0002	0.178
	92238-0004	0.154	92238-0004	0.156	92238-0004	0.158
flux	1.998E+01	0.91%	1.999E+01	0.91%	2.000E+01	0.91%
u235-cap	1.906E-02	1.19%	1.908E-02	1.19%	1.916E-02	1.19%
u235-fis	7.877E-02	1.08%	7.891E-02	1.08%	7.930E-02	1.08%
u238-cap	2.538E-01	0.50%	2.540E-01	0.50%	2.544E-01	0.50%
u238-fis	2.957E-02	4.38%	2.958E-02	4.38%	2.960E-02	4.40%
pu239-cap	9.412E-02	1.01%	9.428E-02	1.02%	9.463E-02	1.03%
pu239-fis	1.710E-01	0.78%	1.713E-01	0.78%	1.719E-01	0.78%
pu240-cap	8.101E-02	0.95%	8.117E-02	0.95%	8.151E-02	0.96%
pu240-fis	6.116E-04	3.56%	6.137E-04	3.56%	6.181E-04	3.55%
pu241-cap	1.699E-02	1.29%	1.546E-02	1.29%	1.222E-02	1.30%
pu241-fis	4.755E-02	1.08%	4.328E-02	1.08%	3.420E-02	1.09%
abs-1	1.289E-02	0.99%	1.289E-02	0.99%	1.288E-02	0.99%
abs-2	1.163E-01	1.29%	1.161E-01	1.29%	1.156E-01	1.29%
fis-1	1.992E-03	1.47%	1.974E-03	1.49%	1.936E-03	1.54%
fis-2	5.708E-02	1.58%	5.627E-02	1.59%	5.458E-02	1.61%
nufis-1	5.443E-03	1.54%	5.389E-03	1.56%	5.274E-03	1.61%
nufis-2	1.580E-01	1.74%	1.556E-01	1.75%	1.506E-01	1.78%
diff-1	1.435E+00	2.29%	1.435E+00	2.30%	1.436E+00	2.30%
diff-2	3.591E-01	0.19%	3.592E-01	0.19%	3.592E-01	0.19%
42095	7.623E-05	0.41%	7.623E-05	0.41%	7.623E-05	0.41%
43099	7.556E-05	0.46%	7.556E-05	0.46%	7.555E-05	0.46%
44101	7.615E-05	0.08%	7.615E-05	0.08%	7.615E-05	0.08%
44106	1.548E-06	0.32%	3.965E-07	0.32%	1.316E-08	0.32%
45103	3.977E-05	1.70%	3.977E-05	1.70%	3.977E-05	1.70%
47109	7.171E-06	1.43%	7.171E-06	1.43%	7.171E-06	1.43%
55133	7.786E-05	1.16%	7.786E-05	1.16%	7.786E-05	1.16%
55134	4.338E-06	4.06%	2.216E-06	4.06%	4.131E-07	4.06%
55135	3.511E-05	2.68%	3.511E-05	2.68%	3.511E-05	2.68%
55137	8.203E-05	0.03%	7.833E-05	0.03%	6.979E-05	0.03%
57139	8.758E-05	0.04%	8.758E-05	0.04%	8.758E-05	0.04%
58140	9.026E-05	0.06%	9.026E-05	0.06%	9.026E-05	0.06%
58142	7.884E-05	0.06%	7.884E-05	0.06%	7.884E-05	0.06%
58144	1.001E-06	0.11%	1.695E-07	0.11%	1.999E-09	0.11%
60142	2.265E-06	0.85%	2.265E-06	0.85%	2.265E-06	0.85%
60143	4.911E-05	2.05%	4.911E-05	2.05%	4.911E-05	2.05%
60145	4.261E-05	2.11%	4.261E-05	2.11%	4.261E-05	2.11%
60146	5.176E-05	1.73%	5.176E-05	1.73%	5.176E-05	1.73%
60148	2.510E-05	0.39%	2.510E-05	0.39%	2.510E-05	0.39%
60150	1.213E-05	0.16%	1.213E-05	0.16%	1.213E-05	0.16%
62147	9.987E-06	2.21%	1.157E-05	2.20%	1.324E-05	2.19%
62148	1.248E-05	1.55%	1.248E-05	1.55%	1.248E-05	1.55%
62149	1.509E-07	1.76%	1.509E-07	1.76%	1.509E-07	1.76%

62150	1.949E-05	1.40%	1.949E-05	1.40%	1.949E-05	1.40%
62151	6.318E-07	3.42%	6.221E-07	3.42%	5.986E-07	3.42%
62152	5.367E-06	2.89%	5.367E-06	2.89%	5.367E-06	2.89%
62154	2.475E-06	0.18%	2.475E-06	0.18%	2.476E-06	0.18%
63151	1.553E-08	3.45%	2.518E-08	3.44%	4.867E-08	3.43%
63153	7.566E-06	3.32%	7.566E-06	3.32%	7.566E-06	3.32%
63154	1.561E-06	8.26%	1.328E-06	8.26%	8.876E-07	8.26%
63155	3.721E-07	5.43%	2.767E-07	5.43%	1.320E-07	5.43%
64154	7.065E-07	7.89%	9.389E-07	7.98%	1.379E-06	8.07%
64155	2.140E-07	5.38%	3.094E-07	5.40%	4.541E-07	5.41%
64156	8.307E-06	3.15%	8.307E-06	3.15%	8.307E-06	3.15%
64158	1.628E-06	4.65%	1.628E-06	4.65%	1.628E-06	4.65%
64160	7.388E-08	0.48%	7.388E-08	0.48%	7.388E-08	0.48%
92233	1.523E-10	12.86%	1.666E-10	11.81%	2.016E-10	9.89%
92234	5.214E-06	5.54%	5.396E-06	5.36%	5.837E-06	4.98%
92235	1.654E-04	2.01%	1.654E-04	2.01%	1.654E-04	2.01%
92236	1.589E-04	1.47%	1.589E-04	1.46%	1.589E-04	1.46%
92238	2.080E-02	0.04%	2.080E-02	0.04%	2.080E-02	0.04%
93237	2.103E-05	3.11%	2.107E-05	3.10%	2.119E-05	3.08%
94238	1.157E-05	3.00%	1.139E-05	3.00%	1.095E-05	3.00%
94239	1.593E-04	2.05%	1.593E-04	2.05%	1.593E-04	2.05%
94240	7.675E-05	2.24%	7.699E-05	2.24%	7.750E-05	2.23%
94241	4.078E-05	1.82%	3.703E-05	1.82%	2.908E-05	1.82%
94242	2.427E-05	3.59%	2.427E-05	3.59%	2.427E-05	3.59%
95241	8.330E-06	2.02%	1.205E-05	1.94%	1.986E-05	1.89%
95243	7.393E-06	6.39%	7.392E-06	6.39%	7.388E-06	6.39%
96244	3.474E-06	7.29%	3.218E-06	7.29%	2.658E-06	7.29%
96246	5.157E-08	13.78%	5.155E-08	13.78%	5.151E-08	13.78%

	50 years cooling time		100 years cooling time		300 years cooling time	
	mean	rel. std. dev.	mean	rel. std. dev.	mean	rel. std. dev.
k-eff	0.8078	1.01%	0.7999	1.03%	0.8104	1.01%
	94239-0452	0.397	94239-0452	0.392	94239-0452	0.406
	94239-0102	0.218	94239-0102	0.223	94239-0102	0.221
	94239-0018	0.207	94239-0018	0.211	94239-0018	0.209
	92238-0002	0.183	92238-0002	0.183	92238-0002	0.180
	92238-0004	0.161	92238-0004	0.161	92238-0004	0.158
flux	2.007E+01	0.92%	2.009E+01	0.92%	2.013E+01	0.91%
u235-cap	1.955E-02	1.19%	1.971E-02	1.18%	2.008E-02	1.17%
u235-fis	8.145E-02	1.08%	8.232E-02	1.08%	8.428E-02	1.05%
u238-cap	2.561E-01	0.50%	2.566E-01	0.50%	2.576E-01	0.49%
u238-fis	2.966E-02	4.46%	2.967E-02	4.48%	2.967E-02	4.48%
pu239-cap	9.630E-02	1.06%	9.697E-02	1.06%	9.841E-02	1.07%
pu239-fis	1.753E-01	0.80%	1.767E-01	0.79%	1.793E-01	0.77%
pu240-cap	8.283E-02	0.98%	8.308E-02	0.99%	8.272E-02	1.00%
pu240-fis	6.330E-04	3.54%	6.338E-04	3.53%	6.215E-04	3.53%
pu241-cap	1.822E-03	1.32%	1.648E-04	1.33%	2.703E-07	12.64%
pu241-fis	5.100E-03	1.13%	4.613E-04	1.14%	7.563E-07	12.56%
abs-1	1.289E-02	1.00%	1.289E-02	1.00%	1.286E-02	1.00%
abs-2	1.129E-01	1.31%	1.119E-01	1.32%	1.101E-01	1.32%
fis-1	1.816E-03	1.70%	1.797E-03	1.73%	1.795E-03	1.73%
fis-2	4.934E-02	1.71%	4.856E-02	1.72%	4.856E-02	1.73%
nufis-1	4.908E-03	1.78%	4.848E-03	1.81%	4.834E-03	1.81%
nufis-2	1.351E-01	1.90%	1.328E-01	1.93%	1.327E-01	1.93%
diff-1	1.437E+00	2.31%	1.437E+00	2.31%	1.437E+00	2.31%
diff-2	3.587E-01	0.19%	3.587E-01	0.19%	3.592E-01	0.19%
42095	7.623E-05	0.41%	7.623E-05	0.41%	7.623E-05	0.41%
43099	7.555E-05	0.46%	7.553E-05	0.46%	7.548E-05	0.46%
44101	7.615E-05	0.08%	7.615E-05	0.08%	7.615E-05	0.08%
44106	1.937E-20	0.32%	0.000E+00		0.000E+00	
45103	3.977E-05	1.70%	3.977E-05	1.70%	3.977E-05	1.70%
47109	7.171E-06	1.43%	7.171E-06	1.43%	7.171E-06	1.43%
55133	7.786E-05	1.16%	7.786E-05	1.16%	7.786E-05	1.16%
55134	6.030E-13	4.06%	3.431E-20	3.99%	0.000E+00	
55135	3.511E-05	2.68%	3.510E-05	2.68%	3.510E-05	2.68%
55137	2.771E-05	0.03%	8.736E-06	0.03%	8.625E-08	0.03%
57139	8.758E-05	0.04%	8.758E-05	0.04%	8.758E-05	0.04%
58140	9.026E-05	0.06%	9.026E-05	0.06%	9.026E-05	0.06%
58142	7.884E-05	0.06%	7.884E-05	0.06%	7.884E-05	0.06%
58144	0.000E+00	0.00%	0.000E+00		0.000E+00	
60142	2.265E-06	0.85%	2.265E-06	0.85%	2.265E-06	0.85%
60143	4.911E-05	2.05%	4.911E-05	2.05%	4.911E-05	2.05%
60145	4.261E-05	2.11%	4.261E-05	2.11%	4.261E-05	2.11%
60146	5.176E-05	1.73%	5.176E-05	1.73%	5.176E-05	1.73%
60148	2.510E-05	0.39%	2.510E-05	0.39%	2.510E-05	0.39%
60150	1.213E-05	0.16%	1.213E-05	0.16%	1.213E-05	0.16%
62147	1.385E-05	2.19%	1.385E-05	2.19%	1.385E-05	2.19%
62148	1.248E-05	1.55%	1.248E-05	1.55%	1.248E-05	1.55%
62149	1.509E-07	1.76%	1.509E-07	1.76%	1.509E-07	1.76%

62150	1.949E-05	1.40%	1.949E-05	1.40%	1.949E-05	1.40%
62151	4.400E-07	3.42%	2.994E-07	3.42%	6.424E-08	3.42%
62152	5.368E-06	2.89%	5.368E-06	2.89%	5.368E-06	2.89%
62154	2.476E-06	0.18%	2.476E-06	0.18%	2.476E-06	0.18%
63151	2.073E-07	3.42%	3.478E-07	3.42%	5.830E-07	3.42%
63153	7.566E-06	3.32%	7.566E-06	3.32%	7.566E-06	3.32%
63154	3.529E-08	8.26%	6.267E-10	8.26%	6.230E-17	8.26%
63155	3.544E-10	5.43%	2.165E-13	5.43%	0.000E+00	
64154	2.232E-06	8.14%	2.266E-06	8.14%	2.267E-06	8.14%
64155	5.857E-07	5.41%	5.861E-07	5.41%	5.861E-07	5.41%
64156	8.307E-06	3.15%	8.307E-06	3.15%	8.307E-06	3.15%
64158	1.628E-06	4.65%	1.628E-06	4.65%	1.628E-06	4.65%
64160	7.388E-08	0.48%	7.388E-08	0.48%	7.388E-08	0.48%
92233	4.904E-10	4.82%	8.985E-10	3.47%	3.043E-09	2.36%
92234	8.804E-06	3.58%	1.141E-05	3.11%	1.569E-05	2.82%
92235	1.656E-04	2.01%	1.658E-04	2.01%	1.668E-04	2.01%
92236	1.593E-04	1.46%	1.597E-04	1.46%	1.613E-04	1.44%
92238	2.080E-02	0.04%	2.080E-02	0.04%	2.080E-02	0.04%
93237	2.344E-05	2.80%	2.691E-05	2.48%	3.875E-05	1.92%
94238	7.992E-06	3.00%	5.390E-06	2.99%	1.117E-06	2.98%
94239	1.591E-04	2.05%	1.589E-04	2.05%	1.582E-04	2.05%
94240	7.926E-05	2.22%	7.933E-05	2.22%	7.775E-05	2.22%
94241	4.218E-06	1.82%	3.779E-07	1.82%	6.081E-10	12.59%
94242	2.427E-05	3.59%	2.427E-05	3.59%	2.427E-05	3.59%
95241	4.248E-05	1.85%	4.285E-05	1.84%	3.140E-05	1.84%
95243	7.360E-06	6.39%	7.326E-06	6.39%	7.190E-06	6.39%
96244	5.751E-07	7.29%	8.487E-08	7.29%	4.025E-11	7.29%
96246	5.121E-08	13.78%	5.084E-08	13.78%	4.937E-08	13.78%

5 Literaturverzeichnis

/NEA 07/ OECD Benchmark for Uncertainty Analysis in Best-Estimate Modeling (UAM) for Design, Operation and Safety Analysis of LWRs, NEA/NSC/DOC(2007)4

SAMPLING BASED NUCLEAR DATA UNCERTAINTY ANALYSIS IN MIXED LWR CALCULATIONS

L. Gallner, M. Klein, B. Krzykacz-Hausmann, A. Pautz, K. Velkov, W. Zwermann

Gesellschaft für Anlagen- und Reaktorsicherheit,
Forschungszentrum, Boltzmannstrasse 14, Garching, Germany, 85748

Winfried.Zwermann@grs.de

Introduction

Evaluated nuclear data are continuously being improved. Recently, the European library was to JEFF-3.1.1 [1], the American library to ENDF/B VII.1 [2], and the Japanese library to JENDL-4.0 [3]. These library improvements are performed on the basis of the newest evaluations of differential experiments. Along with this, growing attention is paid to uncertainty and sensitivity studies concerning the nuclear data evaluations, accompanied by improvements in the covariance data files describing the uncertainties of nuclear cross section data, and the calculation methods using these covariance data.

For the validation of the nuclear data libraries, a large number of integral experiments are used. Descriptions of such experiments are found in the “International Handbook of Evaluated Criticality Safety Benchmark Experiments” [4]. Most of these validation calculations refer to multiplication factors, although other measured quantities like reaction rates and reactivity coefficients are increasingly considered; such experiments are described in the “International Handbook of Evaluated Reactor Physics Benchmark Experiments” [5]. Most systems considered are compact assemblies, mainly at room temperature. Likewise, uncertainty and sensitivity investigations based on covariance data, as performed, e.g., with the TSUNAMI code package [6], primarily consider the multiplication factors of critical assemblies. Such compact critical systems at low temperatures are not necessarily representative for power reactors at operating conditions.

To systematically investigate the influence of nuclear data uncertainties on the results of calculations for large reactors, uncertainty analyses are being performed. For this, the XSUSA (“Cross Section Uncertainty and Sensitivity Analysis”) sequence is used, which has been recently developed at GRS as an extension of the SUSA package for the use with nuclear covariance data.

The XSUSA Method

Within the sampling based GRS method implemented in the code package SUSA (“Software for Uncertainty and Sensitivity Analysis”) [7], many calculations for the problem under consideration are performed with varied input data. The variations of the input data are generated randomly from the given probability distributions of the parameters including possible correlations between them. After performing all the calculations (typically 100 or more), the output quantities of interest are statistically analyzed, and their uncertainty ranges and sensitivities to the input parameters are determined.

So far, the GRS method has been mainly applied to problems with a limited number of parameters and only few correlations between them. However, in the case of its application to the nuclear data uncertainties, various reactions of various nuclides have to be considered. Using the nuclear covariance data from the SCALE-6 code package [8], 44 uncertain parameters for each nuclide and reaction corresponding to the 44 energy group structure are analyzed, resulting in a huge overall number of uncertain parameters. Moreover, a large amount of correlations between the energy group data of each nuclide/reaction combination have to be taken into account, and also cross correlations between data of different reactions and nuclides.
The nuclear data covariance matrices only contain the relative variances and covariances of the nuclear data, i.e. the second moments of the distributions; the types of the distributions are not explicitly known and assumed to be Gaussian.
To use the GRS method with nuclear covariance data, the ENDF/B-VII based 238-group library of SCALE-6 is either used as is, or pre-collapsed to the 44-group structure of the covariance data using a flux spectrum typical for the system under consideration, which can be advantageous when doing full core calculations which require the handling of large amounts of data for the different fuel assemblies in various burn-up states. With this collapsed master library, all necessary spectral calculations are performed, using the Bondarenko method implemented in the BONAMI module for the unresolved resonance regions, and performing 1-D transport calculations by the CENTRM module with continuous energy data in the resolved resonance region. The resulting data libraries are modified according to the uncertainty information in the covariance matrices for each nuclide/reaction combination considered, taking into account, if present, the covariances between different energy groups, different reactions, and different nuclides. After doing so, it has to be assured that the cross section set is entirely consistent, i.e. that sum rules are fulfilled and that 2-d cross sections (e.g. scattering matrices) are compatible with their 1-d counterparts. With the modified cross sections created in this way, the core calculations are performed and the results are statistically evaluated.

Pin Cell Calculations

To make sure that the XSUSA method is correctly implemented, criticality calculations are performed with the 1-D S_N code XSDRN from the SCALE-6 package as transport solver, for two of the fuel pin cells from the KRITZ-2 series of experiments [5, 9]. The results of these calculations, regarding the average multiplication factors and their uncertainties originating from nuclear data uncertainties, are compared with corresponding TSUNAMI-1D results. Series of XSUSA/XSDRN calculations are performed with all relevant nuclide/reaction combinations varied, and separately with variations affecting only the main contributors while using the unvaried data for all other nuclides/reactions (“one-at-a-time variation”). Each of these series consists of 1,000 calculations.

The uncertainties of the multiplication factors due to nuclear data uncertainties are compared in Figs. 1 and 2. In these figures, the overall uncertainties determined with TSUNAMI are given, along with the main contributions from single nuclide/reaction combinations. The overall uncertainty is obtained by adding the squares of the values with positive signs, and subtracting the squares of the values with negative signs, then taking the square root. These values are compared to the corresponding XSUSA/XSDRN results from the overall and one-at-a-time variations. Very satisfactory agreement is obtained; the relative deviations between the

XSUSA/XSDRN and the TSUNAMI values are within 95% confidence intervals obtained from the 1,000 XSUSA/XSDRN, with the exception of the contribution of the fission spectra, which, however, do not contribute substantially to the overall uncertainty.

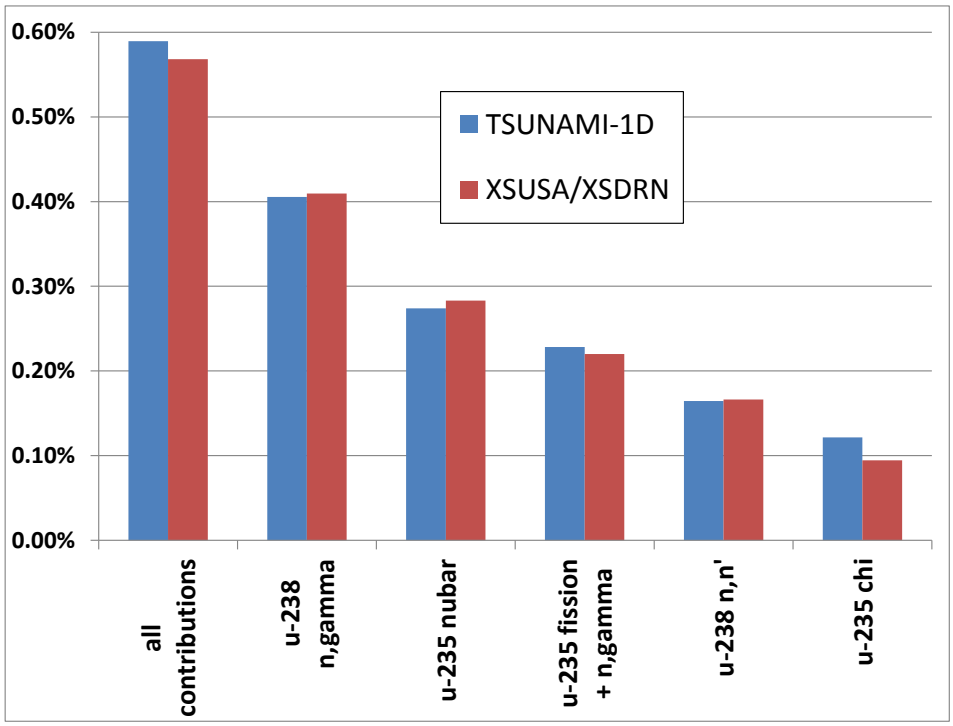

Fig. 1: Main contributions from various nuclides/reactions to the relative 1 σ multiplication factor uncertainty (%) for the UO_2 fuel pin cells from TSUNAMI-1D and XSUSA/XSDRN calculations.

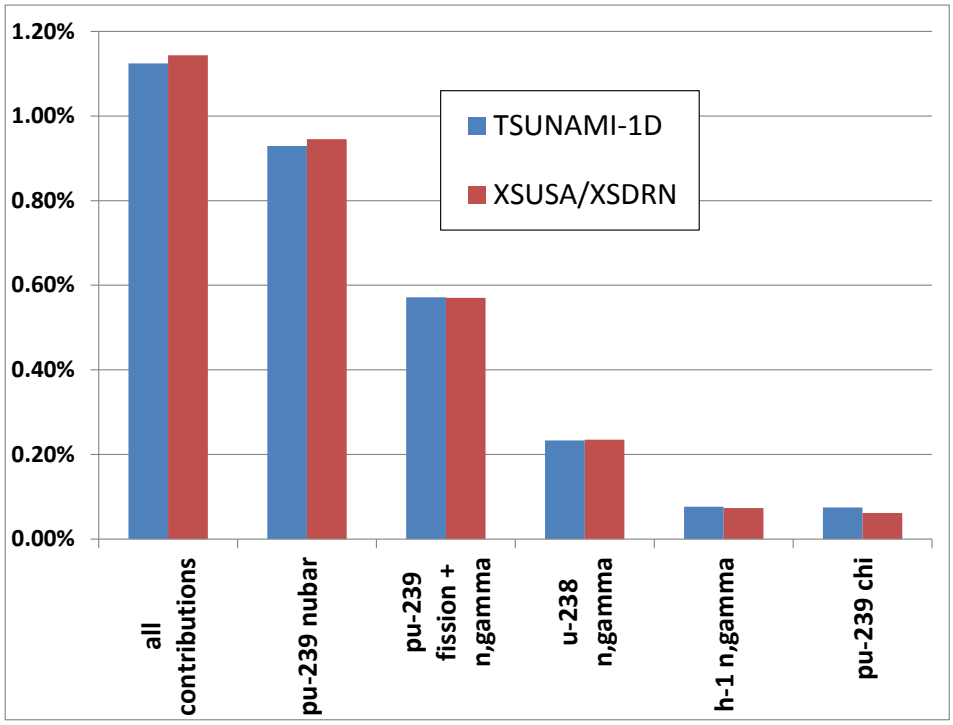

Fig. 2: Main contributions from various nuclides/reactions to the relative 1 σ multiplication factor uncertainty (%) for the MOX fuel pin cells from TSUNAMI-1D and XSUSA/XSDRN calculations.

Core Calculations

The XSUSA method is finally applied to full scale 2-D calculations for two LWR mixed cores specified within international OECD/NEA calculation benchmarks [10, 11]. These are a PWR and a VVER core, both in the uncontrolled state at hot zero power condition, loaded with UO_2 and MOX fuel assemblies in various burn-up states, the latter containing high quality plutonium. The core layouts are displayed in Figs. 3 and 4.

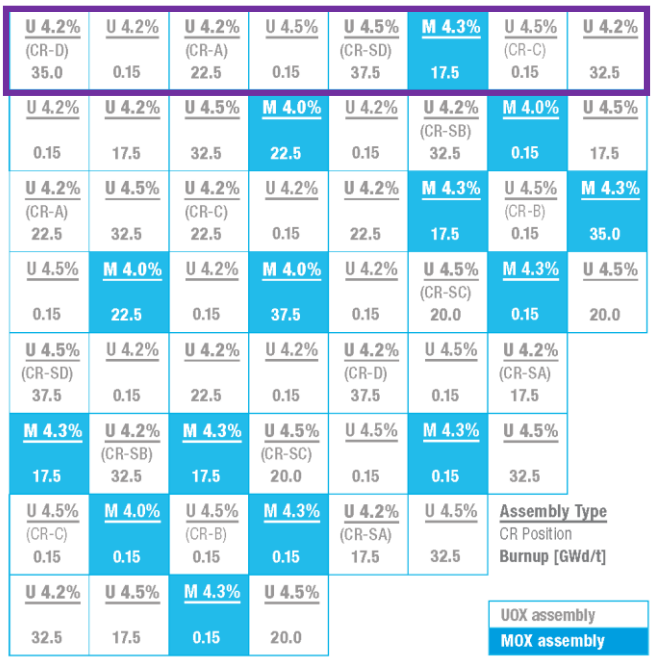

Fig. 3: Layout of the PWR core configuration.

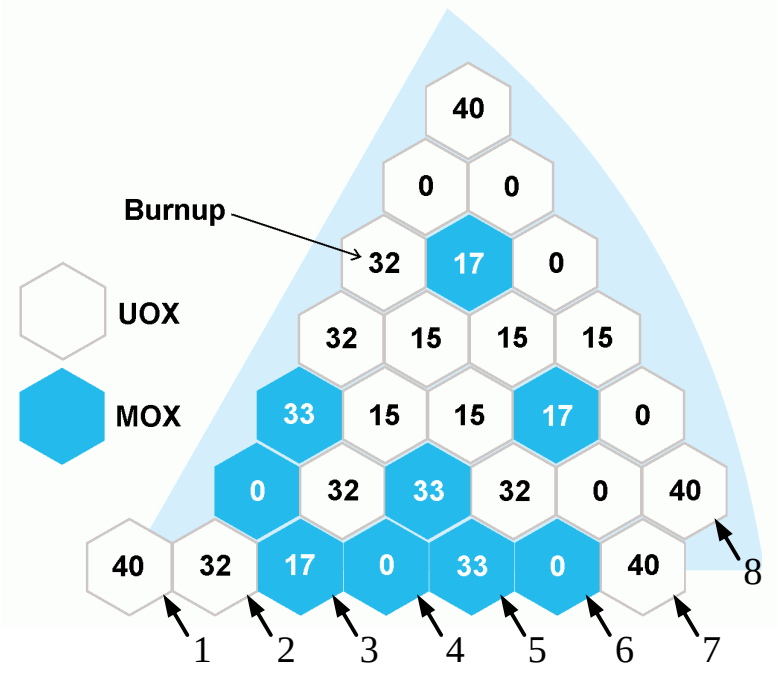

Fig. 4: Layout of the VVER core configuration.

The calculations presented here refer to the hot zero power states, with KENO-Va for the PWR core and MCNP5 for the VVER core, both in multi-group mode, as transport solvers. Spectral calculations were performed with the BONAMI/CENTRM sequence of SCALE-6, starting from a pre-collapsed 44-group master library based on ENDF/B-VII. As covariance data, the SCALE-6 44GROUPCOV set was used. In total, 480 samples were run, each with 1,000 (PWR) or 400 (VVER) millions of neutron histories, to make sure that the fission rate distributions are sufficiently converged, and MC statistical uncertainties are small compared to those originating from nuclear data sampling.

The calculated multiplication factors turn out to lie in a band with a relative standard deviation of 0.55% for the PWR core, and 0.71% for the VVER core, values which one expects for U/Pu LWR systems. For the radial fission rate distributions, however, a much larger influence of the nuclear data variations on the result is observed. This is shown in Figs. 5 and 6, where the reference values and standard deviations are displayed. The resulting standard deviations in the core centres are unexpectedly high. Investigations on a simplified core model [12] have shown that the differences in the fission rate distributions are mainly due to the uncertainties in the average number of neutrons per fission of Pu-239, and the particularly non-uniform distribution of UO_2 and MOX fuel assemblies in the considered core, along with the high amount of Pu-239 in the isotopic composition. Such reactor cores are not yet in operation; uncertainty analyses for standard UO_2 and reactor grade MOX cores will be performed.

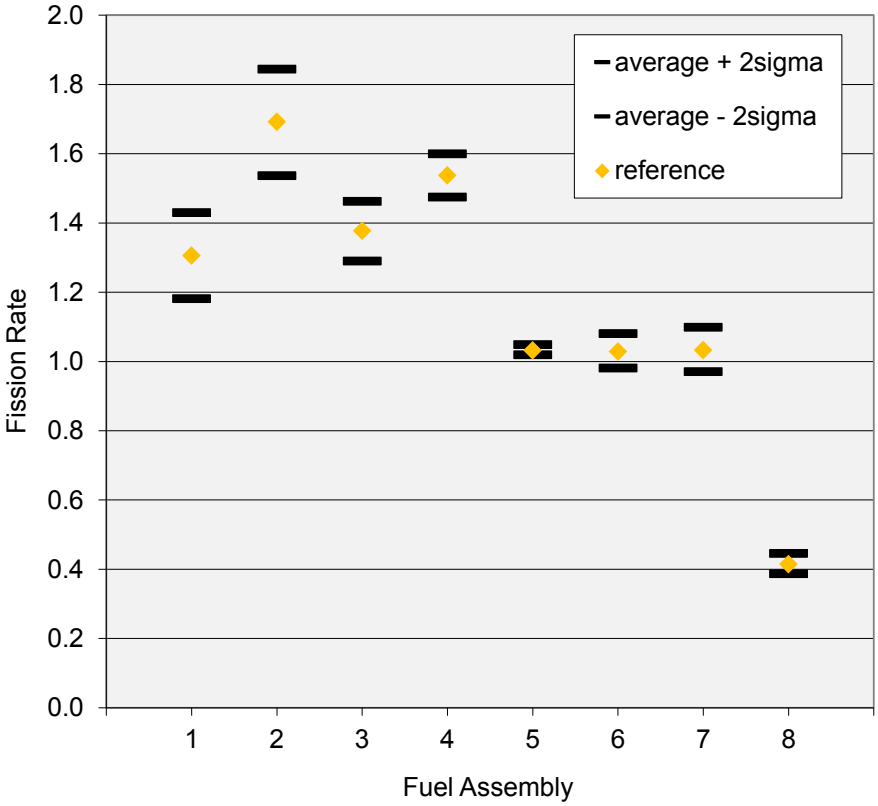

Fig. 5: Radial fission rate distribution for the VVER MOX core (averaged over all fuel assemblies belonging to the same radial column).

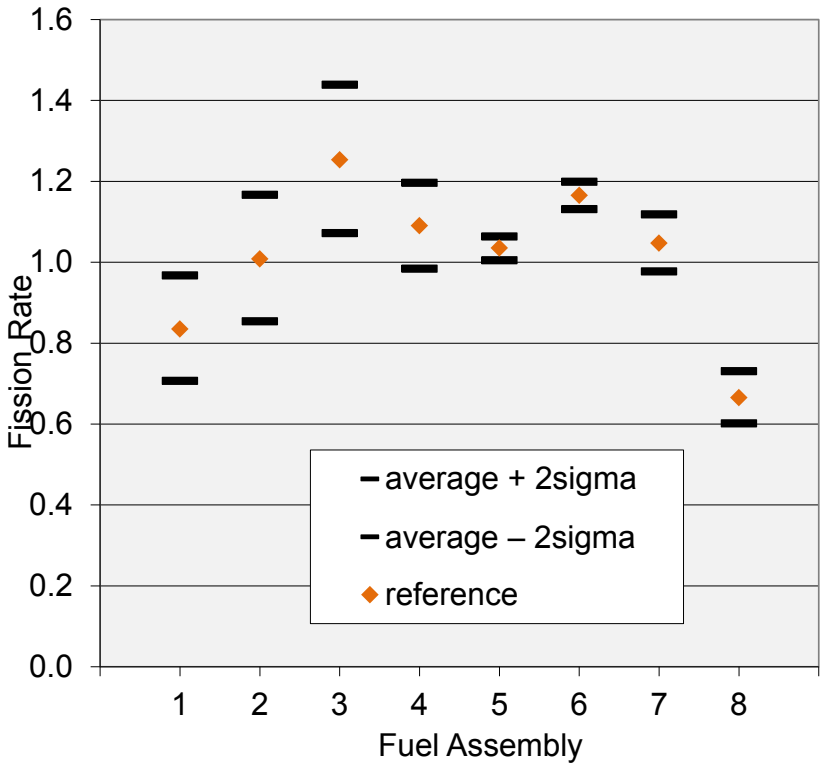

Fig. 6: Radial fission rate distribution for the VVER MOX core (averaged over all fuel assemblies belonging to the same radial column).

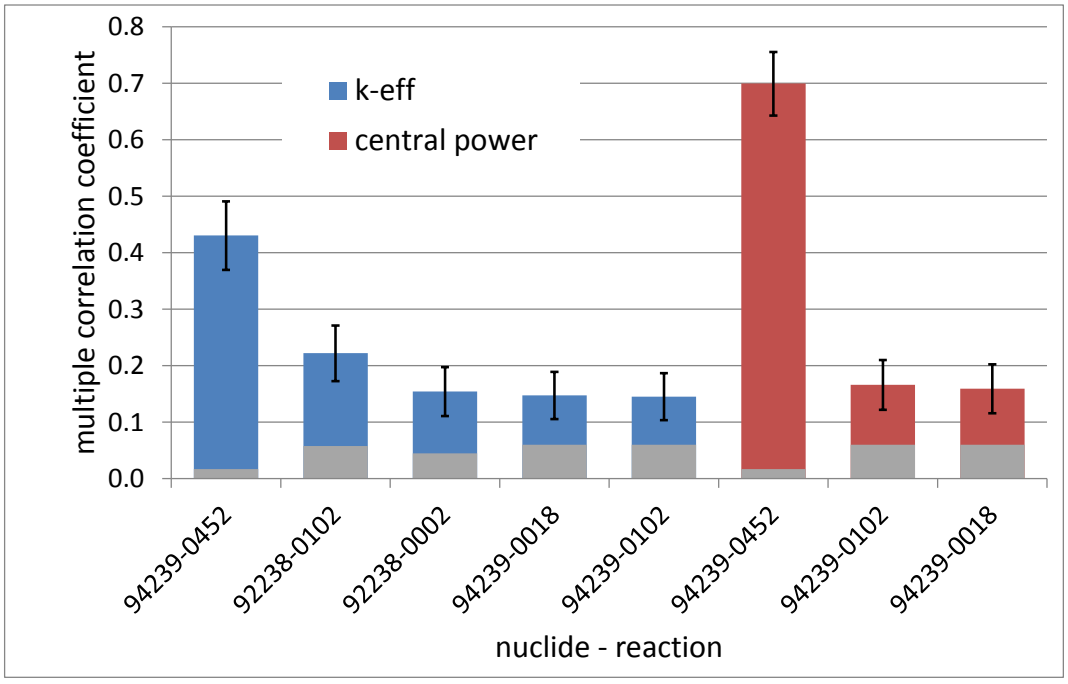

Fig. 7: Sensitivity results for the PWR core: Squared multiple correlation coefficients (R^2) from XSUSA/KENO for k-eff and the central power, along with their 95% confidence intervals indicated by the error bars, and the 95% significance bounds indicated by the grey columns. Reaction IDs: 2 = elastic scattering, 18 = fission, 102 = n,γ capture, 452 = nu-bar.

The calculated multiplication factors turn out to lie in a band with a relative standard deviation of 0.55% for the PWR core, and 0.71%, values which one expects for U/Pu LWR systems. For the radial fission rate distributions, however, a much larger influence of the nuclear data variations on the result is observed. This is shown in

Figs. 5 and 6, where the reference values and standard deviations are displayed. The resulting standard deviations in the core centres are unexpectedly high. Investigations on a simplified core model [12] have shown that the differences in the fission rate distributions are mainly due to the uncertainties in the average number of neutrons per fission of Pu-239, and the particularly non-uniform distribution of UO_2 and MOX fuel assemblies in the considered core, along with the high amount of Pu-239 in the isotopic composition. This can also be seen from Fig. 7, where the so-called "squared multiple correlation coefficients (R^2)" for the multiplication factor and the fission rate in the central fuel assembly in the PWR core for the most relevant reactions are displayed. These serve as sensitivity/uncertainty importance indicator; they can be interpreted as the relative amount of output uncertainty coming from the uncertainty of the respective parameter group.

Summary and Conclusions

The sampling based XSUSA cross section uncertainty and sensitivity analysis sequence was applied to mixed UO_2/MOX cores from OECD/NEA calculation benchmarks using ENDF/B-VII based data and nuclear covariance data from the SCALE-6 system. The resulting uncertainties in the multiplication factors from a number of Monte Carlo transport calculations are as expected; for UO_2 and MOX pin cells, agreement with corresponding TSUNAMI-1D calculations is obtained in 1-D transport calculations. The resulting uncertainties in the calculated radial fission rate distributions are substantial. Due to the main contribution from the uncertainty of the average number of neutrons per fission in Pu-239, the effect is particularly pronounced in UO_2/MOX cores with a high amount of Pu-239 in the isotopic composition. Such reactor cores are not yet in operation; investigations on the uncertainties in the power distribution in standard UO_2 and reactor grade MOX cores will be performed.

In conclusion, it is desirable to routinely accompany reactor calculations by uncertainty and sensitivity analyses in the future, along with aiming for a continuous convergence of different nuclear data evaluations, and a reduction of their uncertainties.

Acknowledgements

This work is supported by the German Federal Ministry of Economics and Technology.

References

1. 2. A. Santamarina et al., "The JEFF-3.1.1 Nuclear Data Library," JEFF Report 22, NEA No. 6807 (2009).
2. 4. M. Herman, "Development of ENDF/B-VII.1 and Its Covariance Components", Journal of the Korean Physical Society, 59, pp.1034–1039 (2011).
3. 6. K. Shibata et al., "JENDL-4.0: A New Library for Innovative Nuclear Energy Systems," Journal of the Korean Physical Society, 59, pp.1046–1051 (2011).
4. "International Handbook of Evaluated Criticality Safety Benchmark Experiments", September 2010 Edition, available on DVD-ROM, NEA/NSC/DOC(95)03.

5. “International Handbook of Evaluated Reactor Physics Benchmark Experiments”, March 2011 Edition, available on DVD-ROM, NEA/NSC/DOC(2006)1.
6. B. T. Rearden, “TSUNAMI Sensitivity and Uncertainty Analysis Capabilities in SCALE 5.1,” Trans. Am. Nucl. Soc. 97, pp. 604-605 (2007).
7. B. Krzykacz, E. Hofer, M. Kloos, “A Software System for Probabilistic Uncertainty and Sensitivity Analysis of Results from Computer Models”, International Conference on Probabilistic Safety Assessment and Management (PSAM-II), San Diego, Ca., USA, March 20 – 25, 1994.
8. “SCALE: A Modular Code System for Performing Standardized Computer Analyses for Licensing Evaluation, Version 6“, ORNL/TM-2005/39 (2009).
9. “Benchmark on the KRITZ-2 LEU and MOX Critical Experiments”, NEA/NSC/DOC(2005)24.
10. T. Kozlowski, T. J. Downar, “The PWR MOX/UO2 Core Transient Benchmark, Final Report”, NEA/NSC/DOC(2006)20.
11. E. Gomin, M. Kalugin, D. Oleynik, “VVER-1000 MOX Core Computational Benchmark – Specification and Results,” NEA/NSC/DOC(2005)17.
12. W. Zwermann, B. Krzykacz-Hausmann, L. Gallner, A. Pautz, “Influence of Nuclear Covariance Data on Reactor Core Calculations,” Proc. WONDER 2009, Cadarache, France, Sep. 29 – Oct. 2, 2009.

PHYSOR 2012 – Advances in Reactor Physics – Linking Research, Industry, and Education
Knoxville, Tennessee, USA, April 15-20, 2012, on CD-ROM, American Nuclear Society, LaGrange Park, IL (2012) Anhang B2

COUPLED MONTE CARLO NEUTRONICS AND THERMAL HYDRAULICS FOR POWER REACTORS

W. Bernnat, M. Buck, M. Mattes
Institut für Kernenergetik und Energiesysteme (IKE), Universität Stuttgart
Pfaffenwaldring 31, D-70569 Stuttgart, Germany
bernnat@ike.uni-stuttgart.de

W. Zwermann, I. Pasichnyk, K. Velkov
Gesellschaft für Anlagen- und Reaktorsicherheit (GRS) mbH
Forschungszentrum, Boltzmannstrase 14, 85748 Garching, Germany

ABSTRACT

The availability of high performance computing resources enables more and more the use of detailed Monte Carlo models even for full core power reactors. The detailed structure of the core can be described by lattices, modeled by so-called repeated structures e. g. in Monte Carlo codes such as MCNP5 or MCNPX. For cores with mainly uniform material compositions, fuel and moderator temperatures, there is no problem in constructing core models. However, when the material composition and the temperatures vary strongly a huge number of different material cells must be described which complicate the input and in many cases exceed code or memory limits. The second problem arises with the preparation of corresponding temperature dependent cross sections and thermal scattering laws. Only if these problems can be solved, a realistic coupling of Monte Carlo neutronics with an appropriate thermal-hydraulics model is possible. In this paper a method for the treatment of detailed material and temperature distributions in MCNP5 is described based on user-specified internal functions which assign distinct elements of the core cells to material specifications (e.g. water density) and temperatures from a thermal-hydraulics code. The core grid itself can be described with a uniform material specification. The temperature dependency of cross sections and thermal neutron scattering laws is taken into account by interpolation, requiring only a limited number of data sets generated for different temperatures. Applications will be shown for the stationary part of the Purdue PWR benchmark using ATHLET for thermal- hydraulics and for a generic Modular High Temperature reactor using THERMIX for thermal- hydraulics.

Key Words: Monte Carlo, Neutronics, Thermal-Hydraulics, PWR, HTR, Cross Sections

1. INTRODUCTION

The Monte Carlo method with continuous energy representation of nuclear cross sections and a detailed description of material composition enables accurate solutions of the transport equation for complex power reactor problems, e.g. by the codes MCNP5 [1] or MCNPX [2]. The performance and quality of these codes were demonstrated by many comparisons with experiments and benchmarks. Difficulties appear if the problem sizes increase, e.g. for pin wise calculation of LWRs, extended LWR fuel clusters, or HTR full core calculations. Since there is a strong dependency of the power distribution and neutron flux spectra on the temperatures of fuel, moderator, structure materials and burnup, these parameters must be taken into account by

subdividing core and reflector into many different material zones since these parameters cannot be represented by continuous functions. The fuel, moderator and structure material temperatures and densities depend on the power distribution and must be separately calculated by means of adequate thermal-hydraulics codes. For complex structures, the assignment of zones of different burnups or temperatures is quite laborious using the standard input processing of MCNP, since the features of repeated structures cannot be used efficiently. Therefore, the assignment of temperatures and atomic fractions of the fuel, moderator and reflector materials will be performed via user-supported functions. The geometry of the core can be effectively described in MCNP by means of repeated structures. Especially regular assemblies with N by N pins or other regular structures can be arranged as clusters or full cores with comparably few input directives. But this feature can be used only for fresh fuel and assembly-wise constant coolant and fuel temperature data. For irradiated fuel and temperature distributions for coolant, moderator and fuel each pin of an assembly must be axially sub-divided and assigned to a distinct material composition via input directive. The necessary number of such directives increases accordingly and may exceed code limitations.

To calculate correct thermal neutron spectra, the temperature distribution must be taken into account. Both cross section data and thermal scattering laws in form of $S(\alpha,\beta)$ tables must correspond to the material data. Since these data are only available for a number of temperature grid points, there must be an effective and sufficiently accurate method to interpolate these tables for actual cell temperatures. One method is to generate all necessary temperature data in advance, either by processing or by any external interpolation procedure. But one can get also acceptable results by means of a limited set of temperature dependent data tables using special weights for the data sets for the neighboring temperature grid points. This enables an almost continuous representation of temperatures for fuel, moderator and structure materials.

In the following Sections, the method is applied to the Purdue PWR benchmark problem [3] and a generic model for a modular pebble bed High Temperature Reactor (HTR) [4]. The neutronics part is always calculated by MCNP5 using internal functions for the material and temperature assignment. The thermal hydraulics for the PWR benchmark was calculated by ATHLET [5], for the HTR by the code THERMIX [6]. The method of interpolation of cross sections and thermal neutron scattering data was separately proven by calculation of cells based on directly processed and interpolated data sets.

2. ASSIGNMENT OF MATERIAL AND TEMPERATURE SPECIFICATION TO LATTICE CELLS

The construction of a core grid by MCNP is comparably easy with the “repeated structure“ option, if all elements of the grid (e. g. pins) have identical materials, see, e.g., Fig. 1. If the materials are not uniform, for every pin and every axial section a different cell name and a different material number must be assigned. For full core models this easily leads to a huge number of cells, which even may exceed the program limits. The geometry parameters of the grid, however, are correctly described. For the particle tracking both the geometry and the material specifications are necessary. The standard solution is to explicitly define the cells with corresponding material composition and temperature. Alternatively, however, this assignment

can be performed internally by means of user-supported functions. Instead of using the cell data of a so called universe filled in the lattice, specific data can be used for lattice cell elements:

$$(c_i < c_j\,[j_x\ j_y\ j_z] < c_k < c_l\,[\,l_x\ l_y\ l_z\,]\ \ldots\ )$$

from user-specified data sets. The material data specified for the universe (number densities, temperatures) will be replaced by the actual material specification of cell c_i (see Fig. 2). This means that the original input material of the universe is re-assigned. For the coupling with the thermal-hydraulics program it is important to define tallies, especially for the power distribution, for the same discretization as for the material specification. This can be realized by means of a user-specified tally routine, e.g. to obtain the axial power distribution for a distinct number of axial sections for every pin of the core grid. The described method based on the user-supported function was implemented into MCNP5 and tested by comparisons with the standard input method for a 2 by 2 assembly cluster of PWR assemblies with 17 by 17 pins. For this cluster, symmetry was assumed along the diagonal from bottom left to top right, see Fig. 3. Fuel temperatures and moderator densities were given (calculated by ATHLET) for every pin for 40 axial fuel zones and 5 axial reflector sections (top and bottom), a total of 46,240 fuel zones. The problem was calculated with standard input (generated with a user program) and by means of internal functions as described.

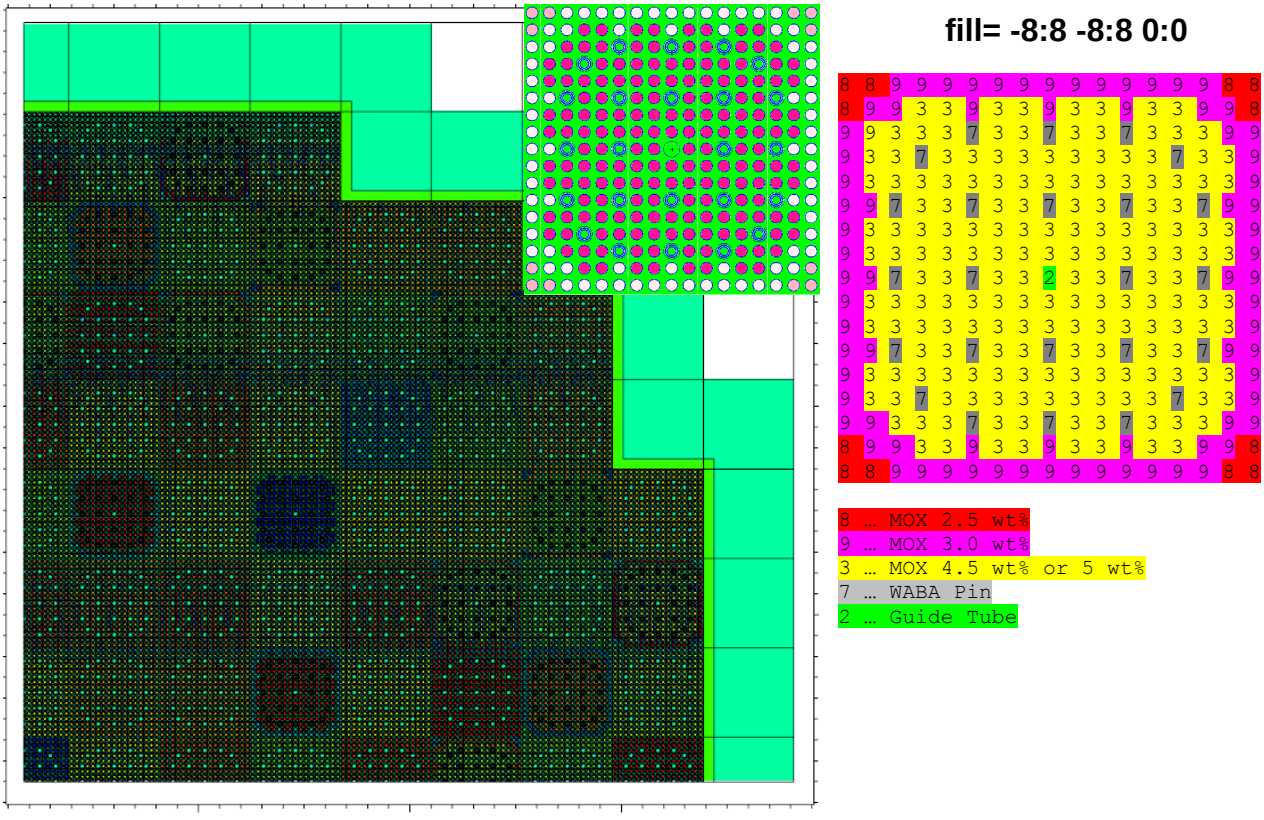

Figure 1. Quarter of PWR core, example of MCNP model based on repeated structures. Example for fill command for a MOX assembly with different Pu content and WABA pins.

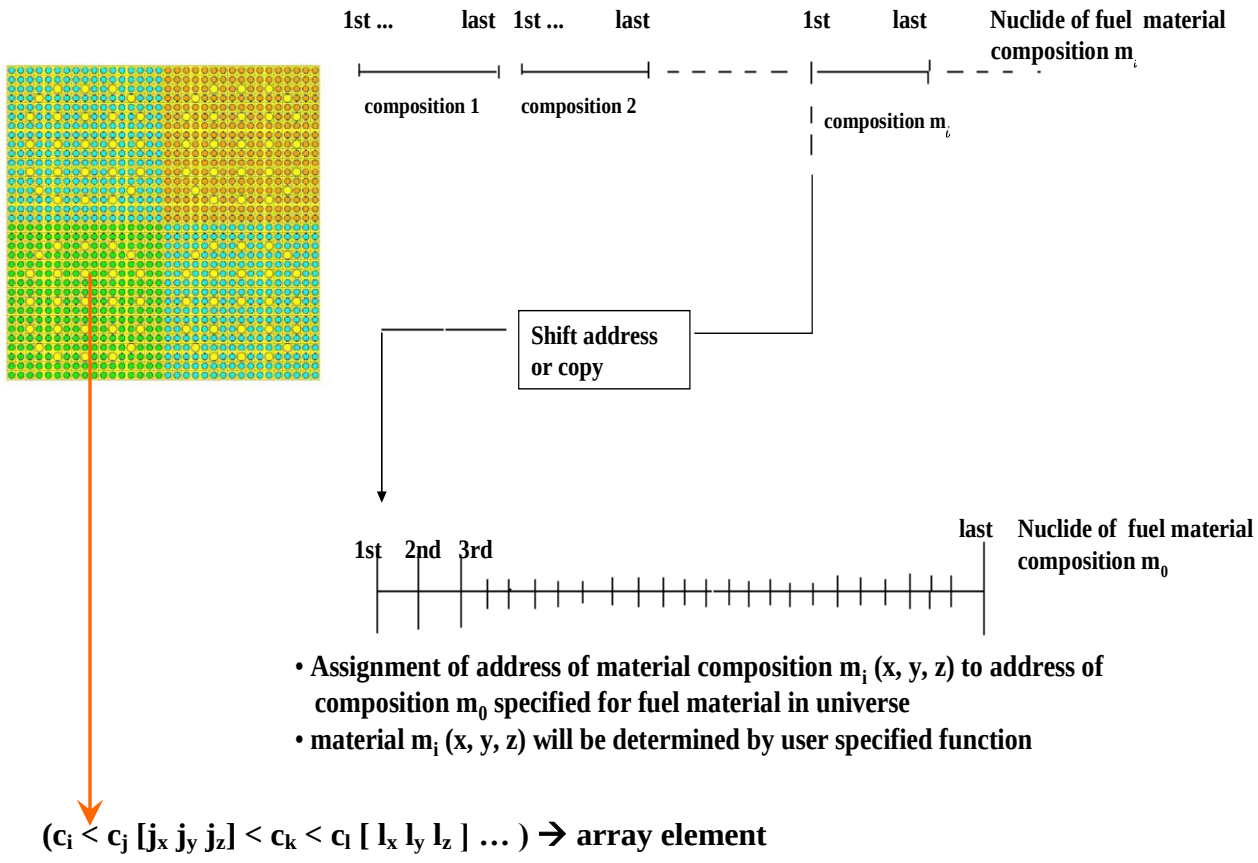

Figure 2. Use of internal function for assignment of material specification and temperature to lattice element.

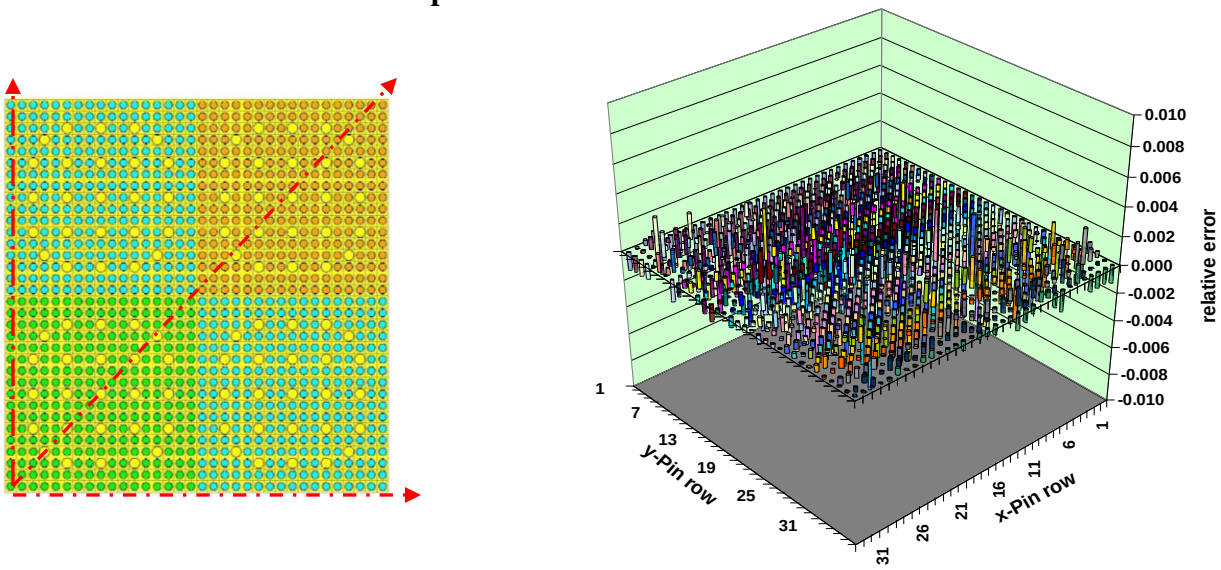

Figure 3. Relative difference in power distribution calculated by direct input and by an internal function for a 2 by 2 PWR assembly array.

3. TEMPERATURE DEPENDENT NEUTRON CROSS SECTIONS AND SCATTERING LAW DATA

The coupling of MCNP with thermal hydraulics requires the consideration of many neutron cross sections for different temperatures. Since both the cross sections and the thermal scattering data are only available or can be generated for distinct temperature points, the actual cell temperature may differ remarkably from the cross section temperature. Since only the elastic scattering cross section can be adjusted to the cell temperature according to the free gas model, there are only two options: generation of a large number of cross sections for all different temperatures or interpolation of cross sections and thermal scattering data between data sets for distinct temperatures. The first option is very time and memory consuming and cannot be used for a problem with many cells of different temperatures. The interpolation requires some more computational effort during tracking, but requires less memory and can be applied with a limited number of data sets. The interpolation principle is the simultaneous use of cross sections for the two grid temperatures enclosing the actual temperature but with appropriate weights [7]. This interpolation works quite well as can be seen in Fig. 4: k-infinity as a function of fuel temperature for a UOX cell with different moderator/fuel volumes, and correspondingly for a MOX cell in Fig. 5. In these figures the difference between results from interpolated cross sections and direct generated cross sections are always in the order of magnitude of the statistical errors. In Fig. 6 the cross sections of important capture resonances of U-238 and Pu-240 are shown: directly processed and interpolated from neighboring grid temperatures. A comparable interpolation can be performed also with thermal scattering law data for H in H_2O using a linear weight, but regarding the correct link between thermal and continuous data sets for H.

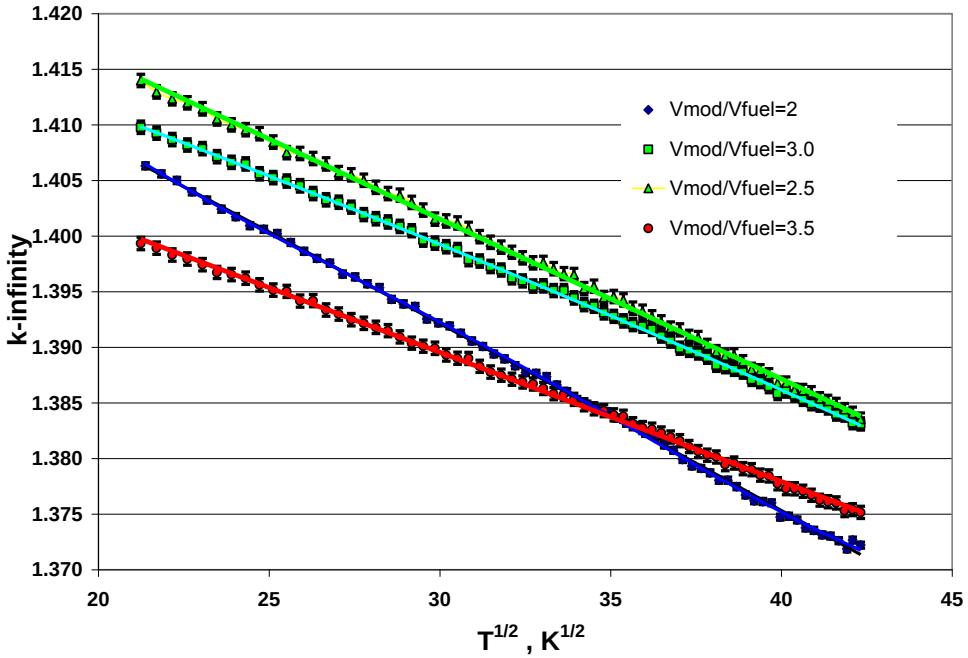

Figure 4. k-infinity as a function of $T^{1/2}$ (fuel temperature) for LWR UOX pincell (different moderator/fuel volume ratios).

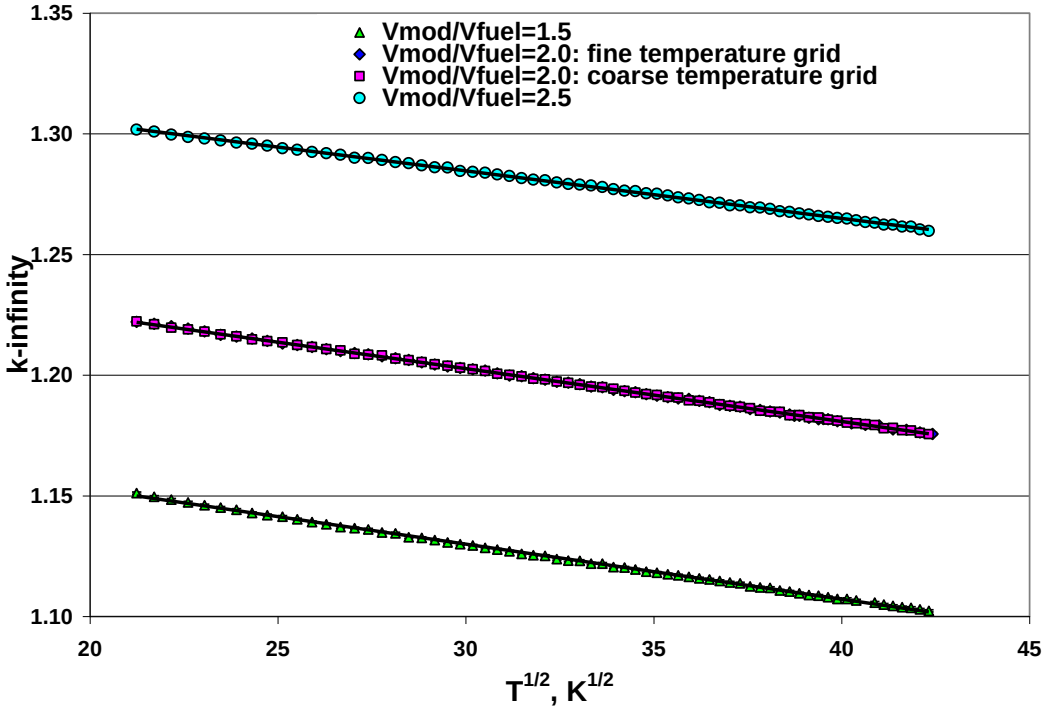

Figure 5. k-infinity as a function of $T^{1/2}$ (fuel temperature) for LWR MOX pincell: (different moderator/fuel volume ratios)

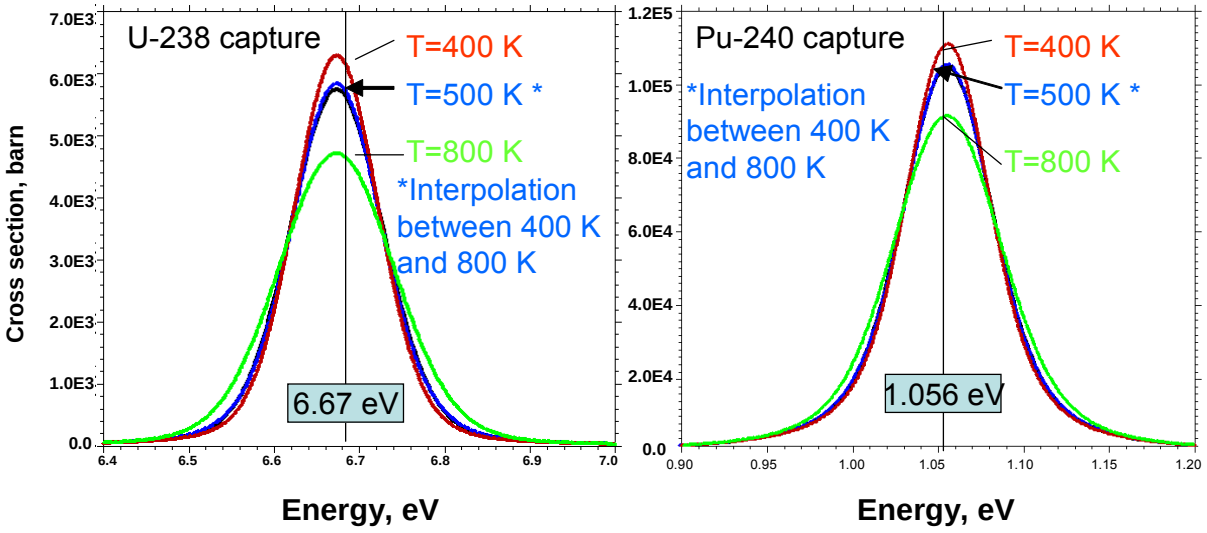

Figure 6. Resonance cross sections processed for 500 K and interpolated from data sets for 400 K and 800 K.

4. COUPLING TO THERMAL HYDRAULICS

With the described models, MCNP5 and an appropriate thermal hydraulics module can be coupled via an interface and successive MCNP and thermal hydraulics calculations can be performed. As thermal hydraulics modules, ATHLET was used for the PWR benchmark and THERMIX for the HTR system. The interface module was developed which transfers the assembly wise axial power distribution from MCNP to the ATHLET or THERMIX input and the results (assembly-wise axial coolant density and temperature and fuel temperature distributions for PWR and mesh wise fuel and moderator temperatures for HTR) back to MCNP. These results are used for the internal function. The MCNP input need not be changed between different iteration steps. A flow chart of the coupled system is shown in Fig. 7.

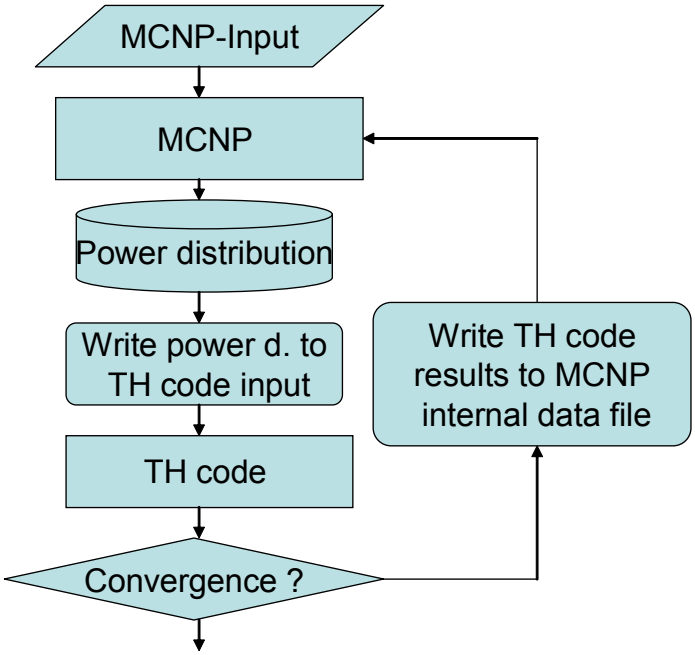

Figure 7. Flow chart for coupled MCNP thermal hydraulics calculations (ATHLET, THERMIX, etc.)

5. APPLICATIONS

5.1 PWR MOX/UO_2 Core Transient Benchmark

The PWR MOX/UO_2 Core Transient Benchmark ("Purdue benchmark") [3] defines a PWR grid of assemblies with 17x17 pins. A quarter of the core and the geometries of the UOX and MOX assemblies are shown in Fig. 8. In this figure, for every assembly the average fissionable content UOX or MOX and the average burnup is shown. The MOX assemblies have fuel pins with depleted uranium and three different high-quality Pu contents. Furthermore, IFBA fuel pins with burnable poisons were used for UOX and WABA burnable poisons in the control rod guide positions for MOX. The core is radially surrounded by a baffle and a reflector. The axial reflectors contain coolant at inlet and outlet temperature condition, respectively. Spacer effects are neglected. The active core zone is subdivided into 23 axial zones. Due to symmetry only a quarter of the core is modeled. The pin and assembly grids are modeled by the repeated structure option of MCNP. The fuel and moderator temperatures were taken into account as calculated by

ATHLET. The calculation of the radially averaged axial power distribution of every assembly was calculated by a special user tally subroutine. JEFF-3.1 cross section data were used [8]. These data contain cross sections for 10 temperatures and thermal scattering data for H in H_2O for 20 temperatures (prepared by IKE [9]). Additionally, for the main actinides U-235, U-238, and the important Pu-isotopes JEFF-3.1 cross sections were generated for a fine temperature grid (30 grid points). The cross sections for the different local temperatures were interpolated internally (in MCNP5) on the basis of the neighboring grid temperatures, see also [7]. The internal interpolation simplifies the geometry representation for MCNP; this means that the axial variation of the coolant temperature, density and fuel temperature need not be formulated for the MCNP input. The variation of these parameters is taken into account during neutron tracking through the pin and assembly lattice by the internal functions.

In the ATHLET core model for the thermal hydraulics part, every assembly was treated as a representative channel with an axial power distribution as calculated by MCNP5. Every representative pin was subdivided into 8 radial zones (with identical power density). The thermal properties for UOX and MOX were taken from the benchmark specification. All channels were connected to a lower plenum and an upper plenum volume. The mass flows of individual channels were calculated by means of the pressure drop iteration. No cross flow was assumed between assembly channels. The inlet pressure was 15.5 MPa. For demonstration (not specified by the benchmark) the assembly C8 was calculated with 264 channels (one for each pin) and the corresponding fuel and moderator temperatures were taken into account for MCNP.

For the demonstration of the method the hot full power condition of the benchmark was analyzed. Beginning with constant temperatures the stationary condition was reached after few iterations. The MCNP5 program was executed on a CRAY XT5 parallel computer using the MPI version with up to 256 processors. The MCNP-ATHLET result is compared with corresponding results from PARCS [10] (from the benchmark) and QUABOX/CUBBOX-ATHLET (QC) [11]. The core averaged axial power distribution is shown in Fig. 9. The axial non-symmetric form is due to the change of coolant state from bottom to top of core. There is a slight difference between the QC and PARCS solution and the MCNP solution. In Fig. 10 the comparison of the radially averaged temperature distribution is shown for different benchmark solutions and MCNP-ATHLET. The integral temperature values of the deterministic programs and MCNP-ATHLET are in good agreement.

The axially averaged assembly powers were also calculated and compared with the QC results. The comparisons (the relative differences) are shown in Fig. 12. These differences are comparably low and lie in the order of differences between QC and PARCS. On the average, the differences are slightly larger for the MOX assemblies (marked in red) than for the UOX assemblies. Further integral results like average fuel and moderator temperatures are in good agreement, too.

Axially averaged pin wise power distributions for selected assemblies show deviations of few per cent. The axially averaged pin wise relative power distribution for the benchmark is shown in Fig. 11.

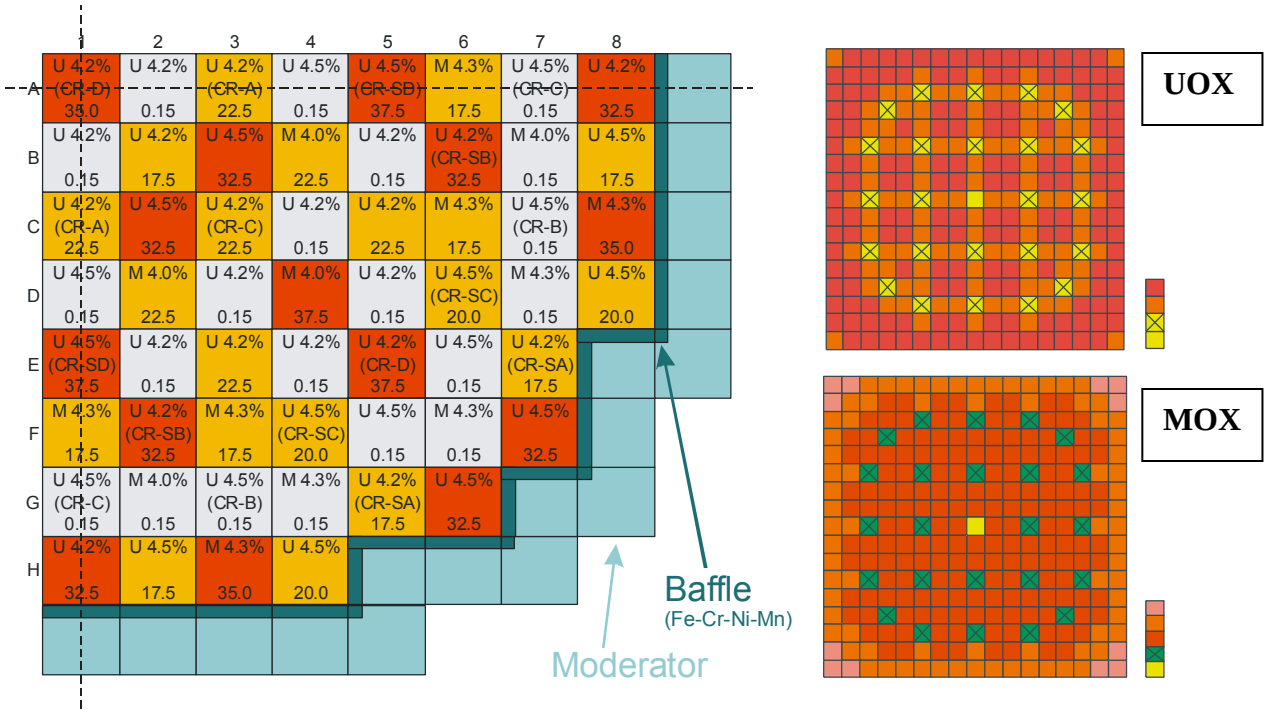

Figure 8. Core configuration and assembly specification of the PWR-MOX/UOX benchmark.

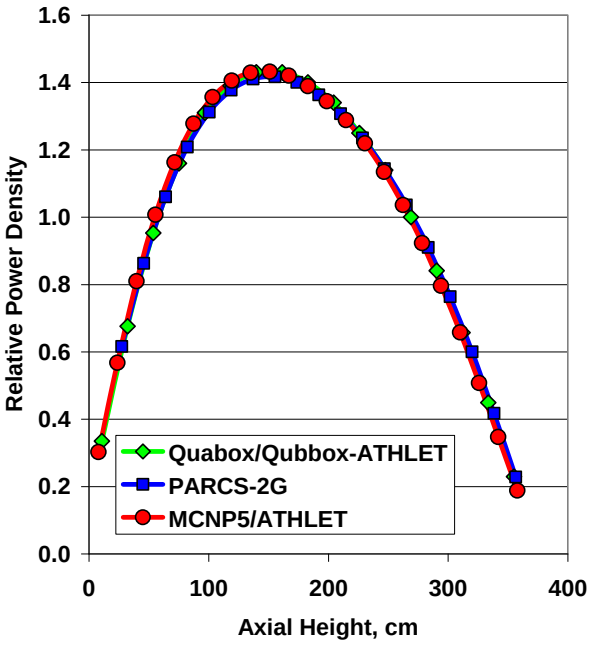

Figure 9. Radially averaged relative power distribution at HFP

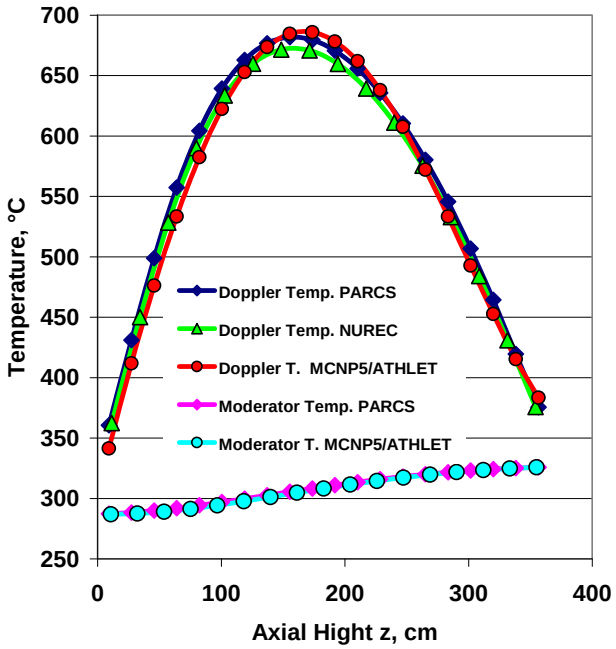

Figure 10. Radially averaged axial fuel and moderator temperature distribution.

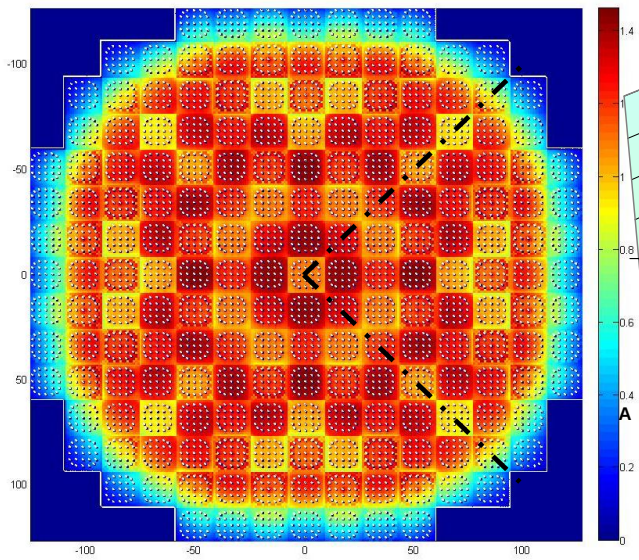

Figure 11. Pin-wise axial averaged power distribution calculated by MCNP/ATHLET

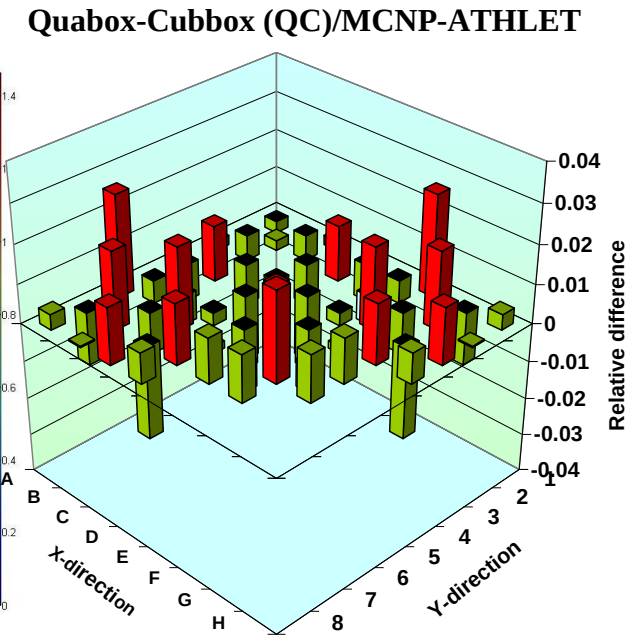

Figure 12. Comparison of relative difference in assembly power calculated by QC and MCNP

5.2 HTR Model

As a model for the modular HTR, the PBMR design was chosen. For the PBMR-400, a benchmark was defined [4] with a simplified core model. The reactor design is shown in Fig. 13. The reactor is He-cooled, the core is a pebble bed with graphite spheres containing UOX fuel in coated particles, see Fig.14. The core has an inner solid graphite column and graphite top, bottom and side reflectors. For the benchmark, a neutronics and a thermal hydraulics model were defined. For these models first burnup calculations were performed with the neutronics system ZIRKUS [12] and the thermal hydraulics model THERMIX [6]. The neutronics model was also used for the MCNP input, e. g. for the accurate calculation of control rod values and other parameters. An interface was used to transmit the burnup dependent data to the pebble bed model of MCNP. The power distribution was calculated for a 2D mesh net. The problem which arises for neutronics calculation is that the core and reflector temperatures strongly influence the local neutron spectra and must be taken into account as detailed as possible. This requires either a fine subdivision of all reflector and core regions or again the use of internal functions to regard the fuel and moderator (reflector) temperature distributions directly taken from the thermal hydraulics program. As for the PWR benchmark this was also realized for the PBMR model. The thermal hydraulic data were taken from THERMIX output via an interface. Both the cross sections for fuel and the scattering law data for graphite were interpolated mesh wise to the actual temperatures. The temperature distribution for the model is shown in Fig. 15, the corresponding thermal flux distribution in Fig. 16. Especially the thermal flux distribution is influenced by the temperature distribution. If the spatial grid for the temperatures is too coarse, the thermal flux distribution shows strong discontinuities at grid boundaries.

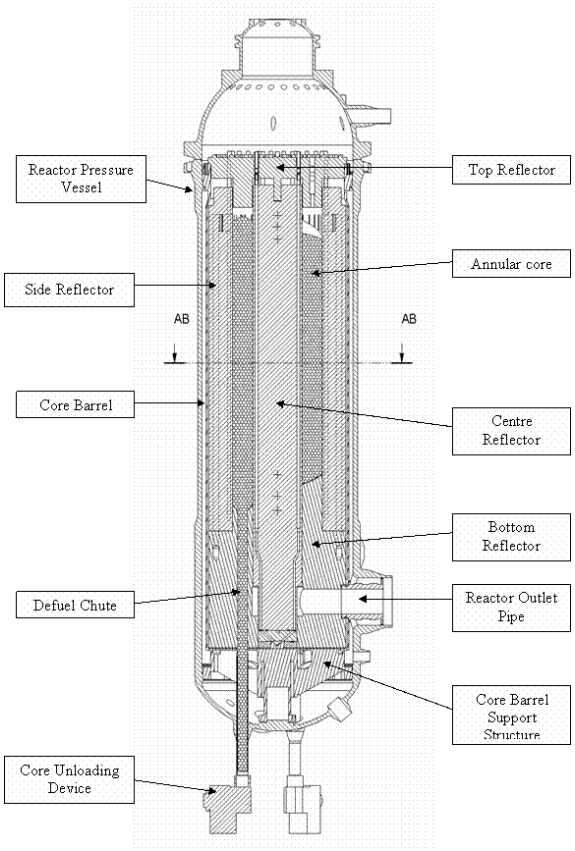

Figure 13. Model of PBMR-400 design

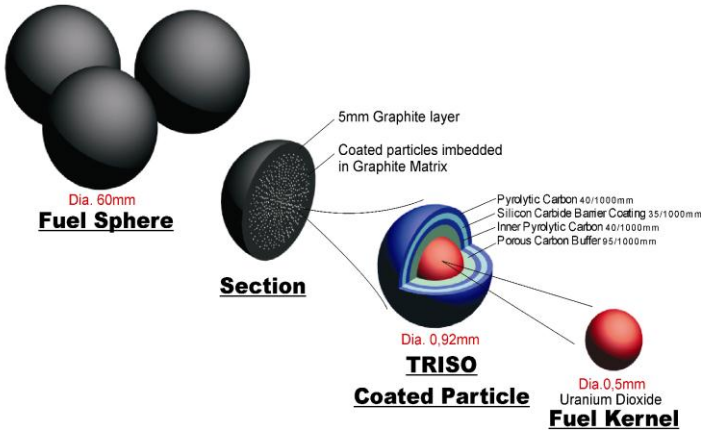

Figure 14. Fuel in pebble bed HTR [4]

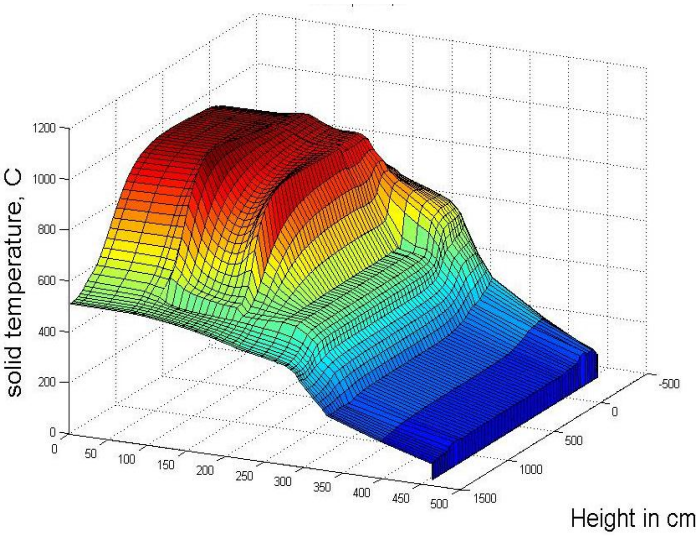

Figure 15. Solid temperature distribution for PBMR 400 at HFP. MCNP/THERMIX result.

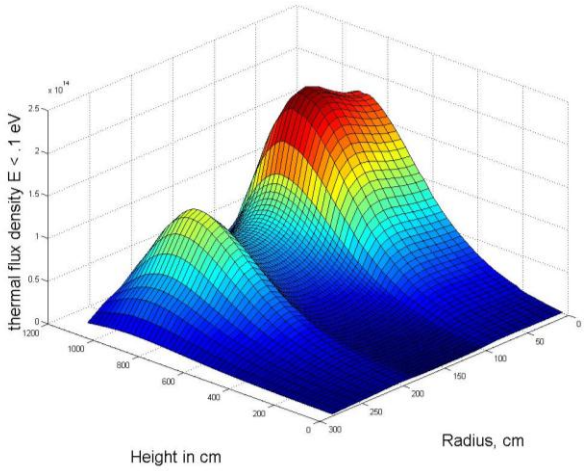

Figure 16. Thermal flux density distribution, PBMR-400, HFP, MCNP/THERMIX result.

6. CONCLUSIONS

The Monte Carlo method is a very powerful tool for a wide field of applications. Using the MCNP5 or MCNPX codes, detailed analyses can be performed for complex systems. Applications with a very large number of different material compositions or temperatures in geometrical regular structures such as LWR assemblies or HTR core grids are complicated, since for all regions with different material, a separate cell and a corresponding material composition or temperature must be defined. This can be simplified by use of user-supported internal functions for the assignment of material specification and temperatures. Furthermore, a large number of zones with different temperatures require an effective interpolation procedure for resonance cross sections and thermal neutron scattering data. The PWR benchmark could be calculated without memory problems even if pin wise material data were used. The simplifications specified for the benchmark are not necessary from a handling and memory requirement point of few. In fact a much higher degree of heterogeneity (e.g. inside the assembly or even inside each pin) could be treated.

ACKNOWLEDGMENT

This work is supported by the German Federal Ministry of Economics and Technology.

REFERENCES

1. X-5 Monte Carlo Team, "MCNP – A General Monte Carlo N-Particle Transport Code, Version 5," LA-UR-03-1987 (2003).
2. D.B. Pelowitz (ed.), "MCNPX™ User's Manual –V. 2.6.0," LA-CP-07-1473 (2008).
3. T. Kozlowski, and T. J. Downar, "The PWR MOX/UO_2 Core Transient Benchmark, Final Report", NEA/NSC/DOC(2006) 20.
4. "OECD/NEA PBMR Coupled Neutronics/Thermal Hydraulics Transient Benchmark - The PBMR-400 Core Design", NEA-1746 ZZ-PBMR-400 (2009).
5. G. Lerchl, H. Austregesilo, "ATHLET Mod 1.2 Cycle A, User's Manual, Rev. 1," GRS-P-1/Vol. 1 (1998).
6. K. Petersen, „Zur Sicherheitskonzeption des Hochtemperaturreaktors mit natürlicher Wärmeableitung aus dem Kern im Störfall". *KFA Jülich Jül-1872*, (Oct. 1983).
7. W. Bernnat, M. Mattes, A. Pautz, W. Zwermann, "Monte Carlo Applications with Consideration of Detailed Material Composition and Temperature Distributions in LWR and HTR," SNA + MC2010, Tokyo, Japan, Oct. 17 – 21, 2010, on CD-ROM, (2010).
8. "MCJEFF3.1NEA: MCNP Neutron Cross Section Library based on JEFF3.1", NEA/NSC/DOC(2006)18 (2006).
9. M. Mattes, J. Keinert, "Thermal Neutron Scattering Data for the Moderator materials H_2O, D_2O and ZrHx in ENDF-6 Format", INDC(NDS)-0470, April 2005
10. T. Downar, et al., "PARCS: Purdue Advanced Reactor Core Simulator," PHYSOR 2002, Seoul, Korea, Oct. 7 – 10, 2002, on CD-RPM, (2002).
11. S. Langenbuch, K.-D. Schmidt, K. Velkov, "Analysis of OECD/NRC Turbine Trip Benchmark by the Coupled-Code System ATHLET-QUABOX/CUBBOX," Nuclear Science and Engineering **148**, pp. 270-280 (2004).

12. W. Bernnat, W. Feltes, “Models for reactor physics calculations for HTR pebble bed modular reactors”, Nuclear Eng. and Design 222 (2003) 331-347.

PHYSOR 2012 – Advances in Reactor Physics – Linking Research, Industry, and Education
Knoxville, Tennessee, USA, April 15-20, 2012, on CD-ROM, American Nuclear Society, LaGrange Park, IL (2012)

Anhang B3

COMPARISON OF XSUSA AND "TWO-STEP" APPROACHES FOR FULL CORE UNCERTAINTY QUANTIFICATION

Artem Yankov
University of Michigan
2355 Bonisteel Blvd
Ann Arbor, MI 48109
yankovai@umich.edu

Markus Klein
Gesellschaft für Anlagen- und Reaktorsicherheit (GRS) mbH
Boltzmannstr. 14, D- 85748 Garching b. München, Germany
Markus.Klein@grs.de

Matthew A. Jessee
Oak Ridge National Laboratory
jesseema@ornl.gov

Winfried Zwermann, Kiril Velkov, Andreas Pautz
Gesellschaft für Anlagen- und Reaktorsicherheit (GRS) mbH
Boltzmannstr. 14, D- 85748 Garching b. München, Germany

Benjamin Collins, Thomas Downar
University of Michigan
bscollin@umich.edu; downar@umich.edu

ABSTRACT

While there are multiple sources of error that are introduced into the standard computational regime for simulating reactor cores, rigorous uncertainty analysis methods are available primarily for quantifying the effects of cross-section uncertainties. Two methods for propagating cross-section uncertainties through core simulators are the XSUSA approach and the "Two-Step" method. The XSUSA approach, which is based on the SUSA code package, is fundamentally a stochastic-based method. Alternatively, the "Two-Step" method utilizes generalized perturbation theory in the first step and stochastic sampling in the second step. The consistency of these two methods in quantifying uncertainties in the multiplication factor and in the core power distribution will be examined in the framework of phase I-3 of the UAM Benchmark. Using the TMI core as a base model for analysis, the XSUSA and "Two-Step" methods are applied with certain limitations and the results are compared to those produced by other stochastic sampling-based codes. Based on the uncertainty analysis results, conclusions are made for which method is currently a more viable option for computing uncertainties in burn-up and transient calculations.

Key Words: UAM Benchmark, XSUSA, Two-Step Method

1. INTRODUCTION

Modeling nuclear reactor stability and performance computationally has evolved into a multi-physics and multi-scale regime. Various computer codes have been developed and optimized to model individual facets of reactor operation such as neutronics, thermohydraulics, and kinetics. These codes are most often coupled to produce more physical results. While it is crucial to be able to produce best-estimate calculations for the design and safety analysis of nuclear reactors, it is equally important to obtain design margins by propagating uncertainty information through the entire computational process. The purpose of the OECD Uncertainty Analysis in Modeling (UAM) benchmark is to produce a framework for the development of uncertainty analysis methodologies in reactor simulations [1]. Three phases comprise the benchmark with each phase building in scale on its predecessors. The first phase deals with uncertainties in neutronics calculations, the second phase deals with neutron kinetics and the final phase requires the propagation of uncertainties through coupled neutronics/thermal-hydraulics simulations.

The neutronics phase of the UAM benchmark deals specifically with the spread of input parameter uncertainties to uncertainties in output parameters on a full-core scale. In the established framework of full-core analyses, lattice homogenized few-group cross-sections are used as inputs to core simulators. Core simulators utilize a number of approximations to the exact transport equation, effectively introducing error into output parameters. Geometrical uncertainties and numerical method simplifications can also be attributed for the introduction of modeling error. While it is important to propagate all known uncertainties when conducting a thorough uncertainty analysis, the necessary methods must still be developed to make this possible. However, rigorous methods have been developed to propagate cross-section uncertainties from lattice transport solvers to core simulators. Consequently, few-group homogenized cross-section errors will be the sole source of modeled uncertainty in the analysis to proceed.

Two primary methods exist for propagating cross-section uncertainties through core simulators. The first method is commonly referred to as the XSUSA (Cross-Section Uncertainty and Sensitivity Analysis) approach, developed at GRS [2]. The XSUSA approach –based on the SUSA code package [11] – is fundamentally a stochastic-based method. An alternate approach, the "Two-Step" method, utilizes generalized perturbation theory in the first step and stochastic sampling in the second step. The purpose of this paper is to show consistency between these two methods in the framework of phase I-3 of the UAM benchmark. As defined in the UAM benchmark specifications, the Three Mile Island Unit-1 (TMI) core will be the focus of application for the XSUSA and "Two-Step" methods. The TMI core is chosen for analysis mainly because it has been the focus of past benchmark problems and is therefore of great familiarity in the nuclear engineering community [3].

2. METHODOLOGY

Both the XSUSA and "Two-Step" methods actively use the modules in SCALE (Standardized Computer Analyses for Licensing Evaluations) to propagate cross-section uncertainties [4]. Also,

both methods make strong use of SCALE's 44-group covariance library. In the XSUSA approach, all input parameters are varied simultaneously and the number of required calculations to achieve a certain statistical accuracy in output parameters of interest is independent of the number of inputs [11]. The number of required runs can be calculated using Wilks' formula, which gives the confidence level that the maximum code output will not be exceeded with some specified probability. Contrarily, the "Two-Step" method does depend on the number of input parameters. The two different methodologies are summarized below.

The covariance matrix between inputs plays a central role in stochastic sampling. Cross-sections are correlated and the degree of correlation can be described by a covariance matrix, which describes how a change in one cross-section will affect all others in the matrix. Cross-sections must be perturbed such that their covariance relations are always preserved. Mathematically, the problem is to generate a matrix $X = (X_1, X_2 \ldots, X_N)$ such that $X \sim N(0, \Sigma)$ where Σ is the covariance matrix for X [6]. Since any linear combination of random normal variables is also normal then for some random normal vector $Z \sim N(0,1)$ the following statement is true

$$a_1 Z_1 + a_2 Z_2 + \cdots + a_n Z_n \sim N(0, \sigma^2) \quad (1)$$

When

$$\sigma^2 = a_1^2 + a_2^2 + \cdots + a_n^2 \quad (2)$$

In matrix form Equ. 1 can be expressed as,

$$A^T Z \sim N(0, A^T A) \quad (3)$$

The Cholesky decomposition defines A such that the covariance matrix can be written as $\Sigma = A^T A$. From Equ. (3) the following result can be easily obtained:

$$X' = X + A^T Z \sim N(X, \Sigma) \quad (4)$$

Hence, to produce perturbed cross-sections X' only the Cholesky decomposition of the cross-sections' covariance matrix is needed along with a random normal vector. In the XSUSA approach, ENDF/B-VII nuclear data in the SCALE 238-group structure is used. Spectral calculations are performed in BONAMI and CENTRM to produce a problem-specific cross-section library, as seen in Fig. 1. Using SCALE's 44-group covariance library with the problem-specific library generated by the spectral calculations, the XSUSA code applies perturbations to create a set of N varied, problem dependent cross-section libraries. The XSUSA code works to make sure varied data is physically consistent.

Each set of N cross-section libraries produced by XSUSA is passed to SCALE's transport solver NEWT, which in turns produces N perturbed, homogenized, few-group cross-section libraries. The perturbed few-group libraries are then used as input for core simulators such as PARCS [7] and QUABOX/CUBBOX [12]. Once all N libraries are processed by the core simulator, statistics can be taken on the output parameters of interest.

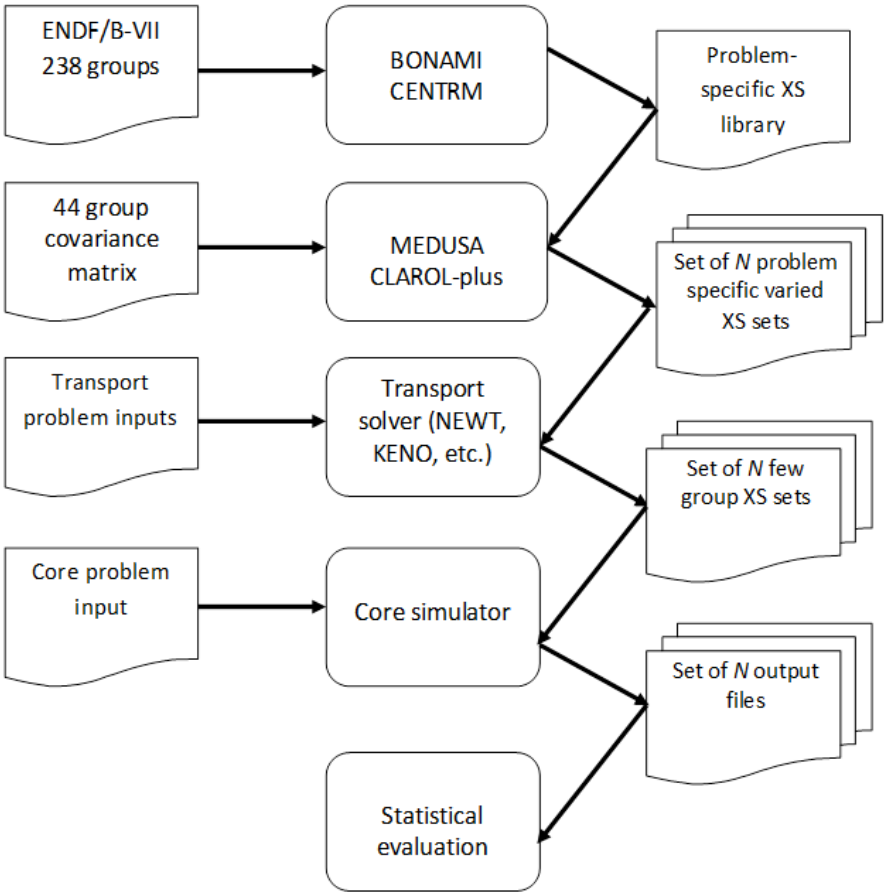

Figure 1: Flow diagram of the XSUSA approach starting from use of the ENDF/B-VII 238 group library and ending with a statistical evaluation of output parameters.

Unlike the XSUSA approach, the "Two-Step" method is only partly based on sampling techniques. In the first step it makes use of the generalized adjoint for the transport equation. In the "Two-Step" method problem-dependent self-shielded data is also generated before any kind of perturbed cross-sections are calculated, as seen in Fig. 2. Using the problem-dependent cross-sections, the TSUNAMI module is applied to calculate the forward transport, adjoint transport, and generalized adjoint transport solutions to the problem at hand. The SCALE module SAMS then uses the problem solutions to calculate sensitivity coefficients for responses of interest. The sensitivity coefficient of the response R_{xG} for reaction type x in broad-group G with respect to some nuclear data parameter σ_n in the transport equation is given as [8],

$$\frac{\Delta R_{xG}}{\Delta \sigma_n} = \frac{\langle \Phi \frac{\partial \Sigma_{xg}}{\partial \sigma_n} \rangle}{\langle \Sigma_{xg} \Phi \rangle} + \langle \Gamma^*_{xG} \frac{\partial (L - \lambda P)}{\partial \sigma_n} \Phi \rangle \qquad (5)$$

where Φ is the solution of the forward transport equation, Σ_{xg} is the fine-group, macroscopic shielded cross-section, L is the migration and loss operator, and P is the production operator. The generalized adjoint Γ^*_{xG} can be obtained by solving the generalized adjoint transport equation in Eq. 6[8].

$$(L^* - \lambda P^*)\,\Gamma^*_{xG} = \frac{\mathrm{d}R_{xG}}{d\Phi} \qquad (6)$$

The solution of Eq. 6 requires the solution of the adjoint transport problem. The pertinent responses of interest are the few-group cross-sections needed for core simulators.

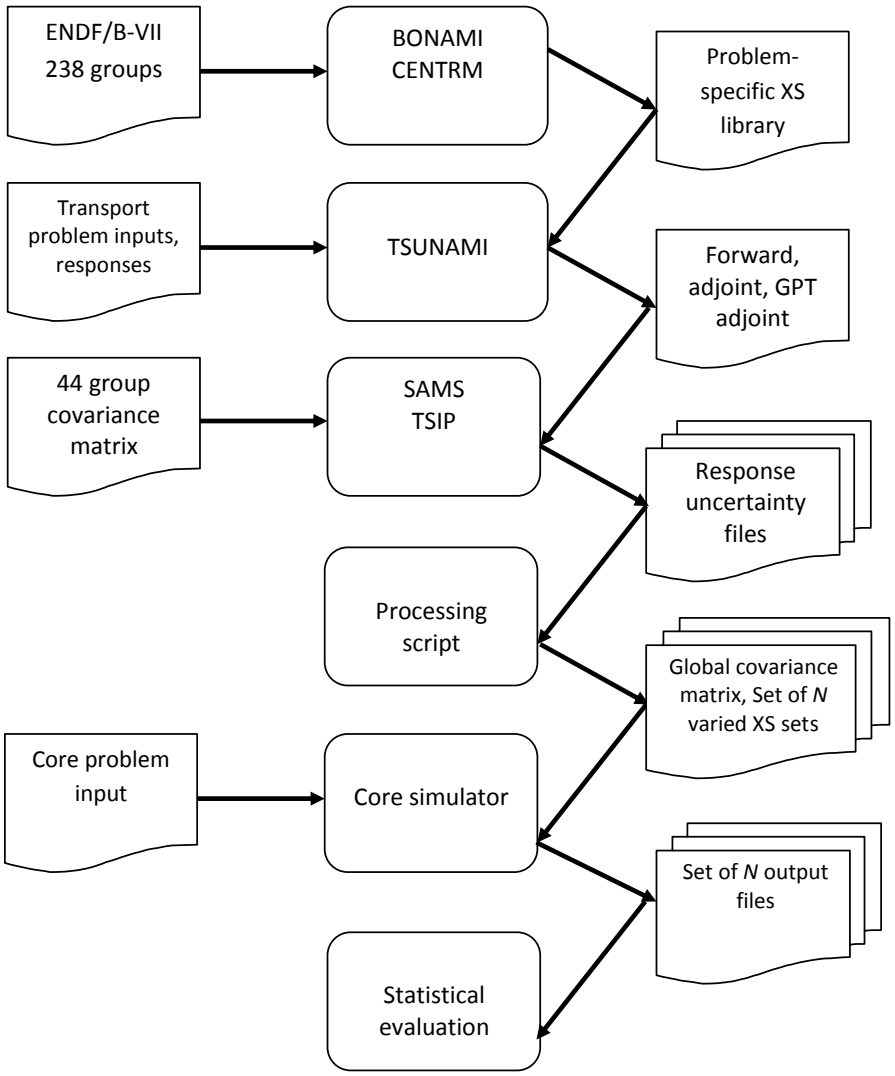

Figure 2[8]: Flow diagram for the proposed "Two-Step" method, which mainly utilizes the generalized perturbation theory modules in SCALE.

If the covariance matrix $\bar{\bar{C}}_i$ of some input parameters is available along with the sensitivities $\bar{\bar{S}}$ relating the change in outputs with respect to the change in input parameters, the "sandwich rule" can be applied to obtain a covariance matrix for the outputs $\bar{\bar{C}}_o$. The "sandwich rule" is expressed in Eq. 7 [9].

$$\bar{\bar{C}}_o = \bar{\bar{S}}\bar{\bar{C}}_i\bar{\bar{S}}^T \quad (7)$$

Consequently, since $\bar{\bar{C}}_i$ is the SCALE 44-group covariance matrix, a covariance matrix for the few-group homogenized cross-sections can be obtained. The SCALE module TSUNAMI-IP is used to generate a global covariance matrix relating the few-group cross-sections in each assembly and reflector regions comprising a full-core problem. Using Eq. 4 this global covariance matrix is sampled to produce N perturbed cross-section libraries that can then be used as input for a core simulator. By applying the XSUSA and "Two-Step" methods to calculate uncertainties in output parameters of interest for the full-core TMI problem, it can be shown that the two different approaches produce consistent results.

3. RESULTS

The TMI core consists of eleven different assemblies and a reflector region placed in 1/8 symmetry. All control rods are ejected from the core, which is at hot zero power [1]. Using the XSUSA and "Two-Step" methods, uncertainties are obtained for the core-wide multiplication factor and for the assembly-wise relative power distribution. The uncertainty analysis is somewhat limited by the current generalized perturbation theory capabilities in SCALE. The limitations mainly affect the "Two-Step" method since it utilizes the generalized perturbation theory modules in SCALE. However, the limitations for this analysis are passed to the XSUSA approach to ensure consistency. Since TSUNAMI only allows for reaction rate ratio responses, the uncertainty in the few-group homogenized transport cross-section cannot be explicitly evaluated [4]. However, uncertainties in the total cross-section can be calculated. To approximate perturbations to the transport cross section Eq. 8 is used.

$$\Sigma_{tr,G}{}^{*} = \Sigma_{t,G} - \bar{\Sigma}_{s1,G} \quad (8)$$

The anisotropic scattering term $\bar{\Sigma}_{s1,G}$ is held constant while the total cross-section $\Sigma_{t,G}$ is perturbed to yield an effectively perturbed transport cross-section $\Sigma_{tr,G}$* that is to be used as input to a core simulator. Also, TSUNAMI is currently unable to provide uncertainties for reflector assembly discontinuity factors (ADF). The remedy is to simply set all ADFs in the core equal to their mean values. Consequently, for a two-group formulation, each assembly in the TMI core requires nine perturbed cross-sections. These are the transport, absorption, kappa-fission, and nu-fission cross-sections along with a down scatter cross-section. The reflector region only requires five cross-section inputs for a total of 104 perturbed cross-sections per core simulation.

In order to check consistency of the intermediate covariance matrix of the "Two-Step" method a statistical covariance matrix of the varied few group cross-sections obtained by XSUSA was computed. It should be noted that this statistical matrix does not serve as an input for any following calculation but that the few-group covariance is contained in the set of *N* few group cross-sections implicitly. Figure 3 shows a comparison of the few-group cross-section

uncertainties of Assembly 6 [1]. Figure 4 shows a comparison of the few-group cross-section correlations and cross correlation coefficients for Assemblies 6 and 7 [1] together with the statistical 99% confidence bounds [2].

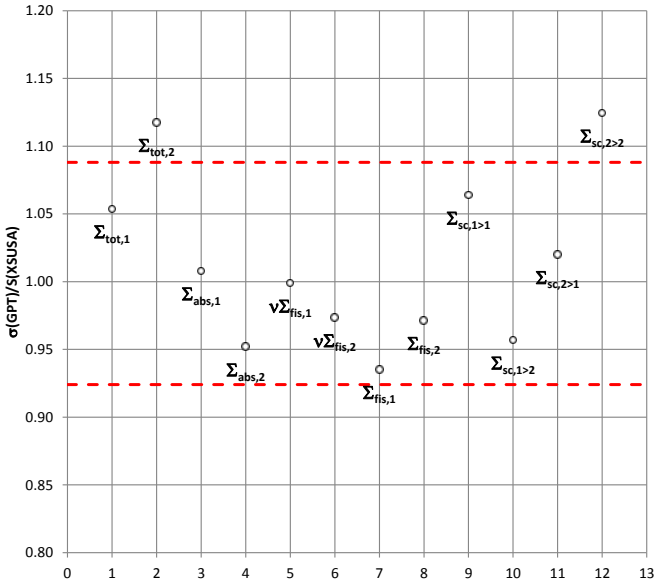

Figure 3: Comparison of few-group cross section uncertainties obtained by GPT $\sigma(GPT)$ and sampling based uncertainties from XSUSA $S(XSUSA)$. The 99% confidence limits are depicted as red lines.

It can be seen that the cross-section uncertainties show good agreement overall, with only the values for $\Sigma_{sc,2>2}$ and $\Sigma_{tot,2}$ being outside the confidence limits. Furthermore, the values of the correlation matrix show good agreement as well. However, several values are outside the confidence limits, a majority of which are connected to scattering cross-sections. The reason for these discrepancies is currently being investigated.

The global covariance matrix for the TMI core consists of the cross-sections for 11 assemblies and one reflector region resulting in a (104 x 104) covariance matrix. While the statistical global covariance matrix obtained by XSUSA was positive definite, the global covariance matrix generated for the TMI core using the "Two-Step" method was slightly non-positive definite. However, the use of a global covariance matrix is essential when sampling cross-sections for an entire core since otherwise the similarity of the nuclide composition of different fuel assembly types is neglected. If the global covariance matrix is not used, the output parameter uncertainties can be greatly misrepresented. Consequently, the "Two-Step" global covariance matrix was made positive definite by making it more diagonally dominant. This was achieved by multiplying the matrix's off-diagonal terms by $1 - \varepsilon$ for some very small value ε.

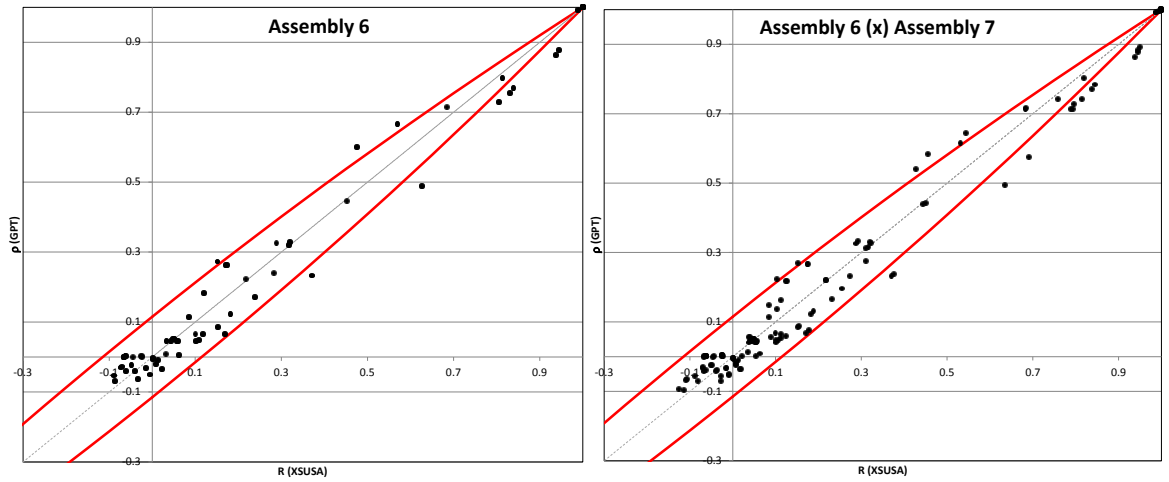

Figure 4: Comparison of few-group cross-section correlations obtained by GPT ρ(GPT) and sampling based uncertainties from XSUSA R(XSUSA). The 99% confidence limits are depicted as red lines.

The core simulator utilized for the proceeding analysis is PARCS. The multi-group NEM nodal kernel is used to execute all 276 core simulations [7]. Initially 300 core simulations were proposed but some of the cross-section perturbations in the "Two-Step" method were too large and so PARCS was unable to produce a converged solution. The large number of core simulation ensures that the largest output values obtained will not be exceeded with a high probability by Wilks' formula. The multiplication factor uncertainty results obtained using XSUSA* (ADFs unperturbed and using Eq. (8) for $\Sigma_{tr,G}$*) and "Two-Step" methods for the TMI core are summarized in Table I. The table clearly shows that the XSUSA and "Two-Step" methods can consistently calculate uncertainties in the multiplication factor.

Table 1. Multiplication factors calculated for the TMI core using the XSUSA* and "Two-Step" methods. All ADFs were set to their mean values and Eq. (8) was used for $\Sigma_{tr,G}$*.

	"Two-Step" Method	XSUSA* Method	Absolute Difference (pcm)
k-eff mean	1.30215	1.30212	3
k-eff stand. deviation	0.00557	0.00583	26
Relative % Error	0.42753	0.44738	

As a "one-step" reference solution, the multiplication factor was calculated using XSUSA/KENO and TSUNAMI-3D. The KENO calculations were performed in accordance with Fig. 1, the only difference being that the transport solver is replaced by KENO. For all XSUSA calculations the same random numbers were used in order to get consistent results. To try to

replicate the TSUNAMI-3D and KENO results as best as possible the XSUSA approach was applied with perturbed ADF values and $\Sigma_{tr,G}$ produced by NEWT using the PARCS and QUABOX/CUBBOX (QC) core simulators. The results are summarized in Table II.

Table II. Multiplication factors calculated for the TMI core using various stochastic approaches. Physical ADF values are used when relevant.

	XSUSA/KENO	TSUNAMI-3D	XSUSA/PARCS	XSUSA/QC
k-eff mean	1.30294	1.30279	1.30200	1.30025
k-eff std. deviation	0.00608	0.00588	0.00582	0.00598
Relative % Error	0.46679	0.45120	0.44732	0.45991

Comparing Table I and Table II, it becomes clear that for the TMI core ADF perturbations do not have a significant effect on the uncertainty in the core multiplication factor. Further analysis of the XSUSA results suggest that the use of ADFs has a minimal effect on the uncertainty in core assembly power distribution despite having a major impact on the mean power distribution values. It is therefore reasonable to compare the power distributions (mean and uncertainties) of the XSUSA/'core simulator' calculations (with varied ADFs), the "two-step" calculations (using non-varied ADFs) and the XSUSA/KENO calculations (not dependent on ADFs). The mean power distributions obtained using XSUSA*/PARCS and the "Two-Step" methods are shown in Fig. 5 along with XSUSA/KENO and XSUSA/QC solutions.

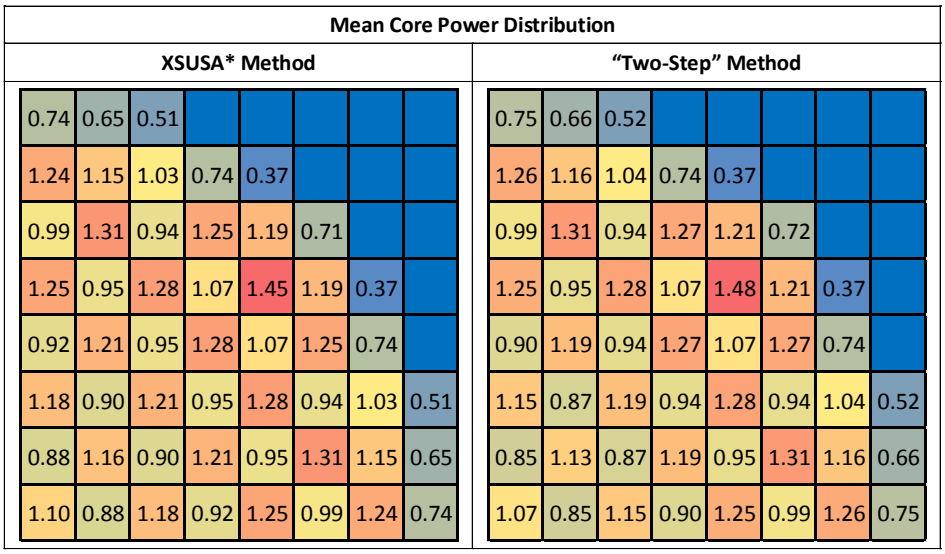

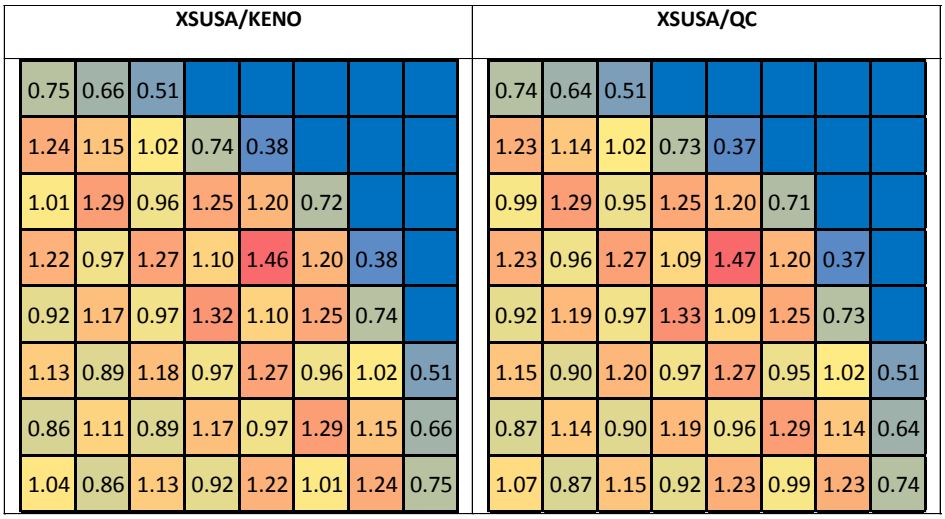

Figure 5: Mean nodal powers in the TMI core calculated using the XSUSA and "Two-Step" methods. Note that the nodal power is normalized such that the average power in the core is unity. Quarter symmetry is displayed.

The values displayed in Fig. 5 are relative power distributions such that the mean power in the core is unity. As expected, the mean power distributions predicted by the XSUSA and "Two-Step" methods are very similar with the largest node-wise discrepancy of some 3%. The relative percent uncertainties in power for each node are shown in Fig. 6.

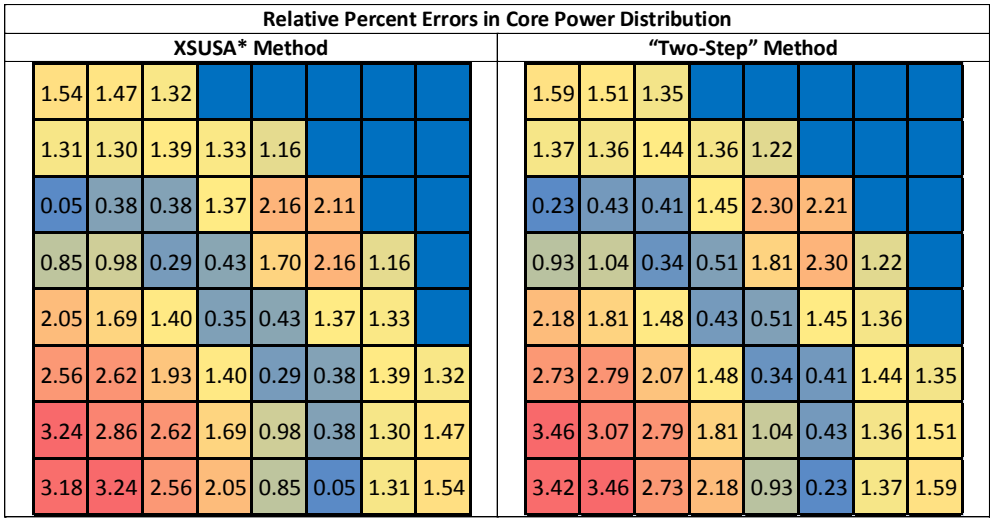

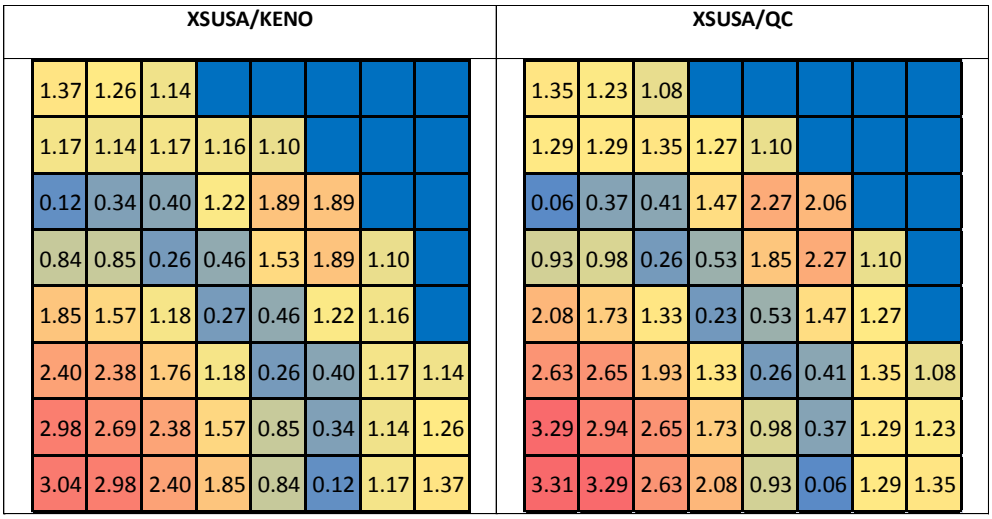

Figure 6: Relative percent error in the nodal powers of the TMI core calculated using the XSUSA and "Two-Step" methods. Quarter symmetry is displayed.

The "Two-Step" method seems to attribute more uncertainty overall to each nodal power. Uncertainties with the highest magnitudes congregate around the center of the core. This is due to the radial heterogeneity of the core configuration [14]. The greatest discrepancy in relative nodal power error occurs in the center of the core, where the XSUSA* and "Two-Step" methods differ by some 7%. Using N=300 samples, the 95%/95% confidence interval for the standard deviation is about 8%. As the two methods do not use the same random numbers, this result does not directly imply a real difference of the results. Both the XSUSA* and "Two-Step" methods compare reasonably well with the "one-step" reference solutions. The small differences can mainly be attributed to the effects of ADF perturbations and complete perturbations in the transport cross-section.

4. CONCLUSIONS

The core simulator output uncertainties for the TMI core obtained using the XSUSA* and "Two-Step" methods indicate that the two methods are consistent in general and are both able to propagate nuclear data uncertainties to the core simulator. Despite some of the current limitations of the generalized perturbation theory implementations in SCALE, both uncertainty quantification methods yield a relatively large uncertainty in the multiplication factor. Some might argue that the uncertainty is unacceptably high given its proximity to the delayed neutron fraction. The multiplication factor uncertainty implies that prompt super criticality is within design margins of the TMI core. Currently, the limitations of generalized perturbation theory as applied in the "Two-Step" method make the XSUSA approach a more robust choice for reactor uncertainty analysis. Even to perform a steady-state uncertainty analysis methods should be developed in the current generalized perturbation theory framework in SCALE in order to capture all of the uncertainty within reach of the XSUSA approach. Methods should also be developed in order to be able to apply "Two-Step" type methods for burn-up and transient calculations, as defined in phases II-III of the UAM benchmark. The XSUSA approach already allows for such calculations, as evident in the works of [10] and [13]. In terms of efficiency, the

XSUSA and "Two-Step" methods require similar computation times if parallel computing is employed. Overall, more work should be done with the "Two-Step" method to make it a viable tool for uncertainty quantification in core simulations. However, the results in this paper suggest that the "Two-Step" method can be made to be fully consistent with more versatile stochastic methods.

REFERENCES

1. Ivanov, K., M. Avramova, I. Kodeli, and E. Sartori. Benchmark for Uncertainty Analysis in Modeling (UAM) for Design, Operation and Safety Analysis of LWRs. Rep. 2nd ed. Nuclear Energy Agency. NEA/NSC/DOC(2007)23.
2. M. Klein, L. Gallner, B. Krzykacz-Hausmann, I. Pasichnyk, A. Pautz, and W. Zwermann. "Influence of Nuclear Data Covariance on Reactor Core Calculations, "International Conference on Mathematics and Computational Methods Applied to Nuclear Science and Engineering" (2011).
3. Ivanov, K., T. M. Beam, Anthony J. Baratta, Adi Irani, and Nick Trikouros. Pressurized Water Reactor Steam Line Break (MSLB) Benchmark. Rep. Nuclear Energy Agency. Print. NEA/NSC/DOC(99)8.
4. SCALE: A Modular Code System for Performing Standardized Computer Analyses for Licensing Evaluations, ORNL/TM-2005/39, Version 6, Vols. I–III, January 2009. Available from Radiation Safety Information Computational Center at Oak Ridge National Laboratory as CCC-750 (2009).
5. Klein, Markus, Igor Pasichnyk, and Winfried Zwermann. "Influence of Nuclear Data Uncertainties on Reactor Core Calculations." Proc. of UAM-5 Workshop, Stockholm, Sweden. 2011. PowerPoint.
6. Bevington, Philip R., and D. Keith. Robinson. Data Reduction and Error Analysis for the Physical Sciences. Boston: McGraw-Hill, 2003.
7. T. Downar, Y. Xu, V. Seker, "PARCSv3.0 Theory Manual," UM-NERS-09-001, October, 2009.
8. Williams, Mark, Matthew Jessee, Ron Ellis, and Brad Rearden. "Sensitivity/Uncertainty Analysis for OECD UAM Benchmark of Peach Bottom BWR." Proc. of UAM-4 Workshop, Pisa, Italy. 2010. PowerPoint.
9. M. A. Jessee, "Cross-Section Adjustment Techniques for BWR Adaptive Simulation," Dissertation, North Carolina State University, Raleigh, North Carolina (2008).
10. I. Pasichnyk, Markus Klein, and Winfried Zwermann. "Influence of Nuclear Data Covariance on Transient Calculations." Proc. of UAM-5 Workshop, Stockholm, Sweden. 2011. PowerPoint.
11. B. Krzykacz, E. Hofer, M. Kloos, "A Software System for Probabilistic Uncertainty and Sensitivity Analysis of Results from Computer Models*," Proc. International Conference on Probabilistic Safety Assessment and Management (PSAM-II),* San Diego, Calif., USA (1994).
12. S. Langenbuch , K. Velkov, "Overview on the Development and Application of the Coupled Code System ATHLET – QUABBOX/CUBBOX", *Proc. of Mathematics and Computation, Supercomputing, Reactor Physics and Nuclear and Biological Applications,* Avignon, France, Sept. 12. – 15. 2005, (2005).

13. L. Gallner, B. Krzykacz-Hausmann, A. Pautz, M. Wagner, W. Zwermann, "Influence of Nuclear Data Uncertainties on the Depletion Chain", *Proc. Jahrestagung Kerntechnik* 2011, Berlin, Germany, May 17. - 19. 2011, (2011).
14. M. Klein, L. Gallner, B. Krzykacz-Hausmann, A. Pautz, K. Velkov, W. Zwermann, "Interaction of Loading Pattern and Nuclear Data Uncertainties in Reactor Core Calculations", *Proc. PHYSOR* 2012, Knoxville, Tennessee, USA, April 15. - 20. 2012, (2012).

PHYSOR 2012 – Advances in Reactor Physics – Linking Research, Industry, and Education
Knoxville, Tennessee, USA, April 15-20, 2012, on CD-ROM, American Nuclear Society, LaGrange Park, IL (2012)

Anhang B4

DEVELOPMENT OF A STATISTICAL SAMPLING METHOD FOR UNCERTAINTY ANALYSIS WITH SCALE

M. Williams, D. Wiarda, H. Smith, M. A. Jessee, B. T. Rearden
Oak Ridge National Laboratory
P.O Box 2008, Oak Ridge, TN 37831-6354, USA*
williamsml@ornl.gov; wiardada@ornl.gov; smithhj@ornl.gov; jesseema@ornl.gov; reardenb@ornl.gov

W. Zwermann, M. Klein, A. Pautz, B. Krzykacz-Hausmann, L. Gallner
Gesellschaft fuer Anlagen- und Reaktorsicherheit (GRS)
Forschungszentrum, Boltzmannstrasse 14, 85748 Garching, Germany
Winfried.Zwermann@grs.de, Markus.Klein@grs.de, Andreas.Pautz@grs.de, Bernard.Krzykacz-Hausmann@grs.de, Lucia.Gallner@grs.de

ABSTRACT

A new statistical sampling sequence called Sampler has been developed for the SCALE code system. Random values for the input multigroup cross sections are determined by using the XSUSA program to sample uncertainty data provided in the SCALE covariance library. Using these samples, Sampler computes perturbed self-shielded cross sections and propagates the perturbed nuclear data through any specified SCALE analysis sequence, including those for criticality safety, lattice physics with depletion, and shielding calculations. Statistical analysis of the output distributions provides uncertainties and correlations in the desired responses.

Key words: uncertainty analysis, statistical sampling, XSUSA, SCALE

1. INTRODUCTION

Over the last ten years a number of sophisticated sensitivity/uncertainty (S/U) tools have been developed for the SCALE code system [1]. They include methods for calculating sensitivity coefficients and response uncertainties (TSUNAMI-1D, 2D, 3D; TSAR), performing similarity analysis (TSUNAMI-IP), and consolidating experimental and computational results through data adjustment (TSURFER) as well as developing a comprehensive library of nuclear data covariance information [1]. The current S/U methodology in SCALE is based on using first-order perturbation theory to calculate response sensitivity coefficients, which are then folded with nuclear data covariances to obtain the response uncertainty [2]. This approach requires an adjoint transport calculation for each response of interest, which may be the critical eigenvalue, the reactivity difference between two reactor states, or the ratio of reactions rates (e.g., peak relative pin power). However, after the adjoint and forward transport calculations are performed, sensitivity coefficients for all input data, including nuclear data and material concentrations, can be computed very efficiently. The SCALE S/U tools have been applied successfully for many applications in criticality safety analysis and steady state reactor lattice physics.

Unfortunately, there are applications where the adjoint-based perturbation methodology is inadequate or is inefficient. These cases tend to fall into three categories:

(a) Cases addressing a large number of responses, such as spatial distributions (e.g., the pinwise fission rate in a depletable fuel assembly). This requires a separate generalized adjoint transport calculation for each pin response in each branch state point and burnup step.

(b) Cases requiring codes for which no adjoint capability has been developed. At present, SCALE has the capability for eigenvalue adjoint solutions with the neutron transport codes XSDRN, NEWT, and KENO and generalized adjoint calculations with XSDRN and NEWT. Multiphysics analysis with coupled neutronics and thermal hydraulics cannot be treated, nor can coupled neutronics-depletion calculations.

(c) Cases for which the linear perturbation assumption is not valid. Discontinuities and bifurcations encountered in reactor dynamics—such as control rod insertion at some time during a transient—are also not amenable to first-order perturbation methods.

In order to eliminate the above restrictions and to provide a robust capability for full core reactor calculations, a completely different approach has been developed recently for uncertainty analysis with SCALE. The new method uses statistical sampling of nuclear data probability density functions (PDFs) based on information in the SCALE covariance library to produce a random sample for the input computational data vector (CDV), which contains all nuclear cross sections used in a transport calculation. If PDFs are available for other input parameters, such as enrichment, dimensions, or depletion data, then they too can be sampled and included in the perturbed CDV. The perturbed data vector can be used in any SCALE sequence or function module to perform a single forward solution for all the desired perturbed responses. The process is repeated for any desired number of randomly sampled input data vectors, and the resulting distribution of results from SCALE can be analyzed with standard statistical analysis tools to obtain the standard deviations and correlation coefficients for all responses.

The random sampling method is not restricted to currently available SCALE modules; any new SCALE modules or other existing codes run through the SCALE driver can be used for the calculations without having to develop the capability for adjoint calculations. Furthermore, the output distributions from SCALE may be propagated to downstream codes for follow-on uncertainty analysis. For example, the TRITON lattice physics sequence can be sampled statistically to produce a number of assembly-averaged, two-group cross section libraries for input to a core simulator code such as PARCS or NESTLE [7]. Each two-group library can be used to perform steady-state or kinetics calculations for a 3D core model, and the output distributions of results will define the response uncertainties (possibly time-dependent) associated with the SCALE input data uncertainties.

Response uncertainties computed with this approach are not limited to first-order accuracy; i.e., they account for all nonlinearities and discontinuities with the same accuracy as the original codes. Thus there are several advantages to the statistical sampling approach. However, the one big drawback is that response sensitivity coefficients cannot be computed efficiently for many practical cases—only the overall response uncertainty due to all data uncertainties is obtained. A full statistical sensitivity analysis requires that every input data parameter be sampled

individually, rather than collectively; this would necessitate a much larger number of SCALE runs. Nevertheless, it is also possible to determine the relative importances from the main nuclide/reaction combinations contributing to the total uncertainty with a moderate number of samples [5]. Fortunately, the calculations are all independent and can be done in parallel, but for standard PCs and small computer clusters in the near future, the statistical method will most likely be limited to computing uncertainties and main importances. In that sense, the statistical sampling method is complementary to the adjoint-based sensitivity method currently in SCALE.

2. METHODOLOGY

The SCALE code package includes generic multigroup (MG) and pointwise (PW) cross-section (XS) libraries for use in transport calculations. SCALE multigroup computation sequences include initial operations that manipulate and perform resonance self-shielding calculations prior to the transport (and possibly depletion) calculations, as shown in Figure 1.

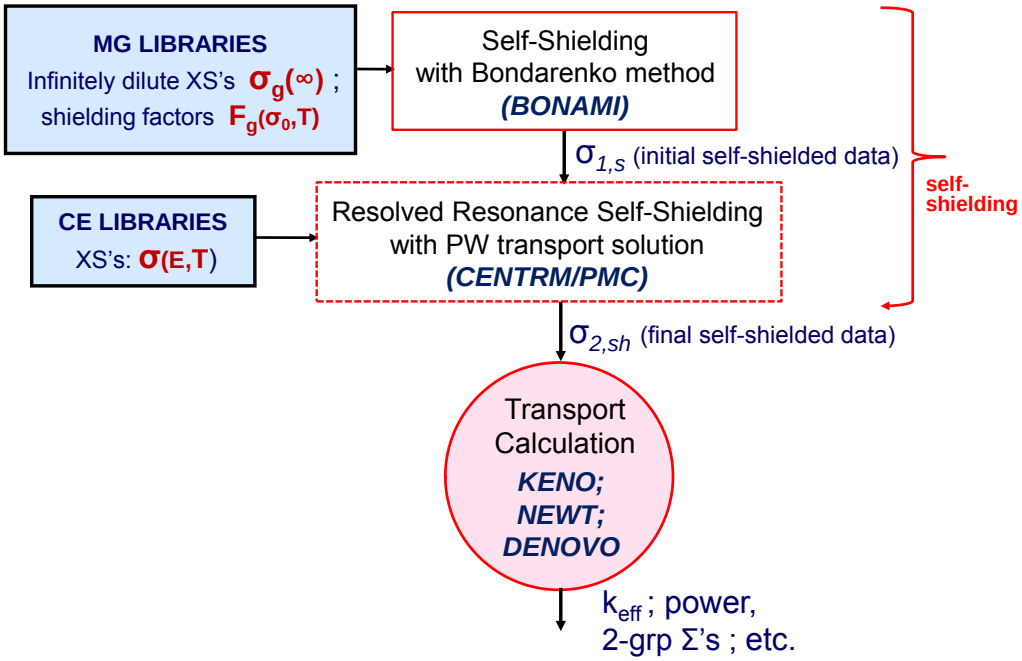

Figure 1. Flow chart of SCALE multigroup computation sequences.

The SCALE libraries contain the following four general types of nuclear data used in MG calculations:

(a) PW 1D data used in CENTRM and PMC self-shielding calculations:

$\sigma_x(E)$ = energy dependent XS for reaction x at energy E processed from ENDF/B;

(b) Infinitely dilute MG 1D data for reaction "*x*":

$$\sigma_{x,g}(\infty) \equiv \frac{\langle \sigma_x(E) \rangle}{\Delta u_g} \ , \tag{1}$$

where Δu_g is the lethargy width of group g ; and brackets $\langle \ \ \rangle$ indicate lethargy integration over g.

(c) Bondarenko self-shielding factors(aka, f-factors) vs background *XS* σ_0*:*

$$f_{x,g}(\sigma_0) \equiv \sigma_{x,g}(\sigma_0) / \sigma_{x,g}(\infty) \ , \tag{2}$$

where $\sigma_{x,g}(\sigma_0)$ is the self- shielded XS at σ_0 , represented as

$$\sigma_{x,g}(\sigma_0) \equiv \left\langle \frac{\sigma_x(E)}{\sigma_t(E)+\sigma_0)} \right\rangle \Big/ \left\langle \frac{1}{\sigma_t(E)+\sigma_0)} \right\rangle \tag{3}$$

(d) 2D scattering distributions:

$$\text{MG data } \sigma_{s,g\to g'}(\infty) \text{ and CENTRM PW thermal kernels, } \sigma_{th}(E \to E')$$

Uncertainties in the calculated results depend upon the uncertainties in each of the above computational data; however, for this development the impact of uncertainties in the 2D distributions is ignored because no uncertainty data are available in the SCALE covariance libraries. Therefore, the remaining three types of input data can be collected into an M-dimensional CDV of the form,

$$X = \left\{ \underbrace{\sigma_x(E), \sigma_y(E) \ldots .}_{\text{PW data for all reactions/nuclides}} \ ; \underbrace{\sigma_{x,g}(\infty), \sigma_{y,g}(\infty) \ldots .}_{\text{MG data for all reactions/nuclides}} \ ; \underbrace{f_{x,g}(\sigma_0), f_{y,g}(\sigma_0) \ldots .}_{\text{shielding factors for all reactions/nuclides}} \right\} \ , \tag{4}$$

where "M" is the number of input nuclear data parameters. These quantities are based on evaluated nuclear data processed from ENDF/B. Uncertainties in the experimental data used in the evaluation process introduce uncertainties into the basic ENDF/B data; thus these quantities should more appropriately be considered as having a range of possible values described by a PDF. Modern ENDF/B data evaluations include not only an estimate for the expected value of the data, but also covariance data to describe the correlated uncertainties. ENDF covariance data are described by a symmetric covariance matrix $\boldsymbol{C}_{\alpha_x,\alpha_y}$, which has variances on the diagonal and covariances off the diagonal. Unfortunately, many older evaluations in ENDF/B do not include covariance information. SCALE includes a comprehensive library of MG covariance data processed from ENDF/B and is supplemented by approximate covariances for materials without ENDF covariances [3]. Uncertainties and correlations in the basic evaluated nuclear data cause uncertainties in the processed data used for calculations, and these uncertainties are responsible for uncertainties in the output responses.

2.1 Sampling Method

The XSUSA code extends the SUSA code package developed by Gesellschaft fuer Anlagen- und Reaktorsicherheit (GRS) [4] to the application with nuclear data covariance. It randomly samples data from available covariance data with the sampling module MEDUSA, applies the samples to the reference nuclear data, and finally performs the statistical analysis of the entity of results. Oak Ridge National Laboratory has worked with GRS to couple the XSUSA sampling code with SCALE computational sequences. At present XSUSA is run to produce random samples for MG data values, although in the future it could also be applied to depletion data such as decay constants and fission product yields and also to delayed neutron parameters that are of major importance for transient calculations. The typical approach is to assume that the MG data PDF is a multivariate normal distribution, which is completely defined by the expected values and covariance matrices for the data. An XSUSA statistical sample consists of a full set of perturbed, infinitely dilute MG data for all groups, reactions, and materials. The SCALE MG covariance data are given as relative values of the infinitely dilute cross sections, so that a random perturbation sample for cross section $\sigma_{x,g}(\infty)$ corresponds to $\frac{\Delta\sigma_{x,g}(\infty)}{\sigma_{x,g}(\infty)}$. XSUSA converts these values to a set of multiplicative perturbation factors $Q_{x,g}$ that are applied to the reference data to obtain the altered values:

$$\sigma'_{x,g} = Q_{x,g}\,\sigma_{x,g}\ , \tag{5}$$

where:

$$Q_{x,g} = 1 + \frac{\Delta\sigma_{x,g}(\infty)}{\sigma_{x,g}(\infty)}\ . \tag{6}$$

The CDV defined in Eq. (4) contains PW cross sections and shielding factors in addition the infinitely dilute MG data. Furthermore, it can be seen from the definitions in Eqs. (1), (2), and (3) that these quantities are highly correlated because the PW cross sections appear in both the infinitely MG data and the self-shielding f-factors. For that reason, the three types of data appearing in the CDV cannot be sampled independently. For example, an energy-dependent perturbation in the PW cross section causes the infinitely MG cross section to be perturbed as shown below,

$$\sigma'_{x,g}(\infty) \equiv \frac{\langle \sigma'_x(E) \rangle}{\Delta u_g} \tag{7}$$

Similarly, the perturbed shielding factor can be obtained using Eqs. (2) and (3):

$$f'_{x,g}(\sigma_0) \equiv \frac{1}{\sigma'_{x,g}(\infty)} \left\langle \frac{\sigma'_x(E)}{\sigma'_t(E)+\sigma_0} \right\rangle \Bigg/ \left\langle \frac{1}{\sigma'_t(E)+\sigma_0} \right\rangle \tag{8}$$

Unfortunately, no SCALE covariance data are available for the energy-dependent PW XSs. For that reason, a simple approximation is used to obtain consistent, correlated perturbations in $\sigma_x(E)$, $\sigma_{x,g}(\infty)$, and $f_{x,g}(\sigma_0)$.

A comparison of the perturbed, infinitely dilute data given by Eqs. (5) and (7) shows that the expressions are equivalent if the PW data are perturbed in the following manner:

$$\sigma'_x(E) = Q_{x,g}\,\sigma_x(E) \text{ , for } E \in g \quad ; \tag{9}$$

i.e., the PW data are changed uniformly at all energy points with a group. Stated in another way, Eq. (9) assumes that PW data are fully correlated within a group. In fact, PW data do have strong short-range correlations of necessity, due to data continuity requirements; however, the correlations may not always extend over an entire group if the energy interval is large. Because different perturbation factors are applied to PW data in different groups, this approach introduces a discontinuity in $\sigma'_x(E)$ at the energy boundaries; however, this approximation is not expected to have much impact on the MG data because the group-averaged value only depends on the energy-dependent cross sections and flux within the group energy interval.

The perturbed MG shielding factor defined in Eq. (8) is evaluated in a similar manner. Applying the approximation in Eq. (9), Eq. (8) can be written as

$$f'_{x,g}(\sigma_0) \equiv \frac{1}{Q_{x,g}\sigma_{x,g}(\infty)} \left\langle \frac{Q_{x,g}\sigma_x(E)}{Q_{t,g}\sigma_t(E)+\sigma_0} \right\rangle \Big/ \left\langle \frac{1}{Q_{t,g}\sigma_t(E)+\sigma_0} \right\rangle , \tag{10}$$

After simplifying, Eq. (10) becomes

$$f'_{x,g}(\sigma_0) \rightarrow f_{x,g}(\sigma'_0) \text{ ; where } \sigma'_0 = \sigma_0 / Q_{x,g} \tag{11}$$

Therefore, the perturbed shielding factor can be obtained by simply evaluating the original f-factor tabulation at a modified background XS value.

In summary, the randomly perturbed CDV for use in SCALE sequence calculations is obtained as follows:

(1) select a value for $\frac{\Delta\sigma_{x,g}(\infty)}{\sigma_{x,g}(\infty)}$ using XSUSA to sample MG covariance data in SCALE,

(2) use Eq. (6) to convert the above relative perturbation into a multiplicative factor,

(3) use Eq. (9) to obtain the perturbed PW data used in CENTRM/PMC,

(4) use Eq. (5) to compute perturbed, infinitely dilute MG data, and

(5) use Eq. (11) to compute the perturbed shielding factor.

3. IMPLEMENTATION OF SCALE STATISTICAL SAMPLING METHODOLOGY

SCALE has several sequences used for a wide range of applications that can benefit from a statistical sampling methodology to perform uncertainty analysis. These include CSAS for criticality safety, TRITON for lattice physics and depletion, Mavric for shielding, and several

others. In order to provide a robust capability for statistical analysis of existing and any new sequences, a "super-sequence" called Sampler has been developed (Figure 2). Sampler generates perturbed MG Master and PW CENTRM libraries based on a random CDV sample containing perturbation factors from XSUSA, and then executes an arbitrary sequence to produce perturbed output results.

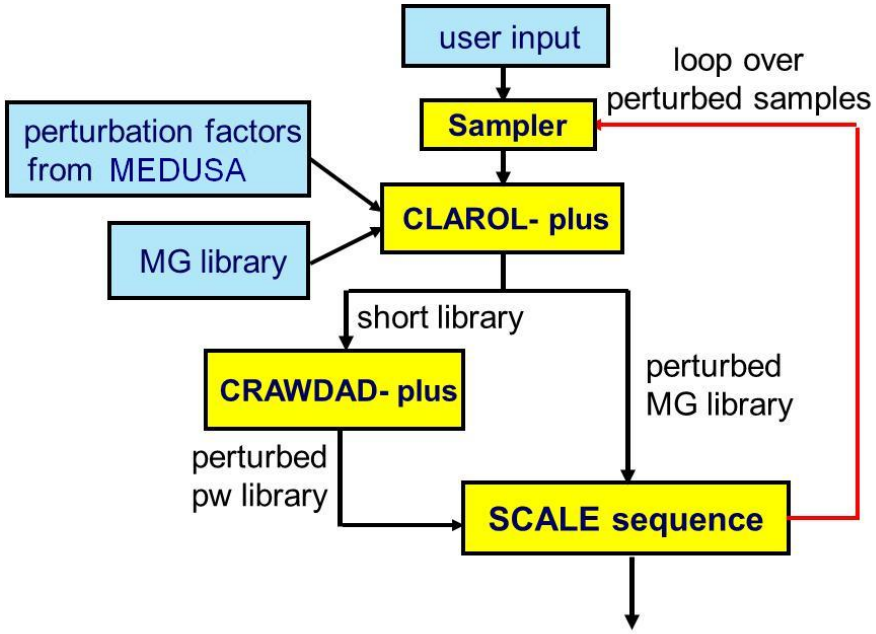

Figure 2. Sampler sequence flow chart.

At present, a precomputed library of nuclear data perturbation factors generated by the XSUSA code is read by Sampler, but in the future it may be desirable to have an option to execute XSUSA within the Sampler sequence so that on-the-fly data sampling can be done. The process is repeated for a specified number of CDV samples, and the distribution of output results is analyzed to determine standard deviations and correlations in any desired output response. The perturbation factors are precalculated and saved in the same format as an AMPX master library. Each sample is treated as "material" with 1D data corresponding to perturbation factors for the respective reaction types. Sampler executes two codes, ClarolPLUS and CrawdadPLUS, that convert perturbation factors into a perturbed MG and PW library, respectively, and then executes a designated sequence. The Sampler sequence performs the following operations:

(1) reads user input for the Sampler options (e.g., the desired number of samples) and reads the desired SCALE sequence input;

(2) prepares the secondary input for the ClarolPLUS and CrawdadPLUS codes;

(3) executes ClarolPLUS and CrawdadPLUS to produce perturbed MG and CENTRM PW libraries;

(4) executes the designated SCALE sequence using the perturbed MG and PW libraries; and

(5) collects sequence output of perturbed results. (The available types of results that can be collected is currently limited but can be easily expanded in the future.)

Sampler repeats steps (2)–(5) for a specified number of samples to obtain a distribution of results that can be converted to a standard deviation and correlation coefficients.

4. EXAMPLE APPLICATION

An earlier work applied the XSUSA/SCALE uncertainty analysis for criticality study [5], but it did not directly include the effects of perturbations in the PW cross sections and Bondarenko factors; instead, the perturbations were applied to the resonance shielded cross sections after the spectral calculations. Also, the calculations were not automated with the new Sampler sequence in SCALE. Here we apply the complete SCALE statistical sampling methodology in Sampler for the critical benchmark experiment LEU-COMP-THERM-008 described in the *International Handbook of Evaluated Criticality Safety Benchmark Experiments* (ICSBEP) [6] to determine uncertainties in the eigenvalue and power distribution, due uncertainties in nuclear data. This experiment corresponds to a 3 × 3 array of pressurized water reactor (PWR) fuel assemblies in a water pool. Figure 3 describes the experiment.

The SCALE CSAS25 sequence was used for the computations. This sequence performs resonance self-shielding calculations using BONAMI, CENTRM, PMC, and WORKER, and the resulting self-shielded cross sections are used in the KenoVa Monte Carlo code. All components of the computational data vector were perturbed (i.e., MG data, Bondarenko factors for BONAMI, and CE data for CENTRM/PMC) as described in Section 2. Perturbation factors were generated by XSUSA based on a multivariate normal distribution with the covariance data given in the SCALE covariance library. MG capture, fission, chi, nubar, elastic, and inelastic reaction data for ^{238}U, ^{235}U, H, and ^{16}O were varied. Three hundred random samples were taken for this example; i.e., 300 CSAS25 sequences were executed using the randomly perturbed nuclear data samples.

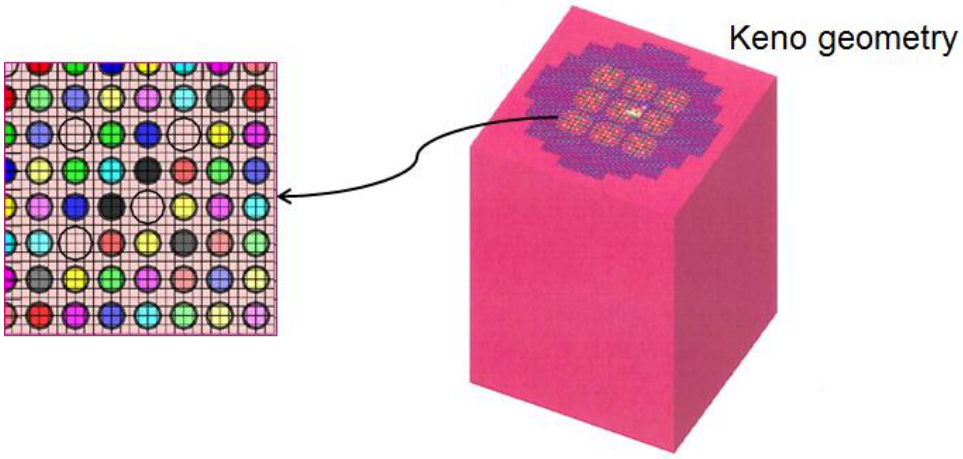

Figure 3. Critical benchmark description:
A 3 × 3 array of PWR fuel assemblies consisting of 15 × 15 array of pins.

Figure 4 illustrates the distribution of computed eigenvalues for this case. Table I shows a comparison of means and variances obtained using conventional perturbation methods in TSUNAMI and with the statistical sampling method. The agreement between uncertainties computed with the two approaches is very good.

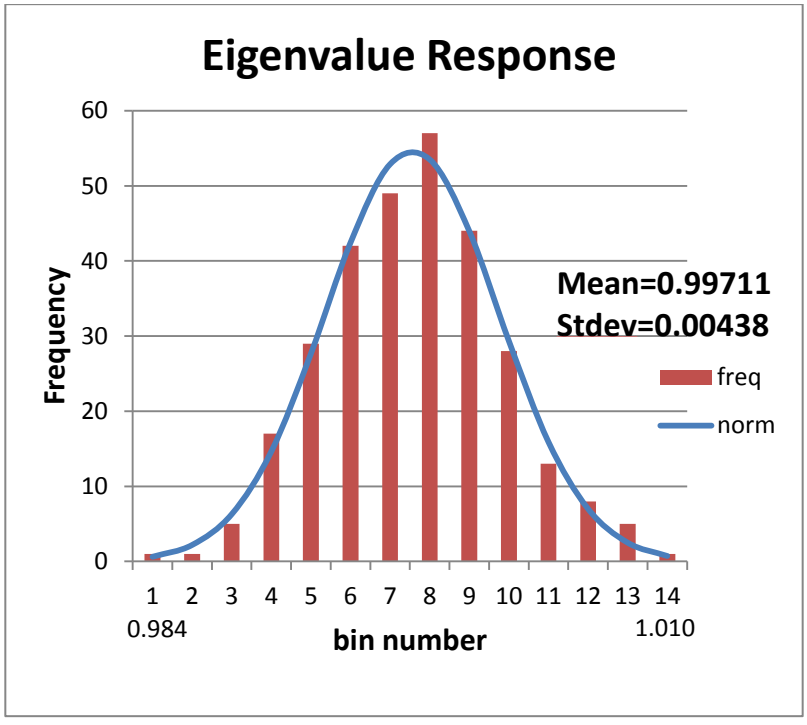

Figure 4. Distribution of computed eigenvalues from 300 random data samples.

Table1. Comparison of k_{eff} means and standard deviations obtained with statistical sampling and perturbation theory

Method	Reference	Mean value	Uncertainty from XS data (%)
XSUSA/MG-Keno (statistical sampling)[a]	0.9966 ± 0.0008	0.9971	0.44
TSUNAMI MG-Keno (perturbation theory)	0.9966 ± 0.0008	0.9966	0.46

[a]XSUSA results based on 300 random samples.

Figure 5 shows the pin power uncertainties computed with the statistical sampling approach based on two different self-shielding methods. The first uses Bondarenko self-shielding with the BONAMI code, and the second uses the CENTRM computed pointwise energy spectrum. The two approaches produce similar uncertainties. To obtain similar results using TSUNAMI, separate generalized adjoint calculations would have to be performed for each pin; however, the sampling method produces all pin uncertainties from the same set of results used for the eigenvalue uncertainty.

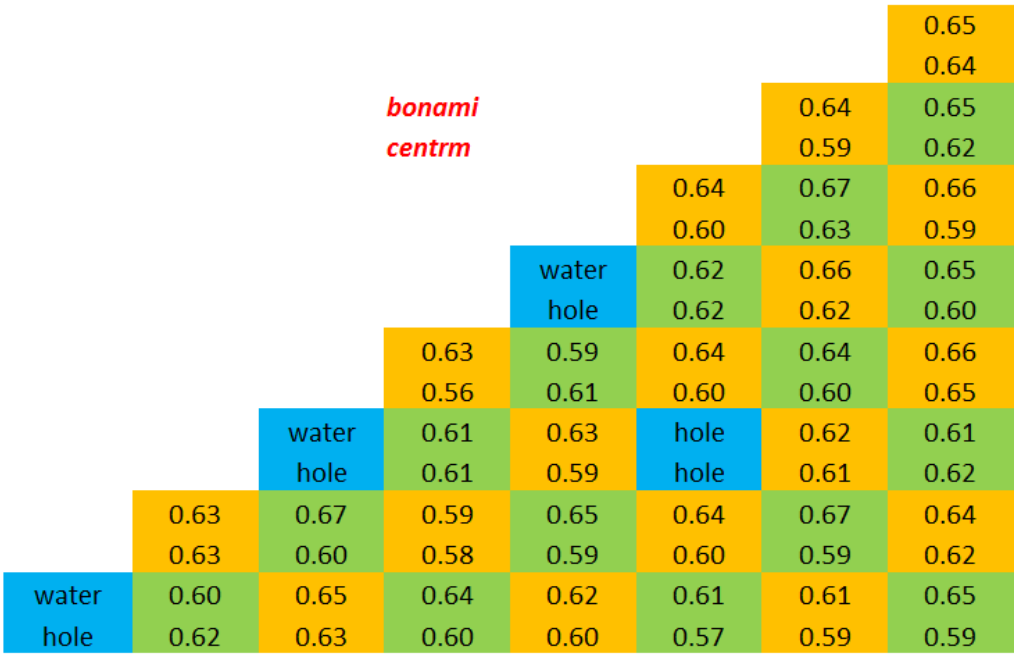

Figure 5. Uncertainties (% standard deviation) in computed pin powers, using BONAMI and CENTRM, respectively, for self-shielding.

5. SUMMARY

A new "super-sequence" called *Sampler* has been developed to perform uncertainty analysis for any SCALE sequence by statistical sampling of the input nuclear data. The random sampling is done by XSUSA using nuclear data probability distributions associated with covariances obtained from the SCALE library. Data variations for multiple samples are stored on a pregenerated perturbation factor library for subsequent use in Sampler. Sampler executes a specified SCALE sequence for the desired number of samples; and the output distribution of results from the SCALE sequence runs can be converted into standard deviations and correlation coefficients for any desired responses computed in the sequence.

The statistical sampling method was applied to a CSAS25 computation sequence (resonance self-shielding + KENO transport solver) for a critical experiment. Uncertainties in the computed eigenvalues and power distribution were determined from 300 random samples. The TSUNAMI-3D sequence was also executed to compute the eigenvalue uncertainty using conventional perturbation theory. The eigenvalue uncertainty obtained with statistical sampling and with perturbation theory agreed well.

Several future improvements are recommended for the Sampler sequence. They include more advanced postprocessing methods and the capability of performing SCALE sequence computations in parallel for multiple samples on several CPUs.

ACKNOWLEDGEMENT: This work was sponsored by the U. S. Nuclear Regulatory Commission Office of Research and the German Federal Ministry of Economics and Technology.

REFERENCES

1. *SCALE: A Modular Code System for Performing Standardized Computer Analyses for Licensing Evaluation*, Version 6, Vols. I–III, ORNL-TM/2005/39, Oak Ridge National Laboratory, Oak Ridge, Tenn. (2009) (Available from Radiation Safety Information Computational Center at Oak Ridge National Laboratory as CCC-750.)
2. M. L. Williams, "Perturbation Theory for Reactor Analysis," *CRC Handbook of Nuclear Reactors Calculations*, Vol. 3, pp. 63–188, CRC Press (1986).
3. M. L. Williams and B. T. Rearden, "Sensitivity/Uncertainty Analysis Capabilities and New Covariance Data Libraries in SCALE," *Nuclear Data Sheets* 109, **12**, 2796–2800 (December 2008).
4. B. Krzykacz, E. Hofer, M. Kloos, "A Software System for Probabilistic Uncertainty and Sensitivity Analysis of Results from Computer Models*," Proc. International Conference on Probabilistic Safety Assessment and Management (PSAM-II)*, San Diego, Calif., USA (1994).
5. W. Zwermann, L. Gallner, M. Klein, B. Krzykacz-Hausmann, A. Pautz, D. Wiarda, M. L. Williams, M. A. Jessee, and B. T. Rearden, "Nuclear Data Uncertainty Analysis For a Fuel Assembly Criticality Benchmark," ICNC 2011 Conference, Edinburgh, U.K, September 19–22, 2011.

6. *International Handbook of Evaluated Criticality Safety Benchmark Experiments*, NEA/NSC/DOC(95) 03/I, Nuclear Energy Agency, Paris (September 2008).
7. M. Klein, L. Gallner, B. Krzykacz-Hausmann, A. Pautz, W. Zwermann, "Influence of Nuclear Data Uncertainties on Reactor Core Calculations", Kerntechnik, 2011/03, 174-178 (2011).

PHYSOR 2012 – Advances in Reactor Physics – Linking Research, Industry, and Education
Knoxville, Tennessee, USA, April 15-20, 2012, on CD-ROM, American Nuclear Society, LaGrange Park, IL (2010)

Anhang B5

ALEATORIC AND EPISTEMIC UNCERTAINTIES IN SAMPLING BASED NUCLEAR DATA UNCERTAINTY AND SENSITIVITY ANALYSES

W. Zwermann, B. Krzykacz-Hausmann, L. Gallner, M. Klein, A. Pautz, K. Velkov
Gesellschaft fuer Anlagen- und Reaktorsicherheit (GRS) mbH
Forschungszentrum, Boltzmannstrasse 14, 85748 Garching, Germany
Winfried.Zwermann@grs.de, Bernard.Krzykacz-Hausmann@grs.de, Lucia.Gallner@grs.de,
Markus.Klein@grs.de, Andreas.Pautz@grs.de, Kiril.Velkov@grs.de

ABSTRACT

Sampling based uncertainty and sensitivity analyses due to epistemic input uncertainties, i.e. to an incomplete knowledge of uncertain input parameters, can be performed with arbitrary application programs to solve the physical problem under consideration. For the description of steady-state particle transport, direct simulations of the microscopic processes with Monte Carlo codes are often used. This introduces an additional source of uncertainty, the aleatoric sampling uncertainty, which is due to the randomness of the simulation process performed by sampling, and which adds to the total combined output sampling uncertainty. So far, this aleatoric part of uncertainty is minimized by running a sufficiently large number of Monte Carlo histories for each sample calculation, thus making its impact negligible as compared to the impact from sampling the epistemic uncertainties. Obviously, this process may cause high computational costs. The present paper shows that in many applications reliable epistemic uncertainty results can also be obtained with substantially lower computational effort by performing and analyzing two appropriately generated series of samples with much smaller number of Monte Carlo histories each. The method is applied along with the nuclear data uncertainty and sensitivity code package XSUSA in combination with the Monte Carlo transport code KENO-Va to various critical assemblies and a full scale reactor calculation. It is shown that the proposed method yields output uncertainties and sensitivities equivalent to the traditional approach, with a high reduction of computing time by factors of the magnitude of 100.

Key Words: Aleatoric and epistemic uncertainties, nuclear data, nuclear covariance data, Monte Carlo transport, XSUSA.

1. INTRODUCTION

Evaluated nuclear data are continuously being improved. During the last years, the European library was updated from JEF-2.2 to JEFF-3.1 [1] and further to JEFF-3.1.1 [2], the American library from ENDF/B-VI to ENDF/B VII.0 [3] and ENDF/B VII.1 [4], and the Japanese library from JENDL-3.2 to JENDL-3.3/AC-2008 [5] and JENDL-4.0 [6]. These library improvements are performed on the basis of the newest evaluations of differential experiments; validation is mainly done by comparing the results of Monte Carlo calculations with a large number of critical experiments covering a wide variety of fuel, moderator, and structure materials in different spectral conditions. However, the precision of evaluated nuclear data is limited by the uncertainties of the underlying measurements and theoretical parameters. Estimated values for these uncertainties are stored in the so-called covariance files accompanying the evaluated nuclear data files. Along

with updates of the nuclear data, current research aims at improved evaluations and augmentation of the covariance files.

Accordingly, growing attention is being paid to uncertainty and sensitivity studies concerning the nuclear data evaluations with respect to the results of neutron transport calculations. So far, most uncertainty investigations with nuclear covariance data, as performed, e.g., with TSUNAMI [7] or SUSD3D [8], are based on first order perturbation theory, and primarily consider the multiplication factors and other integral quantities. In the current version SCALE 6.1, TSUNAMI now also provides generalized perturbation theory capabilities [9] to compute sensitivities and uncertainties for reactor responses such as reaction rate and flux ratios as well as homogenized few-group cross sections. With increasing computer power, sampling based methods, as implemented, e.g., in MCNP-ACAB [10], NUDUNA [11], TMC [12], and XSUSA [13], have become more and more feasible. Within these approaches, the transport calculations are repeated many times with sampled nuclear data, and the results are statistically analyzed, leading to quantification of uncertainties of arbitrary output quantities, and, to a certain degree, to quantification of sensitivities with respect to the uncertain input parameters.

So far, sampling based approaches have been applied with deterministic and Monte Carlo transport solvers. When using a Monte Carlo code for the direct simulation of the neutron transport, an additional source of sampling uncertainty is introduced which results from the finite number of neutron histories sampled in the course of the Monte Carlo simulation ("aleatoric uncertainty"). This adds to the uncertainty due to the incomplete knowledge of the nuclear data ("epistemic uncertainty"). Therefore, if a Monte Carlo code is applied to solve the transport problem, normally a sufficiently large number of neutron histories are used for each nuclear data sample, such that the aleatoric sampling uncertainty becomes negligibly small, and the observed output sampling uncertainty can be attributed to the epistemic nuclear data sampling uncertainty alone. This means that for each of the calculations with sampled nuclear data, the same high number of neutron histories as for the reference calculation is used. Obviously, the computational costs of this procedure may be immense when dealing with large sample sizes.

In the present contribution, a method is proposed to perform the uncertainty analyses with strongly decreased numbers of Monte Carlo histories per calculation, and, nevertheless, without losing substantial information when determining the output uncertainties, thereby reducing the necessary computing times drastically. This method is applied along with the uncertainty and sensitivity analysis code XSUSA ("Cross Section Uncertainty and Sensitivity Analysis") and KENO-Va as Monte Carlo transport solver to a variety of critical assemblies and a full scale reactor configuration. The results are then compared to corresponding results obtained with the "traditional" method with the same high numbers of neutron histories for each nuclear data sample as for the reference calculation.

2. SEPARATION OF ALEATORIC AND EPISTEMIC UNCERTAINTIES

Uncertainty and sensitivity analyses are performed to determine the uncertainties in the output quantities of a calculation describing a physical problem. Output uncertainties result from epistemic input uncertainties. These are due to the incompleteness of the knowledge about the input parameters, e.g. from measurement uncertainties, manufacturing tolerances, etc. As far as nuclear

data are concerned, the uncertainties mainly come from experimental errors and incomplete measurements, as well as uncertainties in physical model parameters. When applying random sampling methods for the uncertainty analysis, as implemented e.g. in the GRS SUSA code package [14], normally deterministic codes are used for solving the physical problem. For steady-state neutron transport in complex geometrical arrangements, however, Monte Carlo codes are best suited to describe the problem by a direct simulation of the microscopic processes, because practically no simplifications of the geometry are necessary. The application of the Monte Carlo method as transport solver, however, introduces an additional kind of uncertainty to the calculation results, which results from the randomness of the calculation procedure performed by the Monte Carlo sampling process ("aleatoric uncertainty"). In "well-behaved" situations, this aleatoric sampling output uncertainty can be reduced or even eliminated by increasing the number of sampled neutron histories in the calculation. In Monte Carlo reference calculations, i.e. without taking epistemic input uncertainties into account, the number of neutron histories is chosen such that the resulting aleatoric uncertainty of the output quantity under consideration, mostly expressed by variance or standard deviation, is below a desired value. When conducting sampling based uncertainty analyses, the complete batch of calculations is usually performed with the same high number of neutron histories in each of the calculation runs. Further effort to separate aleatoric and epistemic sampling uncertainties is unnecessary such that the usual one-dimensional sample based epistemic uncertainty analysis can be performed.

The method presented here shows that for many application cases it is not necessary to perform the full series of runs with such a high accuracy. In fact, it is possible to obtain reliable epistemic uncertainty results with substantially reduced number of neutron histories in each run, such that e.g. the total number of neutron histories for the whole series of all calculations is in the same order of magnitude as for the single high accuracy reference calculation run.

The method works as follows:

Generate two series of calculations.
1st series = the usual two-dimensional aleatoric/epistemic nested sampling with
- Outer (epistemic) loop: nuclear data sample of size N_e,
- Inner (aleatoric) loop: Monte Carlo transport sampling with reduced sample size N_a

2nd series = another two-dimensional aleatoric/epistemic nested sampling with
- Outer (epistemic) loop: the same N_e sample values of nuclear data as in the 1st series
- Inner (aleatoric) loop: new Monte Carlo transport sampling with the same reduced sample size N_a independent of the 1st series.

Thus, for each output quantity of interest the two series of calculations provide two samples of values of size N_e each, or, in other words, a two-dimensional sample of size N_e.

Finally compute the sample covariance of this two-dimensional sample. This sample covariance is the result of principal interest in epistemic uncertainty since it can be considered as the variance of the distribution quantifying the epistemic part of sampling uncertainty alone after having eliminated the effect of aleatoric sampling uncertainty.
The accuracy of the results of this method depends inversely on the relative contribution of the aleatoric sampling uncertainty. It will therefore increase if the aleatoric sample size N_a, i.e. the

number of neutron histories in the Monte Carlo runs will increase. On the other hand, obviously, the accuracy will also increase by increasing the epistemic sample size N_e.

The mathematical basis of this method is the following result about conditional expectations: If two output variables Y and Y' are identically distributed and conditionally independent given the vector of (epistemic) input variables **U**, then their covariance cov(Y,Y') is equal to the variance of the conditional expectation E[Y|**U**] of Y given **U,** i.e. cov(Y,Y') = var(E[Y|**U**]) [15]. In the present context **U** stands for the vector of all epistemic variables representing uncertainties in nuclear data, Y and Y' stand for the output variables corresponding to the two cases considered as functions of the epistemic and aleatoric variables with the reduced aleatoric sample size. The above sampling scheme ensures the assumption that Y and Y' are identically distributed and conditionally independent given **U**. The conditional expectation E[Y|**U**] stands for the epistemic part of the output variable Y from which the aleatoric sampling uncertainty has been eliminated, i.e. averaged out. The result of principal interest is therefore its variance var(E[Y|**U**]) which quantifies the epistemic uncertainty alone separated from the total combined uncertainty from both sources.

It will be demonstrated in the next section that for determining the multiplication factor uncertainties in critical assembly calculations, very small neutron history sample sizes N_a are normally sufficient. It has to be kept in mind that when using extremely small numbers of neutron histories in the Monte Carlo criticality calculations, the results can be falsified by bias and source convergence issues [16]. Therefore one should make sure that averaging over a long series of short Monte Carlo calculations, i.e. with small number of neutron histories without epistemic uncertainties, yields a result compatible with a single reference run obtained with large number of neutron histories. Thus the uncertainty results obtained from the two series of short runs can reasonably be compared with the results from a single series of long runs.

As an example, the performance gain is estimated with some typical values: The reference calculation is performed with N_a=50,000,000 neutron histories. For determining the epistemic uncertainties by the above method, N_e=1,000 nuclear data sample values are used along with the reduced number N_a^*=50,000 of neutron histories per run. One additional series of N_e=1,000 calculations without epistemic uncertainties is also performed for the convergence check of averaging. This finally means that the total number of sampled neutron histories within the entire exercise corresponds to the full number of histories of four long runs, only, i.e. a reduction of computing time by a factor of 250 if compared with 1000 runs with full number of neutron histories (in reality, for the XSUSA/KENO calculations it is a factor of perhaps 100 due to the overhead caused by handling the nuclear data).

3. RESULTS FOR CRITICAL ASSEMBLIES

The method described above is applied for determining multiplication factor uncertainties and sensitivities of various critical assemblies. To cover a wide range of spectral conditions, two Uranium and two Plutonium systems are chosen, with fast as well as thermal spectra. Three of them are described in the International Handbook of Evaluated Criticality Safety Benchmark Experiments [17]: The bare metallic Uranium sphere GODIVA (in the nomenclature of the Handbook HEU-MET-FAST-001), the bare metallic Plutonium sphere ^{239}Pu JEZEBEL (PU-MET-FAST-

001), and one of the P-11 series of bare spheres of Plutonium nitrate solutions (PU-SOL-THERM-011, Case 16-1). KRITZ-2:13 is a light water moderated quadratic array of Uranium fuel pins, described in the International Handbook of Evaluated Reactor Physics Benchmark Experiments [18] as KRITZ-LWR-RESR-003. The XSUSA analyses are performed with KENO-Va from the SCALE 6 code system [19] as Monte Carlo transport solver, with the 238 group ENDF/B-VII neutron cross section library and covariance data included in the SCALE 6 package; the covariance data are from a variety of sources, including high-fidelity evaluations from ENDF/B-VII, ENDF/B-VI, and JENDL-3.3, as well approximate uncertainties obtained from a collaborative project performed by Brookhaven National Laboratory, Los Alamos National Laboratory, and Oak Ridge National Laboratory [20].

Table I. Multiplication factors obtained from KENO-Va for various critical assemblies. Results from one run with a large number of neutron histories and from mean of 1,000 runs with a small number of neutron histories per run.

	GODIVA	JEZEBEL	KRITZ-2:13	P-11, 16-1
(1) Reference long run	0.99989	0.99988	0.99644	1.01040
95% conf. int. of reference	0.00024	0.00026	0.00007	0.00030
(2) Mean of 1,000 short runs	0.99960	0.99992	0.99633	1.01013
95% conf. int. of mean	0.00025	0.00028	0.00008	0.00029
Rel. deviation (2) vs. (1)	-0.029%	0.004%	-0.011%	-0.027%

The reference calculations for GODIVA, JEZEBEL, and the P-11 case are performed with 50,000,000, for KRITZ-2:13 with 400,000,000 active neutron histories. These numbers of histories are also used for determining output uncertainties and sensitivities with negligible aleatoric uncertainties (“long runs”), while for applying the above method to eliminate the aleatoric contributions from the total uncertainty, only 50,000 or 400,000 active neutron histories are considered.

First, it has to be shown that using such small numbers of histories does not lead to biased results. This is done in Table I, where the multiplication factor averages from 1,000 short runs (with 50,000 or 400,000 active neutron histories) are compared with the reference result from a single long run. It can be seen that the differences are sufficiently small, and furthermore that the 95% confidence intervals from the short runs and that given in the long KENO calculation are very similar. Therefore there is no indication in any of the calculation cases that problems might arise by choosing overly small numbers of histories.

After these checks, the actual uncertainty and sensitivity analyses are performed. The results for the output uncertainties are given in Table II. The reference values for the epistemic output uncertainties are those obtained from 1,000 long KENO runs, where there is practically no contri-

bution from the aleatoric sampling uncertainty. When the corresponding calculations are performed with 1,000 short runs, the determined uncertainties are clearly higher, by 4 – 6%. The obvious reason is the influence of a substantial aleatoric sampling uncertainty on the total output uncertainty. After having performed the 2nd series of 1,000 short runs with the same nuclear data samples but new neutron history samples, the covariance between the two series has been computed to eliminate the impact of aleatoric uncertainty, as described in section 2. Now, the resulting output uncertainties have practically the same values as from the 1,000 long runs, with a maximum relative difference of 1.3% for the KRITZ-2:13 assembly, being well inside the 95% confidence interval of the standard deviation, which is approximately +/–4% relatively to the value of the standard deviation. For the GODIVA, JEZEBEL, and P-11 calculations, the aleatoric uncertainties in the short KENO runs are given as 0.3 – 0.8%, in the KRITZ-2:13 calculations as 0.08 – 0.18%; in all cases, these values are smaller than the epistemic uncertainties.

Table II. Multiplication factors and corresponding uncertainties due to nuclear data covariances obtained from KENO-Va with sampled nuclear data. Reference result from a single long run, results from 1,000 runs with a large number of neutron histories per run, from 1,000 runs with a small number of neutron histories per run, and from 2 x 1,000 runs with a small number of neutron histories per run after elimination the aleatoric uncertainties.

	GODIVA	JEZEBEL	KRITZ-2:13	P-11, 16-1
Reference long run	0.99989	0.99988	0.99644	1.01040
Mean of 1,000 long runs	1.00043	0.99985	0.99645	1.01054
Epistemic uncertainty Δk/k (1σ) from 1,000 long runs	1.063%	1.418%	0.529%	1.506%
Mean of 1,000 short runs	0.99889	0.99901	0.99649	1.01055
Total combined uncertainty Δk/k (1σ) from 1,000 short runs	1.125%	1.474%	0.551%	1.586%
Epistemic uncertainty Δk/ k (1σ) from 2 x 1,000 short runs	1.056%	1.415%	0.536%	1.502%

In addition to the quantified output uncertainties, the corresponding sensitivities, i.e. the contributions to these uncertainties from individual nuclide/reaction combinations can be evaluated (sensitivity in the sense of uncertainty importance). To do this, the so-called "squared multiple correlation coefficient (R^2)" is used as sensitivity/uncertainty importance indicator for parameter groups. It can be interpreted as the relative amount of output uncertainty coming from the uncertainty of the respective parameter group. It is basically determined from correlations of the calculated output quantities with the sampled input quantities, i.e. with the sampled nuclear data, taking into account inter-dependencies of input quantities due to non-zero covariance terms [21]. It should be noted that these are not identical to contributions as given by TSUNAMI, and that even the ranking may be quite different due to correlations between different nuclide/reaction

groups. These sensitivities are displayed in Fig. 1 for the five most important parameter groups and for the four application cases, along with their 95% confidence intervals indicated by the error bars. (The contribution from ^{238}U n,γ capture, 92238-0102, should be disregarded because it is below the 95% significance bound).

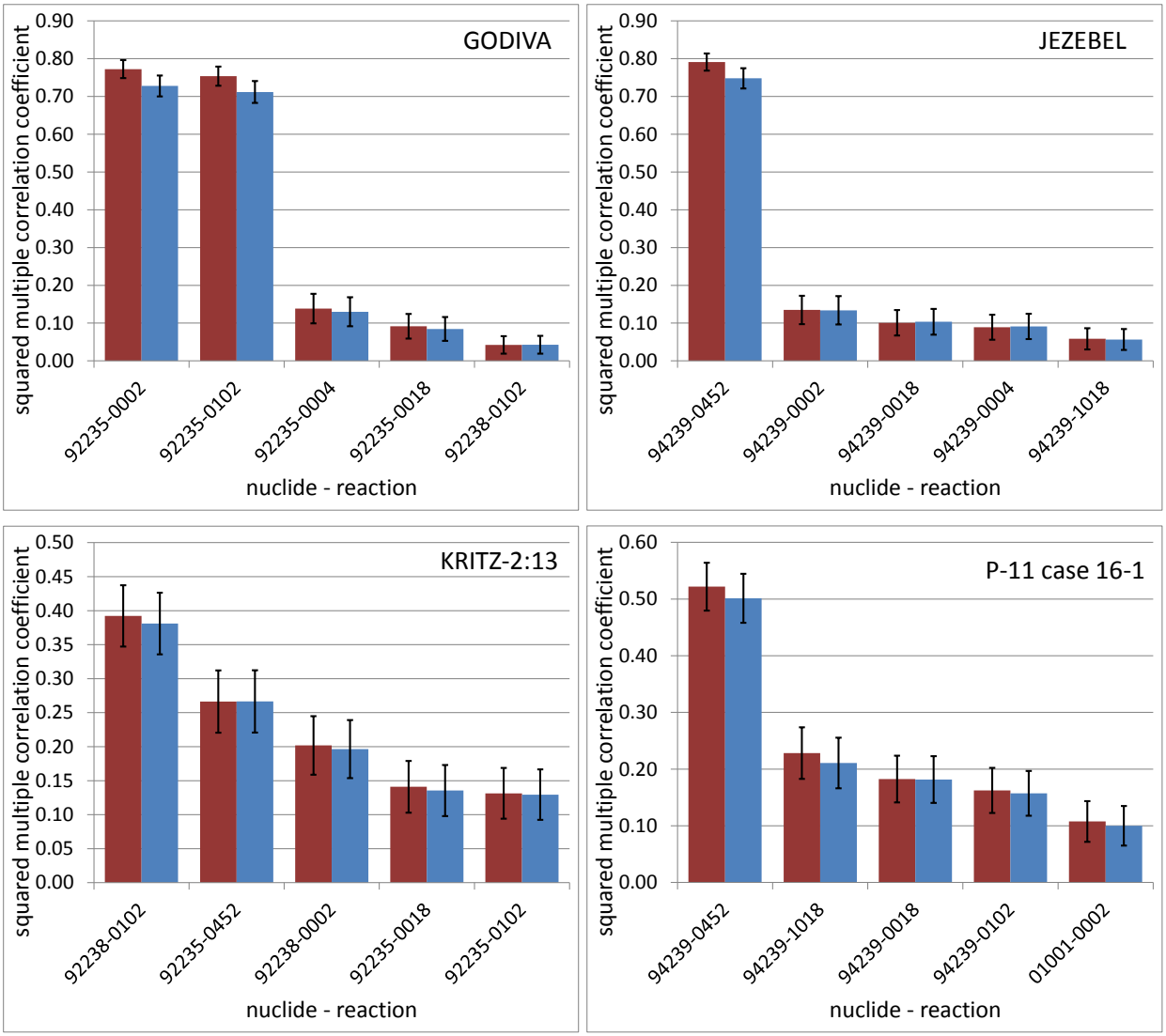

Figure 1. Sensitivity results: Squared multiple correlation coefficients (R^2) from XSUSA/KENO for k-eff of four critical assembly calculations. Red columns: 1,000 long runs; blue columns: 2x1,000 short runs. Reaction IDs: 2 = elastic scattering, 4 = inelastic scattering, 18 = fission, 102 = n,γ capture, 452 = nu-bar, 1018 = fission spectrum.

It can be seen that the sensitivity values determined from the short Monte Carlo runs are generally smaller than those from the long runs. Obviously, this is due to the presence of additional non-negligible aleatoric uncertainties, such that the relative contributions from the groups be-

come smaller. However, the importance ranking of the input quantities is the same from long and short runs, at least for the dominating parameter groups.

Taking KRITZ-2:13 as a typical example of a Monte Carlo critical assembly calculation, the following computing times are necessary (on a 2.53 GHz Intel Xeon CPU): One long KENO run takes approx. 4.5 hours, one short run approx. 40 seconds. Comparing the times for 1,000 long runs and for 3 x 100 short runs plus 1 long reference run, the gain in computational time applying the method described in this paper amounts to a factor of approx. 120. These are wall clock times, i.e. the overhead arising from the nuclear data handling is already taken into account.

The calculations were performed with a Monte Carlo code with multi-group nuclear data; it should be mentioned that this is no restriction, i.e. the described method can also be applied when using continuous energy data. Likewise, it is not restricted to nuclear data uncertainties at all; it can equally well be used for analyses with a Monte Carlo transport solver and epistemic uncertainties from other sources, like manufacturing tolerances considered with the SUnCISTT code [22].

4. RESULTS FOR A FULL CORE ARRANGEMENT

In the previous section, the method of eliminating the aleatoric uncertainties to determine epistemic uncertainties and sensitivities was applied to evaluating the epistemic uncertainty of the multiplication factors of critical assemblies. To demonstrate the possible computing time gain for other output observables, too, this method is applied to the calculation of the fuel assembly power distribution of a full core calculation benchmark [23]. The arrangement is a semi-realistic description of a mixed core with different MOX and UO_2 fuel assemblies in different burn-up states in 2-d representation. The same codes and data as for the critical assembly calculations are used, with the distinction that the 238 group master libraries were pre-collapsed to 44 groups (the same structure as that of the covariance matrices). The long KENO runs are performed with 1,000,000,000 active neutron histories; this large number was used to make sure that sufficiently well converged solutions for fission rate distribution are obtained. In fact, the Monte Carlo solution for a full scale LWR core arrangement may exhibit a rather slow convergence behaviour, and the real uncertainty of the reaction rate distribution can be much larger than the statistical uncertainty estimated in the Monte Carlo calculation [24]. For the short KENO runs, 2,000,000 active neutron histories are used.

Uncertainties and sensitivities are evaluated for the multiplication factor and the fuel assembly powers in a row of fuel assemblies along the x-axis of the core, denoted by p1 – p8. In Fig. 2, the calculated uncertainties are displayed. In this case, the k-eff uncertainties are practically identical, no matter whether a series of long or short runs is used. This is due to the fact that with 2,000,000 neutron histories in the short runs, the aleatoric uncertainty of approx. 0.04% is already negligible as compared to the epistemic uncertainty of approx. 0.5%. For the assembly power uncertainties, the situation is rather different. From one series of long runs, the evaluated total combined uncertainties are much larger than the epistemic uncertainties alone, determined from the series of long runs. However, by using two series of short runs with different Monte Carlo random numbers as described above, the determined uncertainties are in very good agreement with those from the series of long runs.

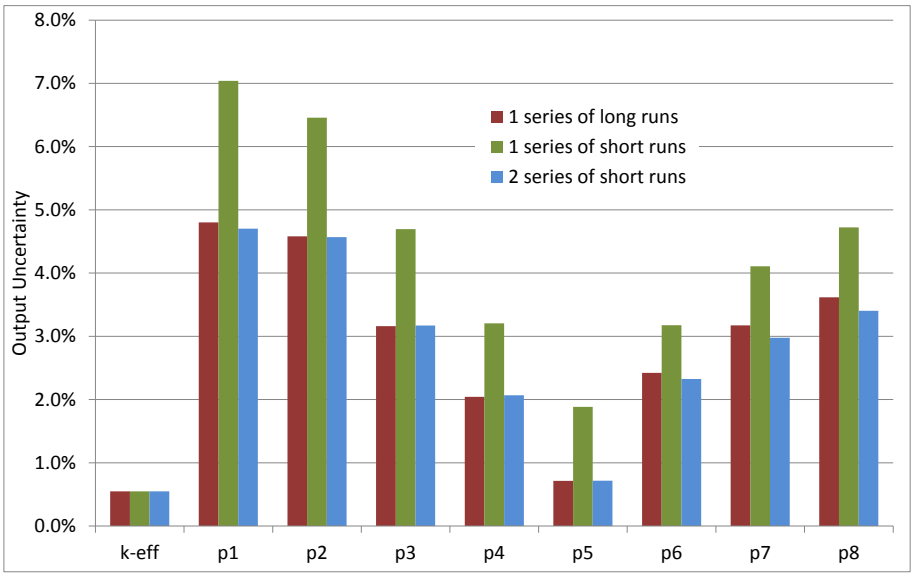

Figure 2. Uncertainties in k-eff and the powers in a row of fuel assemblies (p1 – p8) from full core calculations with XSUSA/KENO. Red columns: 1,000 long runs; green columns: 1,000 short runs; blue columns: 2x1,000 short runs.

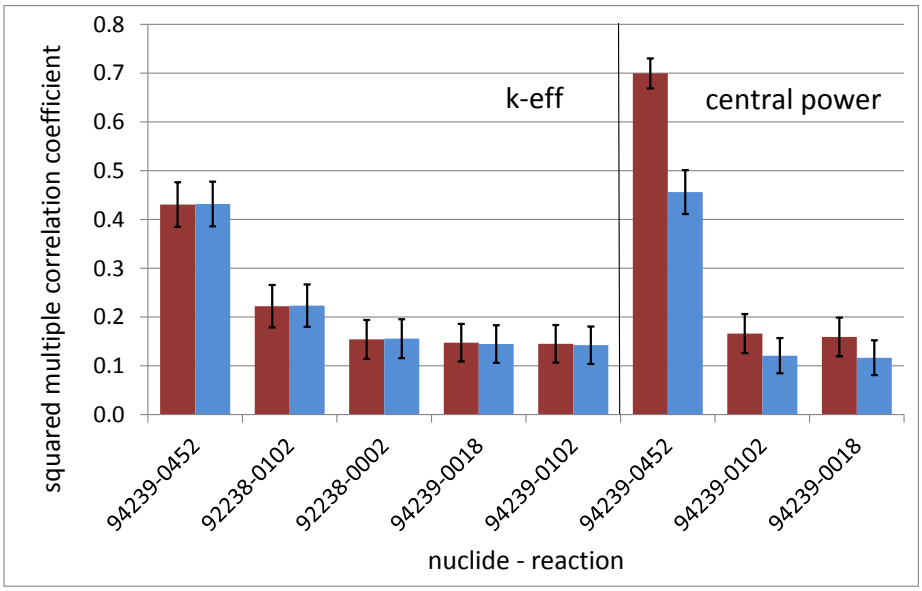

Figure 3. Sensitivity results: Squared multiple correlation coefficients (R^2) from XSUSA/KENO for k-eff and the central power of a full core calculation. Red columns: 1,000 long runs; blue columns: 2x1,000 short runs. Reaction IDs: Same as in Fig. 1.

Correspondingly, the values of sensitivity indices "squared multiple correlation coefficients (R^2)", displayed in Fig. 3 for the main contributions to the k-eff uncertainty are the same for the series of long and short runs; for the assembly powers, the values are significantly larger from the series of long runs than from the short runs, due to the substantial aleatoric uncertainties in

each individual short run. As mentioned before, they provide a similar importance ranking. Each of the long runs takes approx. 13 hours while for a short run approx. 3 minutes are needed, leading to a factor of approx. 80 between the two different approaches.

5. SUMMARY AND CONCLUSIONS

When performing sampling based uncertainty and sensitivity analyses for neutron transport problems with codes directly simulating the microscopic processes, i.e. with the Monte Carlo method, two kinds of uncertainties have to be considered: aleatoric uncertainties which arise from the randomness of the simulation procedure and the limited number of sampled particle histories, and epistemic uncertainties which arise from an incomplete knowledge of the values of input parameters. To determine the influence of the epistemic uncertainties alone, the sample calculations from epistemic sampling can traditionally be performed with a very large number of histories such that the aleatoric uncertainties become negligible and the entire sample output practically reflects only the influence of the epistemic uncertainties. It is clear that this procedure may be computer time consuming. In the present paper, a method was suggested which uses heavily reduced numbers of particle histories in each sample calculation, and, nevertheless, is able to eliminate the aleatoric uncertainty contribution introduced to the output. This is accomplished by evaluating the covariance between two calculation series, each of them performed with identical sampled values of the epistemic variables, but with different and independently generated aleatoric Monte Carlo neutron histories.

Applying this approach, sampling based uncertainty and sensitivity analyses with nuclear covariance data were performed with the XSUSA code and KENO-Va from the SCALE 6 system as Monte Carlo transport solver, for several critical assemblies (fast and thermal, with Uranium and Plutonium), and a full scale steady-state reactor application. Equivalent uncertainty and sensitivity results were obtained as compared to the traditional method of using very large numbers of histories in each sample calculation.

Thereby, computing times could be reduced by factors of the magnitude of 100. The use of multi-group nuclear data is no restriction, i.e. the described method can also be applied when using continuous energy nuclear data. The method can equally well be used for analyses with a Monte Carlo transport solver and epistemic uncertainties from other sources, like manufacturing tolerances. So far, the method was applied to stand-alone Monte Carlo criticality calculations; currently, investigations are being performed with calculations coupling Monte Carlo transport with depletion.

ACKNOWLEDGMENTS

This work is supported by the German Federal Ministry of Economics and Technology.

REFERENCES

1. A. Koning, R. Forrest, M. Kellett, R. Mills, H. Henriksson, and Y. Rugama, “The JEFF-3.1 Nuclear Data Library,” JEFF Report 21, NEA No. 6190 (2006).

2. A. Santamarina et al., "The JEFF-3.1.1 Nuclear Data Library," JEFF Report 22, NEA No. 6807 (2009).
3. M.B. Chadwick et al., "ENDF/B-VII.0: Next Generation Evaluated Nuclear Data Library for Nuclear Science and Technology", *Nuclear Data Sheets*, **107**, pp.2931–3118 (2006).
4. M. Herman, "Development of ENDF/B-VII.1 and Its Covariance Components", *Journal of the Korean Physical Society*, **59**, pp.1034–1039 (2011).
5. O. Iwamoto, T. Nakagawa, N. Otuka, S. Chiba, K. Okumura, and G. Chiba, "JENDL Actinoid File 2008 and Plan of Covariance Evaluation," *Nuclear Data Sheets*, **109**, pp.2885–2889 (2008).
6. K. Shibata et al., "JENDL-4.0: A New Library for Innovative Nuclear Energy Systems," *Journal of the Korean Physical Society*, **59**, pp.1046–1051 (2011).
7. B.T. Rearden and D.E. Mueller, "Uncertainty Quantification Techniques of SCALE/TSUNAMI", *Trans. Am. Nucl. Soc*., **104**, pp.371-373 (2011).
8. I. Kodeli, "The SUSD3D Code for Cross-Section Sensitivity and Uncertainty Analysis – Recent Development," *Trans. Am. Nucl. Soc*., **104**, pp.791-793 (2011).
9. M.A. Jessee, M.L. Williams, M.D. DeHart, "Development of Generalized Perturbation Theory Capability within the SCALE Code Package," *Proc. International Conference on Mathematics, Computational Methods & Reactor Physics (M&C 2009)*, Saratoga Springs, New York, USA, May 3–7, 2009, on CD-ROM (2009).
10. N. García-Herranz, O. Cabellos, J. Sanz, J. Juan, and J. C. Kuijper, "Propagation of Statistical and Nuclear Data Uncertainties in Monte Carlo Burnup Calculations," *Annals of Nucl. Energy*, **35**, pp.714-730 (2008).
11. O. Buss, A. Hoefer, and J.C. Neuber, "NUDUNA – Nuclear Data Uncertainty Analysis," *Proc. International Conference on Nuclear Criticality (ICNC 2011)*, Edinburgh, Scotland, Sep. 19-22, 2011, on CD-ROM (2011).
12. A. J. Koning and D. Rochman, "Towards Sustainable Nuclear Energy: Putting Nuclear Physics to Work," *Annals of Nucl. Energy*, **35**, pp.2024-2030 (2008).
13. W. Zwermann, B. Krzykacz-Hausmann, L. Gallner, A. Pautz, "Influence of Nuclear Covariance Data on Reactor Core Calculations," *Proc. Second International Workshop on Nuclear Data Evaluation for Reactor Applications (WONDER 2009)*, Cadarache, France, 29 Sep. - 2 Oct., 2009, pp.99-104 (2009).
14. B. Krzykacz, E. Hofer, M. Kloos, "A Software System for Probabilistic Uncertainty and Sensitivity Analysis of Results from Computer Models," *Proc. International Conference on Probabilistic Safety Assessment and Management (PSAM-II)*, San Diego, Ca., USA, (1994).
15. J. Peschke, B. Krzykacz-Hausmann, "Methodenentwicklung zur Durchführung von Unsicherheits- und Sensitivitätsanalysen im Rahmen einer probabilistischen Dynamikanalyse," Technical Report GRS-A-3556 (2010).
16. F. Brown, "A Review of Monte Carlo Criticality Calculations – Convergence, Bias, Statistics," *Proc. International Conference on Mathematics, Computational Methods & Reactor Physics (M&C 2009)*, Saratoga Springs, New York, USA, May 3–7, 2009, on CD-ROM (2009).
17. "International Handbook of Evaluated Criticality Safety Benchmark Experiments", September 2010 Edition, available on DVD-ROM, NEA/NSC/DOC(95)03.
18. "International Handbook of Evaluated Reactor Physics Benchmark Experiments", March 2010 Edition, available on DVD-ROM, NEA/NSC/DOC(2006)1.

19. "SCALE: A Modular Code System for Performing Standardized Computer Analyses for Licensing, Version 6," ORNL/TM-2005/39, (2009).
20. R. Little, T. Kawano, G. D. Hale, M. T. Pigni, M. Herman, P. Obložinský, M. L. Williams, M. E. Dunn, G. Arbanas, D. Wiarda, R. D. McKnight, J. N. McKamy and J. R. Felty, "Low-fidelity Covariance Project," *Nuclear Data Sheets* **109**, pp.2828–2833, (2008).
21. H. Glaeser, B. Krzykacz-Hausmann, W. Luther, S. Schwarz, T. Skorek, "Methodenentwicklung und exemplarische Anwendungen zur Bestimmung der Aussagesicherheit von Rechenprogrammergebnissen," Technical Report GRS-A-3443 (2008).
22. M. Kirsch, V. Hannstein, and R. Kilger, "Applications of the SUnCISTT: Monte Carlo Sampling on Uncertain Technical Parameters in Criticality and Burn-Up Calculations," *Proc. International Conference on Nuclear Criticality (ICNC 2011)*, Edinburgh, Scotland, Sep. 19-22, 2011, on CD-ROM (2011).
23. T. Kozlowski, and T. J. Downar, "The PWR MOX/UO_2 Core Transient Benchmark, Final Report", NEA/NSC/DOC(2006) 20.
24. S. Langenbuch, A. Pautz, W. Zwermann, W. Bernnat, and M. Mattes, "Influence of Nuclear Data Evaluations on Full Scale Reactor Core Calculations," *Proc. International Conference on Mathematics, Computational Methods & Reactor Physics (M&C 2009)*, Saratoga Springs, New York, USA, May 3–7, 2009, on CD-ROM (2009).

PHYSOR 2012 – Advances in Reactor Physics – Linking Research, Industry, and Education
Knoxville, Tennessee, USA, April 15-20, 2012, on CD-ROM, American Nuclear Society, LaGrange Park, IL (2012)

Anhang B6

NUCLEAR DATA UNCERTAINTIES BY THE PWR MOX/UO2 CORE ROD EJECTION BENCHMARK

I. Pasichnyk, M. Klein, K. Velkov, W. Zwermann, A. Pautz
Gesellschaft für Anlagen- und Reaktorsicherheit (GRS) mbH
Boltzmannstr. 14, D-85748 Garching b. München, GERMANY
{Ihor.Pasichnyk, Markus.Klein, Kiril.Velkov, Winfried.Zwermann, Andreas.Pautz}@grs.de

ABSTRACT

Rod ejection transient of the OECD/NEA and U.S. NRC PWR MOX/UO2 core benchmark is considered under the influence of nuclear data uncertainties. Using the GRS uncertainty and sensitivity software package XSUSA the propagation of the uncertainties in nuclear data up to the transient calculations are considered. A statistically representative set of transient calculations is analyzed and both integral as well as local output quantities are compared with the benchmark results of different participants. It is shown that the uncertainties in nuclear data play a crucial role in the interpretation of the results of the simulation.

Key Words: rod ejection, uncertainty analysis, XSUSA, nuclear data, ATHLET, QUABOX/CUBBOX

1. INTRODUCTION

According to the current practice of nuclear power plant (NPP) design and safety analysis conservative assumptions and models are required to confirm the fulfilling of the acceptance criteria. Last years a new trend is to be observed – replacement of the conservative analyses with best-estimate calculations in combination of performing of uncertainty and sensitivity analysis (BEPU).The best estimate analysis require for a big class of transients and safety analyses the application of coupled neutronics/thermal-hydraulics codes. An aim of the recently defined OECD Benchmark for Uncertainty Analysis in Modeling (UAM) is to investigate the confidence bounds of the results from simulations and analysis in real applications [1]. One of the proposed reference scenarios for the UAM benchmark is the reactivity initiated accident (RIA) in a pressurized water reactor (PWR).

In Ref. [2] the impact of the nuclear data covariance on reactor core calculations was already considered. The XSUSA method [2], developed in GRS, is applied to steady state analysis of the PWR MOX/UO2 core transient benchmark [3] without taking into account the thermo-hydraulic feedbacks. The XSUSA method is quite universal and well suited for performing full core analysis. In contrast to other state of the art methods, based on the usage of direct and adjoint fluxes in the framework of the generalized perturbation theory [4-6],, with XSUSA uncertainties can be directly propagated through the complete calculation chain.

In the paper the XSUSA method is applied to analyze the rod ejection transient with the coupled system code ATHLET-QUABOX/CUBBOX (A-Q/C) [7]. In Section 2 of the paper, the steady state core with thermo-hydraulic feedbacks is considered, which corresponds to the Part 3 of the

benchmark. In Section 3, where the main results of the paper are discussed, the rod ejection transient with defined boundary conditions from Part 4 of the benchmark is analyzed.

2. HOT ZERO POWER (HZP) ANALYSIS

In the Part 3 of the benchmark the critical boron concentration and the 3D assembly power distribution are required to be calculated. To perform this simulation the GRS coupled system code A-Q/C is used for which the neutronic and thermo-hydraulic parameters are specified as defined in the Benchmark.

2.1. Neutronics model

The neutronics model is a full 3D core layout of 193 fuel assemblies. The core is designed with mixed MOX/UO2 fuel assemblies with different burnup. The quarter of the core load scheme is shown on Figure 1. The core is radially surrounded by a baffle and a reflector. Upper and bottom reflectors are considered also; the spacer effects are neglected. The active core zone is subdivided into 23 axial zones. The fuel and moderator temperature distributions are calculated by ATHLET taking into account the specified initial and boundary conditions

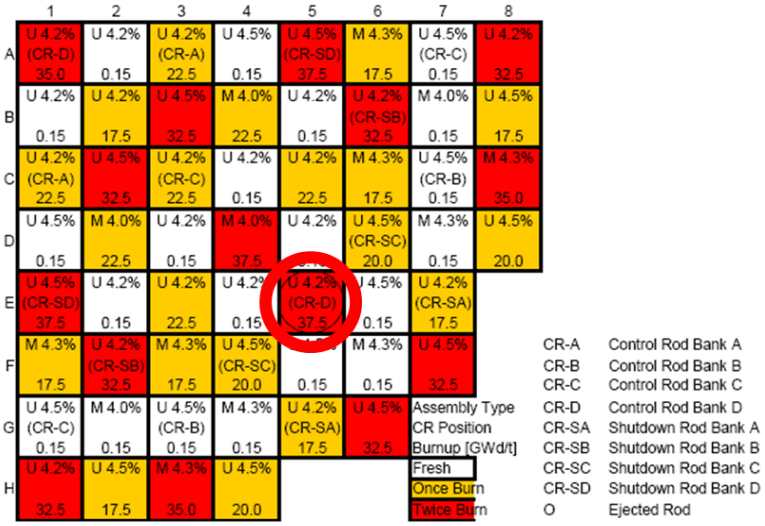

Figure 1 Core configuration (1/4 core) of PWR-MOX/UO2 benchmark. Red circle – ejected rod position

2.2. A set of N = 100 complete two-group cross section libraries (XS) is generated using the XSUSA platform and the spectral code NEWT from SCALE-6 [8]. The generated XS-libraries have the following simplified table structure: two parametric points for fuel temperature (560°K and 900°K), three - for moderator density (661.14 kg/m^3, 711.87 kg/m^3 and 752.00 kg/m^3) and two - for boron concentration (1000 ppm and 2000 ppm).

By calculating each parametric point of each library form the set (fuel assembly type, fuel temperature, moderator density and boron concentration) the same set of random numbers is used. Hence the correlations are naturally preserved and are implicitly contained in the output data. The obtained varied cross-section libraries are then saved [2]. By the simulations with the A-Q/C a linear interpolation algorithm of parametric values in the XS libraries is used. Thermal hydraulics model

Each fuel assembly is treated in ATHLET system code as a single thermo-hydraulic (TH) channel. The whole core is represented by 193 parallel TH channels and all reflector assemblies are lumped in one TH channel. No cross-flows are assumed between the TH-channels. Thermal properties for UOX and MOX are taken from the benchmark specification. The TH boundary inlet conditions for each one of the TH channel are taken to be the same. Each TH-channel has its own time-dependent volume. A converged steady state condition is considered after 10 s of zero transient performed with ATHLET code.

2.3. Results

Figure 2 shows the histogram of critical boron concentration from all performed variation runs. The mean value denotes 1296 ppm and the standard deviation is 88 ppm which is 7% of the mean value.

The mean value of the critical boron concentration calculated by all benchmark participants is 1329 ppm and the difference between the highest and the lowest critical boron concentration denotes 86 ppm. Our simulated variation results are in a good correspondence with the results of other benchmark participants. Moreover there is a good agreement between the critical boron concentrations distribution and the fitted normal distribution.

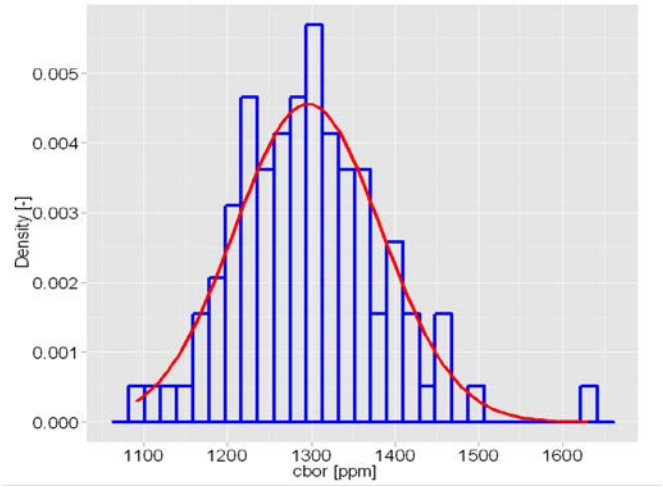

Figure 2 Histogram of critical boron concentrations. Red curve - fitted density of normal distribution

The relative axial power distribution is shown on Figure 3. Again the results of benchmark participants and the simulated variation results are in a good agreement.

The steady state relative assembly power is shown in Figure 4. The left plot compares the A-Q/C mean value with the radial power of DeCART calculation which is considered to be the reference solution of the benchmark. The right plot of Figure 4 shows the standard deviation of A-Q/C variation runs. The maximum deviation between the mean values of A-Q/C assembly power and DeCART assembly power values as well as the pattern of the radial power allow concluding that the initial state of all A-Q/C variation runs is in a good agreement with benchmark results; and the standard deviation of A-Q/C runs covers the difference between A-Q/C assembly power mean value and the benchmark reference value.

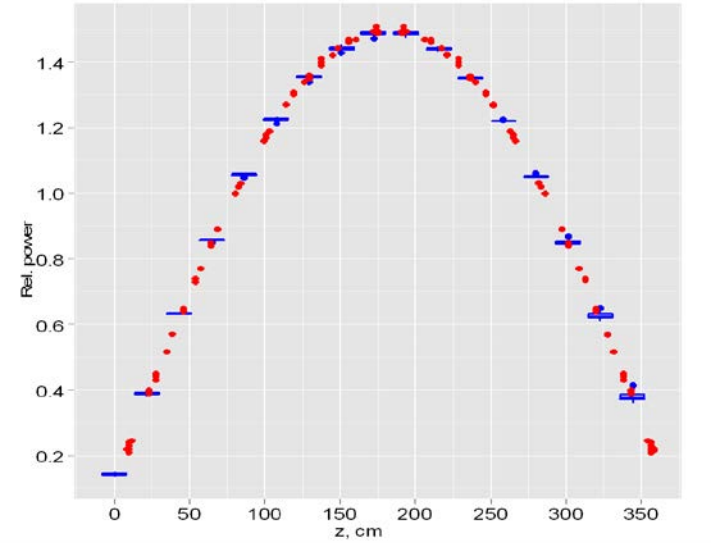

Figure 3 Relative axial power distribution for steady state. Blue bars - plot of nodal calculated values, red dots - benchmark participants' results

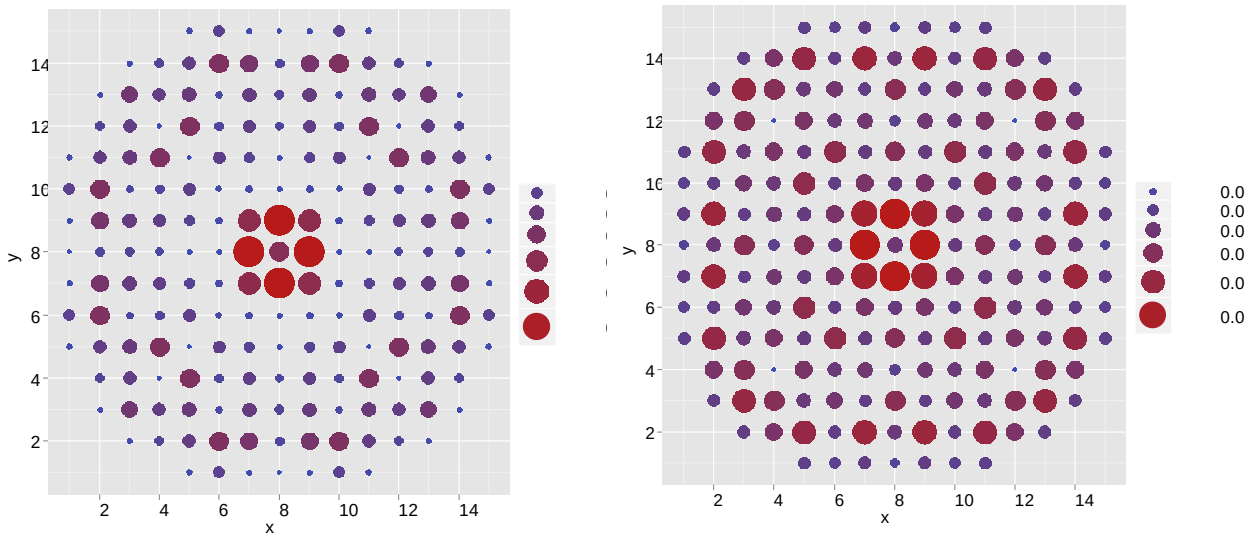

Figure 4 Relative radial assembly power. Left plot: difference between A-Q/C variation runs mean and benchmark reference DeCART; right plot: standard deviation of A-Q/C variation runs

3. TRANSIENT ANALYSIS

The Part 4 of the Benchmark defines the rod withdrawal at position (E, 5) (see Figure 1). The rod is assumed to be fully ejected in 0.1 sec from HZP conditions described in previous Section 2. Small break LOCA is not considered.

For each A-Q/C variation run the corresponding critical boron concentration is taken into account for further analysis. The integration time step by all runs is kept to be constant $\Delta t = 5.0 \cdot 10^{-5}\, s$. Calculations are performed on the Windows HPC Cluster with Intel Xeon 2.5GHz CPU's. The CPU time for each transient calculation with duration of 5 s (10 s for the zero transient should be considered also) is about 5 hours.

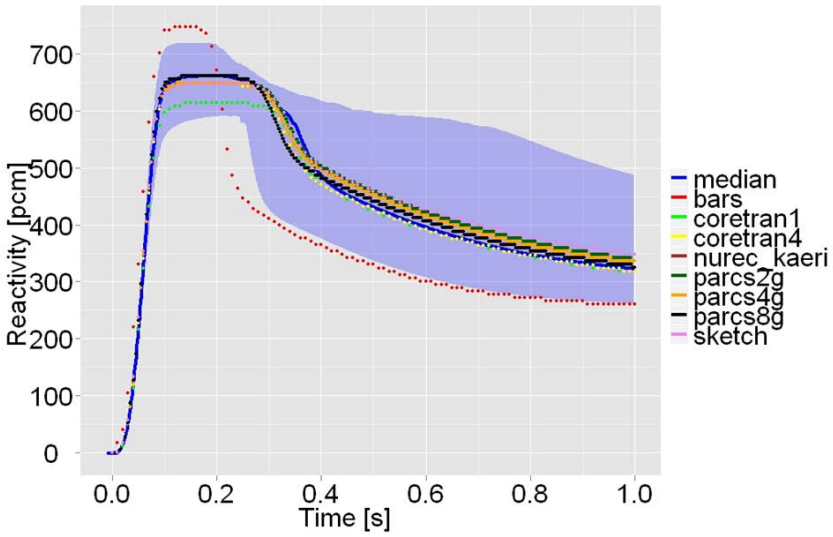

Figure 5 Reactivity evolution. The plot shows benchmark participants' results and the results of all runs with variated XS libraries. Blue ribbon – 95% quantile range; blue curve is the median of all A-Q/C runs

Figure 5 shows the reactivity histories of the rod ejection transient for all benchmark participants. All results with the exception of BARS are similar. The median of A-Q/C variation runs is in a good agreement with majority of benchmark results. The width of the 95%-quantile band at the plateau of the power peak time is approximately 140 pcm. 95%-quantile band goes in a direct vicinity of BARS result. As a matter of fact, all participants except the one that applied BARS code have used the same specified in the Benchmark XS-library. On the contrary, BARS-team [9] prepared its own XS-library using the isotopic compositions and geometry of the benchmark specification. The "outlier" BARS calculation is possibly a consequence of using different XS-library.

More striking is the effect of XS-variations onto the core power history. The Figure 6 shows that already the results from 95%-quantile band can reach peak values that are approximately 3.5 times larger than the nominal power. On the other hand there are results in which the rod ejection leads to a non pronounced power peak during the whole transient. As a result of all calculations a relatively large uncertainty band is formed which is at 95%- quantile level roughly 300% of nominal power. The minimum and maximum power peak values are 21% and 608% of the nominal power. It can be seen also in Figure 6 the difference between the median, which is a numerical value separating the higher half of a distribution from the lower half, and the mean, which is the average of the distribution, values of A-Q/C variation calculations. The median is a better indicator of the most typical value for distributions with outliers. The difference between median and mean values is due to the strongly nonlinear effect of the thermo-hydraulic coupling in the system.

Though the 95%-quantile band does not include BARS result, the range between A-Q/C results with maximum and minimum values of power peak contains even the BARS result. This again indicates that the transient is very sensitive to XS-library variations.

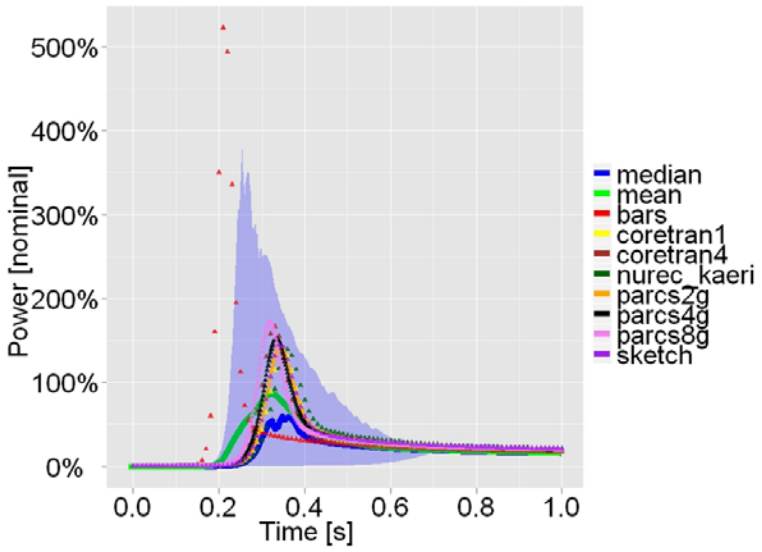

Figure 6 Core power history. The plot shows benchmark participants' results and the results of runs with variated XS libraries. Blue ribbon denotes the 95% quantile range. Blue curve is the median of all A-Q/C variation runs

It is also interesting to look at the nodal distribution of the uncertainties. Figure 7 presents bubble diagrams of the standard deviation of fuel assemblies' normalized power. The snapshot is made at time $t_m = 0.36s$ after beginning of the rod ejection. It is a median value of the power peak times. Left plot of Figure 7 shows the absolute value of standard deviation. Position $(x, y) = (12,4)$ corresponds to the coordinates of the ejected control rod. The assembly power around this position is highest which leads to the largest absolute values of standard deviation. On the other hand, the right plot of Figure 7 shows the relative values of standard deviations normalized to corresponding values of the power mean values. This scaling gives a possibility to reveal a global effect of the rod ejection on to the uncertainties of the assembly power. A local effect of rod ejection leads to responses in the assemblies that are not in its direct vicinity.

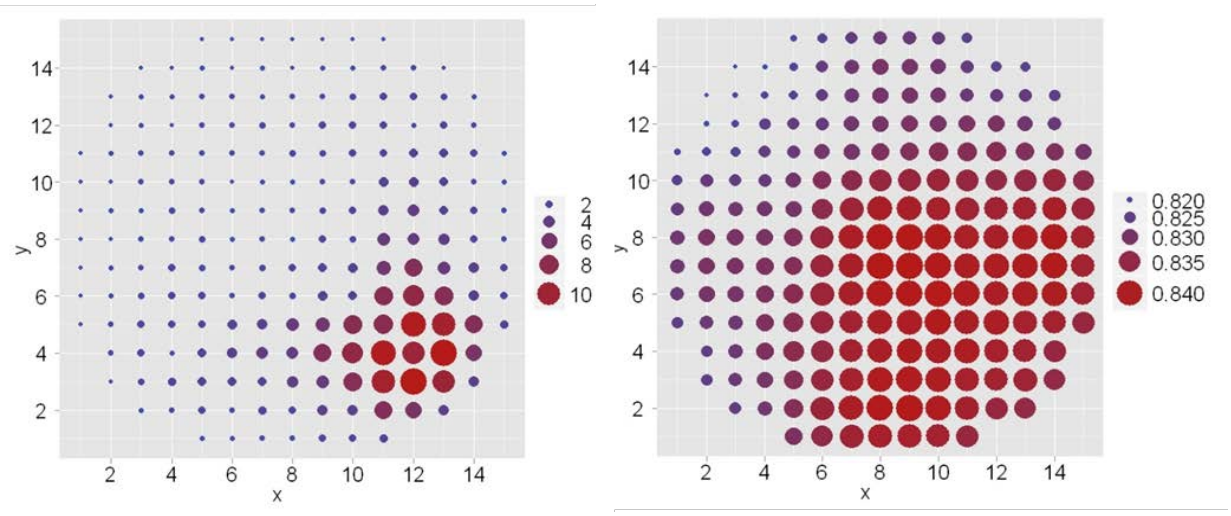

Figure 7 Standard deviation of fuel assembly power at the median value of normalized power peak times. Left – absolute standard deviation; right – relative standard deviation normalized to the corresponding mean value

4. CONCLUSIONS

In the present paper is studied the influence of nuclear data uncertainties for the rod ejection transient. The applied core data is based on the specification of the NEA/OECD MOX/UO2 Benchmark. A significant uncertainty range in the global and local values of the power is observed. The effect of uncertainty spread is global and influences the power distribution in the whole active core. The results of the performed study are compared with the results of all participants in the MOX/UO2 Benchmark. The main parameter distributions of all participants with the exception of one - BARS are covered by the uncertainty range of the performed calculations with A-Q/C based on XS variations sampled with the GRS code XSUSA.
The presented work shows the importance of performing nuclear data uncertainty analysis on the global and local core parameter evolutions and it is a step forward in the development of BEPU methodology.

5. ACKNOWLEDGMENTS

This work was supported by the German Ministry of Economics and Technology.

6. REFERENCES

1. K. Ivanov, M. Avramova, I. Kodeli, and E. Satori, “Benchmark for Uncertainty Analysis in Modeling (UAM) for Design, Operation, and Safety Analysis of LWRs”, NEA/NSC/DOC(2007)23, (2007).
2. M. Klein, L. Gallner, B. Krzykacz-Hausmann, A. Pautz, W. Zwermann, “Influence of Nuclear Data Uncertainties on Reactor Core Calculations” *Kerntechnik*, **2011/03**, p. 174-178, (2011)

3. T. Kozlowski, T. J: Downar, “PWR MOX/UO2 Core Transient Benchmark – Final Report”, NEA/NSC/DOC(2006)20, (2007)
4. M. L. Williams and B. T. Rearden, “SCALE-6 Sensitivity/Uncertainty Methods and Covariance Data”, *Nuclear Data Sheets*, **109** (12), p. 2796, (2009)
5. M. A. Jessee, et al., “Development of Generalized Perturbation Theory Capability within the SCALE Code Package”, *International Conference on Mathematics, Computational Methods & Reactor Physics (M&C 2009)*, Saratoga Springs, NY, (2009) .
6. I. Kodeli, “Multidimensional Deterministic Nuclear Data Sensitivity and Uncertainty Code System: Method and Application“, *Nucl. Sci. Eng.*, **138**, pp. 45-66, (2001).
7. S. Langenbuch and K. Velkov, “Overview on the Development and Application of the Coupled Code System ATHLET – QUABBOX/CUBBOX”, Mathematics and Computation, Supercomputing, Reactor Physics and Nuclear and Biological Applications, Avignon, France, (2005)
8. “SCALE: A Modular Code System for Performing Standardized Computer Analyses Licensing Evaluation, Version 6”, ORNL/TM-2005/39, (2009).
9. A. Avvakumov and V. Malofeev, “Validation of an Advanced Heterogeneous Model for LWR Detailed Pin-by-Pin Calculations,” *Proceedings of the International Conference on the Physics of Nuclear Science and Technology*, USA, October 1998.

PHYSOR 2012 – Advances in Reactor Physics – Linking Research, Industry, and Education
Knoxville, Tennessee, USA, April 15-20, 2012, on CD-ROM, American Nuclear Society, LaGrange Park, IL (2012)

INTERACTION OF LOADING PATTERN AND NUCLEAR DATA UNCERTAINTIES IN REACTOR CORE CALCULATIONS

M. Klein, L. Gallner, B. Krzykacz-Hausmann, A. Pautz, K. Velkov, W. Zwermann
Gesellschaft für Anlagen- und Reaktorsicherheit (GRS) mbH
Boltzmannstr. 14, D- 85748 Garching b. München, GERMANY
Markus.Klein@grs.de

ABSTRACT

Along with best-estimate calculations for design and safety analysis, understanding uncertainties is important to determine appropriate design margins. In this framework, nuclear data uncertainties and their propagation to full core calculations is a critical issue. To deal with this task, different error propagation techniques, deterministic and stochastic are currently developed to evaluate the uncertainties in the output quantities. Among these is the sampling based uncertainty and sensitivity software XSUSA which is able to quantify the influence of nuclear data covariance on reactor core calculations. In the present work, this software is used to investigate systematically the uncertainties in the power distributions of two GEN-III PWR cores. With help of a statistical sensitivity analysis, the main contributors to the uncertainty are determined. Using this information a method is studied with which loading patterns of reactor cores can be optimized with regard to minimizing power distribution uncertainties. It is shown that this technique is able to halve the calculation uncertainties of a MOX/UOX core configuration.

Key Words: uncertainty analysis, sensitivity analysis, nuclear data, covariance, XSUSA, UAM-Benchmark.

1. INTRODUCTION

Nuclear data are the basis of all methods of neutron transport calculation and thus the quality of the nuclear data used is essential for obtaining reliable calculation results. Currently different techniques are developed to quantify the calculation uncertainties on different stages of the reactor core calculation chain. Some of today's uncertainty and sensitivity tools are based on adjoint fluxes in the framework of the generalized perturbation theory [1][2][3][4]. These techniques primarily consider the multiplication factors of small, critical assemblies. Such compact critical assemblies are not necessarily representative for power reactors at operating conditions. To consider these, complex hybrid approaches are currently developed [5]. Other approaches are based on statistical sampling techniques [6][7] including the so called "Total Monte Carlo" method [8], which determines output uncertainties by random sampling the nuclear basis data before generating evaluated files.

The methodology developed and pursued at GRS – XSUSA – is a different sampling approach [9][10]. Based on the GRS method implemented in the code package SUSA ("Software for Uncertainty and Sensitivity Analysis") [11], many varied multi-group input libraries are generated using the evaluated nuclear covariance data shipped with the SCALE 6 code package [12] and the corresponding multi-group ENDF/B-VII library. The variations of the input data are generated randomly from the given probability distributions of the parameters including possible

correlations between them. XSUSA was applied successfully from simple pin cell calculations to burn-up calculations [13] and full core calculations using Monte-Carlo [9][14] and diffusion codes [10]. Thus the method is able to propagate the nuclear data uncertainties through all stages of the reactor core calculation chain.

However, quantifying the output uncertainties is only one aim of the investigations. The second aim is to determine which of the input uncertainties is most responsible for the output uncertainties. These two pieces of information are necessary to reach the third and final goal, namely to find a way to minimize the calculation uncertainties. In this paper an uncertainty analysis is presented concerning with all three aims.

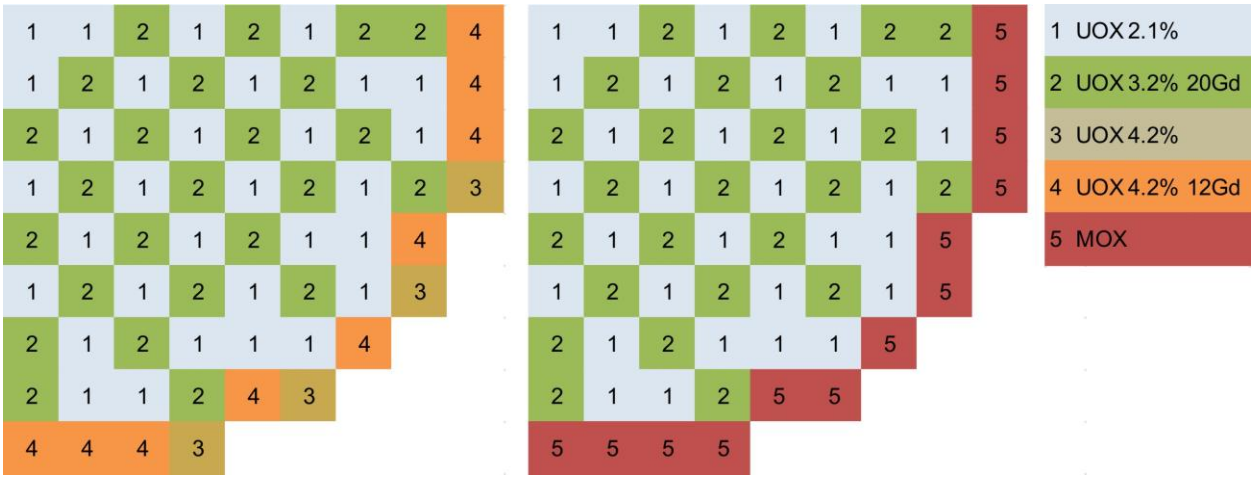

Figure 1. Configurations of the two investigated GEN-III PWR cores.

2. UNCERTAINTY AND SENSITIVITY ANALYSIS OF TWO SIMILAR PWR CORES

2.1. Uncertainty Analysis

Using the XSUSA-Methodology in combination with the spectral code NEWT and with the diffusion code QUABOX/CUBBOX [15] as described in [10] the uncertainties of two similar three-dimensional GEN-III PWR cores introduced in the specification for the OECD UAM-Benchmark [16] are calculated. Both cores have fresh loadings, one with only UOX assemblies and the other with a mixed MOX/ UOX loading as shown in Fig. 1. There are five different types of 17x17 fuel assemblies:

- Type 1: UOX 2.1% ^{235}U assembly without UO_2-Gd_2O_3 rods
- Type 2: UOX 3.2% ^{235}U assembly with 20 UO_2-Gd_2O_3 (1.9% ^{235}U) rods
- Type 3: UOX 4.2% ^{235}U assembly without UO_2-Gd_2O_3 rods
- Type 4: UOX 4.2% ^{235}U assembly with 12 UO_2-Gd_2O_3 (2.2% ^{235}U) rods
- Type 5: MOX assembly without UO_2-Gd_2O_3 rods

The radial reflector is modelled by homogeneous assemblies in stainless steel at the core boundary; beyond this stainless steel reflector, borated water is represented. Concerning the core axial description, the axial reflector at the bottom and the top of the active fuel length is modelled by clads bathed with borated water. For the lower axial reflector, the claddings are filled with a Zircaloy tube and the upper reflector's claddings are filled with a diluted stainless steel material to model springs. The heavy radial reflector is represented on the total core length and the boundary conditions are defined as zero albedo. As can be seen in Fig. 1, the two set-ups show only differences in the outer most row of fuel assemblies. Where the UOX core shows a mixture of assembly types 3 and 4, the outermost row of the MOX/UOX consists only of fuel type 5, i.e. MOX assemblies.

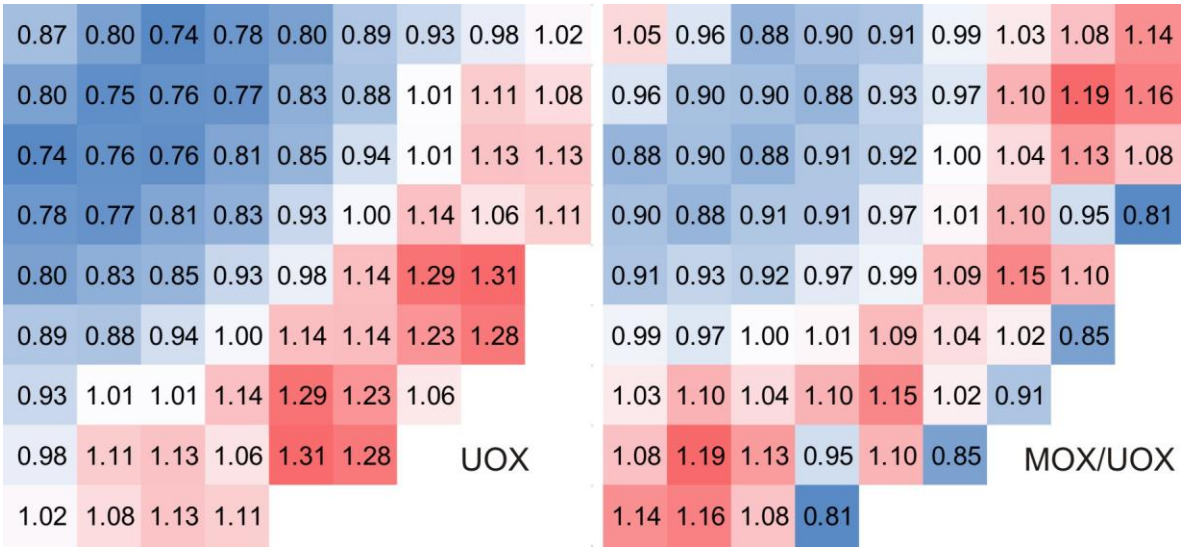

Figure 2. Mean values of the power distribution of the investigated reactor cores for N=300 calculations.

A set of N = 300 complete few-group cross section libraries was generated using XSUSA with the spectral code NEWT from SCALE 6. For all different fuel assemblies (including the reflectors) the same set of random numbers, i.e. the same varied multi-group libraries, was used. Thus the correlations between the cross-sections of different assemblies are preserved naturally and are implicitly contained in the homogenized few-group libraries [10]. These few-group libraries serve as input for the diffusion core model QUABOX/CUBBOX which calculates the multiplication factor and the power distribution for each individual run. The results are then analysed by statistical methods.

Table I. Mean values and statistical standard deviations of k_{eff}.

k_{eff}	mean	uncertainty
UOX	1.00292	0.00513
MOX/UOX	1.00063	0.00488

Table I, Fig. 2 and Fig. 3 show mean values and uncertainties of the full core calculations. For both configurations the mean value of the multiplication factor is a little overcritical. The mean of both radial power distributions are relatively flat with peaking values in the outer region of the core. The uncertainties, calculated as statistical standard deviations, of k_{eff} are about 0.5 % for both, the UOX and the MOX/UOX loading and thus they are in good agreement with values from other UOX dominated systems [9][10][12][13]. The uncertainties of the power distribution also show a similarity: both have a relatively high uncertainty in the center and the outermost region of the core and a very low uncertainty in a circle at half way in-between. However, looking at the magnitude of the uncertainties it becomes apparent, that the MOX/UOX core has a much higher calculation uncertainty. Whereas the uncertainty is smaller than 5 % in every node of the UOX core, it reaches 9.4 % in the outer region and even 13 % in the center of the MOX/UOX core.

The fact that the uncertainty is almost twice as high in the center of the MOX/UOX core is of special interest, as the core loadings show no difference in this region (see Fig. 1). Thus the root of this phenomenon cannot be determined without further investigations.

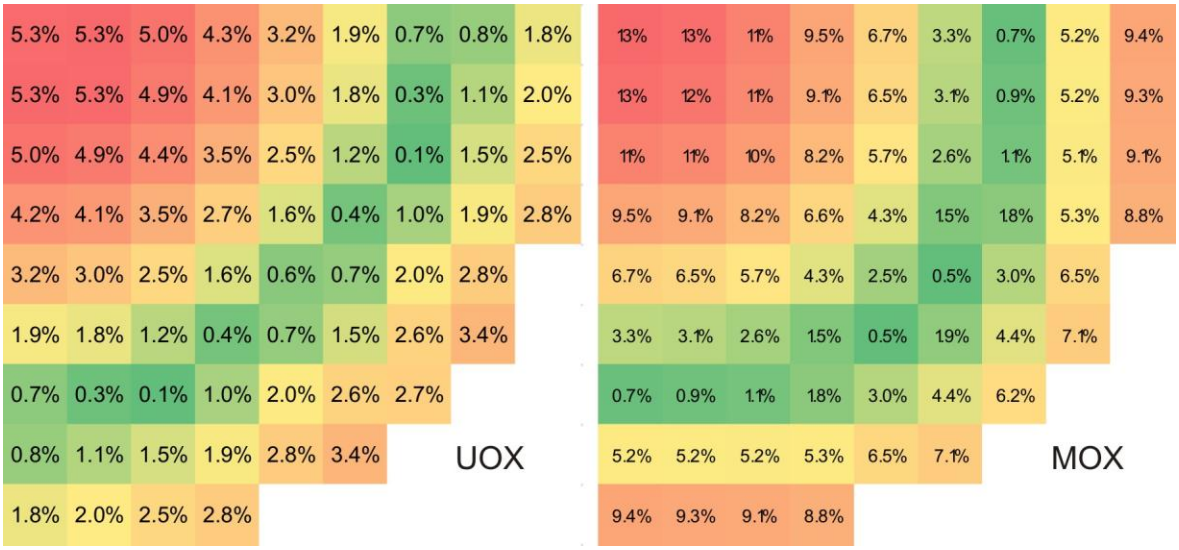

Figure 3. Uncertainties in the power distribution of the investigated reactor cores.

2.2. Sensitivity Analysis

To find out the main contributors for different uncertainties, a statistical sensitivity analysis as implemented in SUSA [17] was performed. The sensitivity measures chosen here are based on Pearson correlation. The method correlates an arbitrary output value (here: k_{eff} or the assembly power in the center of the core) with all different uncertain input values (here: homogenized two-group cross sections) and gives back a statistical sensitivity coefficient between [-1;1]. A value of 1 (-1) means a total correlation (total anti correlation) between input and output value, whereas a value of 0 means that there exists no correlation between the input and output value.

The left side of Fig. 4 shows the statistical sensitivity coefficients for Δk_{eff} of the UOX core. It can be seen that the coefficients are group-wise approximately the same for the different assembly types for each cross section. This is due to strong correlations between the uncertain input cross-sections (i.e. Σ_{fis} of assembly type 1 to 4 are correlated due to similar nuclide inventories) which are not taken into account in this sensitivity measure. The most important contributors to the uncertainty of k_{eff} are $\nu\Sigma_{fis}^{2}$ – which is due to the large uncertainties of ν of ^{235}U – and Σ_{abs}^{1} – which is due to the large uncertainties of the absorption of ^{238}U. Looking at the right side of the same Fig. 4 one sees that the same input cross sections contribute also most to Δk_{eff} of the MOX/UOX core. The cross sections of the MOX assembly seem to play an unimportant role in this case which is maybe due to sheer numbers (n_{UOX}/n_{MOX} = 193/48). This result is in good agreement with the fact that Δk_{eff} is almost the same for both cases. The reflector plays no important role in this case.

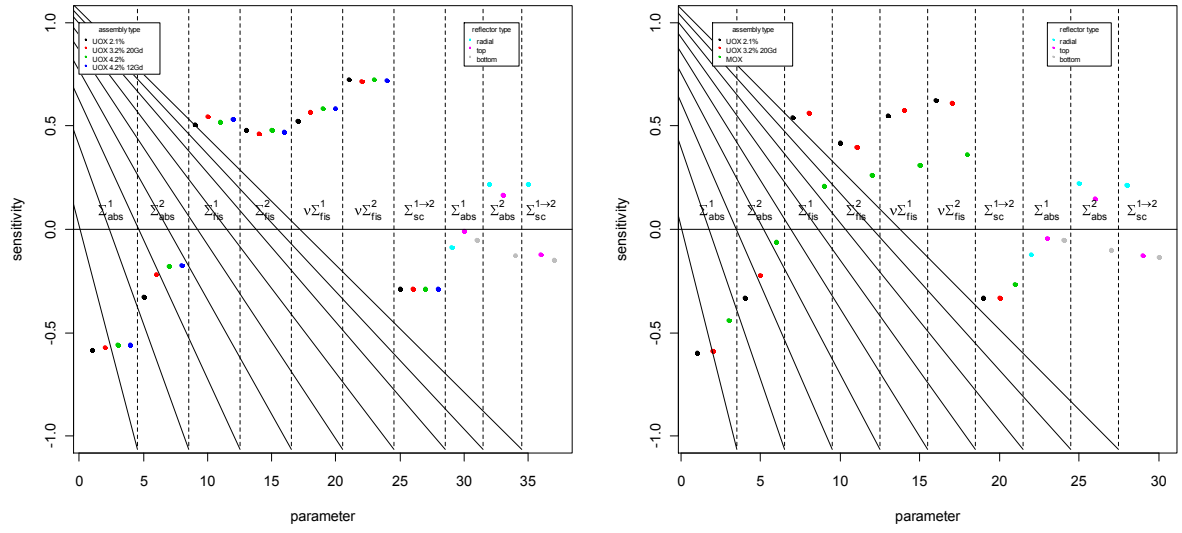

Figure 4. Statistical sensitivity coefficients for the uncertainty in k_{eff} for the UOX core (left side) and the MOX/UOX core (right side).

To find out the reason of the bigger uncertainties in the power distribution of the MOX/UOX core, the same analysis was performed for the assembly power of the central assembly. The results are displayed in Fig. 5. For the UOX core (left side) it becomes apparent that many of the cross-sections in the fast energy group, especially the down-scatter cross-section and Σ_{abs}^{1}, are the main contributors to the uncertainty. However, the situation is completely different for the MOX/UOX core (right side). All the parameters that are important in the UOX core have much lesser importance in this core. Instead the main contributors are by far the MOX cross-sections, especially $\nu\Sigma_{fis}^{2}$. That means that the outermost row of assemblies has a big influence not only locally but on the global power distribution of the core.

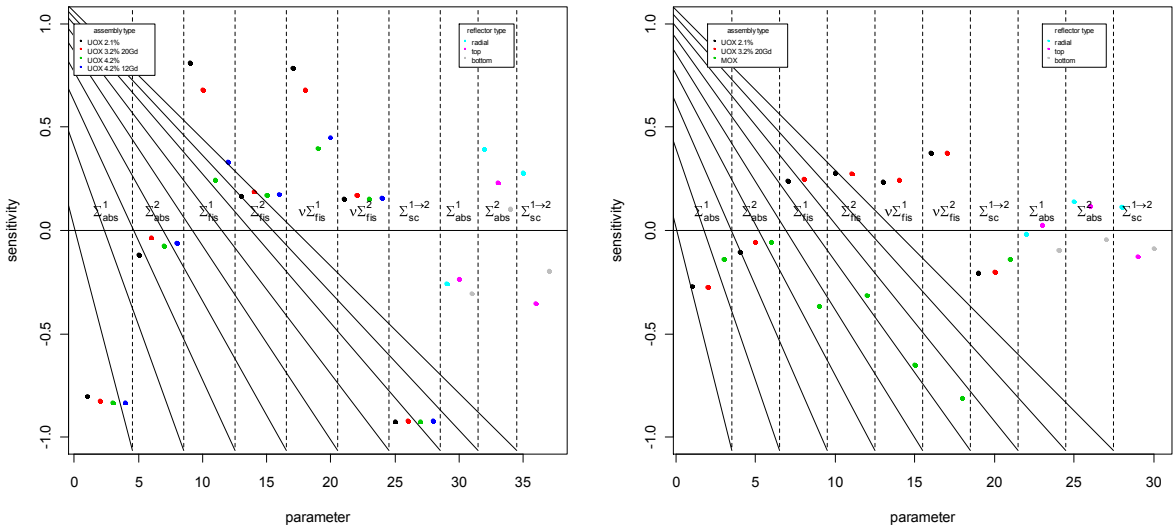

Figure 5. Statistical sensitivity coefficients for the uncertainty in the nodal power of the central fuel assembly for the UOX core (left side) and the MOX/UOX core (right side).

2.3. Minimizing the effect of nuclear data uncertainties on the power distribution using a superposition technique

The sensitivity analysis only reveals that the MOX assemblies are the main contributors to the uncertainty of the power distribution but it does not tell if MOX assemblies are *per se* the main source of uncertainties or if it is just the special geometric configuration of this particular core. To analyze this, a simplified one-dimensional reactor model is investigated. The model consists of 17 MOX assemblies in a chain, with heavy-reflector assemblies on both ends (see Fig. 6). The boundary conditions are vacuum on the reflector side and reflective else where. To investigate how local cross-section uncertainties of one special assembly influence the global set-up only the cross-sections of some particular assemblies are assumed to be uncertain, i.e. a XSUSA investigation was performed, where only some of the cross-sections were varied while all the

others were kept constant. The fuel assemblies with varied cross-sections are denoted by an arrow in Fig. 6.

In the first one-dimensional calculation only the cross-sections of the central assembly (see configuration 1 in Fig. 6) were assumed to be uncertain. This results in large uncertainties in the center and a smaller peak in the outer part of the chain while in-between these peaks there is almost no uncertainty. This behavior can be understood better when the bias of the deviation from the mean value is taken into account also. This is shown in the lower part of Fig. 6, where the deviations in the varied assembly are always defined to be in positive direction. One can see, that the deviations in the second peak have always the opposite direction than the central peak, which is a consequence of the power normalization.

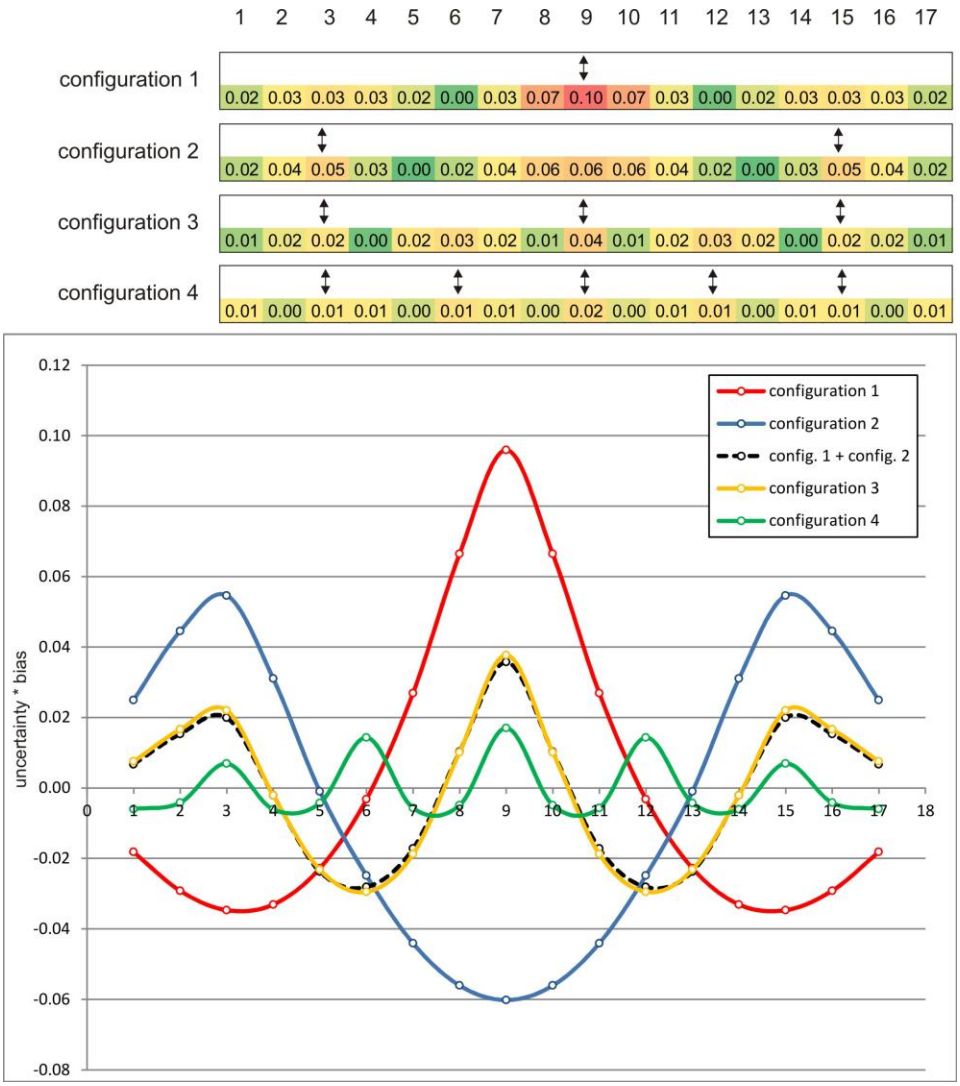

Figure 6. Uncertainties in the power distribution of the one-dimensional reactor model. The arrows denote the positions where uncertain cross-sections were assumed in the individual configurations.

In a second calculation two assemblies at positions 3 and 15 are assumed to have uncertain cross-sections (see configuration 2 in Fig. 6). The biased result is two positive uncertainty peaks at position 3 and 15 and one negative peak in the center of the core. Thus the biased uncertainty in configuration 2 has just the opposite direction than in configuration 1. The uncertain cross-sections are totally correlated in this example, i.e. if they deviate in a positive direction at position 3 they will also deviate positively at position 15. The same should be true if we introduce even more assemblies with uncertain cross-sections, e.g. additionally at position 1. If the individual assemblies do not influence each other too much, the result of this should then be a superposition of the results of configurations 1 and 2 (see black dashed line in Fig. 6).

That this assumption is true can be seen with sampling configuration 3. In the center of the chain, one can see that the positive biased uncertainty stemming from the central assembly cancels out the combined negative biased uncertainty from assemblies 3 and 15. The assemblies seem not to interact too much, as the resulting line lies almost exactly on the superposed line of configurations 1 and 2. One can continue the superposition technique by adding more uncertain cross-sections at positions with negative biased uncertainty, e.g. positions 6 and 12. The result of this (see configuration 4) can be seen as the green line in Fig. 6: the highest resulting uncertainty is only one fifth of the highest uncertainty in the initial configuration 1.

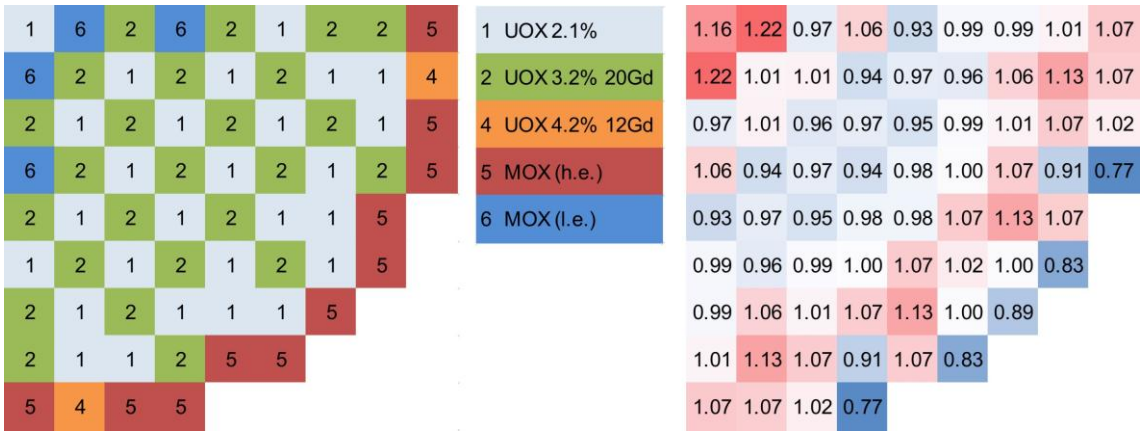

Figure 7. New configuration and power distribution of the MOX/UOX core.

This simple example on the one-dimensional model reactor shows, that the superposition technique can minimize the calculation uncertainties in the power distribution by applying a different core configuration. In order to show that the technique is suitable for realistic three-dimensional reactor core models as well, it was applied to the MOX/UOX core. The sensitivity analysis in the preceding section showed, that the MOX assemblies in the outer section of the

reactor are the main contributors to the uncertainties of the power distribution. A closer investigation also showed that the biased uncertainties have opposite signs in the center and the outer regions of the core. The positions of eight MOX assemblies were exchanged with eight central positioned UOX assemblies. In order not to change the power distribution in the core too much and keep the multiplication factor near criticality (k_{eff} = 1.00009; Δk_{eff} = 0.00494), the enrichment of the central MOX assemblies was lowered a little bit and the enrichment of the new outer UOX assemblies was increased. However, the new MOX/UOX core has almost the same nuclide inventory as the original core. The configuration and the mean values of the resulting power distribution are shown in Fig. 7, the uncertainties of the power distribution in Fig. 8. It can be seen, that the resulting uncertainties are much smaller than the ones in the original configuration. This can be seen in particular in the right part of the Fig. 8 which shows the uncertainties in the central row of fuel assemblies of all three investigated core configurations. It shows that the uncertainties in the new MOX/UOX configurations are in the order of the ones of the UOX core.

This example demonstrates that the superposition technique can be applied to minimize the calculation uncertainties of realistic reactor cores. It also shows that MOX/UOX configurations do not have to be *per se* responsible for a uncertain power distribution but only in combination with a special core configuration. Therefore it is important to investigate every different configuration.

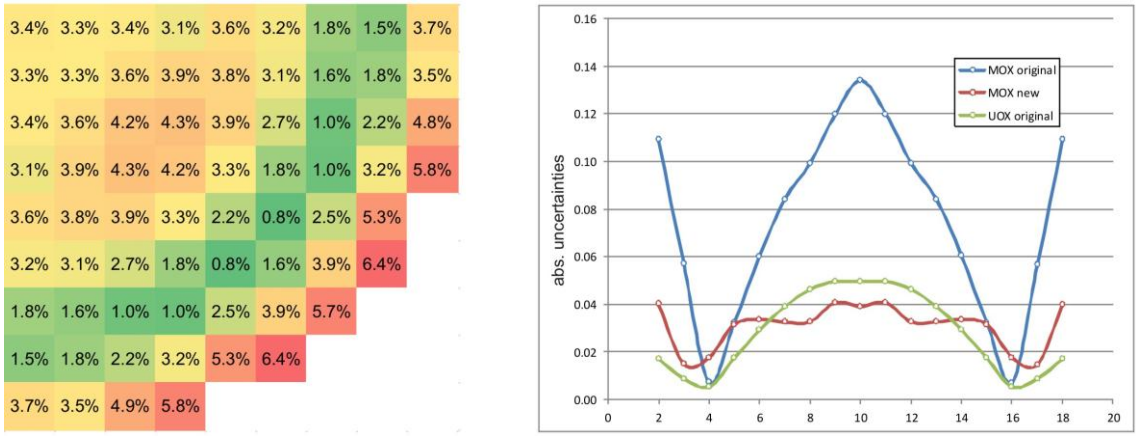

Figure 8. Uncertainties in the power distribution of the new configured MOX/UOX core (left side). The right graph shows the magnitude of uncertainties in the central horizontal row of assemblies for all three investigated three-dimensional reactor cores.

3. SUMMARY AND CONCLUSIONS

The influence of nuclear data uncertainties on reactor core calculations was investigated systematically using the sampling based uncertainty and sensitivity software XSUSA. The method was applied to three-dimensional steady state calculations of two GEN-III reactor cores.

While the uncertainty in k_{eff} was about the same for both reactor cores, the uncertainties in the nodal power distribution were much higher in the MOX/UOX core than in the UOX core. They reached 13% in the central fuel assembly. A statistical sensitivity analysis revealed that the MOX assemblies were the main contributors to the uncertainties in the power distribution.

Using a simplified one-dimensional reactor core model it was demonstrated that calculation uncertainties can be minimized by an appropriate core configuration. The same technique was applied to the MOX/UOX core. By rearranging eight fuel assemblies the calculation uncertainties could be halved in value and thus had the same magnitude as the uncertainties for the UOX core.

In conclusion, it is desirable to routinely accompany reactor calculations by uncertainty and sensitivity analyses in the future. Especially MOX/UOX configurations have to be investigated as some core loading patterns can have high calculation uncertainties.

ACKNOWLEDGMENTS

This work was supported by the German Ministry of Economics and Technology.

REFERENCES

1. M. L. Williams and B. T. Rearden, "SCALE-6 Sensitivity/Uncertainty Methods and Covariance Data", *Nuclear Data Sheets,* **109**(12), p.2796, (2009).
2. M. A. Jessee, et al., "Development of Generalized Perturbation Theory Capability within the SCALE Code Package", *International Conference on Mathematics, Computational Methods & Reactor Physics (M&C 2009),* Saratoga Springs, NY, (2009).
3. I. Kodeli, "Multidimensional Deterministic Nuclear Data Sensitivity and Uncertainty Code System: Method and Application", *Nucl. Sci. Eng.,* **138**, pp.45-66, (2001).
4. I. Kodeli, "The SUSD3D Code for Cross-Section Sensitivity and Uncertainty Analysis – Recent Development", *Trans. Am. Nucl. Soc.*, **104**, pp.791-793 (2011).
5. H. S. Abdel-Khalik, P. J. Turinsky, and M.A. Jessee, "Efficient Subspace Methods-Based Algorithms for Performing Sensitivity, Uncertainty, and Adaptive Simulation of Large-Scale Computational Models", Nuclear Science and Engineering, 159, 256-272 (2008)
6. N. García-Herranz, O. Cabellos, J. Sanz, J. Juan, and J. C. Kuijper, "Propagation of Statistical and Nuclear Data Uncertainties in Monte Carlo Burnup Calculations," *Annals of Nucl. Energy*, **35**, pp.714-730 (2008).
7. O. Buss, A. Hoefer, and J.C. Neuber, "NUDUNA – Nuclear Data Uncertainty Analysis," *Proc. International Conference on Nuclear Criticality (ICNC 2011)*, Edinburgh, Scotland, Sep. 19-22, 2011, on CD-ROM (2011).
8. A. J. Koning and D. Rochman, "Towards Sustainable Nuclear Energy: Putting Nuclear Physics to Work," *Annals of Nucl. Energy*, **35**, pp.2024-2030 (2008).
9. W. Zwermann, B. Krzykacz-Hausmann, L. Gallner, A. Pautz, "Influence of Nuclear Covariance Data on Reactor Core Calculations," *Proc. Second International Workshop on Nuclear Data Evaluation for Reactor Applications (WONDER 2009)*, Cadarache, France, 29 Sep. - 2 Oct., 2009, pp.99-104 (2009).

10. M. Klein, L. Gallner, B. Krzykacz-Hausmann, A. Pautz, W. Zwermann, "Influence of Nuclear Data Uncertainties on Reactor Core Calculations", *Kerntechnik,* **2011/03**, 174-178 (2011).
11. B. Krzykacz, E. Hofer, M. Kloos, "A Software System for Probabilistic Uncertainty and Sensitivity Analysis of Results from Computer Models," *Proc. International Conference on Probabilistic Safety Assessment and Management (PSAM-II)*, San Diego, Ca., USA, (1994).
12. "SCALE: A Modular Code System for Performing Standardized Computer Analyses for Licensing, Version 6," ORNL/TM-2005/39, (2009).
13. L. Gallner, B. Krzykacz-Hausmann, A. Pautz, M. Wagner, W. Zwermann, "Influence of Nuclear Data Uncertainties on the Depletion Chain", *Proc. Jahrestagung Kerntechnik 2011*, Berlin, Germany, May 17. - 19. 2011, (2011).
14. L. Gallner, M. Klein, B. Krzykacz-Hausmann, A. Pautz, W. Zwermann, "Sampling Based Nuclear Data Uncertainty Analysis in Reactor Calculations", *Proc. ANS Annual Meeting*, Hollywood (FL), USA, June 26. – 30. 2011, (2011).
15. S. Langenbuch , K. Velkov, "Overview on the Development and Application of the Coupled Code System ATHLET – QUABBOX/CUBBOX", *Proc. of Mathematics and Computation, Supercomputing, Reactor Physics and Nuclear and Biological Applications*, Avignon, France, Sept. 12. – 15. 2005, (2005).
16. K. Ivanov, M. Avramova, S. Kamerow, I. Kodeli, E. Satori, "Benchmark for Uncertainty Analysis in Modeling (UAM) for Design, Operation, and Safety Analysis of LWRs", Volume I: Specification and Support Data for the Neutronics Cases (Phase I), Version 2.0 NEA/NSC/DOC(2011), (2011).
17. E. Hofer, "Sensitivity analysis in the context of uncertainty analysis for computational intensive models", *Computer Physics Communications*, **117**, pp. 21-34 (1999).

Pin-by-Pin Calculations with QUABOX/CUBBOX using the Super Homogenization Method

E. Lemarchand, M. Klein, I. Pasichnyk, K. Velkov, W. Zwermann

Gesellschaft für Anlagen- und Reaktorsicherheit (GRS) mbH
Boltzmannstr. 14, D-85748 Garching, Germany

markus.klein@grs.de

Introduction

The diffusion approximation of the transport equation is usually applied for production calculation for the analysis of the current generation of light water reactors (LWR), because the transport equation is very costly to solve for full core-sized problems. Advanced coarse-mesh and nodal methods have been successfully developed to spatially discretize the diffusion equation for a long time. Such a coarse-mesh or nodal approach is the method implemented in QUABOX-CUBBOX (QC) [1] which has been widely used for performing accident analysis because of the good accuracy and low CPU and memory expenses.

Currently, the state of art of performing accident analysis for PWR and BWR is based on applying coarse-mesh neutron codes that use cross sections homogenized over large spatial regions, typically of the size of one fuel assembly. The results generated are well validated and proved to be reliable. However, current trends towards increased operation flexibility stimulate the utilities to consider more complicated reactor core designs and operation strategies, such as cores loaded partially with mixed-oxide fuel or high burn-up loadings. Such cores may feature a highly heterogeneous flux/power profile inside the reactor. To estimate the impact of such heterogeneities on safety relevant quantities, it is desirable to have an exact knowledge of the pin-power distribution both at steady-state conditions and during transients. With an appropriate cross section treatment using the so called Super Homogenization method (SPH) [2,3], it will be shown that the neutron diffusion code QC can be applied not only for coarse mesh analyses, but for pin-by-pin investigations on a full-core scale, as well.

The SPH procedure is an equivalence procedure which was developed by Kavenoky and Hébert in the 1980s. The aim of this procedure is to preserve the reaction rates and the currents at the pin-cells interfaces in a single assembly calculation. As developed in [3], this method can provide an appropriate set of SPH factors without a normalization condition. The method uses a lattice code providing the heterogeneous solution and a diffusion (or transport) code to provide a pin-wise homogenized solution. However no modification of both lattice and diffusion code has to be done to compute the SPH factors: a new set of SPH corrected cross sections can be processed using the output data given by both codes.

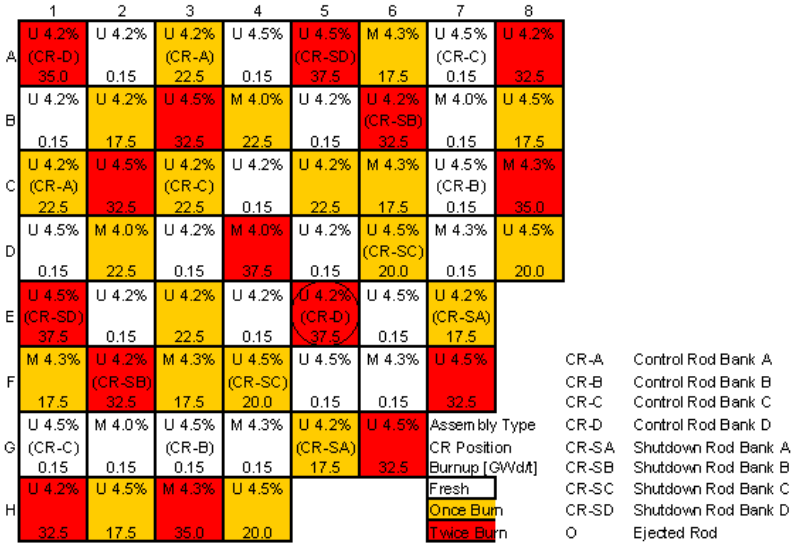

Figure 1 Core configuraion of the OECD MOX/UO2 Benchmark core [6].

Application of the method to the MOX/UO_2 Benchmark core

Earlier studies showed that the combination of QC and SPH is capable to exactly reproduce the pin-power values and the eigenvalue of heterogeneous fuel assemblies with reflective boundary conditions [4]. Though, as mentioned above, no normalization is needed on a single assembly level it is obvious that the SPH factors can be multiplied by any arbitrary constant without modifying the reaction rates in the calculation. However, the normalization factor becomes important when larger setups (i.e. reactor cores) are calculated using different kinds of fuel assemblies.

As described in [5], there are several ways to normalize the SPH factors after the SPH iterations. The first idea described initially by Hébert in [3], is to use the Flux-Volume normalization. This normalization preserves the average flux over the assembly in each group. Further studies showed that the normalization by so called Generalized Selengut factors yields the best results for heterogeneous core configurations with an excellent treatment of the assembly interfaces [5]. Own studies supported this observation such that for the calculations shown here this normalization was applied.

In order to demonstrate that the method is suitable to describe even highly heterogeneous core configurations it was applied to calculate the OECD MOX/UO_2 Benchmark core [6]. As shown in Figure 1, the core distribution is composed of four different assembly types at different burn-up values. There are two different UO_2 Assemblies with 4.2% and 4.5% enrichment and two different MOX assemblies with 4.0% and 4.3% enrichment, where the Pu-vector contains 94% fissile isotopes. Based on Westinghouse design, there are five different types of pin cells: fuel, guide tubes, control rods, IFBA (Integral Fuel Burnable Absorber) and WABA (Wet Annular Burnable Absorber) pins. Taking the burn-up into consideration there are 25 different assemblies types.

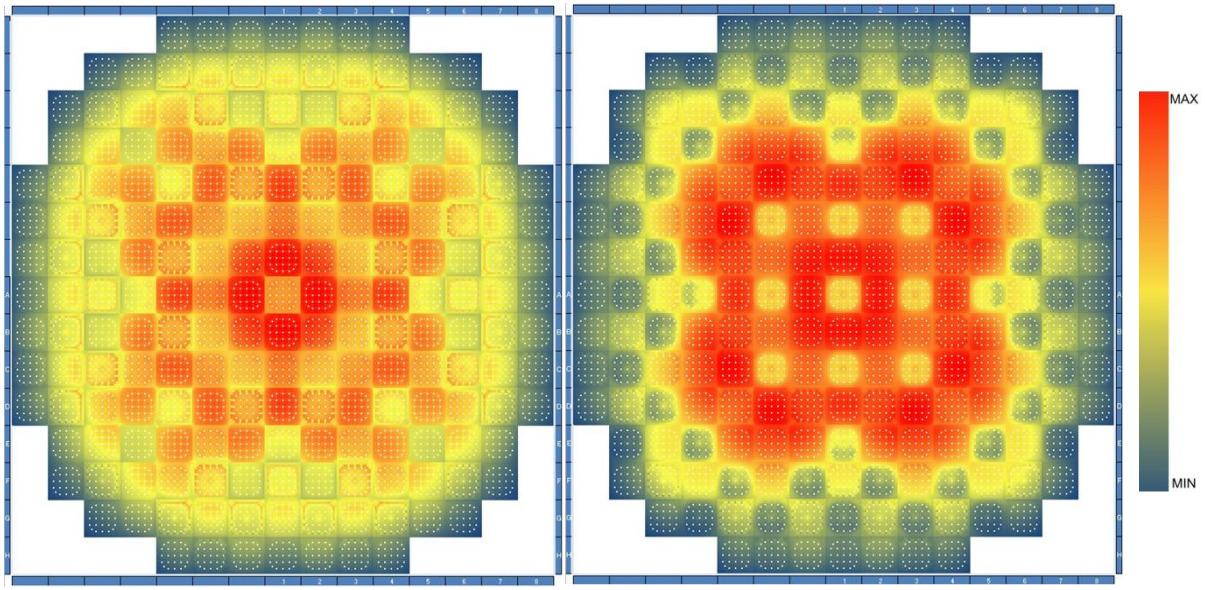

Figure 2 Color map of the power distribution for the ARO state (left) and the ARI state (right) at HZP conditions.

The lattice code HELIOS was applied to generate the pin-wise cross sections and the heterogeneous flux for the fuel assemblies. For the reflector the tested model from [7] including reflector discontinuity factors was applied. All cross sections were modified by SPH factors as described in [5]. It is mentioned that the calculated power distribution significantly depends on the basis data used for this core calculation [7]. The results were compared to a MCNP reference solution based on JEF-2.2 nuclear data. The 2D 'all-rods-out' (ARO) and the 'all-rods-in' (ARI) states at fixed T/H conditions (ρ_M = 752.06 kg/m^3, T_{core} = 560 K, SB = 1000.0 ppm) were calculated with QC. Figure 2 shows a color map of the power distribution of both calculated states.

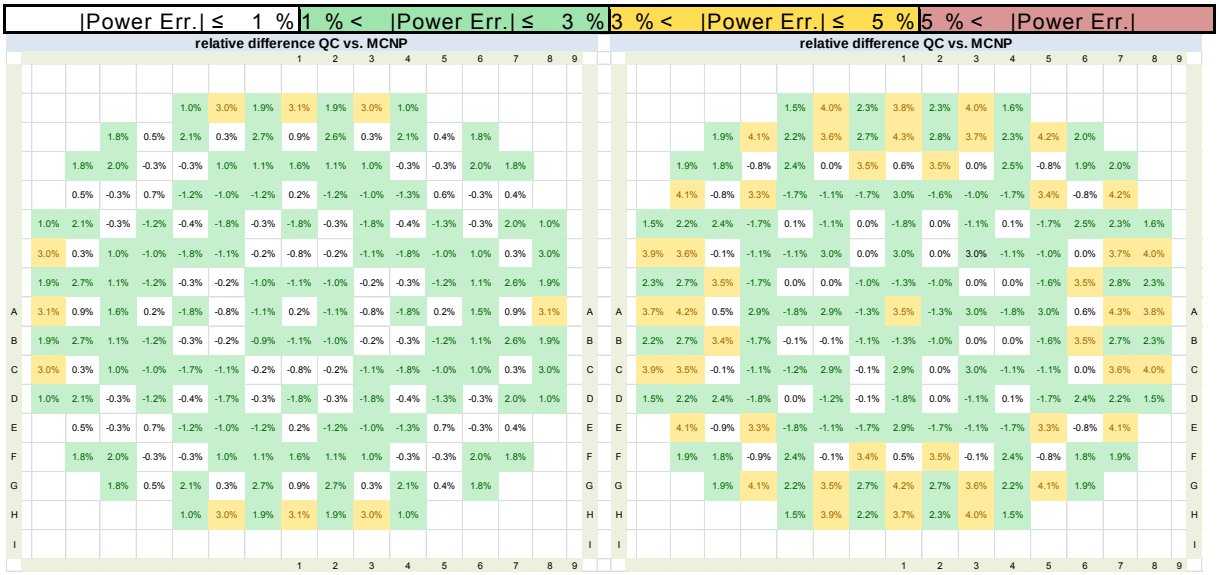

Figure 3 Relative difference of the assembly averaged power distribution between MCNP (ref.) and QUABOX/CUBBOX for the ARO (left) and the ARI (right) states at HZP conditions. Note that the slight asymmetry comes from the statistical error of the Monte-Carlo solution.

Table I Eigenvalues for the ARO and ARI states at HZP conditions obtained with different codes.

	ARO	*ARI*
MCNP (ref.)	1.06065	0.99001
QUABOX/CUBBOX with SPH	1.06000	0.98728

Table I displays the calculated multiplication factors with reference values. The QC solution shows only a deviation of 65 pcm for the ARO state and 273 pcm for the ARI state. To get an overview of the quality of global power distribution the power was averaged assembly wise and compared to the MCNP reference. As can be seen in Figure 3 the QC solution for the ARO state shows a very good agreement. Both, the UOX and the MOX assemblies are represented equally well. Only some assemblies in the outermost row show a significant deviation of about 3%. The situation slightly changes when the control rods are inserted in the ARI state. However the differences stay below 3% in most of the fuel assemblies and the maximum difference stays well below 5%.

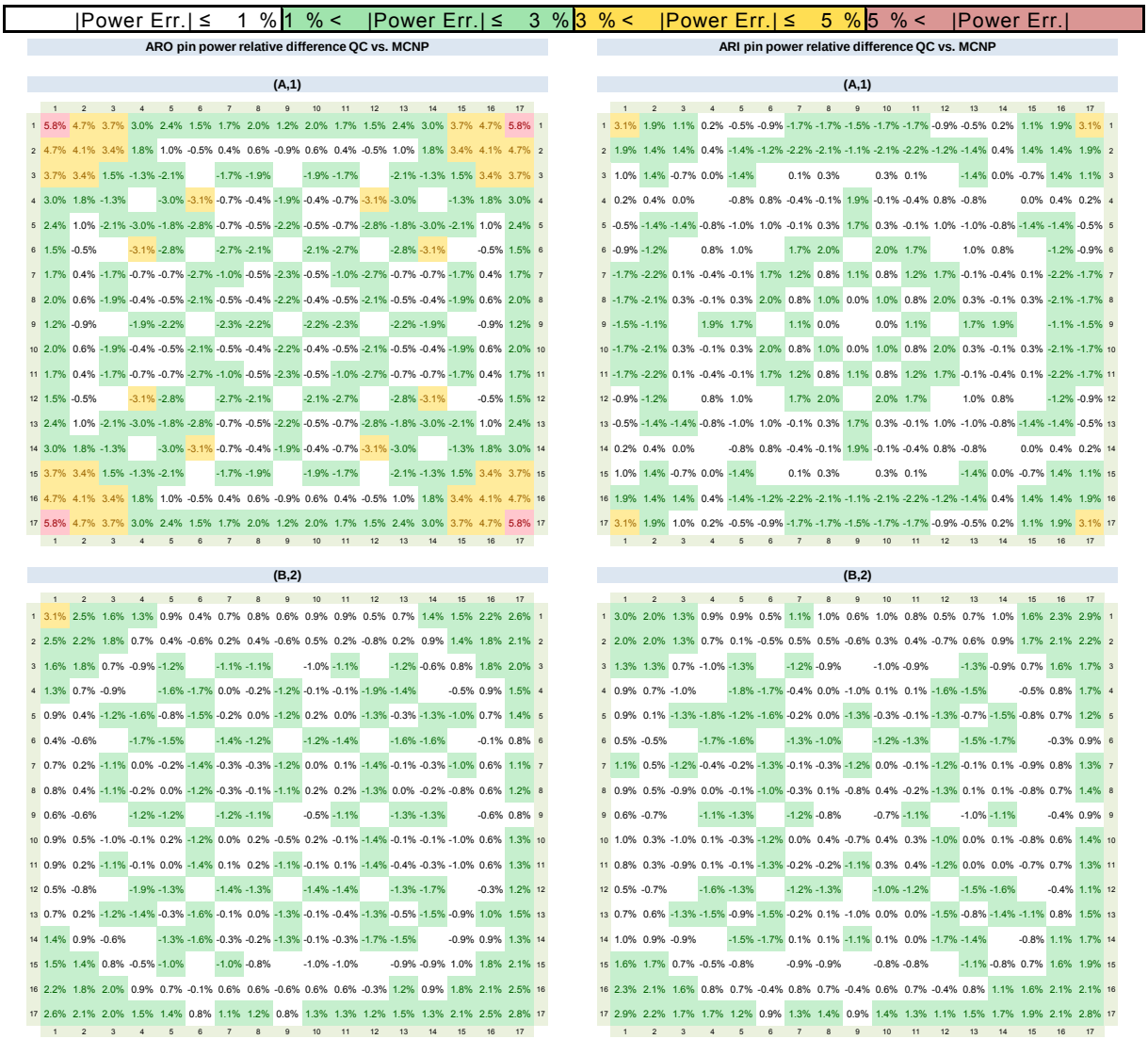

Figure 4 Relative differences of the pin-power distributions between MCNP (ref.) and QUABOX/CUBBOX. The left side shows values for the ARO state, the right side shows values for the ARI state.

|Power Err.| ≤ 1 %	1 % < |Power Err.| ≤ 3 %	3 % < |Power Err.| ≤ 5 %	5 % < |Power Err.|

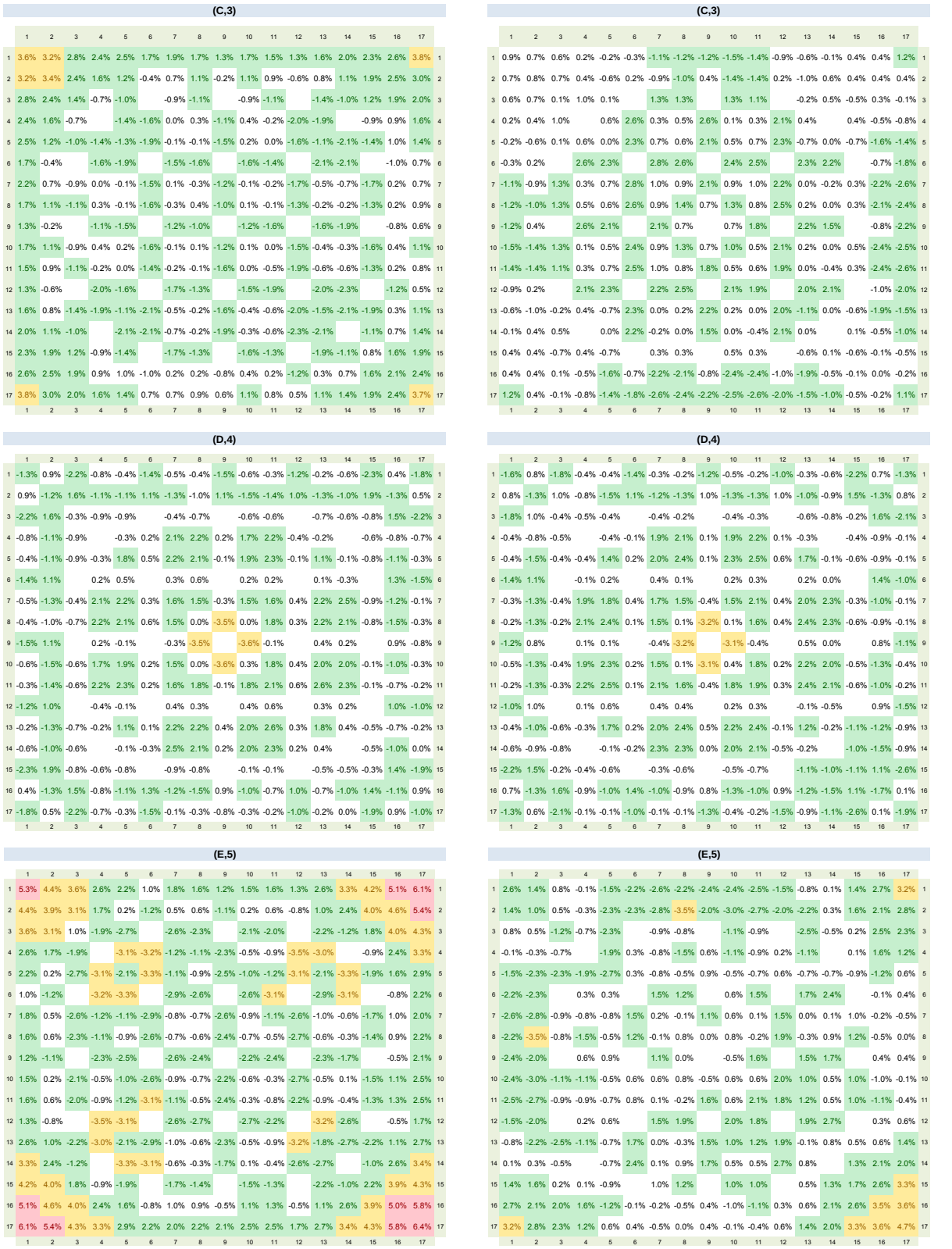

Figure 5 Relative differences of the pin-power distributions between MCNP (ref.) and QUABOX/CUBBOX. The left side shows values for the ARO state, the right side shows values for the ARI state.

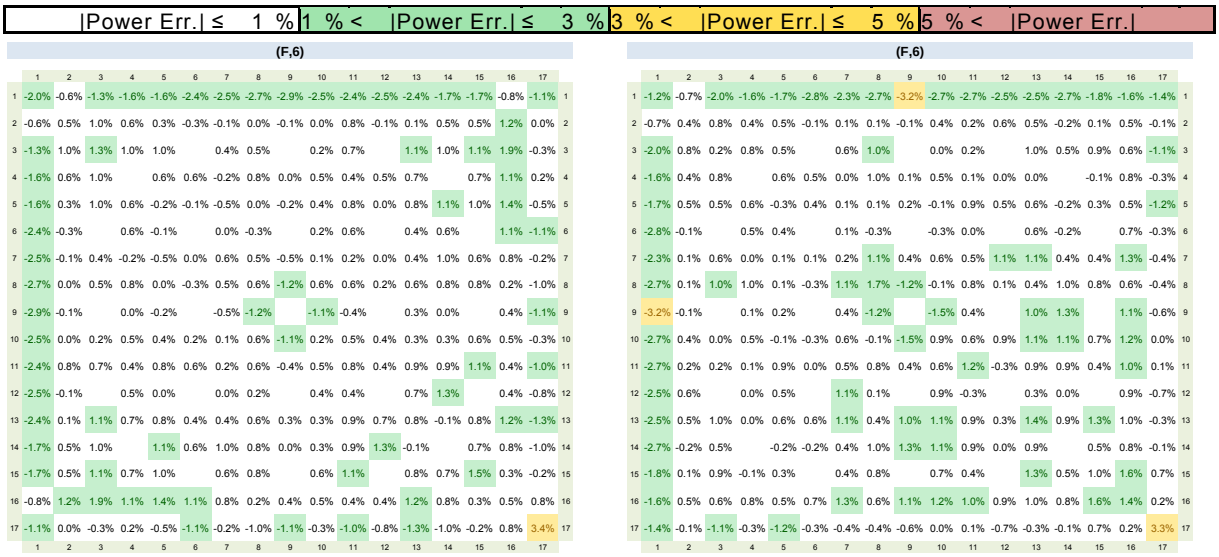

Figure 6 Relative differences of the pin-power distributions between MCNP (ref.) and QUABOX/CUBBOX. The left side shows values for the ARO state, the right side shows values for the ARI state.

The pin-wise power distribution along the diagonal (A,1) to (F,6) is compared to the MCNP reference in Figure 4 to Figure 6 (left side: ARO, right side: ARI). It can be seen that the representation of the inter assembly power distribution is very good as well for the ARO as for the ARI state. Most of the pin-powers show a difference of less the 3% and only few pins show a difference above 5% in the corners of the assemblies (A,1) and (E,5). Somewhat smaller deviations in the values of the corner pins of (B,2) and (C,3) suggest that the most erroneous pin powers are positioned in corners where a fresh UOX assembly is located near a highly burned-up UOX assembly. However, it should be noted especially that the UOX/MOX (i.e. (D,4) and (F,6)) and controlled/uncontrolled (i.e. ARI state (A,1), (C,3) and (E,5)) assembly interfaces reproduce the Monte-Carlo reference accurately.

Summary and Conclusions

In this paper it was demonstrated that QUABOX/CUBBOX is capable to calculate a highly heterogeneous full-core problem with a pin-wise resolution. Using pin-wise homogenized cross sections adjusted by SPH factors it was demonstrated that the pin-power distribution for as well UOX and MOX assemblies can be obtained with a high accuracy. Compared to transport solvers the needed CPU time is very low such that coupled accident analysis using a pin-wise resolution comes into reach for standard application.

Acknowledgements

This work is supported by the German Federal Ministry of Economics and Technology.

References

[1] S. Langenbuch, K. Velkov, *"Overview on the Development and Application of the Coupled Code System ATHLET – QUABOX/CUBBOX"*, Mathematics and Computation, Supercomputing, Reactor Physics and Nuclear and Biological Applications, Avignon, France, Sept. 12 – 15, 2005, (2005)

[2] A. Hébert, *"A Consistent Technique for the Pin-by-Pin Homogenization of a Pressurized Water Reactor Assembly",* Nucl. Sci. Eng. ,113, 227-238, (1993).

[3] A. Hébert, and G. Mathonnière, *"Development of a Third-Generation Superhomogénéisation Method for the Homogenization of a Pressurized Water Reactor Assembly",* Nucl. Sci. Eng. ,115, 129-141, (1993).

[4] M. Klein, I Pasichnyk., A. Pautz, K. Velkov, and W. Zwermann, *"Accuracy Enhancements of the Coarse-Mesh Diffusion Core Model QUABBOX/CUBBOX for Highly Heterogeneous Core Configurations"*, PHYSOR 2010, Pittsburgh, Pennsylvania, USA, May 9-14, 2010, (2010).

[5] T. Courau, M. Cometto, E. Girardi, D. Couyras, and N. Schwartz, *"Elements of Validation of Pin-by-pin Calculations with the Future EDF Calculation Scheme Based on APOLLO2 and COCAGNE Codes",* ICAPP 08 Anaheim, California, June 8-12, 2008, (2008)

[6] T. Kozlowski, T. Downar, *"Pressurized Water Reactor MOX/UO2 Core Transient Benchmark – Final Report"*, NEA/NSC/DOC(2006)20, (2006)

[7] M. Klein, L. Gallner, B. Krzykacz-Hausmann, A. Pautz, W. Zwermann, *"Influence of Nuclear Data Uncertainties on Reactor Core Calculations"*, Kerntechnik, 2011/03, 174-178, (2011).

APPLICATION OF XSUSA WITH ALEATORIC AND EPISTEMIC UNCERTAINTIES

Lucia Gallner, Markus Klein, Bernard Krzykacz-Hausmann,
Andreas Pautz, Kiril Velkov, Winfried Zwermann

Gesellschaft für Anlagen- und Reaktorsicherheit (GRS) mbH,
Forschungszentrum, Boltzmannstrasse 14, 85748 Garching, Germany

Lucia.Gallner@grs.de, Markus.Klein@grs.de, Bernard.Krzykacz-Hausmann@grs.de,
Andreas.Pautz@grs.de, Kiril.Velkov@grs.de, Winfried.Zwermann@grs.de

Introduction

Neutron transport calculations for criticality and other parts of the nuclear calculation chain have reached a very high level of precision. The Monte Carlo method with its direct simulation of nuclear reactions is used for reference calculations; a comparable accuracy can also be obtained with deterministic transport methods which solve the Boltzmann equation on a fine spatial grid without homogenization of large regions, and a multi-group representation for the energy dependence of the nuclear data. An indispensable pre-requisite for such high-accuracy calculations is the quality of the nuclear data used; correspondingly, evaluated nuclear data are continuously being improved, resulting in the current versions JEFF-3.1.1 [1], ENDF/B-VII.1 [2], and JENDL-4.0 [3] of the most important nuclear data libraries.
However, the precision of the calculation results is limited by the uncertainties of the input parameters. For criticality calculations, which are normally performed without thermal-hydraulic feedback, the uncertain input quantities are technological parameters due to, e.g., manufacturing tolerances, and nuclear data due to uncertainties of the underlying measurements and theoretical parameters. Estimated values for the nuclear data uncertainties are stored in the so-called covariance files accompanying the evaluated nuclear data files.
With respect to nuclear data uncertainties, deterministic tools based on perturbation theory like TSUNAMI [4] and SUSD3D [5], as well as sampling based methods as implemented in MCNP-ACAB [6], NUDUNA [7], TMC [8], and XSUSA [9] have been developed. The sampling tool SUnCISTT [10] based on the GRS method [11] is available for the treatment of uncertainties in technological parameters.
The present contribution focuses on the application of the GRS tool XSUSA [9] with a Monte Carlo code as neutron transport solver. A method is proposed and applied to perform the uncertainty and sensitivity analyses with strongly decreased numbers of Monte Carlo histories per calculation as compared to the conventional application and, nevertheless, without losing substantial information when determining the output uncertainties, thereby reducing the necessary computing times drastically. After giving an outline of the method, its application to a criticality benchmark, which is being investigated within an OECD/NEA working group, is described.

Separation of Aleatoric and Epistemic Uncertainties

Uncertainty and sensitivity analyses are performed to determine the uncertainties in the output quantities of a calculation describing a physical problem. Output

uncertainties result from epistemic input uncertainties. These are due to the incompleteness of the knowledge about the input parameters.
So far, sampling based approaches have been applied with deterministic and Monte Carlo transport solvers. When using a Monte Carlo code, an additional source of sampling uncertainty results from the finite number of neutron histories sampled in the course of the Monte Carlo simulation ("aleatoric uncertainty"). This adds to the uncertainty due to the incomplete knowledge of the parameters ("epistemic uncertainty"). Therefore, if a Monte Carlo code is applied to solve the transport problem, normally a sufficiently large number of neutron histories are used for each nuclear data sample, such that the aleatoric sampling uncertainty becomes negligibly small, and the observed output sampling uncertainty can be attributed to the epistemic nuclear data sampling uncertainty alone. That means that the complete batch of calculations is performed with the same high number of neutron histories in each of the calculation runs. Further effort to separate aleatoric and epistemic sampling uncertainties is unnecessary such that the usual one-dimensional sample based epistemic uncertainty analysis can be performed.
The method presented here shows that for many application cases it is not necessary to perform the full series of runs with such a high accuracy. In fact, it is possible to obtain reliable epistemic uncertainty results with substantially reduced number of neutron histories in each run, such that e.g. the total number of neutron histories for the whole series of all calculations is in the same order of magnitude as for the single high accuracy reference calculation run. The quintessence of the method consists in running two series of calculations with heavily reduced numbers of Monte Carlo histories each, instead of running one series with the full number of Monte Carlo histories. It is important that these two series are performed using identical nuclear data variations for each pair of calculations, but different Monte Carlo random numbers (by choosing different random number seeds). By evaluating the covariance between the two calculation series it is possible to widely eliminate the aleatoric uncertainty from the result. The details of the method as well as its mathematical basis are discussed in [12].

Uncertainty and Sensitivity Analysis for the EG-UACSA Benchmark Phase II

Although the EG-UACSA Benchmark Phase II [13] is mainly dedicated to estimating the influence of manufacturing tolerances, one optional task refers to the influence of nuclear data uncertainties, which is investigated in the present paper. Uncertainty and sensitivity analyses referring to manufacturing tolerances with the GRS method are presented in [10].
The arrangement is a two-dimensional representation of an infinite lattice of fuel assemblies, simulating a storage situation. The fuel assemblies consist of 17x17 pin cells, 25 of which contain control rod guide or instrumentation tubes; the fuel is fresh UO_2 with 4 wt.-% ^{235}U enrichment, moderated by light water at room temperature. The fuel assemblies are placed inside square stainless steel support channels. A slight sub-criticality is obtained by the presence of borated steel welds around the fuel pin arrays. For criticality calculations at nominal geometry, as it is the case for the nuclear data uncertainty and sensitivity analyses presented here, the description of one quarter of a fuel assembly with reflecting boundary conditions on all surfaces is appropriate.

The calculations were performed with the Monte Carlo code KENO-Va from the SCALE 6 [14] system as transport solver, with reflecting boundary conditions on all surfaces to account for the 2D problem geometry. For comparison, the 2D S_N transport code NEWT was also applied. In all calculations, the SCALE 6 general-purpose 238-group ENDF/B-VII based library was used, along with the SCALE 6 covariance data for the uncertainty analyses. In both the calculation routes, the same spectral calculations with the SCALE modules BONAMI and CENTRM for the unresolved and resolved resonance regions were used to obtain problem specific multi-group data.

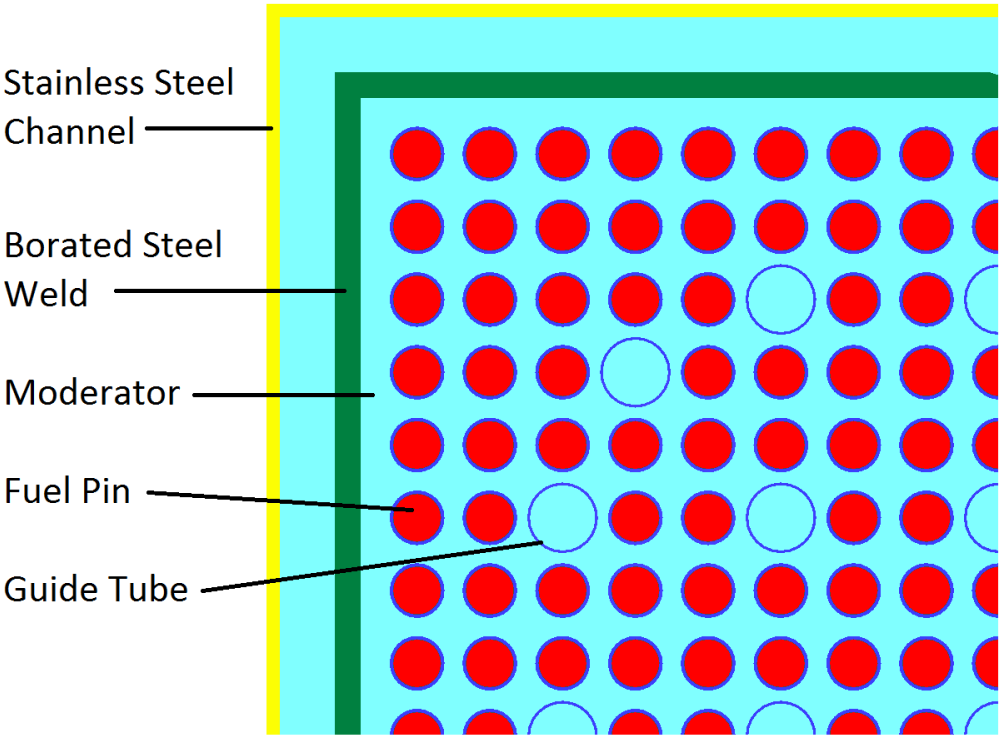

Fig. 1: Calculation model for the arrangement of the EG-UACSA benchmark phase II.

Uncertainty and Sensitivity Analysis with XSUSA were performed with both the deterministic transport solver NEWT and the Monte Carlo transport solver KENO-Va. In all cases, a sample size of 1000 was chosen (i.e. 1000 calculations with randomly varied nuclear data were performed). The high number of calculations is performed in order to be able to determine the main contributions to the total uncertainty. When using the deterministic code NEWT, there is no aleatoric uncertainty in the solution method, and therefore, the reference calculation with nominal nuclear data has to be repeated in full length with sampled nuclear data, leading to a multiplication of the calculation time by a factor of 1000. When using the Monte Carlo code KENO-Va, the conventional method of performing all calculations with sampled data using the same number of histories as for the reference calculations, leads to similar results. To be specific, 50 x 10^6 histories per run were used, resulting in a calculation time of approximately 25 min per run, practically the same as the time needed for one NEWT calculation. In this case, the aleatoric uncertainty due to the stochastic treatment of the neutron transport is estimated to be 0.01% per run, which is negligible as compared to the epistemic uncertainty of 0.42% due to the nuclear data covariance.
When reducing the number of Monte Carlo histories by a factor of 1000, i.e. applying only 50 x 10^3 histories per run, the corresponding aleatoric uncertainty of 0.35% is substantial and in the same order of magnitude as the epistemic uncertainty, leading

to a combined uncertainty which significantly overestimates the true epistemic uncertainty. By performing a second series of calculations and determining the covariance of these two series, one finally arrives at an uncertainty value which is practically identical to the true epistemic uncertainty. The gain in CPU time is dramatic: While approximately 400 hours were necessary to perform the 1000 long runs, the method just described takes less than 3 hours. These are wall clock times, i.e. the overhead arising from the nuclear data handling is already taken into account. These results are summarized in Table 1.

Table 1: Multiplication factors for the EG-UACSA Phase II benchmark and corresponding uncertainties due to nuclear data covariance obtained from NEWT and KENO-Va with sampled nuclear data. Reference results from single long runs, results from 1000 runs with a large number of neutron histories per run, from 1000 runs with a small number of neutron histories per run, and from 2 x 1000 runs with a small number of neutron histories per run after elimination the aleatoric uncertainties.

	k	*Δk/k aleatoric*	*Δk/k total*	*CPU time per run*	*CPU time total*
NEWT (ref.)	0.99212	-		25 min	
XSUSA/NEWT (1000 runs)	0.99226	-	0.424%	25 min	400 h
KENO (ref. long run)	0.99293	0.01%		25 min	
XSUSA/KENO (1000 long runs)	0.99308	0.01%	0.418%	25 min	400 h
XSUSA/KENO (1000 short runs)	0.99306	0.35%	0.544%	5 sec	1.5 h
XSUSA/KENO (2 x 1000 short runs)	0.99305	0.35%	0.411%	5 sec	3 h

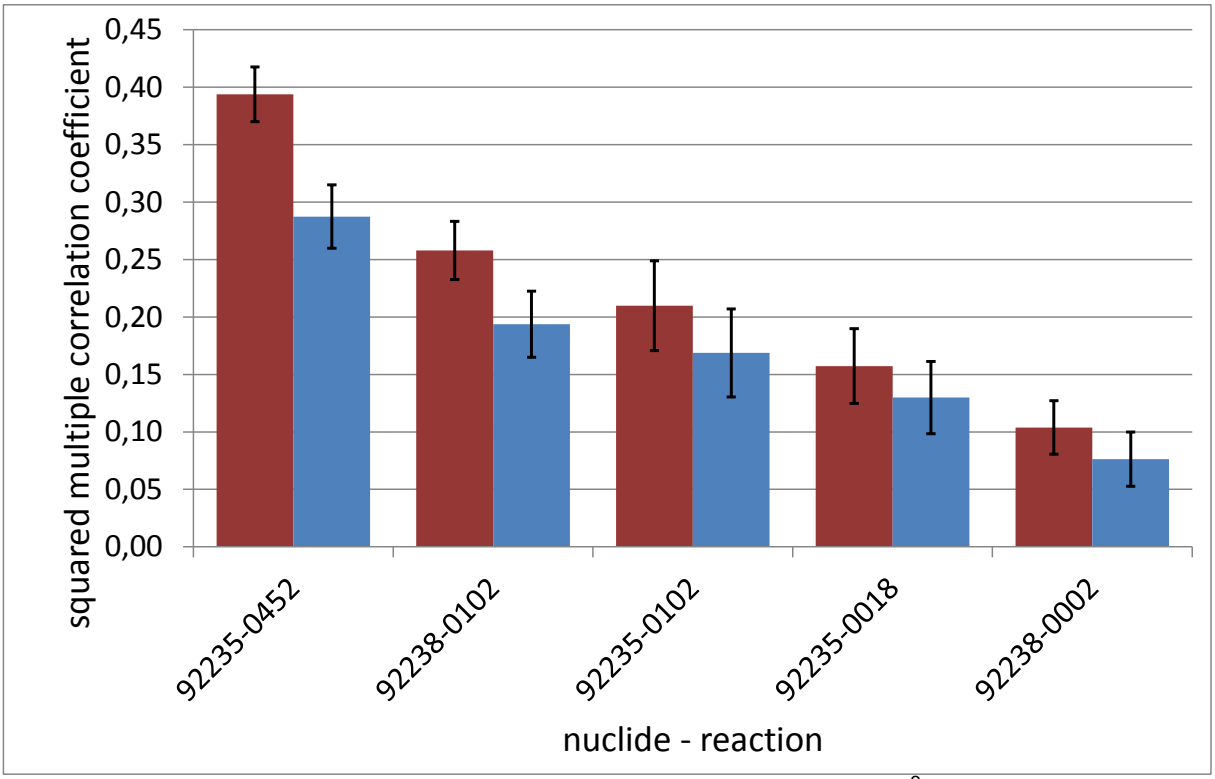

Fig. 2: Sensitivity results: Squared multiple correlation coefficients (R^2) from XSUSA/KENO for k-eff of the EG-UACSA Phase II benchmark. Red columns: 1000 long runs; blue columns: 2 x 1000 short runs. Reaction IDs: 2 = elastic scattering, 18 = fission, 102 = n,γ capture, 452 = prompt multiplicity.

In addition to the quantified output uncertainties, the corresponding sensitivities, i.e. the contributions to these uncertainties from individual nuclide/reaction combinations can be evaluated. To do this, the so-called “squared multiple correlation coefficient (R^2)” is used as sensitivity/uncertainty importance indicator for parameter groups. It can be interpreted as the relative amount of output uncertainty coming from the uncertainty of the respective parameter group. It is basically determined from correlations of the calculated output quantities with the sampled input quantities, i.e. with the sampled nuclear data, taking into account inter-dependencies of input quantities due to non-zero covariance terms [15]. These sensitivities are displayed in Fig. 2 for the five most important parameter groups, along with their 95% confidence intervals indicated by the error bars. It can be seen that the sensitivity values determined from the short Monte Carlo runs are generally smaller than those from the long runs. Obviously, this is due to the presence of additional non-negligible aleatoric uncertainties, such that the relative contributions from the groups become smaller. However, the importance ranking of the input quantities is the same from long and short runs, at least for the dominating parameter groups.

Summary and Conclusions

When performing sampling based uncertainty and sensitivity analyses for neutron transport problems with the Monte Carlo method, two kinds of uncertainties have to be considered, namely aleatoric uncertainties arising from the stochastic nature of the simulation procedure, and epistemic uncertainties arising from an incomplete knowledge of the values of input parameters. To determine the influence of the epistemic uncertainties alone, the sample calculations from epistemic sampling can traditionally be performed with a very large number of histories such that the aleatoric uncertainties become negligible and the total uncertainty practically only comes from the influence of the epistemic uncertainties. This procedure may be CPU time intensive. In the present paper, a method was applied which uses heavily reduced numbers of particle histories in each sample calculation, and, nevertheless, is able to largely eliminate the aleatoric uncertainty contribution introduced to the output.

Applying this approach, sampling based uncertainty and sensitivity analyses with nuclear covariance data were performed with the XSUSA code and KENO-Va from the SCALE 6 system as Monte Carlo transport solver, for an international criticality benchmark. Equivalent uncertainty and sensitivity results were obtained as compared to the traditional method of using very large numbers of histories in each sample calculation.

Thereby, computing times could be reduced by factors of the magnitude of 100. The use of multi-group nuclear data is no restriction, i.e. the described method can also be applied when using continuous energy nuclear data. The method can equally well be used for analyses with a Monte Carlo transport solver and epistemic uncertainties from other sources, like manufacturing tolerances. So far, the method was applied to stand-alone Monte Carlo criticality calculations; currently, investigations are being performed with calculations coupling Monte Carlo transport with depletion.

Acknowledgements

This work is supported by the German Federal Ministry of Economics and Technology.

References

1. A. Santamarina et al., “The JEFF-3.1.1 Nuclear Data Library,” JEFF Report 22, NEA No. 6807 (2009).
2. M. Herman, “Development of ENDF/B-VII.1 and Its Covariance Components”, Journal of the Korean Physical Society, 59, pp.1034–1039 (2011).
3. K. Shibata et al., “JENDL-4.0: A New Library for Innovative Nuclear Energy Systems,” Journal of the Korean Physical Society, 59, pp.1046–1051 (2011).
4. B.T. Rearden and D.E. Mueller, “Uncertainty Quantification Techniques of SCALE/TSUNAMI”, Trans. Am. Nucl. Soc., 104, pp.371-373 (2011).
5. I. Kodeli, “The SUSD3D Code for Cross-Section Sensitivity and Uncertainty Analysis – Recent Development,” Trans. Am. Nucl. Soc., 104, pp.791-793 (2011).
6. N. García-Herranz, O. Cabellos, J. Sanz, J. Juan, and J. C. Kuijper, “Propagation of Statistical and Nuclear Data Uncertainties in Monte Carlo Burnup Calculations,” Annals of Nucl. Energy, 35, pp.714-730 (2008).
7. O. Buss, A. Hoefer, and J.C. Neuber, “NUDUNA – Nuclear Data Uncertainty Analysis,” Proc. International Conference on Nuclear Criticality (ICNC 2011), Edinburgh, Scotland, Sep. 19-22, 2011, on CD-ROM (2011).
8. A. J. Koning and D. Rochman, “Towards Sustainable Nuclear Energy: Putting Nuclear Physics to Work,” Annals of Nucl. Energy, 35, pp.2024-2030 (2008).
9. W. Zwermann, B. Krzykacz-Hausmann, L. Gallner, A. Pautz, “Influence of Nuclear Covariance Data on Reactor Core Calculations,” Proc. Second International Workshop on Nuclear Data Evaluation for Reactor Applications (WONDER 2009), Cadarache, France, 29 Sep. - 2 Oct., 2009, pp.99-104 (2009).
10. M. Kirsch, V. Hannstein, and R. Kilger, “Applications of the SUnCISTT: Monte Carlo Sampling on Uncertain Technical Parameters in Criticality and Burn-Up Calculations,” Proc. International Conference on Nuclear Criticality (ICNC 2011), Edinburgh, Scotland, Sep. 19-22, 2011, on CD-ROM (2011).
11. B. Krzykacz, E. Hofer, M. Kloos, “A Software System for Probabilistic Uncertainty and Sensitivity Analysis of Results from Computer Models,” Proc. International Conference on Probabilistic Safety Assessment and Management (PSAM-II), San Diego, Ca., USA, (1994).
12. W. Zwermann, B. Krzykacz-Hausmann, L. Gallner, M. Klein, A. Pautz, K. Velkov, “Aleatoric and Epistemic Uncertainties in Sampling Based Nuclear Data Uncertainty and Sensitivity Analyses”, Proc. International Conference on the Physics of Reactors (PHYSOR 2012), Knoxville, TN, USA, 15 – 20 Apr. 2012, to be published.
13. J. C. Neuber, “Proposal for an UACSA benchmark study on the reactivity impacts of manufacturing tolerances of parameters characterizing a fuel assembly configuration,” available online at http://www.oecd-nea.org/science/wpncs/UACSA/.
14. “SCALE: A Modular Code System for Performing Standardized Computer Analyses for Licensing Evaluation, Version 6“, ORNL/TM-2005/39 (2009).
15. H. Glaeser, B. Krzykacz-Hausmann, W. Luther, S. Schwarz, T. Skorek, “Methodenentwicklung und exemplarische Anwendungen zur Bestimmung der Aussagesicherheit von Rechenprogrammergebnissen,“ Technical Report GRS-A-3443 (2008).

Hindawi Publishing Corporation
Science and Technology of Nuclear Installations
Volume 2012, Article ID 767096, 9 pages
doi:10.1155/2012/767096

Anhang B10

Research Article

A Two-Step Approach to Uncertainty Quantification of Core Simulators

Artem Yankov,[1] Benjamin Collins,[1] Markus Klein,[2] Matthew A. Jessee,[3] Winfried Zwermann,[2] Kiril Velkov,[2] Andreas Pautz,[2] and Thomas Downar[1]

[1] *Department of Nuclear Engineering and Radiological Sciences, University of Michigan, 2355 Bonisteel Boulevard, Ann Arbor, MI 48109, USA*
[2] *Reactor Safety Research Division, Gesellschaft für Anlagen- und Reaktorsicherheit (GRS) mbH, Boltzmannstraße 14, 85748 Garching bei München, Germany*
[3] *Reactor and Nuclear Systems Division, Oak Ridge National Laboratory, P.O. Box 2008 MS6172, Oak Ridge, TN 37831, USA*

Correspondence should be addressed to Artem Yankov, yankovai@umich.edu

Received 30 July 2012; Accepted 7 December 2012

Academic Editor: Kostadin Ivanov

For the multiple sources of error introduced into the standard computational regime for simulating reactor cores, rigorous uncertainty analysis methods are available primarily to quantify the effects of cross section uncertainties. Two methods for propagating cross section uncertainties through core simulators are the XSUSA statistical approach and the "two-step" method. The XSUSA approach, which is based on the SUSA code package, is fundamentally a stochastic sampling method. Alternatively, the two-step method utilizes generalized perturbation theory in the first step and stochastic sampling in the second step. The consistency of these two methods in quantifying uncertainties in the multiplication factor and in the core power distribution was examined in the framework of phase I-3 of the OECD Uncertainty Analysis in Modeling benchmark. With the Three Mile Island Unit 1 core as a base model for analysis, the XSUSA and two-step methods were applied with certain limitations, and the results were compared to those produced by other stochastic sampling-based codes. Based on the uncertainty analysis results, conclusions were drawn as to the method that is currently more viable for computing uncertainties in burnup and transient calculations.

1. Introduction

Computational modeling of nuclear reactor stability and performance has evolved into a multiphysics and multiscale regime. Various computer codes have been developed and optimized to model individual facets of reactor operation such as neutronics, thermal hydraulics, and kinetics. These codes are most often coupled to produce more realistic results. While it is crucial to produce best-estimate calculations for the design and safety analysis of nuclear reactors, it is equally important to obtain design margins by propagating uncertainty information through the entire computational process. The purpose of the OECD (Organization for Economic Cooperation and Development) Uncertainty Analysis in Modeling (UAM) benchmark is to produce a framework for the development of uncertainty analysis methodologies in reactor simulations [1]. Three phases comprise the benchmark, with each phase building in scale on its predecessors. The first phase deals with uncertainties in neutronics calculations, the second phase deals with neutron kinetics, and the final phase requires the propagation of uncertainties through coupled neutronics/thermal-hydraulics simulations.

The neutronics phase of the UAM benchmark deals specifically with the propagation of input parameter uncertainties to uncertainties in output parameters on a full-core scale. In the established framework of full-core analyses, lattice homogenized few-group cross sections are used as inputs to core simulators. Core simulators utilize a number of approximations to the exact transport equation, effectively introducing uncertainties into output parameters. Geometrical uncertainties and numerical method simplifications can also be attributed to the introduction of modeling uncertainties. While it is important to propagate all known uncertainties when conducting a thorough uncertainty analysis,

the necessary methods to make this possible must still be developed. However, rigorous methods already have been developed to propagate cross section uncertainties from lattice transport solvers to core simulators. Consequently, few-group homogenized cross section errors are assumed for now to be the sole source of uncertainty in the subsequent analyses.

Two methods already exist for propagating cross section uncertainties through core simulators. The first method is commonly referred to as the stochastic sampling (Monte Carlo) method. The XSUSA (Cross Section Uncertainty and Sensitivity Analysis) code system is representative of this approach [2]. XSUSA was developed by GRS based on the SUSA code package [3]. An alternate approach, the two-step method, utilizes generalized perturbation theory in the first step and stochastic sampling in the second step [4, 5]. The purpose of this paper is to show consistency between these two methods in the framework of phase I-3 of the UAM benchmark. As defined in the UAM benchmark specifications, the Three Mile Island Unit 1 (TMI) core will be the focus of application for the XSUSA and two-step methods. The TMI core is chosen for analysis mainly because it has been the focus of past benchmark problems and is therefore of great familiarity in the nuclear engineering community [6].

The two-step method is motivated largely by the computationally expensive solution of the transport equation. In the stochastic sampling approach there is effectively a one-to-one mapping between the solutions of the transport equation and the set of homogenized cross section inputs for a core simulator. Alternatively, for practical problems the two-step method provides a means by which an unlimited number of core simulator inputs can be generated at the cost of relatively few transport-type solutions. The means mentioned above is a few-group covariance matrix whose elements are generated with linear perturbation theory. Hence, the quality of the core simulator inputs produced by the two-step method is limited by the extent to which linear perturbation theory can describe the system under study. Contrarily, stochastic sampling through the XSUSA approach produces core simulator random inputs whose distributions are not subject to linear approximations. This paper shows that the linear approximations used in the two-step method can be remarkably accurate.

2. Methodology

Both the stochastic and two-step methods actively use the modules in SCALE to propagate cross section uncertainties [7]. Also, both methods make strong use of SCALE's 44-group covariance library. The multigroup cross sections are assumed to follow a multivariate normal distribution and so expected values and a covariance matrix suffice to fully describe the distribution. In the XSUSA approach, all input parameters are varied simultaneously, and the number of required calculations to achieve a certain statistical accuracy in output parameters of interest is independent of the number of inputs [2]. The number of required runs can be calculated by Wilks' formula, which gives the confidence level that the maximum code output will not exceed with some specified probability. Contrarily, the two-step method depends on the number of input parameters since each input requires a transport-like solution. The two different methodologies are summarized below.

2.1. XSUSA Approach. The covariance matrix between inputs plays a central role in stochastic sampling. Cross section uncertainties are correlated, and the degree of correlation can be described by a covariance matrix. Cross section uncertainties must be perturbed such that their correlation relations are always preserved. If $\overline{X}$ is a vector of mean values whose covariance relations are defined by the matrix $\overline{\overline{\Sigma}}$, then correlated random variables $\overline{X}'$ can be generated by applying [8]

$$\overline{X}' = \overline{X} + \overline{\overline{A}}^T \overline{Z}. \tag{1}$$

In (1) the operator $\overline{\overline{A}}^T$ is the upper right triangular matrix obtained by taking the Cholesky decomposition of the covariance matrix. Every covariance matrix is Hermitian and positive definite; thus, all covariance matrices have a Cholesky decomposition $\overline{\overline{\Sigma}} = \overline{\overline{A}}^T \overline{\overline{A}}$. The vector $\overline{Z}$ in (1) is a random normal vector. When $\overline{\overline{A}}^T$ multiplies $\overline{Z}$, linear combinations of the uncertainties are taken in accordance with their covariance relations, and so $\overline{X}'$ is normally distributed with covariance $\overline{\overline{\Sigma}}$.

Hence, to produce perturbed cross sections $\overline{X}'$, only the Cholesky decomposition of the cross section's covariance matrix is needed along with a random normal vector. In the XSUSA approach, ENDF/B-VII nuclear data in the SCALE 238-group structure are used. Spectral calculations are performed in BONAMI and CENTRM to produce a problem-specific cross section library, as seen in Figure 1. By use of SCALE's 44-group covariance library with the problem-specific library generated by the spectral calculations, the XSUSA code applies perturbations to create a set of N varied, problem-dependent cross section libraries. Specifically, the MEDUSA module samples the 44-group covariance library that is enlarged to accommodate all problem-specific nuclides and reactions. CLAROL-plus then takes the output from MEDUSA and creates a problem-specific multigroup library. The XSUSA code works to make sure varied data are physically consistent. This procedure does not include the implicit effects of uncertainties in self-shielding, but extensions are currently being made to include these effects [9].

Each set of N cross section libraries produced by XSUSA is passed to SCALE's lattice physics transport solver NEWT, which in turns produces N perturbed, homogenized, few-group cross section libraries. The perturbed few-group libraries are then used as input for core simulators such as PARCS [11] and QUABOX/CUBBOX [12]. Once all N libraries are processed by the core simulator, statistics can be taken on the output parameters of interest. As indicated in Figure 1, NEWT can be replaced by any of SCALE's

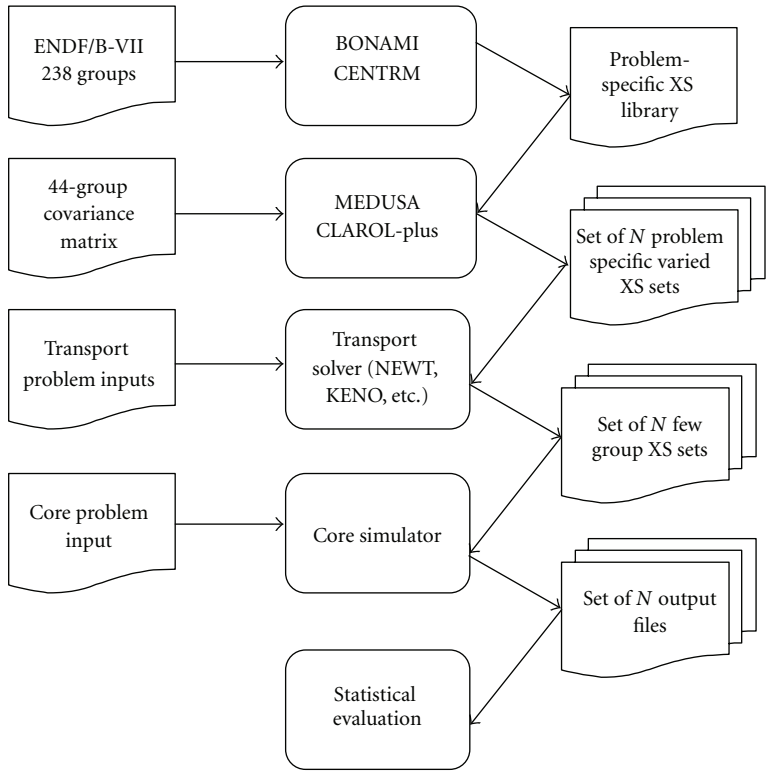

Figure 1: Flow diagram of the XSUSA approach starting from use of the ENDF/B-VII 238-group library and ending with a statistical evaluation of output parameters.

transport solvers. For example, XSDRN can be used for one-dimensional (1D) calculations and KENO for Monte Carlo reference solutions [2].

2.2. Two-Step Method. Unlike the XSUSA approach, the two-step method is only partly based on sampling techniques. In the first step it makes use of the generalized adjoint for the transport equation [13]. In the two-step method, problem-dependent self-shielded data are also generated before any perturbed cross sections are calculated, as seen in Figure 2. Using the problem-dependent cross sections, the TSUNAMI module is applied to calculate the forward transport, adjoint transport, and generalized adjoint transport solutions to the problem at hand. The SCALE module SAMS then uses the problem solutions to calculate sensitivity coefficients for responses of interest. A response R_{xG} for reaction type x in broad-group G is defined as a ratio of inner products with the forward neutron flux [10]:

$$R_{xG} = \frac{\langle H_1 \Phi \rangle}{\langle H_2 \Phi \rangle}. \tag{2}$$

The explicit sensitivity coefficient of the response R_{xG} with respect to some nuclear data parameter σ_{ng} in the transport equation is then given as [10]

$$\frac{\partial R_{xG}}{\partial \sigma_{ng}} = \frac{\left\langle \Phi\left(\partial H_1/\partial \sigma_{ng}\right)\right\rangle}{\langle \Phi H_1 \rangle} - \frac{\left\langle \Phi\left(\partial H_2/\partial \sigma_{ng}\right)\right\rangle}{\langle \Phi H_2 \rangle} + \left\langle \Gamma^*_{xG} \frac{\partial (L - \lambda P)}{\partial \sigma_{ng}} \Phi \right\rangle, \tag{3}$$

where Φ is the solution of the forward transport equation, L is the migration and loss operator, and P is the production operator.

The generalized adjoint Γ^*_{xG} can be obtained by solving the generalized adjoint transport equation in [10]

$$(L^* - \lambda P^*)\Gamma^*_{xG} = \frac{1}{R_{xG}} \frac{dR_{xG}}{d\Phi}. \tag{4}$$

The solution of (4) requires the solution of the adjoint transport problem for each response. The pertinent responses of interest are the homogenized few-group cross sections needed for core simulators. Equations (3) and (4) above are used to compute explicit sensitivity coefficients. The TSUNAMI methodology incorporates implicit sensitivity effects arising from resonance self-shielding [10].

If the covariance matrix $\overline{\overline{C}}_i$ of some input parameters is available along with the sensitivities $\overline{\overline{S}}$ relating the change in outputs with respect to the change in input parameters, the "sandwich rule" can be applied to obtain a covariance matrix for the outputs $\overline{\overline{C}}_o$. The "sandwich rule" is expressed in [14]

$$\overline{\overline{C}}_o = \overline{\overline{S}}\,\overline{\overline{C}}_i \overline{\overline{S}}^T. \tag{5}$$

Consequently, since $\overline{\overline{C}}_i$ is the SCALE 44-group covariance matrix, a covariance matrix for the few-group homogenized cross sections can be obtained. The SCALE module TSUNAMI-IP is used to generate a global covariance matrix relating the few-group cross sections in each assembly and

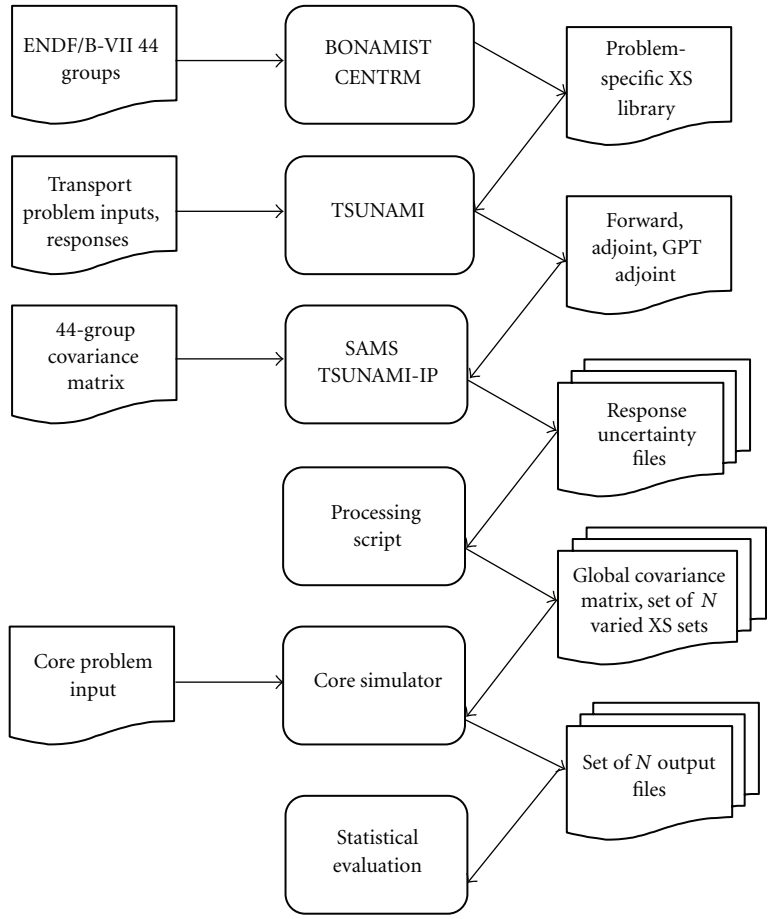

Figure 2: Flow diagram for the proposed two-step method, which mainly utilizes the generalized perturbation theory modules in SCALE [10].

reflector regions comprising a full-core problem. With (1), this global covariance matrix is sampled to produce N perturbed cross section libraries that can then be used as input for a core simulator. By applying the XSUSA and two-step methods to calculate uncertainties in output parameters of interest for the full-core TMI problem, it can be shown that the two different approaches produce consistent results.

3. Application

3.1. Implementation. The computational implementation of the two-step and XSUSA methods strays somewhat from their theoretical formulations. Specifically, modifications must be made since the generalized perturbation theory capabilities in SCALE are currently limited to only some of the responses required by core simulators. First, the TSUNAMI module currently cannot compute the uncertainty in the few-group homogenized transport cross section. However, uncertainties in the total and scatter cross sections can be calculated. To approximate perturbations to the transport cross section, is used the following:

$$\Sigma^*_{tr,G} = \Sigma_{t,G} - \overline{\mu}\Sigma_{s,G}. \quad (6)$$

The average cosine of the scattering angle $\overline{\mu}$ is held constant while the total cross sections $\Sigma_{t,G}$ and scatter cross sections $\Sigma_{s,G}$ are perturbed to yield an effectively perturbed transport cross section $\Sigma^*_{tr,G}$ that can be used as input to a core simulator. Normally a critical spectrum based on either the P1 or B1 approximation is utilized to compute few-group cross sections. However, the critical spectrum cannot be correctly accounted for in the TSUNAMI generalized perturbation theory methodology. Consequently, in the proceeding analysis the default B1 critical spectrum calculation in SCALE is disabled in favor of the simplified P1 formulation shown in (6). Similarly, TSUNAMI does not generate uncertainties for kappa, the average energy release per fission event. To calculate a perturbed kappa-fission cross section, the average value of kappa $\overline{\kappa}$ is multiplied by a perturbed fission cross section $\Sigma_{f,G}$ to obtain an effectively perturbed kappa-fission cross section $\kappa\Sigma^*_{f,G}$ as shown in

$$\kappa\Sigma^*_{f,G} = \overline{\kappa}\Sigma_{f,G}. \quad (7)$$

A more subtle modification must be made when calculating the uncertainties in assembly discontinuity factors (ADFs). At the assembly level where reflective boundary conditions are used, TSUNAMI can approximate ADF uncertainties

very well by taking the ratio of the average flux of a thin surface at the assembly boundary to the assembly averaged flux [15]. A cell volume normalization factor is also needed to account for the size of the thin surface at the assembly boundary. While this approach is valid for an infinite system, TSUNAMI is currently not capable of accurately quantifying ADF uncertainties at reflector interfaces due to leakage effects. To calculate uncertainties in few-group ADFs along reflector interfaces, a method developed by Yankov et al. is used [15]. The method is based on the 1D adjoint diffusion approximation generally used to treat reflector interface ADFs, the neutron balance equation on a fuel assembly/reflector interface, and the "sandwich rule."

The two-step method is presented algorithmically in Table 1. The majority of the algorithm consists of file manipulations. In the second step of the algorithm, it is important to check that the global covariance matrix produced by TSUNAMI-IP is positive definite. The global covariance matrix consists of examining the correlations among few-group cross sections between all assemblies in the core. Use of a global covariance matrix is essential when sampling cross sections for an entire core, since otherwise the similarity of the nuclide composition of different fuel assembly types is neglected. If the global covariance matrix is not used, the output parameter uncertainties can be greatly misrepresented. In most cases, the global covariance matrix produced by TSUNAMI-IP will only be nearly positive definite due to a lack of diagonal dominance. However, the matrix can be made more diagonally dominant by multiplying the matrix's off-diagonal terms by $1 - \epsilon$ for some very small value ϵ.

Note that the XSUSA approach does not require any of these modifications since it is fundamentally a statistically based approach, whereas the two-step method uses a deterministic approach in the first step.

Table 1: Algorithm for applying the two-step method using SCALE and a core simulator.

(1)	For each assembly and reflector in the core, create a TSUNAMI-2D input file. In each input, responses should correspond to the few-group total, absorption, nu-fission, fission, Chi, and scatter cross sections. Responses for ADFs should also be specified. The TSUNAMI-2D input files can be executed in parallel.
(2)	From the ".sdf" sensitivity files in TSUNAMI-2D outputs, use TSUNAMI-IP to generate a global covariance matrix along with mean and standard deviations of the responses. Verify that the global covariance matrix is positive definite.
(3)	Sample the covariance matrix to produce N perturbed cross section sets. Using (6) and (7), process the perturbed cross sections to obtain perturbed values for the transport and kappa-fission cross sections. Also, apply the method developed by Yankov et al. [15] to determine uncertainties in the reflector ADFs.
(4)	Using each set of perturbed cross sections, produce N input files for the core simulator.
(5)	Execute the core simulator N times using a different cross section set each time. These executions can be done in parallel.
(6)	Scanning the core simulator's N output files, extract relevant data. Perform a statistical analysis on the relevant output data.

3.2. Results

3.2.1. Pin-Cell Calculations. Before the two-step and XSUSA methods are applied to a full core problem, it is prudent to perform a preliminary investigation on an easily tractable problem. Such a tractable problem consists of a single TMI pin-cell, as defined in the UAM benchmark [1]. Since the two methods of interest fundamentally work with covariances, the preliminary investigation will compare how the two-step and XSUSA methods can calculate variances and covariances for few-group parameters. Recall that SCALE/TSUNAMI, the underlying code system used in the two-step method, considers both the explicit and implicit contributions from cross sections. The XSUSA method only considers explicit effects for the same perturbations. Consequently, to produce a fair comparison the implicit sensitivity coefficient component is disabled in TSUNAMI. To this end, 1000 XSUSA samples of few-group scatter and fission cross sections are compared to those produced by the modified TSUNAMI code.

First, the standard deviations for the scatter and fission cross sections are compared in Figure 3, which depicts ratios of standard deviations produced by XSUSA and SCALE. In Figure 3, two different SCALE results are shown. The first result, labeled "GPT(explicit)," considers only the explicit sensitivity coefficients in SCALE. The second result, labeled "GPT(explicit, XSUSA)," not only considers the explicit sensitivity coefficients but also utilizes the same perturbation factors generated by the XSUSA simulations. For an in-depth discussion of how perturbation factors are used in the pertinent methodologies the interested reader is referred to [16]. Ideally, all ratios in Figure 3 would be identical unity in the case where the responses depend linearly on the uncertain parameters. However, since XSUSA is a statistical method, some variability is present in the results. Some variability can also result from nonlinear phenomena. When the same perturbation factors are used in SCALE and XSUSA, all points are well contained in the 95% confidence interval bounds. The same phenomenon can be observed when the generalized perturbation theory and statistically generated covariance matrices are compared in Figure 4.

In Figure 4 the correlation coefficients should ideally lay along the dotted line, representing a one-to-one relationship. Figure 4(b) has points concentrated more closely around the dotted line because identical perturbation factors are used in XSUSA and SCALE. All effects considered, the slight discrepancies visible in Figure 4(b) must be from nonlinear effects. The black lines bounding the points in Figure 4 represent the 95% confidence bounds for the correlation coefficients calculated with the Fisher transformation [17].

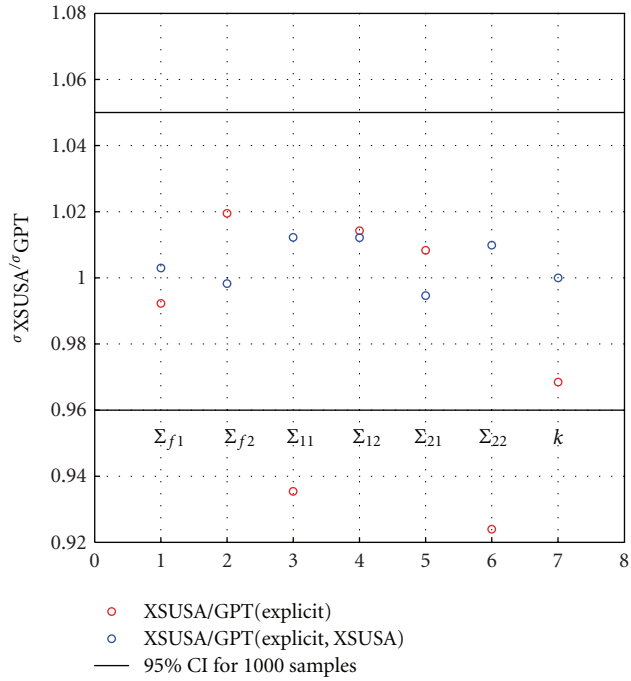

Figure 3: The ratio of the stochastic to generalized perturbation theory standard deviations of few-group cross sections. The independent axis represents various cross section indices.

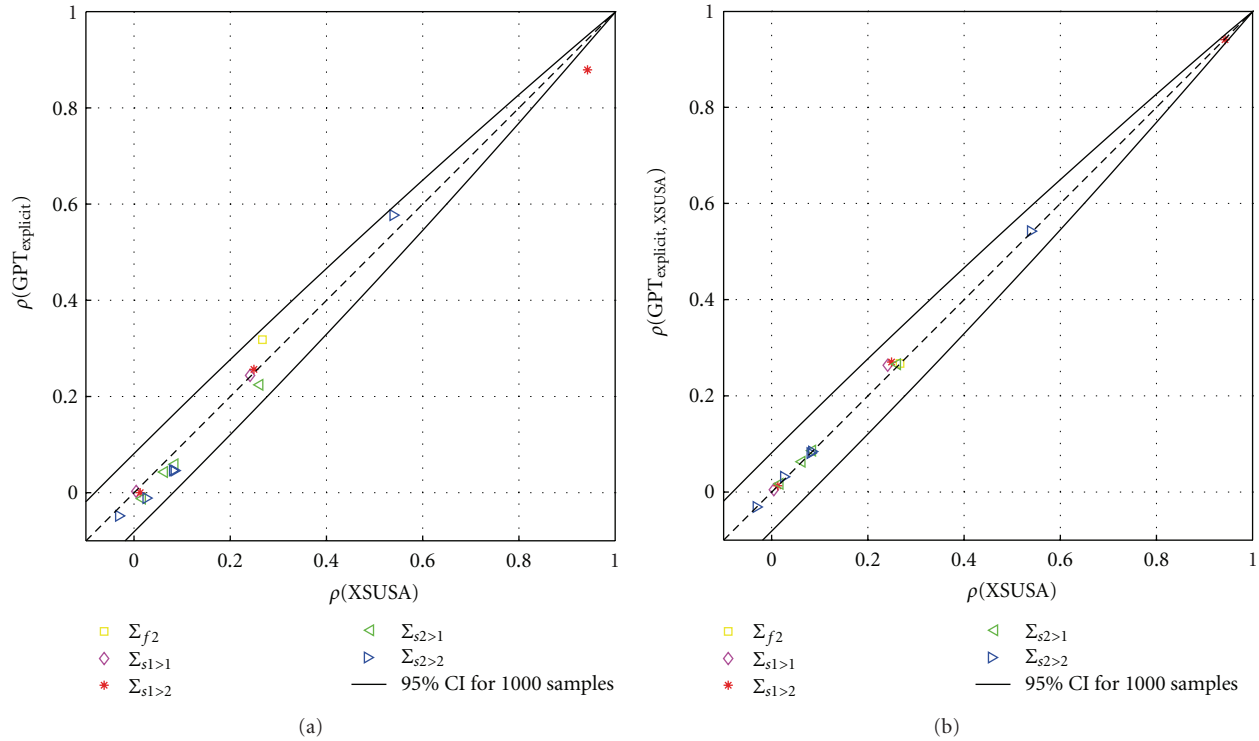

Figure 4: Correlation coefficients calculated by XSUSA compared to those calculated by SCALE. (a) Only the explicit effect is represented in the SCALE coefficients. (b) The explicit effect and the XSUSA perturbation factors are considered.

Table 2: Uncertainty in the effective multiplication factor from using the two-step and XSUSA methods with a sample size of 290.

	Two-step method	XSUSA method	Absolute difference (pcm)
k-eff mean	1.30268	1.30330	62
k-eff stand. deviation	0.00569	0.00564*	5
Relative SD %	0.43706	0.43272	

* The 95% confidence interval is [0.00522, 0.00614].

Table 3: Uncertainty in the effective multiplication factor from using "one-step" schemes.

	XSUSA/KENO	TSUNAMI-3D	Absolute difference (pcm)
k-eff mean	1.30294	1.30279	15
k-eff stand. deviation	0.00608*1	0.00588*2	20
Relative SD %	0.46679	0.45120	

*1 The 95% confidence interval is [0.00563, 0.00661]. *2The 95% confidence interval is [0.00544, 0.00639].

3.2.2. Full-Core Calculations. The TMI core under consideration consists of 11 different UO_2 assemblies and a reflector region placed in 1/8 symmetry. All control rods are ejected from the core, which is at hot zero power [1]. By use of the XSUSA and two-step methods, uncertainties are obtained for the core-wide multiplication factor and for the assembly-wise relative power distribution. For a two-group formulation, each assembly in the TMI core requires 11 perturbed cross sections. These are the transport, absorption, kappa-fission, and nu-fission cross sections along with a down-scatter cross section and two ADFs. The reflector region requires only 7 cross section inputs for a total of 128 perturbed cross sections per core simulation.

The core simulator utilized for the proceeding analysis is PARCS. The multigroup NEM nodal kernel is used to execute all 290 core simulations [11]. Initially 300 core simulations were proposed, but some of the cross section perturbations in the two-step method were too large, so PARCS was unable to produce a converged solution. The large number of core simulations ensures that the largest output values obtained will not be exceeded with a high probability by Wilks' formula. The multiplication factor uncertainty results obtained with the XSUSA and two-step methods for the TMI core are summarized in Table 2. The table clearly shows that the XSUSA and two-step methods can consistently calculate uncertainties in the multiplication factor.

Both the "one-step" reference solutions and the two-step and XSUSA methods produced results that are well within statistical uncertainty of each other, as evidenced by comparing Tables 2 and 3. The agreement between the "one-step" reference solutions and between the two-step and XSUSA methods appears to be better than the overall agreement among all four calculation schemes.

The mean power distributions obtained from the XSUSA/PARCS and two-step methods are shown in Figure 5 along with XSUSA/KENO reference solutions. The values displayed in Figure 5 are relative power distributions such that the mean power in the core is unity. As expected, the mean power distributions predicted by the XSUSA and two-step methods are very similar, with the largest node-wise discrepancy being less than 1%. The relative standard deviation (%) in power for each node is shown in Figure 6.

Before looking at the numerical values of the uncertainty in the core power distribution calculated by the three methods in Figures 6 and 7, it is evident that the distribution of uncertainty is spread evenly in all the methods. Uncertainties with the highest magnitudes congregate around the center of the core. This is due to the radial heterogeneity of the core configuration [18]. The two-step method seems to attribute less uncertainty overall to each nodal power. Although the reasons for this observation are currently under investigation, the authors have noticed that the relative power distribution uncertainties are particularly sensitive to the way in which uncertainties are propagated to the transport cross section in the two-step method.

4. Conclusions

The core simulator output uncertainties for the TMI core obtained with the XSUSA and two-step methods indicate that both methods are consistent in general and are able to propagate nuclear data uncertainties to the core simulator. However, further investigation is needed to explain some of the discrepancies observed between the two methods, especially in the calculation of uncertainty in the relative power distribution. Since the TMI core used in this analysis is relatively homogeneous, the linear approximations employed by the two-step method are completely satisfactory. While the authors anticipate that the linear approximations will hold for more inhomogeneous cores, such as the MOX cores specified in the UAM benchmark [1], this matter should be examined in greater detail.

Despite some of the current limitations of the generalized perturbation theory implementations in SCALE, both uncertainty quantification methods yield an uncertainty of $\Delta k = 0.5\%$ in the core simulator k-effective. Currently, the limitations of generalized perturbation theory as applied in the two-step method make the XSUSA approach a more robust choice for reactor uncertainty analysis. In order to perform a steady-state uncertainty analysis, methods should be developed in the current generalized perturbation theory framework in SCALE to capture all uncertainty within reach of the XSUSA approach. Methods should

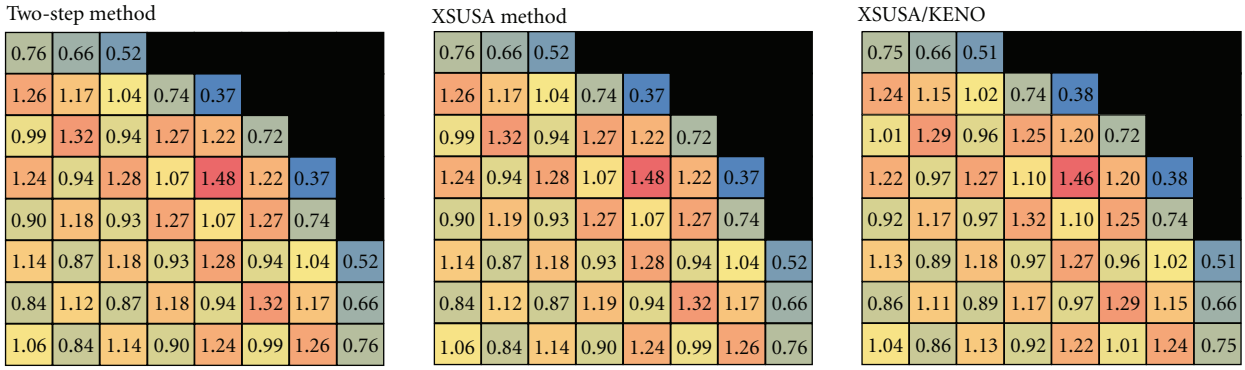

Figure 5: Mean power distribution calculated by the two-step and XSUSA methods along with the XSUSA/KENO reference. Values shown are calculated such that unity is the core average power. Quarter symmetry is displayed.

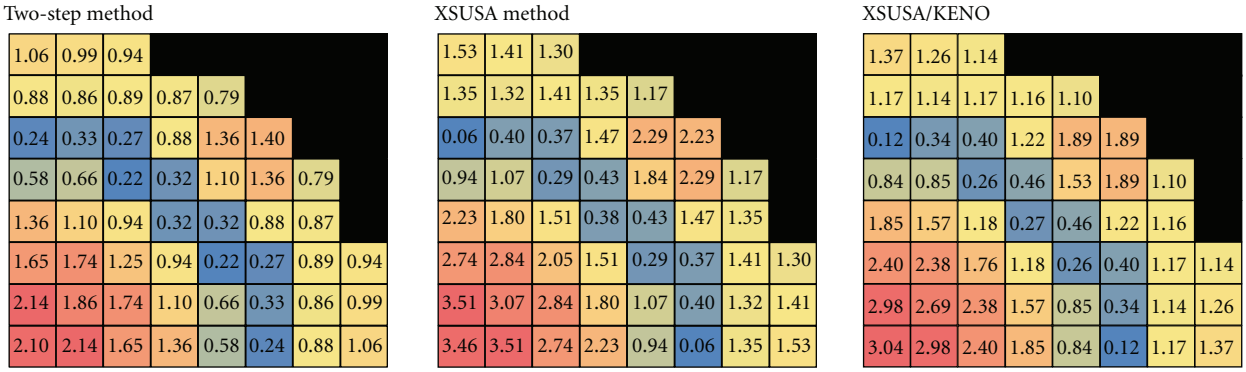

Figure 6: Relative standard deviation (%) calculated by the two-step and XSUSA methods along with the XSUSA/KENO reference. Uncertainties in assembly discontinuity factors are included. Quarter symmetry is displayed.

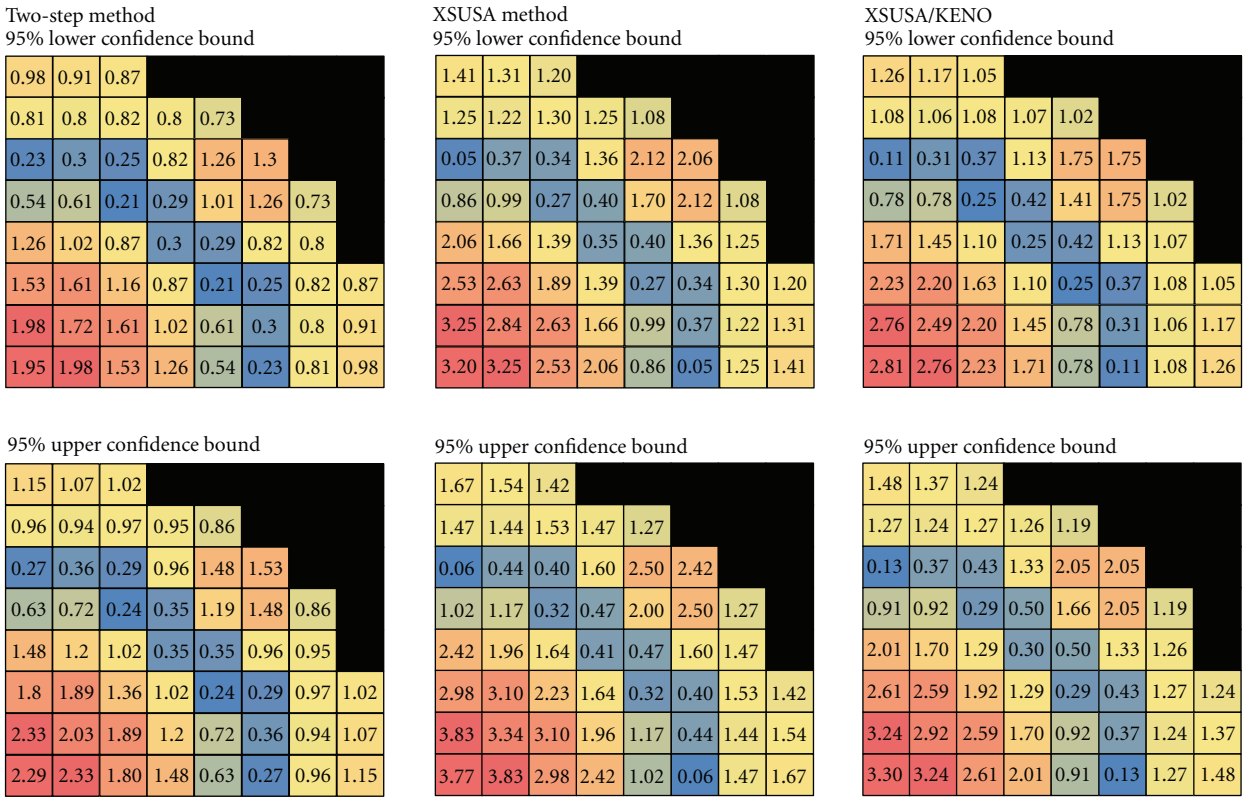

Figure 7: The 95% confidence bounds are shown for the relative standard deviations corresponding to Figure 6.

also be developed so that two-step-type methods can be applied to burnup and transient calculations, as defined in phases II-III of the UAM benchmark. The XSUSA approach already allows for such calculations, as evident from [16, 19].

In terms of efficiency, the XSUSA and two-step methods require similar computation times if parallel computing is employed. For the TMI core, 128 transport-like solutions on an assembly were required to obtain a global covariance matrix in TSUNAMI, one solution for each response. To obtain the desired statistical accuracy this covariance matrix was sampled around 300 times. Relatively speaking, sampling the covariance matrix and running the perturbed cross sections through a core simulator are free. Since no covariance matrix is used in the XSUSA approach, some 3600 full transport solutions on an assembly are needed to be able to execute 300 core simulations (11 assemblies plus 1 reflector, multiplied by 300 perturbed cross section sets). To summarize, for full-core problems the computational burden is much less when the two-step method is used. However, due to the nature of parallel processing the two-step and XSUSA methods can take the same amount of time. Overall, more work should be done with the two-step method to make it a viable tool for uncertainty quantification in core simulations. However, the results in this paper suggest that the two-step method can be made to be fully consistent with more versatile stochastic methods.

Acknowledgments

This work was supported by the German Ministry of Economics and Technology and the US Nuclear Regulatory Commission. This paper has been authored by UT-Battelle LLC under Contract no. DE-AC05-00OR22725 with the U.S. Department of Energy. The United States Government retains and the publisher, by accepting the paper for publication, acknowledges that the United States Government retains a nonexclusive, paid-up, irrevocable, world-wide license to publish or reproduce the published form of this paper, or allow others to do so, for the United States Government purposes.

References

[1] K. Ivanov, M. Avramova, I. Kodeli, and E. Sartori, *Benchmark for Uncertainty Analysis in Modeling (UAM) for Design, Operation and Safety Analysis of LWRs*, Rep. NEA/NSC/DOC(2007) 23, Nuclear Energy Agency, 2nd edition, 2007.

[2] M. Klein, L. Gallner, B. Krzykacz-Hausmann, A. Pautz, and W. Zwermann, "Influence of nuclear data uncertainties on reactor core calculations," *Kerntechnik*, vol. 76, no. 3, pp. 174–178, 2011.

[3] B. Krzykacz, E. Hofer, and M. Kloos, "A software system for probabilistic uncertainty and sensitivity analysis of results from computer models," in *Proceedings of the International Conference on Probabilistic Safety Assessment and Management (PSAM '94)*, San Diego, Calif, USA, 1994.

[4] M. Williams, M. A. Jessee, R. Ellis, and B. Rearden, "Sensitivity and uncertainty analysis for OECD UAM benchmark of peach bottom BWR," in *Proceedings of the 4th Uncertainty Analysis in Modelling Benchmark Meeting*, Pisa, Italy, April 2010.

[5] A. Yankov, M. Klein, M. A. Jessee et al., "Comparison of XSUSA and "two-step" approaches for full-core uncertainty quantification," in *Proceedings of the International Conference on the Physics of Reactors (PHYSOR '12)*, Knoxville, Tenn, USA, April 2012.

[6] K. Ivanov, T. M. Beam, A. J. Baratta, A. Irani, and N. Trikouros, "Pressurised water reactor Main Steam Line Break (MSLB) benchmark," Tech. Rep. NEA/NSC/DOC(99)8, Nuclear Energy Agency, 1999.

[7] *SCALE: A Comprehensive Modeling and Simulation Suite for Nuclear Safety Analysis and Design*, ORNL/TM-2005/39, Version 6. 1, Radiation Safety Information Computational Center at Oak Ridge National Laboratory as CCC-785, Oak Ridge, Tenn, USA, 2011.

[8] P. R. Bevington and K. Robinson, *Data Reduction and Error Analysis for the Physical Sciences*, McGraw-Hill, Boston, Mass, USA, 2003.

[9] M. Williams, D. Wiarda, H. Smith et al., "Development of a statistical sampling method for uncertainty analysis with scale," in *Proceedings of the International Conference on the Physics of Reactors (PHYSOR '12)*, Knoxville, Tenn, USA, April 2012.

[10] M. A. Jessee, M. L. Williams, and M. D. DeHart, "Development of generalized perturbation theory capability within the scale code package," in *Proceedings of the International Conference on Mathematics, Computational Methods, and Reactor Physics (M&C '09)*, Saratoga Springs, New York, NY, USA, May 2009.

[11] T. Downar, Y. Xu, and V. Seker, "PARCSv3. 0 Theory Manual," UM-NERS-09-001, October 2009.

[12] S. Langenbuch and K. Velkov, "Overview on the development and application of the coupled code system ATHLET—QUABBOX/CUBBOX," in *Proceedings of the Mathematics and Computation, Supercomputing, Reactor Physics and Nuclear and Biological Applications*, Avignon, France, September 2005.

[13] M. Williams, "Perturbation theory for nuclear reactor analysis," in *CRC Handbook of Nuclear Reactor Calculations*, vol. 3, pp. 63–188, 1986.

[14] M. A. Jessee, *Cross section adjustment techniques for BWR adaptive simulation [Dissertation]*, North Carolina State University, Raleigh, NC, USA, 2008.

[15] A. Yankov, B. Collins, M. A. Jessee, and T. Downar, "A generalized adjoint approach for quantifying reflector assembly discontinuity factor uncertainties," in *Proceedings of the International Conference on the Physics of Reactors (PHYSOR '12)*, Knoxville, Tenn, USA, April 2012.

[16] M. L. Williams, G. Ilas, M. A. Jessee et al., "A statistical sampling method for uncertainty analysis with SCALE and XSUSA," submitted to *Nuclear Technology*.

[17] R. Fisher, "On the 'probable error' of a coefficient of correlation deduced from a small sample," *Metron*, vol. 1, pp. 3–32, 1921.

[18] M. Klein, L. Gallner, B. Krzykacz-Hausmann, A. Pautz, K. Velkov, and W. Zwermann, "Interaction of loading pattern and nuclear data uncertainties in reactor core calculations," in *Proceedings of the International Conference on the Physics of Reactors (PHYSOR '12)*, Knoxville, Tenn, USA, April 2012.

[19] I. Pasichnyk, M. Klein, K. Velkov, W. Zwermann, and A. Pautz, "Nuclear data uncertainties by the PWR MOX/UO2 core rod ejection benchmark," in *Proceedings of the International Conference on the Physics of Reactors (PHYSOR '12)*, Knoxville, Tenn, USA, April 2012.

EPJ Web of Conferences **42**, 03003 (2013)
DOI: 10.1051/epjconf/20134203003

Status of XSUSA for Sampling Based Nuclear Data Uncertainty and Sensitivity Analysis

W. Zwermann, L. Gallner, M. Klein, B. Krzykacz-Hausmann, I. Pasichnyk, A. Pautz, K. Velkov

Gesellschaft für Anlagen- und Reaktorsicherheit, Forschungszentrum, Boltzmannstrasse 14, Garching, Germany, 85748, Winfried.Zwermann@grs.de

Abstract. In the present contribution, an overview of the sampling based XSUSA method for sensitivity and uncertainty analysis with respect to nuclear data is given. The focus is on recent developments and applications of XSUSA. These applications include calculations for critical assemblies, fuel assembly depletion calculations, and steady-state as well as transient reactor core calculations. The analyses are partially performed in the framework of international benchmark working groups (UACSA - Uncertainty Analyses for Criticality Safety Assessment, UAM - Uncertainty Analysis in Modelling). It is demonstrated that particularly for full-scale reactor calculations the influence of the nuclear data uncertainties on the results can be substantial. For instance, for the radial fission rate distributions of mixed UO_2/MOX light water reactor cores, the 2σ uncertainties in the core centre and periphery can reach values exceeding 10%. For a fast transient, the resulting time behaviour of the reactor power was covered by a wide uncertainty band. Overall, the results confirm the necessity of adding systematic uncertainty analyses to best-estimate reactor calculations.

1 Introduction

Evaluated nuclear data files are continuously being improved. Recently, the European library was updated to JEFF-3.1.1 [1], the American library to ENDF/B VII.1 [2], and the Japanese library to JENDL-4.0 [3]. These library improvements are performed on the basis of the newest evaluations of differential experiments. Nevertheless, their precision is limited by the uncertainties of the underlying measurements and theoretical parameters. There is an increasing effort to improve the amount and quality of the covariance files accompanying the major data libraries. For now, a rather complete set of covariance data is provided in multi-group format with the SCALE 6 system [4]. In the past, most uncertainty investigations with nuclear covariance data, as performed, e.g., with TSUNAMI [5] or SUSD3D [6], were based on first order perturbation theory, and primarily consider the multiplication factors and other integral quantities. With increasing computer power, another approach has become possible, namely random sampling of nuclear data, as implemented in MCNP-ACAB [7], NUDUNA [8], TMC [9], and XSUSA [10]. Meanwhile, the GRS code package XSUSA ("Cross Section Uncertainty and Sensitivity Analysis") has been used for a wide variety of calculations for fissionable systems, including neutron transport calculations for pin cells, fuel assemblies, critical experiments, and full-scale reactor calculations, fuel assembly depletion calculations, as well as coupled neutron transport/thermo-hydraulic steady-state and transient reactor core calculations.

2 The XSUSA Method

Within the sampling based GRS method implemented in the code package SUSA ("Software for Uncertainty and Sensitivity Analysis") [11], many calculations for the problem under consideration are performed with varied input data. The variations of the input data are generated randomly from the given probability distributions of the parameters including possible correlations between them. After performing the complete series of calculations, the output quantities of interest are statistically analysed, and their uncertainty ranges and sensitivities to the input parameters are determined.

Originally, the GRS method has been mainly applied to problems with a limited number of parameters and only few correlations between them, such as thermo-hydraulic or technological parameters. However, in the case of its application to the nuclear data uncertainties implemented in XSUSA, various reactions of various nuclides have to be considered. Using the nuclear covariance data from the SCALE 6 code package, 44 uncertain parameters for each nuclide and reaction corresponding to the 44-group structure are analysed, resulting in a huge overall number of uncertain parameters. Moreover, a large amount of correlations between the energy group data of each nuclide/reaction combination have to be taken into account, and also cross correlations between data of different reactions and nuclides.

The nuclear data covariance matrices only contain the relative variance and covariance values of the nuclear data, i.e. the second moments of the distributions; the types of the distributions are not explicitly known and assumed to be Gaussian.

To use the GRS method with nuclear covariance data, the ENDF/B-VII based 238-group library of SCALE 6 is either used as is, or pre-collapsed to the 44-group structure of the covariance data using a flux spectrum typical for the system under consideration, which can be advantageous when doing full core calculations which require the handling of large amounts of data for the different fuel assemblies in various burn-up states. With the original or the collapsed master library, all necessary spectral calculations are performed, using the Bondarenko method implemented in the BONAMI module for the unresolved resonance regions, and performing 1-D transport calculations by the CENTRM module with continuous energy data in the resolved resonance region. The resulting data libraries are modified according to the uncertainty information in the covariance matrices for each nuclide/reaction combination considered. After doing so, it has to be assured that the cross section set is entirely consistent, i.e. that sum rules are fulfilled and that 2-D cross sections (e.g. scattering matrices) are compatible with their 1-D counterparts.

3 Applications

In this Section, uncertainty and sensitivity analysis results are presented for a variety of neutron transport applications.

3.1 Critical Assembly Calculations

In order to apply XSUSA to systems with different spectral conditions, Uranium and Plutonium systems are chosen, with fast and thermal spectra. Three of them are described in the International Handbook of Evaluated Criticality Safety Benchmark Experiments [12]: The bare metallic Uranium sphere GODIVA (in the nomenclature of the Handbook HEU-MET-FAST-001), the bare metallic Plutonium sphere 239Pu JEZEBEL (PU-MET-FAST-001), and one of the P-11 series of bare spheres of Plutonium nitrate solutions (PU-SOL-THERM-011, Case 16-1). KRITZ-2:13 is a light water moderated quadratic array of Uranium fuel pins, described in the International Handbook of Evaluated Reactor Physics Benchmark Experiments [13] as KRITZ-LWR-RESR-003. Due to their spherical shapes, GODIVA, JEZEBEL, and the P-11 sample were calculated with the 1-D deterministic XSDRN code as transport solver, while for KRITZ-2:13, the 3-D Monte Carlo code KENO-Va was used, both with XSUSA and TSUNAMI. Both XSDRN and KENO-Va are part of

the SCALE 6 system. In the XSUSA analysis, 1,000 samples were evaluated. The multiplication factor uncertainties from both the approaches agree very well.

Table 1. Multiplication factors and corresponding uncertainties due to nuclear data covariances obtained from XSUSA and TSUNAMI with sampled nuclear data.

	GODIVA	JEZEBEL	KRITZ-2:13	P-11, 16-1
Multiplication factor	1.00016	1.00035	0.99644	1.01042
Uncertainty from XSUSA	1.063%	1.418%	0.512%	1.506%
Uncertainty from TSUNAMI	1.069%	1.389%	0.529%	1.475%

3.2 Steady-State Core Calculations

The XSUSA method has been applied to a variety of full-scale reactor core calculations; as an example, a 2-D calculation for the uncontrolled hot zero-power state of a PWR mixed core specified within an international OECD/NEA benchmark [14] is chosen. Figure 1 displays the XSUSA uncertainty results (relative 1σ values) in the radial power distribution from the reference Monte Carlo calculations with KENO (left side). In addition, nodal calculations were performed with the GRS diffusion code QUABOX-CUBBOX with two-group fuel assembly homogenized cross sections obtained with the lattice code NEWT from SCALE 6. The corresponding results are given on the right side of Fig. 1.

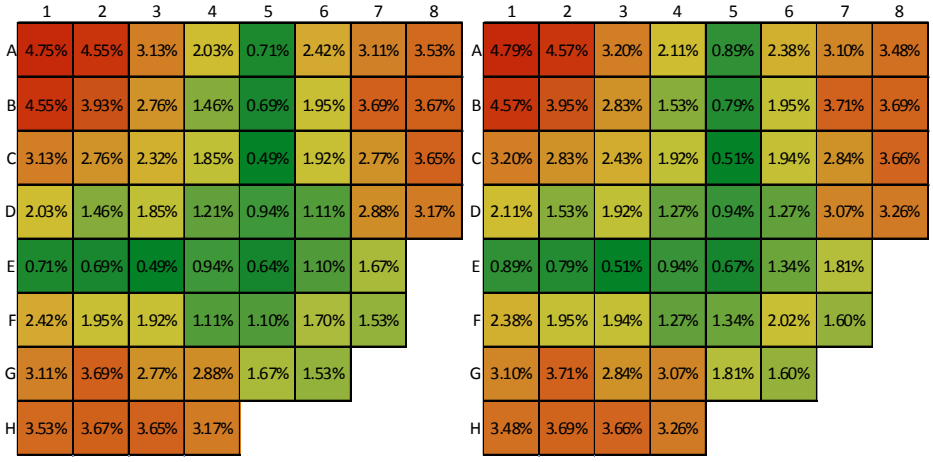

Fig. 1. Uncertainties of the radial fuel assembly power distribution of a mixed PWR core. Left: XSUSA/KENO; right: XSUSA/NEWT/QUABOX-CUBBOX

.

The resulting 1σ uncertainty is almost 5% for the power in the central fuel assembly; depending on the core layout, even larger uncertainties have been observed in full-scale core calculations. In addition, it is remarkable that the uncertainty distributions of both calculations are practically identical, demonstrating that the output uncertainties are hardly influenced by the additional calculation steps performed by the lattice code.

3.3 Time-dependent Core Calculations

For the same benchmark, an exercise for a transient was specified, namely the ejection of one control rod. This transient was analysed with the coupled GRS code system QUABOX-CUBBOX/ ATHLET. Figure 2 shows a substantial uncertainty band for the evolution of the reactor power,

ranging from practically no power excursion at all to a power peak of several times the nominal full reactor power.

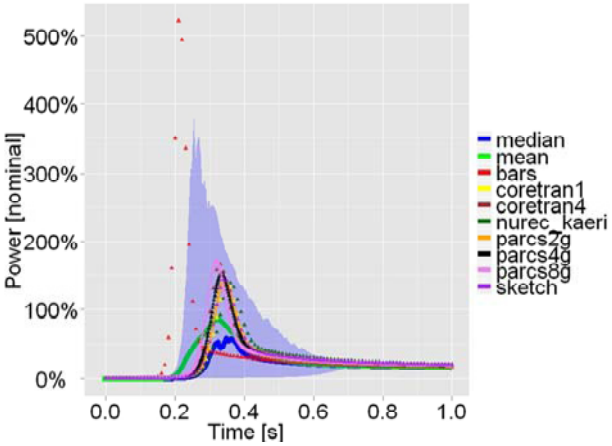

Fig. 2. Core power history for a rod ejection transient of a mixed PWR core. The XSUSA/QUABOX-CUBBOX/ATHLET uncertainty band is compared with the results of the benchmark participants.

3.4 Burn-Up Calculations

XSUSA is also applied for determining uncertainties in the relevant output quantities of pin cell and fuel assembly burn-up calculations, such as nuclide inventories and few-group cross sections for subsequent core simulations. Figure 3 gives an example for the isotope uncertainties arising in a UO_2 fuel pin during five years of irradiation and five years of cooling time. The calculations were performed with the SCALE 6 depletion sequence TRITON.

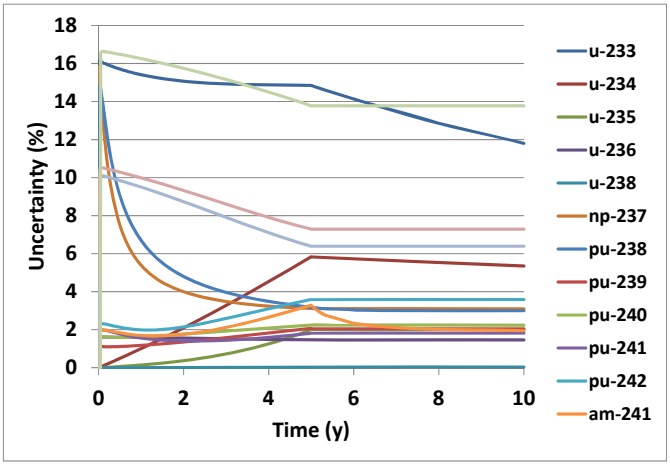

Fig. 3. Nuclide inventory uncertainty in a UO_2 pin cell burn-up calculation.

4 Conclusions and Outlook

The sampling based XSUSA cross section uncertainty and sensitivity analysis sequence has reached a mature state and is being applied to a variety of neutron transport calculations, namely criticality, depletion, lattice, and full core calculations, using both Monte Carlo and deterministic transport

methods. So far, the analyses were restricted to neutron cross sections as uncertain parameters. This is currently being extended to additional quantities relevant for burn-up calculations, namely fission yield and decay data. Another extension is being performed concerning the inclusion of delayed neutron multiplicity uncertainties, which may be important for the time-dependent behaviour of fissionable systems. When using Monte Carlo codes as transport solvers, methods are under investigation to drastically reduce the number of neutron histories without losing much information on the output uncertainties.

In conclusion, it is desirable and feasible to routinely accompany all parts of reactor calculations by uncertainty and sensitivity analyses, along with aiming for evaluated nuclear data of highest quality, as well as reliable and complete nuclear data uncertainty information.

This work is supported by the German Federal Ministry of Economics and Technology.

References

1. A. Santamarina et al., “The JEFF-3.1.1 Nuclear Data Library,” JEFF Report 22, NEA No. 6807 (2009).
2. M. Herman, “Development of ENDF/B-VII.1 and Its Covariance Components”, Journal of the Korean Physical Society, **59**, pp.1034–1039 (2011).
3. K. Shibata et al., “JENDL-4.0: A New Library for Innovative Nuclear Energy Systems,” Journal of the Korean Physical Society, **59**, pp.1046–1051 (2011).
4. “SCALE: A Modular Code System for Performing Standardized Computer Analyses for Licensing Evaluation, Version 6“, ORNL/TM-2005/39 (2009).
5. B.T. Rearden and D.E. Mueller, “Uncertainty Quantification Techniques of SCALE/ TSUNAMI”, Trans. Am. Nucl. Soc., **104**, pp.371-373 (2011).
6. I. Kodeli, “The SUSD3D Code for Cross-Section Sensitivity and Uncertainty Analysis – Recent Development,” Trans. Am. Nucl. Soc., **104**, pp.791-793 (2011).
7. N. García-Herranz, O. Cabellos, J. Sanz, J. Juan, and J. C. Kuijper, “Propagation of Statistical and Nuclear Data Uncertainties in Monte Carlo Burnup Calculations,” Annals of Nucl. Energy, **35**, pp.714-730 (2008).
8. O. Buss, A. Hoefer, and J.C. Neuber, “NUDUNA – Nuclear Data Uncertainty Analysis,” Proc. International Conference on Nuclear Criticality (ICNC 2011), Edinburgh, Scotland, Sep. 19-22, 2011, on CD-ROM (2011).
9. A. J. Koning and D. Rochman, “Towards Sustainable Nuclear Energy: Putting Nuclear Physics to Work,” Annals of Nucl. Energy, **35**, pp.2024-2030 (2008).
10. W. Zwermann, B. Krzykacz-Hausmann, L. Gallner, A. Pautz, “Influence of Nuclear Covariance Data on Reactor Core Calculations,” Second International Workshop on Nuclear Data Evaluation for Reactor Applications (WONDER 2009), Cadarache, France, 29 Sep. - 2 Oct., 2009, pp.99-104 (2009).
11. B. Krzykacz, E. Hofer, M. Kloos, “A Software System for Probabilistic Uncertainty and Sensitivity Analysis of Results from Computer Models,” Proc. International Conference on Probabilistic Safety Assessment and Management (PSAM-II), San Diego, Ca., USA, (1994).
12. “International Handbook of Evaluated Criticality Safety Benchmark Experiments”, September 2010 Edition, available on DVD-ROM, NEA/NSC/DOC(95)03.
13. “International Handbook of Evaluated Reactor Physics Benchmark Experiments”, March 2010 Edition, available on DVD-ROM, NEA/NSC/DOC(2006)1.
14. T. Kozlowski, T. J. Downar, “The PWR MOX/UO2 Core Transient Benchmark, Final Report”, NEA/NSC/DOC(2006)20.

Evaluation of Uncertainties in β_{eff} by Means of Deterministic and Monte Carlo Methods

I. Kodeli[1,*] and W. Zwermann[2]

[1] *Jožef Stefan Institute, Jamova 39, 1000 Ljubljana, Slovenia*
[2] *Gesellschaft fuer Anlagen- und Reaktorsicherheit (GRS) mbH, Forschungszentrum, Boltzmannstrasse 14, 85748 Garching, Germany*

(Dated: April 2, 2013)

Due to the influence of delayed neutrons on the reactor dynamics an accurate estimation of the effective delayed neutron fraction (β_{eff}), as well as good understanding of the corresponding uncertainty, is essential for reactor safety analysis. This paper presents the β_{eff} sensitivity and uncertainty analysis based on the derivation of Bretscher's prompt k-ratio equation. Performance of both deterministic (SUSD3D generalised perturbation code) and Monte Carlo (XSUSA random sampling code) methods applied with the multi-group neutron transport codes XSDRN and DANTSYS were compared on a series of ICSBEP critical benchmarks. Using the JENDL-4.0m and SCALE-6.0 covariance matrices the typical β_{eff} uncertainty was found to be around 3-4% and is generally dominated by the uncertainty of delayed nu-bar; depending on the considered assembly, the nu-prompt, inelastic, elastic and fission cross-section uncertainties may also significantly contribute to the overall uncertainty. The β_{eff} measurements in combination with the sensitivity and uncertainty analysis can be therefore exploited for validation of nuclear cross-section, such as delayed fission yields, ^{238}U elastic and inelastic cross section, complementing thus the information obtained from the k_{eff} measurements.

I. INTRODUCTION

The effective delayed neutron fraction β_{eff} is a key reactor safety parameter involved in the control rods worth calculations and transient (reactivity feedbacks effect) studies, playing an important role in reactivity accident analysis. Its accuracy should be therefore precisely understood and evaluated. The interest in calculating kinetics parameters and propagating their uncertainties was expressed within the Uncertainty Analysis in Modelling (UAM) project [1] of the OECD/NEA and methods for β_{eff} uncertainty evaluation were proposed and demonstrated at the UAM meetings in 2011-12 [2]-[5].

The uncertainty in the effective delayed neutron fraction β_{eff} was already studied by Hammer (1979) [6], D'Angelo et al. (1987, 1990) [7, 8] and A. Zukeran et al. (1999) [9]. Hammer [6] estimated the β_{eff} uncertainty for power reactor to about 5%, decomposed into the uncertainty due to those in the direct and adjoint neutron flux (∼2%), uncertainty in the fission cross-section x neutron yield, $\sigma_f\bar{\nu}$ (∼1.5%) and in the delayed fission spectra, χ_d (∼0.5%). Similar uncertainty of about 5% is reported for fast reactors in [7, 8]. The main sources were the uncertainty in the delayed neutron yield, $\bar{\nu}_d$ (∼2%) and the delayed fission spectra, χ_d (∼0.5%). Zukeran et al. (1999) used the generalised perturbation method and estimated the β_{eff} uncertainty to about 4 - 5%, the principal components being the uncertainty in $\bar{\nu}_d$ (∼2.5%), σ_f especially of ^{238}U (∼1.6%) and χ_d (∼0.5%).

II. CALCULATION OF THE EFFECTIVE DELAYED NEUTRON FRACTION

According to the conventional definition given in [10] the effective delayed neutron fraction (β_{eff}) for a mixture of fissionable isotopes, m, is given by:

$$\beta_{\text{eff}} = \frac{\sum_m \int \overline{\Phi^+ \sum_i \alpha_{i,m}\chi_{i,m}}\bar{\nu}_{d,m}\Sigma_{f,m}\Phi dE d\Omega d\vec{r}}{\sum_m \int \overline{\Phi^+\chi_m}\bar{\nu}_m\Sigma_{f,m}\Phi dE d\Omega d\vec{r}}. \quad (1)$$

where Φ and Φ^+ symbolise the direct and the adjoint angular fluxes, $\Sigma_{f,m}$ represents the macroscopic fission cross section of the fissile isotope m, $\chi_{i,m}$, χ_m are the corresponding i^{th}-group delayed and total neutrons fission spectra, and $\bar{\nu}_{d,m}$, $\bar{\nu}_m$ the delayed and total fission neutron yields (nu-bar). α_i represents the delayed-neutron fraction of the i^{th}-group.

As demonstrated in [2, 5] the above definition of beta-effective is equivalent to the sensitivity of the k_{eff} with

* Corresponding author, electronic address: ivan.kodeli@ijs.si

respect to the delayed fission neutron yields ($S^k_{\bar{\nu}_d}$) calculated using the first-order Perturbation Theory:

$$\beta_{\text{eff}} = \sum_{g,m} S^k_{\bar{\nu}_d,m,g}. \quad (2)$$

Calculation of β_{eff} by Eq. 1 or 2 is suitable for deterministic neutron transport codes. On the contrary, due to the complexity of the adjoint Monte Carlo transport calculations an alternative formulation to Eq. 1 is often used to calculate the β_{eff}. The method is based on Bretscher's approximation, also called the prompt k-ratio method [11, 12]:

$$\beta_{\text{eff}} = 1 - \frac{k_p}{k}. \quad (3)$$

where k_p is the effective multiplication factor (k_{eff}) taking into account only prompt neutrons and k is the usual total (prompt and delayed neutron) k_{eff}.

III. SENSITIVITY OF BETA-EFFECTIVE TO NUCLEAR DATA

The sensitivity and uncertainty in β_{eff} was obtained by deriving above mentioned Bretscher's k-ratio method, as already presented in 2011/12 [2, 3, 5]. From the Eq. 3 the sensitivities can be readily obtained as a difference between two standard sensitivity terms:

$$S^\beta_\sigma = -\frac{\sigma}{\beta_{\text{eff}}} \frac{\partial \frac{k_p}{k}}{\partial \sigma} = \frac{(1-\beta_{\text{eff}})}{\beta_{\text{eff}}} \left(S^k_\sigma - S^{k_p}_\sigma \right). \quad (4)$$

The two terms S^k_σ and $S^{k_p}_\sigma$ correspond to the sensitivities of k and k_p which can be obtained using the standard linear perturbation theory. Note however that due to a small difference between the two terms a high accuracy is required for these sensitivity calculations. Eq. 4 is similar to the one used in [8], differing only by a factor of $(1-\beta_{\text{eff}})$ which originates from the derivation of the denominator in Eq. 2.

IV. BENCHMARK ANALYSIS

The following benchmarks were selected from the International Handbook of Evaluated Criticality Safety Benchmark Experiments (ICSBEP) [13] database for the inter-comparison study:
- Jezebel (PU-MET-FAST-001): bare sphere of ^{239}Pu metal, 6.385-cm radius (4.5 at.%. ^{240}Pu, 1.02 wt.% Ga);
- Popsy (PU-MET-FAST-006 - Flattop-Pu): $\sim$ 20-cm natural U reflected ^{239}Pu sphere, 4.4-cm radius;
- Topsy (HEU-MET-FAST-028 - Flattop-25): $\sim$ 20-cm natural U reflected ^{235}U sphere, 6.045-cm radius;

Table I compares the β_{eff} values calculated using the above Eqs. 2 and 3 with the measured values for several benchmark experiments.

TABLE I. Measured values of β_{eff} compared with those calculated using the Eqs. 2 and 3.

Benchmark	Measured (pcm)	Calculated (pcm) Eq. 2 SUSD3D	Prompt k-ratio (Eq. 3) DANTSYS	XSUSA
Jezebel	194 ± 10	185	186	185
Popsy	276 ± 7	277	278	288
Topsy	665 ± 13	688	690	698

Two different approaches both based on the above derivation of the β_{eff} sensitivities (Eq. 4) were used. In the first approach the k and k_p cross-section sensitivities were calculated using the first order perturbation code SUSD3D [14, 15] based on the direct and adjoint neutron fluxes calculated by the DANTSYS package [16]. For the specific needs of the β_{eff} sensitivity analysis the accuracy of the SUSD3D sensitivity calculations was increased due to the small difference between the two sensitivity terms in Eq. 4. SUSD3D is available from the OECD/NEA Data Bank and RSICC. The benchmarks were calculated in 1D spherical geometry using ONEDANT. The cross-sections were taken from the ENDF/B-VII.0 evaluation [17] and processed into 33 energy groups by NJOY-99 [18]. The covariance matrices for most reactions were taken from the SCALE-6.0 [19] package which were made available to the UAM project together with the ANGELO2-LAMBDA [20] processing/verification tools. However, since SCALE-6.0 does not include covariances of the delayed nu-bar, essential for the β_{eff} studies, these data were taken from the JENDL-4.0m [21] evaluations, the only evaluation providing these matrices.

In addition, XSUSA [22] with XSDRN as transport code has been used to calculate uncertainties by random sampling of the nuclear data on the basis of the SCALE 6 covariance data. Again, these have been supplemented by delayed nu-bar covariance data from JENDL-4.0m. To evaluate sensitivities as given in the figures below, a group-by-group direct perturbation has been applied to the neutron cross section data.

The energy-integrated sensitivity coefficients for the Jezebel, Popsy and Topsy benchmarks benchmark are given in Tables II, VI and IV, respectively, and the corresponding uncertainties in Tables III, VII and V. β_{eff} in the Jezebel and Topsy benchmarks is shown to be particularly sensitive to the delayed and prompt neutron yields. According to the JENDL-4.0m covariances the uncertainties in the delayed fission neutron yields are by far the main sources of uncertainty, leading to the total uncertainty in β_{eff} of $\sim$3%. These benchmarks can be therefore considered as suitable above all for the validation of the delayed fission neutron yields.

On the other hand, β_{eff} in the Popsy benchmark is sensitive, in addition to the prompt and delayed neutron yields, in particular also to the fission, inelastic and capture neutron cross-sections. The total uncertainty in β_{eff} is around 4%.

The fact that an important part of the total uncertainty

comes from the ^{238}U inelastic cross-section uncertainty makes these benchmarks potentially suitable for the validation of these nuclear reaction data. Examples of the β_{eff} sensitivity to the ^{238}U inelastic data compared to the k_{eff} sensitivity are shown on Figures 1 and 2 for the Popsy and Topsy benchmarks, respectively. Due to the different shapes of the sensitivity profiles it is expected that the combined use of criticality and β_{eff} measurements could provide a better insight and an efficient validation of these nuclear data in the energy range above ∼1 MeV.

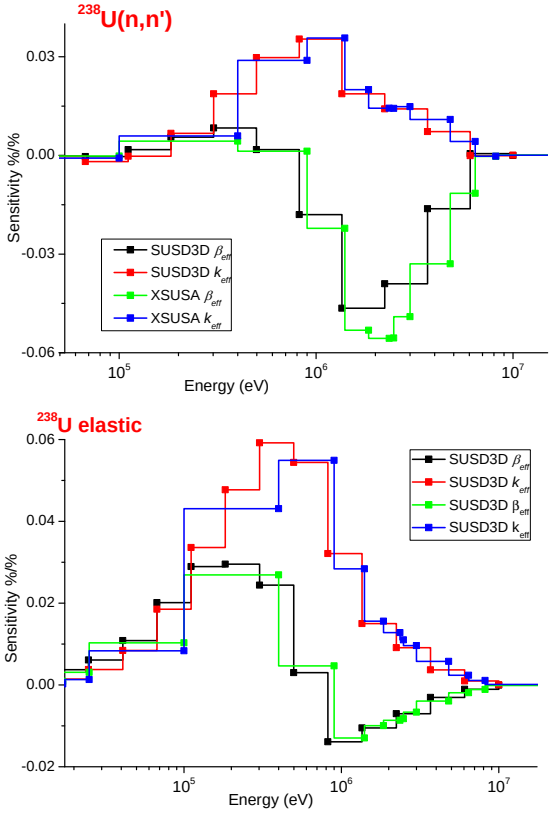

FIG. 1. Topsy benchmark: Comparison of the sensitivities of k_{eff} and β_{eff} with respect to the ^{238}U inelastic cross sections calculated using the SUSD3D and XSUSA codes.

TABLE II. Jezebel: Sensitivity of β_{eff} relative to ^{239}Pu nuclear cross-sections.

	Sensitivity (%/%)					
	elastic	inelastic	(n,f)	$\bar{\nu}_d$	$\bar{\nu}_p$	$\bar{\nu}_t$
SUSD3D	0.0794	0.0086	-0.0137	**0.948**	**-0.947**	0.002
XSUSA	0.0786	0.0082	-0.0129	**0.944**	**-0.946**	-0.002

V. CONCLUSIONS

The sensitivity coefficients of the effective delayed neutron fraction β_{eff} were obtained by deriving Bretscher's prompt k-ratio formula with respect to the basic nuclear data.

The sensitivity and uncertainty method was successfully implemented in the SUSD3D first order nuclear data perturbation code and the XSUSA random sampling code. Applied to the sensitivity and uncertainty analysis of several fast reactor benchmarks the two methods were demonstrated to be consistent and suitable for detailed analysis of various components of β_{eff} uncertainty, vali-

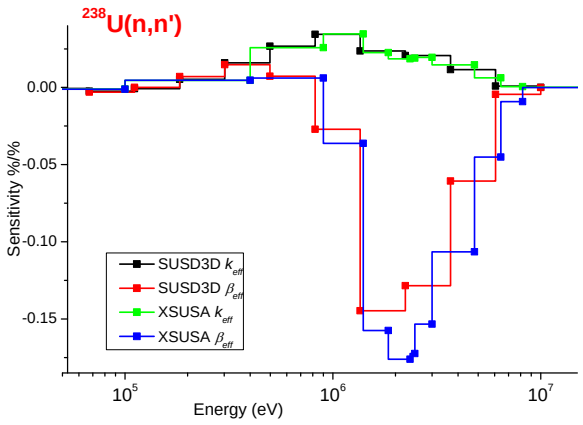

FIG. 2. Popsy benchmark: Comparison of the sensitivities of k_{eff} and β_{eff} with respect to the ^{238}U inelastic cross sections calculated using the SUSD3D and XSUSA codes.

TABLE III. Jezebel: Uncertainty in β_{eff} due to ^{239}Pu cross-sections uncertainties.

MAT	Uncertainty (%)				
	scattering	(n,f)	(n,γ)	$\bar{\nu}_d$	$\bar{\nu}_p$
SUSD3D	0.250	0.257	0.168	2.130	1.761
XSUSA	0.26			2.37	1.80

TABLE IV. Topsy: Sensitivity of β_{eff} relative to cross-sections.

MAT	Sensitivity (%/%)					
	elastic	inelastic	(n,f)	(n,γ)	$\bar{\nu}_d$	$\bar{\nu}_p$
SUSD3D						
^{235}U	0.0158	-0.0141	-0.0585	-0.033	**0.836**	**-0.843**
^{238}U	0.0472	-0.0512	0.0282	-0.0133	**0.153**	**-0.140**
XSUSA						
^{235}U	0.0157	-0.0177	-0.076		**0.818**	**-0.847**
^{238}U	0.0437	-0.0648	0.0441	-0.0126	**0.171**	

TABLE V. Topsy: Uncertainties in β_{eff} due to nuclear data uncertainties.

Code	MAT	Uncertainty (%)				
		scattering	(n,f)	(n,γ)	$\bar{\nu}_d$	$\bar{\nu}_p$
SUSD3D	^{235}U	0.09	0.08	1.01	2.41	0.14
	^{238}U	0.88	0.02	0.02	0.51	0.16
XSUSA	^{235}U			1.02	2.40	
	^{238}U	1.17			0.58	

TABLE VI. Popsy: Sensitivity of β_{eff} relative to nuclear data.

MAT	Sensitivity (%/%)					
	elastic	inelastic	(n,f)	(n,γ)	$\bar{\nu}_d$	$\bar{\nu}_p$
SUSD3D						
^{238}U	**0.103**	**-0.170**	**0.261**	-0.050	**0.361**	-0.083
^{239}Pu	-0.010	-0.042	**-0.305**	-0.017	**0.588**	**-0.879**
XSUSA						
^{238}U	**0.089**	**-0.195**	**0.316**	-0.047	**0.413**	
^{239}Pu	-0.030	-0.046	**-0.358**		**0.561**	**-0.918**

TABLE VII. Popsy: Uncertainties in β_{eff} due to nuclear data uncertainties.

Code	MAT	Uncertainty (%)				
		scattering	(n,f)	(n,γ)	$\bar{\nu}_d$	$\bar{\nu}_p$
SUSD3D	^{238}U	**3.236**	0.137	0.065	1.206	0.113
	^{239}Pu	0.654	0.280	0.151	1.364	1.397
XSUSA	^{238}U	**4.18**			1.39	
	^{239}Pu	0.72	0.280	0.151	1.38	1.46

dating in this way the mathematical methods and procedures developed. The method is robust provided sufficiently high precision is used in the calculations.

The results of the sensitivity and uncertainty analysis are valuable for nuclear data validation. According to the used covariance data the total uncertainty in β_{eff} was found to be in general around 3-4%. The β_{eff} uncertainty comes predominantly from the uncertainties in delayed neutron yields, contributing in the bare sphere experiments Jezebel and Topsy major part to the total uncertainty. In the case of the Popsy benchmark the inelastic and elastic scattering (contributing 3-4%), delayed and prompt neutron yields ($\sim$1%) and fission cross sections ($\sim$ 0.3%) play an important role. Due to the high sensitivity and the specific sensitivity profiles of β_{eff} the latter experiments can provide a complementary information to critical experiments for the validation of other reactions than ν_d. ^{238}U inelastic scattering is one example where β_{eff} measurements would contribute to improve nuclear data evaluations.

ACKNOWLEDGMENTS: This work is supported by the German Federal Ministry of Economics and Technology.

[1] K. Ivanov, *et al.*, Benchmark for Uncertainty Analysis in Modelling (UAM) for Design, Operation and Safety Analysis of LWRs, Volume I: Specification and Support Data for the Neutronics Cases (Phase I), Ver.2.0, (2012)

[2] I. Kodeli, Sensitivity and Uncertainty in the Effective Delayed Neutron Fraction β_{eff} (Method & SNEAK-7A Example), Proc. 5^{th} Workshop for the OECD Benchmark for Uncertainty Analysis in Best-Estimate Modelling (UAM-5), Stockholm (April 13-15, 2011), NEA-1769/04 package, OECD-NEA Data Bank.

[3] I. Kodeli, Sensitivity and uncertainty in beta-effective - new results, Proc. OECD Benchmark for Uncertainty Analysis in Best-Estimate Modelling (UAM-6), Karlsruhe, Germany, May 9-11, 2012

[4] E. Ivanov and I. Kodeli, Kinetics parameters S/U deterministic analysis, Proc, UAM-6 Workshop, Karlsruhe, May 9-11, 2012

[5] I. Kodeli, Sensitivity and Uncertainty in the Effective Delayed Neutron Fraction (β_{eff}), Proc. PHYSOR 2012 Conference, Knoxville, Tennessee, USA, Apr.15-20, 2012, ANS, LaGrange Park, IL (2012)

[6] P. Hammer, Requirements of delayed neutron data for the design, operation, dynamics and safety of fast breeder and thermal power reactors, Proc. Consultants Meeting on Delayed Neutron Properties, Vienna, 26-30 March 1979, INDC (NDS)-107/G+Special.

[7] A. D'Angelo, B. Vuillemin and J.C. Cabrillat: NEACRP-A-766, (1987).

[8] A. D'Angelo, A Total Delayed Neutron Yields Adjustment Using "ZPR" and "SNEAK" Effective-beta Integral Measurements, Proc. PHYSOR'90 Conf., Marseille (1990).

[9] A. Zukeran *et al.* J. Nucl. Sci. and Technology, **36**, No.1, 61 (1999).

[10] G. R. Keepin, *Physics of Nuclear Kinetics*, Addison-Wesley, Reading, Massachusets (1965).

[11] M. M. Bretscher, Evaluation of reactor kinetics parameters without the need for perturbation codes, Proc. Int. Meeting on Reduced Enrichment for Research & Test Reactors, Jackson Hole, Wyoming. USA, Oct.5-10, 1997.

[12] R. K. Meulekamp, S. C. van der Marck, Nucl. Sci. and Eng., 152, 142-148 (2006).

[13] International Handbook of Evaluated Criticality Safety Benchmark Experiments, OECD/NEA, NEA/NSC/DOC(95)03, Paris (2011).

[14] I. Kodeli, Nucl. Sci. Eng., **138**, 45-66 (2001).

[15] I. Kodeli, Transactions of American Nuclear Society, **104**, 2011.

[16] R.E. Alcouffe *et al.*, DANTSYS 3.0, - A Diffusion-Accelerated, Neutral-Particle Transport Code System, LA-12969-M, RSICC Code Package CCC-0547/08.

[17] M.B. Chadwick *et al.*, Nuclear Data Sheets **107**, 2931 (2006).

[18] R.E. MacFarlane, D.W. Muir, The NJOY Nuclear Data Processing System Version 99, LA-12740-M, RSICC Code Package PSR-368 (1999)

[19] "SCALE: A Modular Code System for Performing Standardized Computer Analyses for Licensing Evaluations", ORNL/TM-2005/39, Ver. 6.0, Vols. I-III, Jan.2009

[20] I. Kodeli, ANGELO-LAMBDA, Covariance matrix interpolation and mathematical verification, NEA-DB Computer Code Collection, NEA-1798/02 (2008).

[21] K. Shibata *et al.*, J.Nuclear Sci.& Technology, **48**, 1, 130 (2011).

[22] W. Zwermann *et al.*, "Influence of Nuclear Covariance Data on Reactor Core Calculations," Proc. 2^{nd} Int. Workshop on Nuclear Data Evaluation for Reactor Applications (WONDER 2009), Cadarache, France, 29 Sep. - 2 Oct., 2009, 99-104 (2009).

Uncertainty propagation with fast Monte Carlo techniques

D. Rochman,[1,*] S.C. van der Marck,[1] A.J. Koning,[1] H. Sjöstrand,[2] and W. Zwermann[3]

[1] *Nuclear Research and Consultancy Group NRG, Petten, The Netherlands*
[2] *Department of Physics and Astronomy, Uppsala University, Uppsala, Sweden*
[3] *Gesellschaft für Anlagen- und Reaktorsicherheit (GRS) mbH Forschungszentrum, Garching, Germany*

(Dated: February 26, 2013)

Since 2008, several new methods for nuclear data uncertainty propagation based on Monte Carlo techniques were developed and presented. They are based on a two-step approach: (1) the random sampling of nuclear model parameters to generate n random nuclear data libraries with observables such as cross sections, nubar (or alternatively n perturbations of nuclear observables, based on covariance information), and (2) the use of these random nuclear data in n calculations with a particle transport code ($n \simeq 1000$). With the use of a stochastic simulation code, each individual calculation is usually time-consuming because the statistical uncertainty of the stochastic simulation should be smaller than the nuclear data uncertainty. Repeated n times, the Monte Carlo uncertainty propagation with a Monte Carlo particle transport code becomes a large computer-time consumer. To remedy this problem, two methods of "fast" uncertainty propagation with a Monte Carlo simulation code are presented in this paper. In favorable cases, the uncertainty of a quantity can be calculated in only twice (or less) the amount of computer time that is needed for the quantity itself.

I. INTRODUCTION

As accredited scientists, one of our obligations is to report reliable uncertainties. Focusing on computer simulations, one source of uncertainty lies in the use of predictive models. They require a set of known inputs to predict an outcome. These inputs, however, are not known with certainty, and users are interested in accounting for that lack of certainty in their models.
In the case of Monte Carlo simulations, it is crucial to assess the impact of the model and parameter uncertainties without being distracted by the statistical uncertainty. The underlying necessity is to obtain the less approximate answer within a conceivable and practicable time. For instance, the most exact solution for uncertainty propagation might be obtained by repeating the same simulation, varying each time a given input parameter, for all the combinations of other input parameters. This solution is rapidly becoming unmanageable for large numbers of input parameters and is therefore not feasible.
In this paper, we are presenting possible solutions to this problem for nuclear applications. Conscious of the main drawback of the original TMC method, we are proposing faster solutions, providing uncertainties with a small additional calculation time compared to a unique calculation with nominal parameters.

* Corresponding author: rochman@nrg.eu

II. FAST METHODS

In 2008 a Monte Carlo method to propagate nuclear data uncertainties to parameters of large-scale nuclear systems was presented in Ref. [1], later acquiring the name of "Total Monte Carlo" (or TMC).
This original TMC method had the merit to propose an alternative way of propagating uncertainties for a nuclear system, compared to the well-established and accepted perturbation methods. It also allows the propagation of uncertainties for quantities where the perturbation methods were not applied for different practical reasons.It can nevertheless be recognized that TMC is an inefficient way of propagating uncertainties with Monte Carlo simulation codes, due to the minimization of the statistical uncertainty. The long calculation time is often considered as the main drawback of TMC and TMC-like methods, arguing that perturbation/sensitivity methods were in general more appropriate for a large number of applications, even if only providing an approximate answer. In the case of *extremely* long calculation time for a single simulation (such as weeks on hundreds of processors), it is not realistic to apply the TMC method and other solutions should be used. In the following, two "fast" alternatives are presented with an application on simple examples (see Table I for a schematic presentation).

(1) An original approach toward a faster TMC was taken in Ref. [2], where the advantages of the properties of identically distributed and conditionally independent output variables are exploited. In the following, this

method is called the "fast GRS method". Detailed descriptions can be found in Ref. [2] with several examples. Considering that $\vec{A}_{i=1..n}$ are n sets of random input parameters (A_i is of large dimension, containing for instance random cross sections of ^{235}U), and given that a unique calculation $C_1(m)$ provides $\sigma_{\text{stat\_1}}$ within T_1 sec. and m histories ($\sigma_{\text{stat\_1}}$ satisfactory small), the following should be performed:

1. repeating n times $C_1(\frac{m}{n})$, using different $\vec{A}_{i=1..n}$ and a unique seed s_1,
2. repeating n times $C_1(\frac{m}{n})$, using different $\vec{A}_{i=1..n}$ and a unique seed s_2,
3. then the covariance between the calculations (1) and (2) is equal to the variance due to $\vec{A}$ (see Table I for the description of the equations).

(2) A second alternative to bypass the difficulty of repeating n times long simulations (called fast TMC in the following) can be used and provide uncertainties due to input quantities in one to twice the time for a single calculation $C_1(m)$. It can be described as follows:

1. repeating n times $C_1(\frac{m}{n})$ with $\vec{A}_{i=1..n}$ and each time a different seed s_i, provides an observed σ_k^* and $\overline{\sigma^*}_{\text{statistics}} \simeq \sigma_{\text{stat\_1}}$ in $\approx T_1$ sec.
2. then $\sigma_k^{*2} = \overline{\sigma^*}_{\text{stat}}^{\,2} + \sigma^2_{\text{nucl.data.}}$.

In the case of possible bias in the estimation of the statistical uncertainties from the Monte Carlo transport code (such as MCNP), a second set of calculations is necessary to evaluate $\sigma_{\text{statistics}}$ by repeating the same calculations, only changing the seed of the random number generator. A full description will be presented in Ref. [3].

III. APPLICATION ON SIMPLE BENCHMARKS

In these examples of criticality and shielding benchmarks, reaction rates, neutron/gamma fluxes or k_{eff} are calculated, together with the uncertainties due to the random data (^{239,240,241}Pu, ^{235,238}U, ^{56}Fe and $^{\text{nat}}$W). This gives the flexibility to investigate small uncertainties (less than 100 pcm) to large ones (above 1000 pcm and a few tens of percent for shielding benchmarks) by selecting a given benchmark in combination with random nuclear data for selected isotopes: see Fig. 1.

In this figure, the calculated uncertainties for either k_{eff}, reaction rates or neutron and gamma spectra from the fast methods (fast TMC and the fast GRS method) are plotted as a function of the "original" TMC method. If the fast methods would yield to the same answer as the "original" TMC, all uncertainty values could be represented on a single $y = x$ line. From Fig. 1 it can be seen that the results are scattered along the $y = x$ line

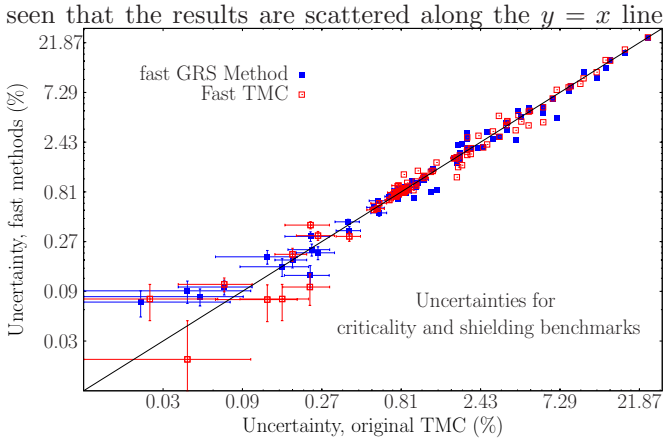

FIG. 1. Results for the criticality and shielding benchmarks (FNS, FNG and OKTAVIAN).

for both fast methods. One should nevertheless notice that for small nuclear data uncertainties and k_{eff} calculations, a difference up to a factor 2 can be observed.

IV. CONCLUSIONS

In 2008, the TMC method was presented to propagate nuclear data uncertainties, with the handicap of multiplying the required calculation time by the number of random cases considered nT, ($n \simeq 1000$). Five years later, we now present two faster solutions in the case of Monte Carlo simulations leading to a consequent decrease in nT (nT $\approx$ 2T). This means that uncertainty estimation will soon become standard for any Monte Carlo calculation involving nuclear data. Simple presented examples show the good performance compared to the original TMC method. A full detailed description will be presented in Ref. [3].

The work of GRS is supported by the German Federal Ministry of Economics and Technology.

[1] A.J. Koning, D. Rochman, Ann. of Nucl. Energy **35**, 2024 (2008).
[2] W. Zwermann *el al.*, "Aleatoric and epistemic uncertainties in sampling based nuclear data uncertainty and sensitivity analyses", in the proceedings of the PHYSOR-2012 conference, Knoxville, TN, USA, American Nuclear Society, April 15-20.
[3] D. Rochman, S.C. van der Marck, A.J. Koning, H. Sjöstrand and W. Zwermann, "Efficient use of Monte Carlo: uncertainty propagation", to be submitted in 2013

TABLE I. Simplified presentation of the three types of nuclear uncertainty propagation methods considered in this paper.

	TMC					fast TMC					fast GRS method				
	neutron histories	run time	seed	Nuclear data	Observed	neutron histories	run time	seed	Nuclear data	Observed	neutron histories	run time	seed	Nuclear data	Observed
run 1	m	T	s_0	ND_1	$k_1 \pm \sigma_{stat1}$	m/n	T/n	s_1	ND_1	$k_1^* \pm \sigma_{stat1}^*$	m/n	T/n	s_0	ND_1	$k_1^\bullet$
run 2	m	T	s_0	ND_2	$k_2 \pm \sigma_{stat2}$	m/n	T/n	s_2	ND_2	$k_2^* \pm \sigma_{stat2}^*$	m/n	T/n	s_0	ND_2	$k_2^\bullet$
⋮	⋮		⋱		⋮	⋮		⋱		⋮	⋮		⋱		⋮
run n	m	T	s_0	ND_n	$k_n \pm \sigma_{statn}$	m/n	T/n	s_n	ND_n	$k_n^* \pm \sigma_{statn}^*$	m/n	T/n	s_0	ND_n	$k_n^\bullet$
subTotal															$\overline{k^\bullet} \pm \sigma_1^\bullet$
run $n+1$											m/n	T/n	s_1	ND_1	k_1°
run $n+2$											m/n	T/n	s_1	ND_2	k_2°
⋮											⋮		⋱		⋮
run 2n											m/n	T/n	s_1	ND_n	k_n°
subTotal											m	T			$\overline{k^\circ} \pm \sigma_2^\circ$
Total	m	nT			$\overline{k}, \sigma_k, \overline{\sigma}_{stat}$	m	T			$\overline{k^*}, \sigma_k^*, \overline{\sigma^*}_{stat}$	$2 \times m$	2T			$\sigma_1^\bullet, \sigma_2^\circ$
Method	$\sigma_k^2 = \overline{\sigma}_{stat}^2 + \sigma_{nucl.data.}^2$					$\sigma_k^{*2} = \overline{\sigma^*}_{stat}^{\,2} + \sigma_{nucl.data.}^2$					$\sigma_{nucl.data.}^2 = \mathrm{cov}(\vec{k^\circ}, \vec{k^\bullet}) = \mathrm{corr}(\vec{k^\circ}, \vec{k^\bullet}) * \sigma_1^\bullet * \sigma_2^\circ$				

Verteiler

		Exemplare: gedruckte Form	Exemplare: pdf
BMWi			
Referat III C 7		1 x	
GRS-PT/B			
Projektbegleiter	(ket)	3 x	1 x
GRS			
Geschäftsführung	(wfp, stj)		je 1 x
Bereichsleiter	(moe, prg, san, stc, stu, uhl, ver)		je 1 x
Abteilungsleiter	(kig, luw, vek)		je 1 x
Projektleiter	(zww)	5 x	
Projektbetreuung	(hak, bna)		je 1 x
Informationsverarbeitung	(nit)		1 x
Autoren	(aur, muh, krz, ktz, pas, per, vek, zma, zww)	je 1 x	je 1 x
Bibliothek	(Köln)	1 x	

Gesamtauflage	**Exemplare**	**19**

Gesellschaft für Anlagen- und Reaktorsicherheit (GRS) mbH

Schwertnergasse 1
50667 Köln
Telefon +49 221 2068-0
Telefax +49 221 2068-888

Forschungszentrum
85748 Garching b. München
Telefon +49 89 32004-0
Telefax +49 89 32004-300

Kurfürstendamm 200
10719 Berlin
Telefon +49 30 88589-0
Telefax +49 30 88589-111

Theodor-Heuss-Straße 4
38122 Braunschweig
Telefon +49 531 8012-0
Telefax +49 531 8012-200

www.grs.de